Synthesis of Novel Serine β-Lactamase Inhibitors

Justin Young Ho

Wadham College

Hilary Term 2026

A thesis submitted to the Board of the Faculty of Mathematical, Physical & Life Sciences in partial fulfilment of the requirements for the degree of Doctor of Philosophy at the University of Oxford

Abstract

The widespread emergence of bacterial resistance to β-lactam antibiotics, driven primarily by serine β-lactamases (SBLs), continues to threaten the clinical utility of this cornerstone class of antibacterial agents. Although β-lactamase inhibitors such as sulbactam and tazobactam have historically restored the activity of partner antibiotics, their effectiveness has been eroded by the proliferation of inhibitor-resistant enzymes, particularly class C (AmpC) and class D (OXA) β-lactamases. Consequently, there remains a pressing need for new inhibitor scaffolds that combine potent enzyme inhibition with improved chemical stability and tunable physicochemical properties.

This thesis explores sulfoximine substitution on the penam scaffold as a strategy to expand the chemical and biological properties of β-lactamase inhibitors. Sulfoximines offer distinct advantages over classical sulfones, including stereochemical control, dual hydrogen-bond donor/acceptor capability, and enhanced opportunities for structural diversification. Leveraging recent advances in nitrene-transfer chemistry, robust and stereocontrolled synthetic routes to penam-sulfoximines were developed from sulbactam-derived sulfoxides. Both (*S*)- and (*R*)-configured penam sulfoximines were prepared, including synthetically challenging *NH*-sulfoximines that closely mimic the parent sulbactam framework. Single-crystal X-ray diffraction confirmed stereochemical integrity and structural assignments.

The scope and limitations of sulfoximine *N*-functionalization were systematically investigated, enabling access to amide, urea, and *N*-aryl derivatives while revealing intrinsic stability constraints of the penam core under basic or reductive conditions. These studies establish a versatile synthetic platform for the generation of structurally diverse penam-sulfoximines suitable for biological evaluation.

Biochemical and microbiological studies demonstrated that penam-sulfoximines are potent inhibitors of clinically relevant SBLs, including AmpC and OXA-type enzymes. A free *NH* penam-sulfoximine displayed particularly strong enzyme inhibition and measurable antibacterial activity against *Acinetobacter baumannii*, supported by enzyme inhibition assays, protein-binding studies, antimicrobial susceptibility testing, and structural characterization of enzyme–inhibitor complexes. However, many substituted sulfoximines exhibited reduced stability under physiological conditions, highlighting a trade-off between potency and chemical robustness.

Overall, this work establishes penam-sulfoximines as a chemically accessible and biologically active class of β-lactamase inhibitors, delineates key structure–stability–activity relationships, and provides a foundation for the future design of sulfoximine-based agents targeting resistant Gram-negative pathogens.

Acknowledgements

I would like to express my deepest gratitude to my supervisor, Professor Christopher Schofield, for his unwavering support and scientific insight throughout my doctoral studies. His guidance, perspective, and encouragement have been instrumental not only in shaping this thesis but also in my development as a scientist. I am also sincerely grateful to Dr. Lennart Brewitz for his patience, mentorship, and constant willingness to discuss ideas, troubleshoot challenges, and provide thoughtful advice at every stage of this work.

I gratefully acknowledge the Ineos Oxford Institute for Antimicrobial Research for partially funding this work and for their support of research addressing antimicrobial resistance.

I am profoundly thankful to my parents, Alice and Kennic, for their unconditional support, sacrifices, and belief in me throughout my life. Their encouragement made it possible for me to pursue my academic goals across continents. I am equally grateful to my siblings, Maria and Lawson, whose support and perspective have been a constant source of strength and grounding.

My time in Oxford would not have been the same without the friends who helped keep me sane, balanced, and motivated. I would like to thank Sara, Ed, Victor, Hamish, Ziggy, and Raphael for their friendship, shared experiences, and countless moments of laughter during my studies. I am deeply grateful to all my friends from around the world who took the time to visit me in Oxford and made this chapter of my life even more meaningful: Jerry, Lucas, Zach, Angel, Daniel, Hunter, Chris, Tony, Sean, Pae, Nicole, Max, Fabi, Joe, Jamie, Irene, and Camelia. Your visits, facetimes, and friendship made Oxford feel like home.

Declaration and Author Contributions

I declare that I carried out all of the work described in this thesis, except where stated below:

Chapters 2 and 3:

- Single-crystal X-ray diffraction data for small-molecule compounds were collected by the Oxford Crystallography Service, Department of Chemistry, University of Oxford. Structure solution and refinement were performed by the service.

Chapter 4:

- Dr. Karina Calvopina and Emily Freeman expressed and purified the serine β-lactamase (SBL) enzymes AmpC, TEM-116, OXA-10, OXA-48.
- Dr. Karina Calvopina and Emily Freeman performed SBL inhibition assays.
- Emily Freeman performed SPE-MS protein binding assays with AmpC and OXA-10.
- Emily Freeman crystallized sulfoximine inhibitors in complex with AmpC and solved the crystal structure of the AmpC:**37a** complex.
- Dr. Ana Ramos da Silva performed antimicrobial susceptibility testing.

Chapter 5:

- Tazobactam-derived penam-sulfoximine compounds described in **Figure 5.2-1** were synthesized by Ben Spivey, a Master's Part II student, under my direct supervision.

All experimental design (unless otherwise stated), data analysis, interpretation, and preparation of figures and text for this thesis were carried out by the author.

Table of Contents

Abbreviations

6-APA	6-Aminopenicillanic acid
7-ADCA	7-Aminodesacetoxycephalosporanic acid
A. baumannii	*Acinetobacter baumannii*
ADME	Adsorption, distribution, metabolism, excretion
AEC	Acyl–enzyme complex
AmpC	Ampicillin-hydrolyzing class C β-lactamase
AST	Antimicrobial susceptibility testing
Boc	*tert*-Butyloxycarbonyl
Bzh	Benzhydryl
CBZ	Benzyloxycarbonyl
CDK	Cyclin-dependent kinase
CMY	Cephamycinase
CNS	Central nervous system
CRE	Carbapenem-resistant Enterobacteriaceae
CTX-M	Cefotaximase (Munich)
cUTI	Complicated urinary tract infection
DBO	Diazabicyclooctane
DBU	1,8-Diazabicyclo(5,4,0)undec-7-ene
DCAD	Bis(4-chlorobenzyl) (*E*)-diazene-1,2-dicarboxylate
DCC	*N*,*N*′-Dicyclohexylcarbodiimide
DCE	Dichloroethane
DCM	Dichloromethane
DEAD	Diethyl azodicarboxylate
DHA	Dhahran AmpC β-lactamase
DIAD	Diisopropyl azodicarboxylate
DIPEA	*N*,*N*-Diisopropylethylamine
DMAP	4-Dimethylaminopyridine
DME	Dimethoxyethane
DMF	*N*,*N*-Dimethylformamide
DMS	Dimethyl sulfide
DMSO	Dimethyl sulfoxide
DPH	*O*-(2,4-Dinitrophenyl)hydroxylamine
EDC	1-(3-Dimethylaminopropyl)-3-ethylcarbodiimide
EDCI	1-(3-Dimethylaminopropyl)-3-ethylcarbodiimide hydrochloride
ESBL	Extended-spectrum β-lactamase
ESI	Electrospray ionization
EtOAc	Ethyl acetate
E. coli	*Escherichia coli*
FC-5	Fluorogenic cephalosporin probe-5
FDA	Food and Drug Administration
FOX	Cefoxitin-hydrolyzing β-lactamase
HCl	Hydrochloric acid
HRMS	High resolution mass spectrometry
HSV	Herpes simplex virus
IMP	Imipenemase
IR	Infrared
K. pneumoniae	*Klebsiella pneumoniae*
KOtBu	Potassium *tert*-butoxide

KOTMS	Potassium trimethylsilanolate
KPC	*Klebsiella pneumoniae* carbapenemase
LHMDS	Lithium bis(trimethylsilyl)amide
MBL	Metallo-β-lactamase
MeCN	Acetonitrile
MeOH	Methanol
MIC	Minimum inhibitory concentration
*m*CPBA	*meta*-Chloroperoxybenzoic acid
MS	Mass spectrometry
MSH	*O*-(Mesitylenesulfonyl)hydroxylamine
NDM	New Delhi metallo-β-lactamase
NMR	Nuclear magnetic resonance
OXA	Oxacillinases
P. aeruginosa	*Pseudomonas aeruginosa*
PCy_3	Tricyclohexylphosphine
Pd/C	Palladium on carbon
PMB	*para*-Methoxybenzyl
PNB	*para*-Nitrobenzyl
PBP	Penicillin-binding proteins
$Rh_2(esp)_2$	Bis rhodium(α,α,α',α'-tetramethyl-1,3-benzenedipropionic acid
$Rh_2(TPA)_4$	Rhodium (II) triphenylacetate dimer
RMSD	Root mean square deviation
SAR	Structure–activity relationship
SBL	Serine β-lactamase
SHV	Sulfhydryl variable β-lactamase
SM	Starting material
SPE-MS	Solid-phase extraction mass spectrometry
STAB	Sodium triacetoxyborohydride
TEM	Temoniera β-lactamase
TEA	Triethylamine
TBAF	Tetrabutylammonium fluoride
TFA	Trifluoroacetic acid
THF	Tetrahydrofuran
TLC	Thin-layer chromatography
TMSE	Trimethylsilyl ethyl
TPSA	Total polar surface area
UV	Ultraviolet
VIM	Verona integron-encoded metallo-β-lactamase

Standard 3 letter or single letter abbreviations for amino acids, standard SI unit abbreviations and chemical element symbols are used throughout this thesis.

Chapter 1 | Introduction

1.1 Penicillin and other β-lactam antibiotics

The discovery of penicillin marked the beginning of the modern antibiotic era which revolutionized medicine. In 1928, Alexander Fleming observed the antibacterial activity produced by *Penicillium notatum*, noting the fungus' ability to inhibit the growth of *Staphylococcus aureus* colonies on agar plates.[1] It was not until the early 1940s however, that Howard Florey, Ernst Chain, and colleagues succeeded in partially purifying and producing "penicillin" on a scale sufficient for pioneering therapeutic use. Subsequent work lead to purified penicillin G, which played a pivotal role in combatting disease during World War II.[2, 3] This breakthrough ushered in the "golden age" of antibiotics, leading to the development of a broad class of structurally related antibiotics containing a β-lactam ring – including penicillins (**1**), cephalosporins (**2**) , carbapenems (**3**), and monobactams (**4**) – that have remained a cornerstone of antibacterial chemotherapy for more than eight decades (**Figure 1.1-1**).[4]

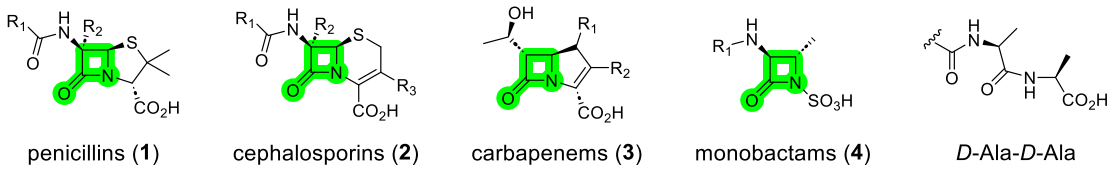

Figure 1.1-1. Structures of β-lactam antibiotics and the PBP natural substrate (*D*-Ala-*D*-Ala).

A conserved structural feature of all β-lactam antibiotics vital for antibacterial activity is the presence of a strained β-lactam ring, which acts as a structural mimic and competitor of the *D*-Ala-*D*-Ala terminus of peptidoglycan precursors.[5] β-lactam antibiotics inhibit bacterial cell wall biosynthesis via covalently acylating the nucleophilic active site serine of penicillin-binding proteins (PBPs) – a class of transpeptidases responsible for cross-linking the bacterial cell wall peptidoglycan

mesh.[5, 6] This covalent acyl-enzyme complex blocks transpeptidation, halting peptidoglycan cross-linking and leading to weakened cell wall integrity. The resulting defects render bacteria susceptible to osmotic lysis, explaining the potent bactericidal effect of β-lactam antibiotics.[7]

The extraordinary clinical success of β-lactam antibiotics is not only due to their broad-spectrum efficacy, but also to their relatively low toxicity in humans, as mammalian cells lack peptidoglycan cell walls. Nevertheless, the widespread use of these agents has been accompanied by the emergence of bacterial resistance, particularly through the production of β-lactamases and altered PBPs – a challenge that has shaped antibiotic development from the mid-20th century to the present day.[4]

1.2 β-Lactamase mediated resistance

Just one year after the therapeutic potential of penicillin was demonstrated in 1940, Abraham and Chain described an enzyme produced by *Escherichia coli* capable of hydrolyzing penicillin – the first β-lactamase to be reported.[8] Abraham and Chain's discovery foreshadowed the central challenge of β-lactam therapy: the continual emergence and spread of β-lactamases alongside each new generation of antibiotics – a challenge that has shaped antibiotic development from the mid-20th century to the present day. β-Lactamases have now become the most widespread and clinically significant mechanism of resistance to β-lactam drugs, with genes encoding these enzymes rapidly spreading among pathogenic bacteria.[9, 10]

β-Lactamases are divided into four Ambler classes (A–D) based on amino acid sequence homology and structural features.[11, 12] Ambler classes A, C, and D are serine β-lactamases (SBLs), which utilize a catalytic serine residue to react with the β-lactam ring giving a covalent acyl-enzyme intermediate, whereas class B β-lactamases

comprises the metallo-β-lactamases (MBLs) that rely on one or, more commonly, two Zn(II) ions to activate water for hydrolysis of the β-lactam ring (**Figure 1.2-1**).[13, 14]

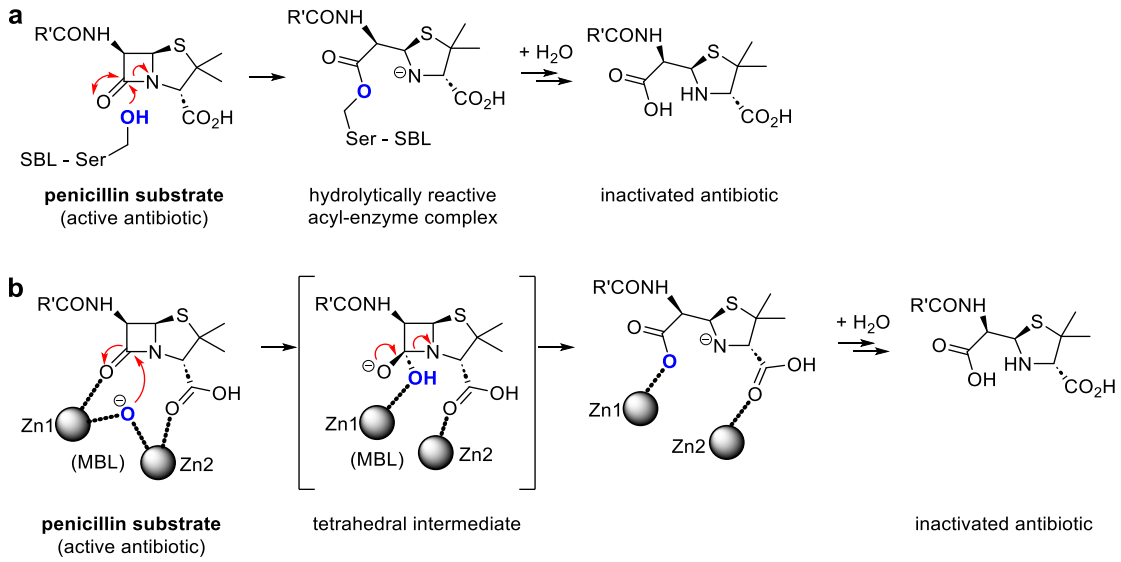

Figure 1.2-1. Outline mechanism of **a**) SBLs[13] and **b**) MBLs[14] with penicillin antibiotics.

The class A enzymes are among the most clinically prevalent β-lactamases (*e.g.*, TEM, SHV, and CTX-M), which have evolved from once narrow-spectrum penicillinases into extended-spectrum β-lactamases (ESBLs) capable of hydrolyzing third-generation cephalosporins.[15] Many ESBLs are plasmid-encoded, facilitating rapid dissemination across *Enterobacteriaceae*. A particularly concerning subset of class A enzymes is the KPC (*Klebsiella pneumoniae* carbapenemase**)** subfamily, which efficiently hydrolyzes carbapenems, long considered last-resort antibiotics.[16] Importantly, many class A β-lactamases can be inhibited by clinically established mechanism-based inhibitors such as clavulanic acid, sulbactam, or newer diazabicyclooctane based β-lactamase inhibitors (*i.e.*, avibactam), although resistance to all of these due to inhibitor-resistant variants is increasingly reported.[9]

The Class B β-lactamases, the MBLs, are mechanistically distinct in that they coordinate one or two Zn^{2+} ions in their active site.[17] These metal cofactors activate a

water molecule to directly attack the β-lactam carbonyl, bypassing the need for a covalent acyl-enzyme intermediate.[18] The MBLs are subdivided into the B1-3 groups, of which the B1 MBLs are most clinically important. B1 MBLs include the IMP, VIM, and NDM β-lactamases, which confer resistance to nearly all β-lactams, including carbapenems, though monobactams such as aztreonam are typically unreactive.[17] Unlike the SBLs, MBLs are not inhibited by classical β-lactamase inhibitors, meaning treatment options for infections caused by bacteria producing them are severely restricted. The global spread of NDM-producing *Enterobacteriaceae* illustrates the critical public health threat posed by β-lactamases.[17, 18]

The class C SBLs, sometimes known as AmpC β-lactamases, are typically encoded on the chromosome of many Gram-negative bacteria such as *Enterobacter*, *Citrobacter*, and *Pseudomonas* species, where they confer resistance to penicillins and cephalosporins.[12, 19] AmpC β-lactamases gene expression is often inducible by β-lactam exposure through regulatory pathways involving ampR, but can become constitutive via mutations, leading to high-level resistance.[20, 21] In recent decades, plasmid-borne AmpC variants such as CMY, DHA, and FOX have been identified, accelerating their spread among *E. coli* and *K. pneumoniae*.[22, 23]

The class D β-lactamases, or oxacillinases (OXAs), were initially identified for their ability to hydrolyze isoxazolyl penicillins such as oxacillin and cloxacillin.[24, 25] This class is highly diverse, with over 800 variants being reported, including enzymes with clinically important carbapenemase activity.[26, 27] Among these, OXA-48-like enzymes have disseminated widely in *Enterobacteriaceae*, while OXA-23, OXA-24/40, and OXA-58 are associated with carbapenem resistance in *Acinetobacter baumannii*.[28, 29] Many OXA enzymes hydrolyze carbapenems poorly, but their clinical relevance is amplified by high-level expression or synergistic resistance mechanisms such as porin

loss and efflux pump activity.[26, 30] As with AmpC β-lactamases, most OXA β-lactamases are poorly inhibited by classical β-lactamase inhibitors, and even avibactam demonstrates limited efficacy against certain OXA-variants.[24]

1.3 β-Lactamase inhibitors

In response to the threat that β-lactamases pose to the clinical utility of β-lactam antibiotics, inhibitors to them have been developed to restore the activity of companion antibiotics against resistant pathogens (**Figure 1.3-1**).[8, 9]

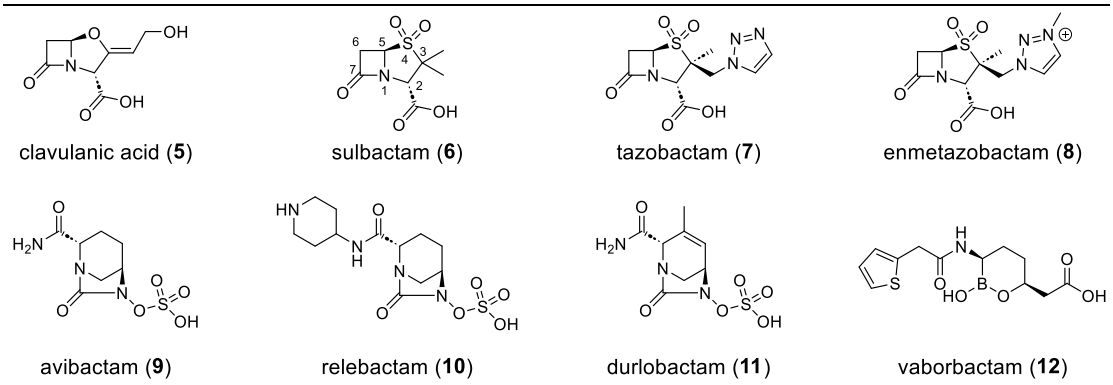

Figure 1.3-1. Structures of clinically approved β-lactamase inhibitors.

1.3.1 Clavulanic acid

The emergence of plasmid-encoded β-lactamases in the 1960s and 1970s rapidly undermined the efficacy of penicillins, prompting efforts to identify agents capable of restoring their activity.[31] The discovery of the first clinically useful β-lactamase inhibitor, clavulanic acid, was reported in 1976, following its purification from the fermentation broth of *Streptomyces clavuligerus*.[31] Structurally, clavulanic acid contains a β-lactam ring but exhibits minimal intrinsic antibacterial activity; instead, it functions as a mechanism-based covalent inhibitor of many class A SBLs.[32] Upon binding to the β-lactamase's nucleophilic active-site serine, clavulanic acid undergoes

a ring opening and series of tautomerizations that result in an acid-promoted fragmentation, causing inactivation of the enzyme (**Figure 1.3-2**).[33]

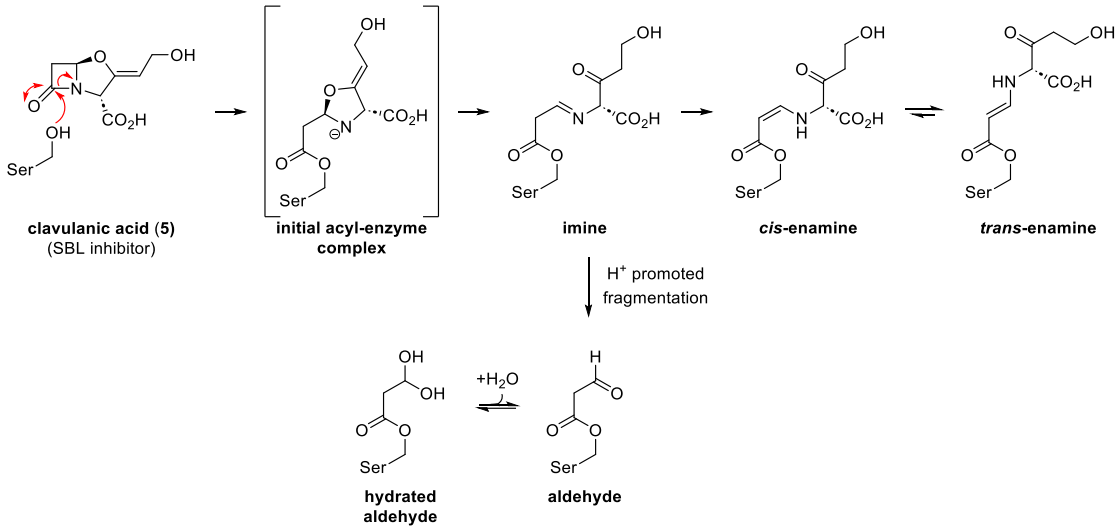

Figure 1.3-2. Outline mechanism for reaction of clavulanic acid (**5**) with SBLs.[33]

Clavulanic acid entered clinical use in the early 1980s in fixed-dose combinations with broad-spectrum penicillins. The most widely used formulation, amoxicillin–clavulanate (Augmentin), was introduced in 1981 and remains a frontline therapy for community-acquired infections such as respiratory tract infections, urinary tract infections, and skin and soft tissue infections.[34, 35] Clavulanic acid containing combinations include ticarcillin-clavulanate, which was used for severe hospital-acquired infections, though the ticarcillin-clavulanate combination has been largely supplanted by newer agents.[36] Despite the introduction of more modern inhibitors, amoxicillin-clavulanate is increasingly used and remains one of the most frequently prescribed antibiotics globally, underscoring the enduring clinical relevance.[4]

Clavulanic acid is not universally effective, and exhibits strong potency against many class A SBLs, including TEM-1, SHV-1, and related penicillinases. However, resistance to clavulanic acid has emerged in the form of inhibitor-resistant TEM (IRT) and SHV variants, as well as CTX-M ESBLs, which are variably inhibited.[9, 15] In

contrast, class C (AmpC) and class D (OXA) enzymes generally display poor inhibition by clavulanic acid, and class B MBLs are completely unaffected by clavulanic acid due to their distinct Zn^{2+}-dependent mechanism.[19, 26]

Thus, clavulanic acid remains a cornerstone β-lactamase inhibitor in clinical use nearly five decades after its discovery. Limitations against AmpCs, OXAs, and MBLs have driven the development of new generations of inhibitors such as sulbactam, tazobactam, and non-β-lactam scaffolds like diazabicyclooctanes (DBOs).[4]

1.3.2 Sulbactam

Following the discovery and clinical success of clavulanic acid, attention turned to developing additional mechanism-based serine β-lactamase (SBL) inhibitors with improved pharmacological properties. Sulbactam (**6**), a semi-synthetic penicillanic acid sulfone, was introduced in the early 1980s as the second clinically approved SBL inhibitor.[37, 38] Like clavulanic acid, sulbactam lacks significant intrinsic activity against most, but not all, bacteria, and similarly acts as a covalent inhibitor of many class A SBLs. As for clavulanic acid, the penam sulfone SBL inhibition mechanism involves acylation of the active-site serine residue followed by ring-opening, tautomerization, and acid-promoted fragmentation to a stable, covalently modified enzyme that is catalytically inactivated (**Figure 1.3-3**).[39]

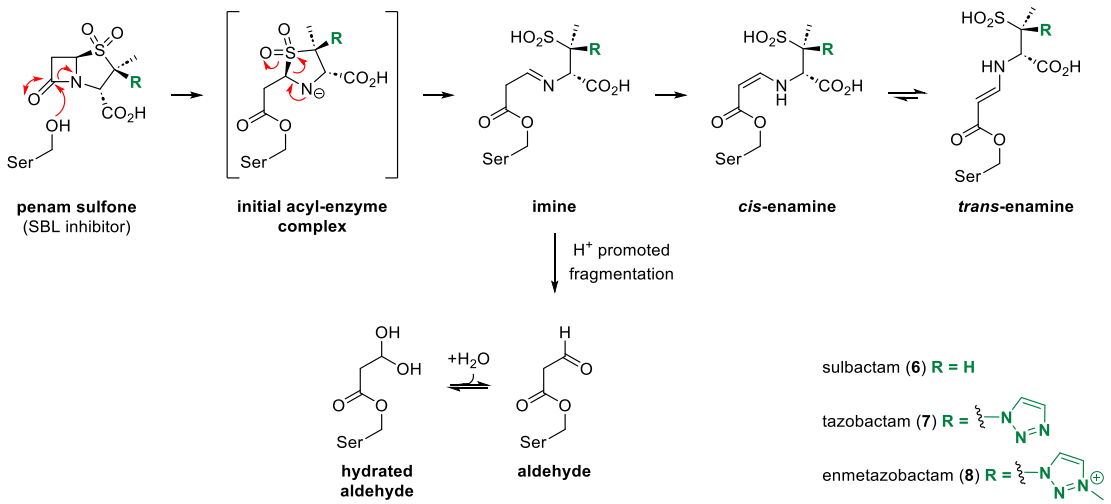

Figure 1.3-3. Outline mechanism for the reaction of penam sulfones with SBLs.[39]

Sulbactam has been widely deployed in fixed-dose combinations with broad-spectrum penicillins. The most notable formulation is ampicillin-sulbactam (Unasyn), first approved in 1987, which remains in use for a broad range of infections including intra-abdominal, skin and soft tissue, gynecological, and respiratory tract infections.[40, 41] Another early combination, cefoperazone–sulbactam has found particular utility in Asia and parts of Europe, especially for infections caused by Gram-negative *Nosocomial bacilli*.[42] These combinations were developed to counter the increasing prevalence of plasmid-encoded class A β-lactamases in *Enterobacteriaceae* and *Haemophilus* influenzae that rendered penicillins and some cephalosporins ineffective.[22]

Like clavulanic acid, sulbactam's spectrum of inhibition is confined to class A SBLs; it has activity against TEM, SHV, and some CTX-M SBLs. However, many inhibitor-resistant TEM (IRT) variants, ESBLs, and carbapenemases are poorly inhibited by sulbactam.[4, 15] Sulbactam is also largely ineffective against class C (AmpC) SBLs, class D oxacillinases, and class B MBLs, highlighting the limitations of early SBL inhibitors and the clinical need that later drove the development of tazobactam and

non-β-lactam inhibitors.[19, 26] Despite these limitations, sulbactam remains clinically used today, particularly in ampicillin–sulbactam formulations.

1.3.3 Tazobactam

The limitations of clavulanic acid and sulbactam against plasmid-encoded SBLs spurred the development of tazobactam (**7**), a second-generation penicillanic acid sulfone inhibitor distinguished by a 1,2,3-triazol-1-yl substituent at the *C3* position of the penam nucleus (**Figure 1.3-1**).[43] This heteroaryl group enhances inhibitory potency compared with sulbactam, particularly against TEM and SHV SBLs, by stabilizing the acyl–enzyme complex.[9, 10] Mechanistically, tazobactam resembles sulbactam and clavulanic acid in acting as a mechanism-based inhibitor: the β-lactam ring undergoes irreversible acylation of the active-site serine, leading to enzyme inactivation (**Figure 1.3-3**).[39]

Clinically, tazobactam was approved for use the late 1980s and is most widely used in combination with piperacillin (Zosyn, introduced in 1993), which quickly became a cornerstone of hospital therapy.[44] This fixed-dose formulation offers broad-spectrum coverage against Gram-negative and Gram-positive pathogens and remains a first-line option for serious nosocomial infections, including intra-abdominal infections, pneumonia, urinary tract infections, and febrile neutropenia.[45] Other combinations, such as cefepime–tazobactam, have been investigated but have not gained comparable clinical adoption.[46]

Despite these advances, tazobactam has limitations: although it is active against many class A SBLs, including TEM and SHV, tazobactam shows reduced activity against CTX-M-type ESBLs and is largely ineffective against class C (AmpC), class D (OXA), and class B MBLs.[19, 26] The global rise of ESBL- and AmpC-producing

Enterobacteriaceae in the 1990s and 2000s diminished its effectiveness in many regions. Nevertheless, piperacillin–tazobactam remains one of the most widely prescribed β-lactam/β-lactamase inhibitor combinations, underscoring the clinical value of tazobactam nearly three decades after its introduction.

1.3.4 Enmetazobactam

The development of resistance to classical SBL inhibitors (clavulanic acid, sulbactam, and tazobactam), particularly through ESBLs and inhibitor-resistant TEM/SHV variants, drove the search for new SBL inhibitors with improved potency and broader coverage. Enmetazobactam (**8**) is a novel penicillanic acid sulfone closely related to tazobactam, distinguished by the presence of an additional *N*-methyl group on the triazolyl substituent (**Figure 1.3-1**).[43] This modification enhances penetration into Gram-negative bacteria and increases stability against hydrolysis, thereby conferring superior inhibitory activity against class A β-lactamases, including ESBLs such as CTX-M enzymes.[47, 48]

Enmetazobactam has been co-formulated with cefepime in the investigational cefepime-enmetazobactam combination, which has shown potent *in vitro* activity against *Enterobacteriaceae* producing ESBLs and has progressed to late-stage clinical development.[48] A Phase 3 trial (ALLIUM study) demonstrated that cefepime-enmetazobactam was non-inferior, and in some endpoints superior, to piperacillin-tazobactam for the treatment of complicated urinary tract infections, including acute pyelonephritis.[49] In this trial, cefepime-enmetazobactam achieved higher clinical cure and microbiologic eradication rates, particularly against ESBL-producing *E. coli* and *K. pneumoniae*.

Mechanistically, enmetazobactam retains activity against many class A β-lactamases (including TEM, SHV, and CTX-M families), with limited activity against class C enzymes and minimal inhibition of class D β-lactamases and class B MBLs.[50] As such, enmetazobactam's primary clinical role lies in addressing the rising global prevalence of ESBL-producing *Enterobacteriaceae*, a critical resistance mechanism driving multidrug-resistant infections worldwide.

1.3.5 Diazabicyclooctane SBL inhibitors

The clinical limitations of β-lactam-based SBL inhibitors highlighted the need for new scaffolds with broader inhibitory activity. This led to the development of diazabicyclooctanes (DBOs), the first clinically approved class of non-β-lactam SBL inhibitors (**Figure 1.3-1**). Unlike mechanism based inhibitors such as clavulanic acid, DBOs do apparently not undergo extensive degradation during inhibition; instead, they form a reversible covalent bond with the catalytic serine of SBLs, allowing potent, sustained inhibition of class A and class C SBLs, as well as partial activity against some class D SBLs.[51, 52] Importantly, DBOs lack intrinsic antibacterial activity but serve to restore the activity of partner β-lactams against resistant pathogens.[48]

Avibactam (**9**) was the first DBO approved for clinical use (FDA 2015), in fixed-dose combinations with ceftazidime and ceftaroline.[53, 54] It exhibits potent inhibition of class A enzymes (including KPC carbapenemases and ESBLs), class C AmpC enzymes, and some class D SBLs such as OXA-48-like carbapenemases.[55, 56] However, avibactam is inactive against class B MBLs.[51] Clinically, ceftazidime-avibactam has become an important treatment for complicated intra-abdominal infections, urinary tract infections, and hospital-acquired pneumonia due to multidrug-resistant *Enterobacteriaceae* and *Pseudomonas aeruginosa*.[57]

Relebactam (**10**), a structural analogue of avibactam with an added piperidine moiety, was approved in 2019 in combination with imipenem/cilastatin.[58] This modification improves penetration and inhibitory potency against certain class C enzymes and enhances activity against multidrug-resistant *P. aeruginosa* while maintaining strong inhibition of class A carbapenemases (KPCs).[59, 60] Imipenem-relebactam is approved for the treatment of complicated UTIs, intra-abdominal infections, and hospital-acquired pneumonia, expanding therapeutic options against carbapenem-resistant *Enterobacteriaceae* that do not produce MBLs.

Durlobactam (**11**) is the most recently approved DBO (FDA 2023); it was developed specifically to address resistance in *Acinetobacter baumannii*.[61] Unlike avibactam and relebactam, which primarily target *Enterobacteriaceae*, durlobactam has been optimized for potent inhibition of class D OXA-type β-lactamases, which are the dominant carbapenemases in *A. baumannii*.[62, 63] Approved in combination with sulbactam, durlobactam restores sulbactam's intrinsic antibacterial activity against *A. baumannii–calcoaceticus* complex, providing the first pathogen-targeted β-lactam/β-lactamase inhibitor therapy for drug-resistant *Acinetobacter* infections.

1.3.6 Vaborbactam

While DBO inhibitors expanded the spectrum of SBL inhibition to include class A carbapenemases (KPC) and class C SBLs, resistance mediated by KPC-producing *Enterobacteriaceae* continued to pose a major global threat. This promoted the development of boronic acid–based inhibitors, which exploit the ability of boronic acids to form a reversible covalent bond with the catalytic serine of SBLs, mimicking the high-energy tetrahedral intermediate of β-lactam hydrolysis.[64]

Vaborbactam (**12**) is a cyclic boronic acid β-lactamase inhibitor, which was FDA-approved in 2017 for use in combination with meropenem (Vabomere®) for the treatment of complicated urinary tract infections (cUTI), including pyelonephritis (**Figure 1.3-1**).[65] Its spectrum includes potent inhibition of class A carbapenemases, especially KPC enzymes, and broad activity against class C AmpC enzymes.[66] Unlike avibactam, however, vaborbactam has little to no activity against most class D (OXA-type) SBLs and does not inhibit class B MBLs (NDM, VIM, IMP).[67]

In clinical studies, meropenem–vaborbactam demonstrated superiority over piperacillin–tazobactam in the TANGO I trial for the treatment of cUTI, and non-inferiority compared to best available therapy in the TANGO II trial for infections due to carbapenem-resistant *Enterobacteriaceae* (CRE), with improved safety and lower mortality.[68, 69] These results established vaborbactam as a potentially important therapeutic option against KPC-producing CRE, where few alternatives exist. Mechanistically, vaborbactam's high affinity and reversible covalent interaction with KPC enzymes allows durable suppression of carbapenem hydrolysis, restoring meropenem's bactericidal activity.[66] Its lack of activity against MBLs and OXAs, however, underscores the need for next-generation boronate inhibitors such as taniborbactam, which aim for broader inhibition across Ambler classes.

Inhibitor	Chemical class	Year of approval	Common combinations	Effective against	Key limitations
Clavulanic acid	Clavams	1984	Amoxicillin – clavulanate (Augmentin); Ticarcillin-clavulanate	Class A (narrow spectrum, TEM, SHV)	Poor against ESBLs, AmpC, OXA, MBLs
Sulbactam	Penicillanic acid sulfone	1986	Ampicillin–sulbactam (Unasyn)	Class A (limited), some Acinetobacter PBPs	Weak against ESBLs, AmpC, OXA, MBLs
Tazobactam	Penicillanic acid sulfone	Late 1980s	Piperacillin–tazobactam (Zosyn)	Class A (TEM, SHV); weak vs. ESBLs	Ineffective vs. CTX-M, AmpC, OXA, MBLs
Enmetazobactam	Penicillanic acid sulfone	2020s (EU)	Cefepime–enmetazobactam (Exblifep)	Class A incl. ESBLs (TEM, SHV, CTX-M)	Poor vs. AmpC, OXA, MBLs
Avibactam	DBO	2015	Ceftazidime–avibactam (Avycaz)	Class A (incl. KPC, ESBLs), Class C (AmpC), some Class D (OXA-48)	No activity vs. MBLs
Relebactam	DBO	2019	Imipenem–cilastatin–relebactam (Recarbrio)	Class A (incl. KPC), Class C (AmpC)	Ineffective vs. MBLs, most OXAs
Durlobactam	DBO	2023	Sulbactam–durlobactam (Xacduro)	Class A, C, D; restores sulbactam activity vs. *A. baumannii*	No activity vs. MBLs
Vaborbactam	Cyclic boronate	2017	Meropenem–vaborbactam (Vabomere)	Class A (esp. KPC carbapenemases)	No activity vs. MBLs, OXAs, limited vs. AmpC

Table 1.3-4. Summary table of clinically approved β-lactamase inhibitors.

Importantly, many class A SBLs can be inhibited by mechanism-based inhibitors such as clavulanic acid, sulbactam, or newer diazabicyclooctane (DBO)-based inhibitors (*i.e.*, avibactam), although resistance for all these due to inhibitor-resistant variants is increasingly reported.[9]

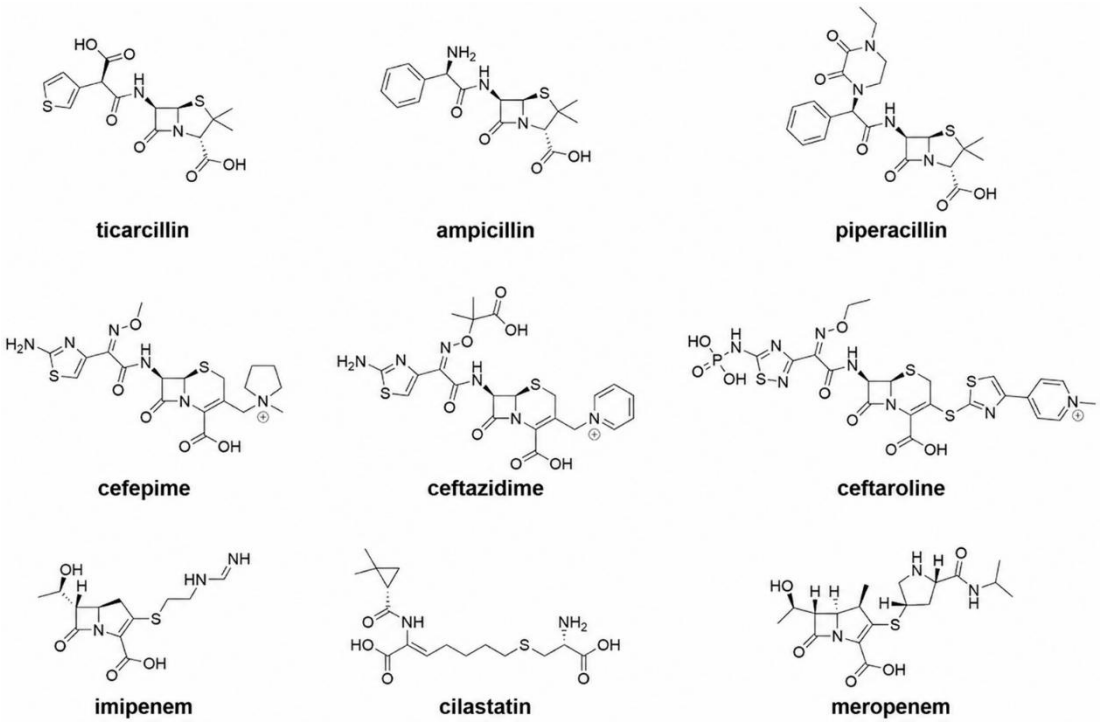

Figure 1.3-5. Structures of antibiotics mentioned used in combination with β-lactamase inhibitors.

1.4 Antibiotic properties of sulbactam against *A. baumannii*

Unlike most SBL inhibitors, sulbactam possesses intrinsic antibacterial activity against *A. baumannii*. This activity stems from its relatively strong affinity for penicillin-binding proteins (PBPs), specifically PBPs 1a, 1b, and 3, which it inhibits by acylation to disrupt peptidoglycan cross-linking and ultimately cause bacterial cell death.[70] The ability of sulbactam to effectively target PBPs distinguishes it from clavulanic acid and tazobactam, which lack potent intrinsic antibacterial properties.[61]

Since sulbactam was approved in the 1980s for use in a fixed-dose combination with ampicillin (ampicillin-sulbactam; Unasyn), it has been widely used to treat severe infections caused by *A. baumannii*, particularly in hospital settings where multidrug-resistant (MDR) strains are prevalent.[71] The antibiotic activity of sulbactam versus *A. baumannii* is unusual because it does not have a *C6* sidechain. However, its utility as monotherapy is compromised by the widespread emergence of resistance, particularly

mediated by Ambler class D OXA-type SBLs that hydrolyze sulbactam and reduce its efficacy.[70]

To overcome this limitation, sulbactam has been paired with novel β-lactamase inhibitors that protect it from enzymatic inactivation. Notably, the DBO durlobactam has potent activity against class A, C, and D enzymes and has been shown to restore sulbactam's antibacterial activity against carbapenem-resistant *A. baumannii* both *in vitro* and *in vivo*.[61] The sulbactam-durlobactam combination (Xacduro), received FDA approval in 2023 for the treatment of hospital-acquired and ventilator-associated bacterial pneumonia caused by *A. baumannii* complex, reflecting the enduring clinical importance of sulbactam's intrinsic antibacterial properties and the value of potentiating them through novel inhibitors.[63]

1.5 Sulfoximines in medicinal chemistry

Sulfoximines have attracted significant attention in medicinal chemistry over the past decade, yet for much of their history they remained a relatively neglected and underutilized functional group. The first sulfoximine to be identified, L-methionine-(*S*)-sulfoximine, was described in the 1950s as a potent and irreversible inhibitor of glutamine synthetase, and its profound biological activity highlighted the potential of this motif early on,[72, 73] which, however, did not translate into broad adoption in drug discovery.[74] The relative obscurity of sulfoximines has likely stemmed in part from synthetic limitations: traditional routes required hazardous oxidants or unstable intermediates, raising concerns for scalability and industrial application.[74, 75]

In recent years, however, interest in sulfoximines has undergone a remarkable resurgence. This renewed interest has been driven by two key developments: (i) the

advent of modern, safer, and more versatile synthetic methodologies, and (ii) the advancement of pioneering sulfoximine drug candidates into clinical trials.

1.5.1 Physiochemical properties of sulfoximines

A defining feature of the sulfoximine group is its tetrahedral sulfur atom, which is both constitutionally and configurationally stable.[76] Incorporation of a nitrogen atom at sulfur generates a stereogenic center, yielding configurationally stable, optically active isomers.[77] The ability to exploit stereochemistry is highly advantageous when targeting chiral biological macromolecules, where subtle differences in spatial arrangement can drive potency, selectivity, and differentiated pharmacology. By contrast with bioisosteric achiral sulfones, sulfoximines thus enable investigations on enantiomer-specific protein interactions and optimize target engagement (**Figure 1.5-1**).

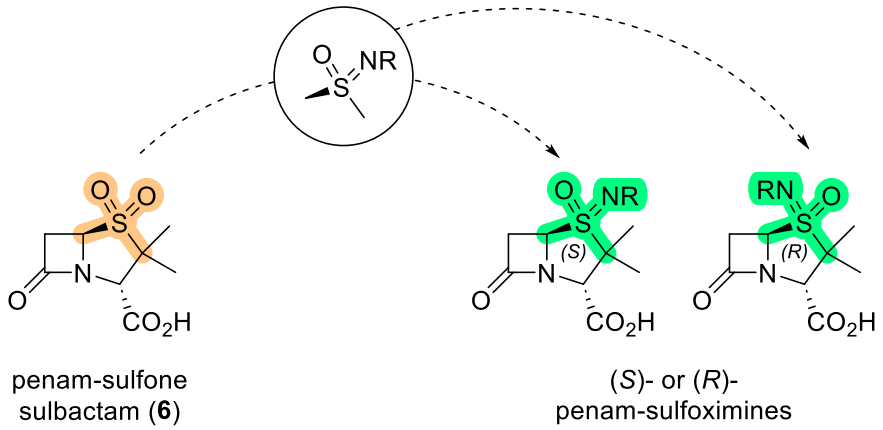

Figure 1.5-1. Replacement of sulfone (orange) of sulbactam with sulfoximine (green).

The unique hydrogen-bonding characteristics of sulfoximines are also important. Whereas sulfones function only as hydrogen-bond acceptors, unsubstituted *NH* sulfoximines combine donor and acceptor properties within a compact, metabolically stable unit.[78] The sulfur-bound oxygen and nitrogen atoms provide hydrogen-bond

acceptor sites, while the *NH* proton can act as a hydrogen-bond donor, enabling sulfoximines to engage in complex, directional hydrogen-bonding networks within a protein binding site.[75] This dual functionality expands the range of interaction motifs accessible in drug design and has been shown to enhance both affinity and selectivity.

Sulfoximines can also confer favorable physicochemical properties. Simple low-molecular-weight sulfoximines are notably soluble in protic solvents such as water and alcohols, a consequence of strong solvation around the sulfoximine moiety.[74] Improved aqueous solubility can mitigate one of the most persistent hurdles in drug development: poor bioavailability due to limited dissolution.[79] Beyond solubility, sulfoximines exhibit high chemical and metabolic stability, enabling compounds to withstand physiological and enzymatic environments.[80] This robustness contributes to improved pharmacokinetic profiles and longer duration of action, both of which are desirable for therapeutic candidates.

The nitrogen atom of sulfoximines provides additional opportunities for fine-tuning electronic and physicochemical behavior.[76] The group is mildly basic (p*K*a = 2.7 for NH_2^+ in water), permitting salt formation and metal coordination. The acidity of the *NH* proton is highly tunable depending on the *N*-substituent, ranging from p*K*a = 24 in DMSO (for R_3 = H) to 32 (for R_3 = Me), or 23 (for R_3 = tosyl) (**Figure 1.5-2**).[74, 76] This chemical flexibility enables precise control over ionization at physiological pH, allowing medicinal chemists to optimize membrane permeability, target engagement, and avoidance of off-target effects.

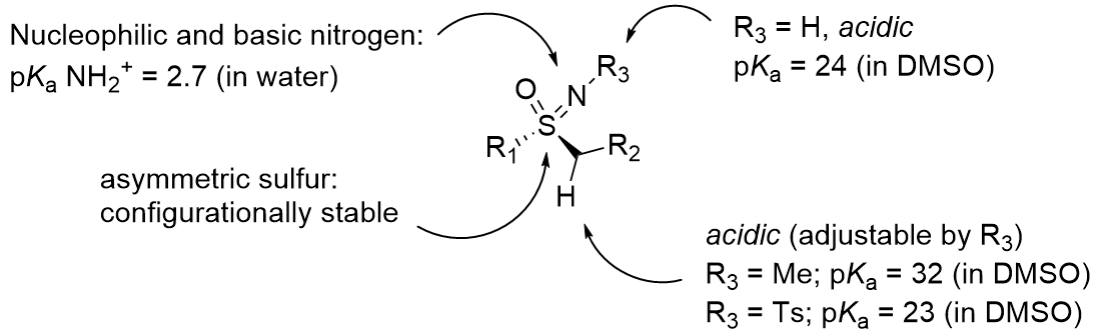

Figure 1.5-2. Chemical properties of sulfoximines.[74, 76]

Perhaps most striking is the bioisosteric versatility of sulfoximines. Sulfoximines have been successfully deployed as replacements for a wide range of functional groups, including sulfones, sulfonamides, and even non-sulfur motifs (*i.e.*, alcohols, acids, amidines).[74, 81]

1.5.2 Sulfoximine-containing drugs and clinical candidates

The first sulfoximine to enter human trials was roniciclib (BAY 1000394), a pan-cyclin-dependent kinase (CDK) inhibitor, which validated the feasibility of the scaffold in oncology (**Figure 1.5-3**).[82] Despite promising preclinical efficacy, development was discontinued after Phase II due to toxicity.[77] In an effort to improve selectivity and tolerability, Bayer subsequently developed atuveciclib (BAY 1143572), the first selective CDK9 inhibitor to reach the clinic, in which the sulfoximine group contributed to improved aqueous solubility and oral bioavailability.[83] Although clinical development was halted due to dose-limiting neutropenia, the program laid the foundation for enitociclib (BAY 1251152), a second-generation CDK9 inhibitor with improved pharmacological properties. Enitociclib, delivered intravenously, has demonstrated good tolerability and encouraging activity in hematologic malignancies and is in clinical evaluation.[84]

Another example is the ATR kinase inhibitor ceralasertib (AZD-6738) developed by AstraZeneca. Here, the replacement of a sulfone with a sulfoximine eliminated CYP3A4 inhibition and markedly improved solubility, enabling clinical development.[85] Ceralasertib is currently in multiple Phase II trials.[86]

Beyond applications in oncology, sulfoximines have also found application in antiviral drug design. IM-250, a helicase-primase inhibitor developed by Innovative Molecules for herpes simplex virus (HSV), incorporates a sulfoximine in place of a sulfonamide to reduce total polar surface area (TPSA), increase lipophilicity, and improve central nervous system (CNS) penetration. Preclinical studies demonstrated superior efficacy compared to the benchmark pritelivir, and IM-250 has progressed into early-stage clinical trials.[87]

These examples demonstrate the breadth of applications enabled by the sulfoximine functional group. In diverse chemical series, sulfoximines have contributed to improved physiochemical properties, enhanced pharmacokinetic performance, novel binding interactions, and reduced off-target liabilities. Their continued clinical advancement underscores their value as a versatile design element in contemporary medicinal chemistry.

Compound	Target / indication	Company	Clinical Stage	Role of Sulfoximine
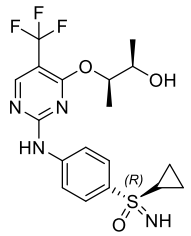 **Roniciclib**	Pan-CDK inhibitor (oncology)	Bayer	Phase II (discontinued)	Improved solubility, potency, reduced carbonic anhydrases (CAs) liabilities
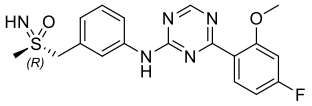 **Atuveciclib**	Selective CDK9 inhibitor (oncology)	Bayer	Phase I (discontinued)	Increased solubility, oral bioavailability, reduced CYP induction
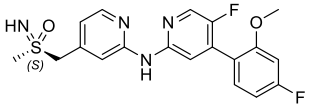 **Enitociclib**	CDK9 inhibitor (hematologic malignancies)	Bayer	Phase I/II (ongoing)	Excellent solubility (IV), improved selectivity and tolerability
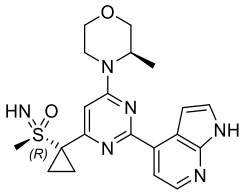 **Ceralasertib**	ATR kinase inhibitor (oncology)	AstraZeneca	Phase II (ongoing)	Replaced sulfone to improve solubility and avoid CYP3A4 inhibition
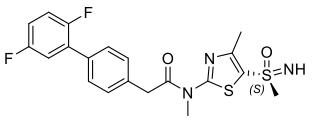 **IM-250**	HSV helicase-primase inhibitor (antiviral)	Innovative Molecules	Phase I (early clinical)	Replaced sulfonamide to reduce TPSA, increase lipophilicity, improve CNS penetration

Figure 1.5-3. Clinical candidates containing sulfoximines.

Beyond their expanding role in medicinal chemistry, sulfoximines have also found important applications in agrochemistry. The most prominent example of a sulfoximine containing agrochemical is sulfoxaflor, the first and only sulfoximine-based insecticide to reach the market, which was introduced by Dow AgroSciences in 2013 (**Figure 1.5-4**).[88] Sulfoxaflor acts as a systemic insecticide targeting nicotinic acetylcholine receptors, which disrupts synaptic transmission and causes rapid feeding cessation and insect death. Importantly, sulfoxaflor binds to receptor subtypes distinct from those targeted by neonicotinoids, enabling effective control of resistant sap-feeding pests such

as aphids, whiteflies, and planthoppers.[89] Its introduction has provided growers with a valuable alternative in integrated pest management, particularly in regions where resistance to older insecticide classes is widespread.

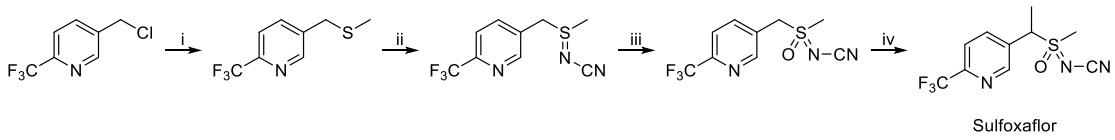

Figure 1.5-4. Synthesis of Sulfoxaflor. Reagents and conditions: (i): $NaSCH_3$, DMSO, 25 °C, 67%; (ii): H_2NCN, $PhI(OAc)_2$, CH_2Cl_2, 0 °C, 14%; (iii) *m*CPBA, K_2CO_3, $EtOH/H_2O$, 0 °C, 44%; (iv):, CH_3I, potassium hexamethyldisilazane (KHMDS), hexamethylphosphoramide (HMPA), THF, –78 °C, 59%.

Overall, sulfoximines represent a valuable addition to structure-activity relationship studies for medicinal chemistry and agrochemical purposes.

1.5.3 Classical synthetic approaches to sulfoximines

The first reported syntheses of sulfoximines in the 1960s were based on routes that introduced nitrogen and oxygen sequentially onto divalent sulfur. Two main pathways dominated these early developments: the sulfilimine pathway and the sulfoxide pathway. In the sulfilimine approach, sulfides were aminated to sulfilimines, which could then be oxidized to sulfoximines (**Figure 1.5-5, A-C**).[78] However, sulfilimines are intrinsically unstable, and this instability restricted the synthetic scope and limited their practical application.

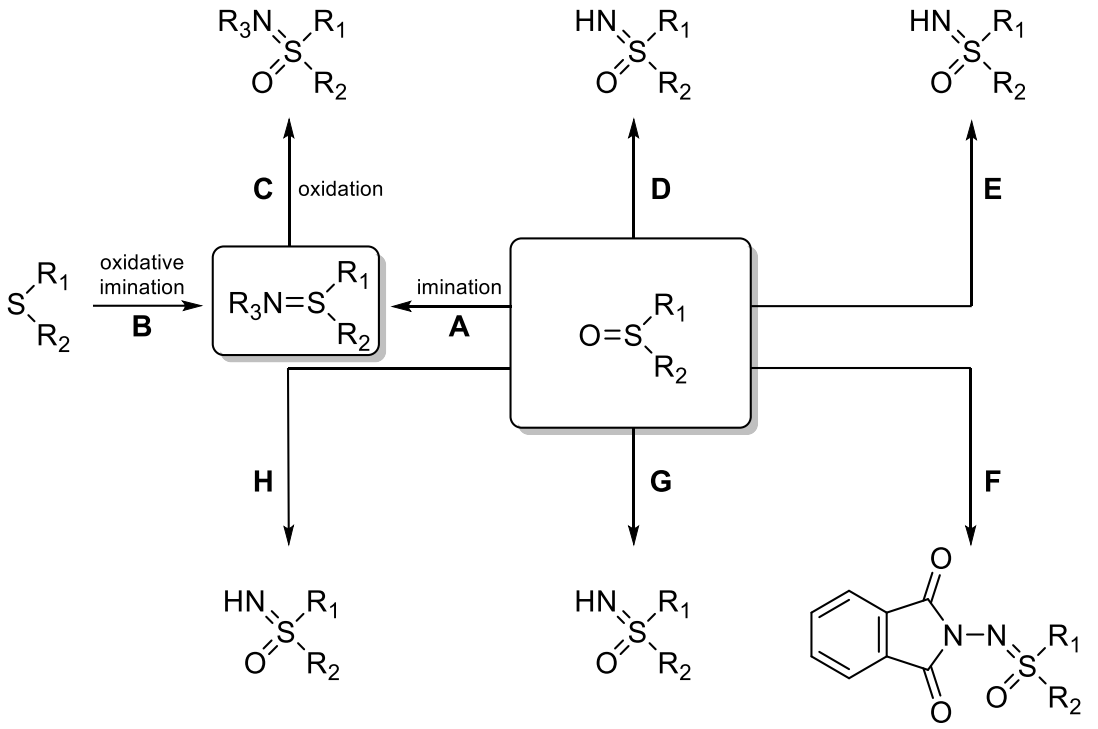

Figure 1.5-5. Classical synthetic routes to sulfoximines. Reagents and conditions: (**A**) $(TsN)_2S$, pyridine;[90] (**B**) *t*BuOCl, $Na^+{}^-NHCN$, Et_2O;[91] (**C**) *m*CPBA, CH_2Cl_2;[92] (**D**) NaN_3, P_2O_5, HSO_3CH_3;[93] (**E**) MSH, $NaOCH_3$, MeOH;[94] (**F**) $Pb(OAc)_4$, $PhthNH_2$, CH_2Cl_2;[95] or $PhthNH_2$, Pt anode, $NEt_3H^+OAc^-$, MeCN;[96] (**G**) $Rh_2(esp)_2$, DPH, TFE;[97] (**H**) NH_2COONH_4, $PhI(OAc)_2$, MeCN.[98]

The more established route involved oxidation of sulfides to sulfoxides, followed by imination. Historically, this *N*-transfer step required extremely hazardous reagents, the most notable being hydrazoic acid generated *in situ* from sodium azide and polyphosphoric acid (**Figure 1.5-5, D**).[99] While this transformation was effective, the explosive and toxic nature of hydrazoic acid posed major safety concerns. To address this, alternative nitrogen donors were introduced, including *O*-(mesitylenesulfonyl)hydroxylamine (MSH), but this reagent itself was shock-sensitive and unsuitable for scale-up (**Figure 1.5-5, E**).[100, 101] These drawbacks, combined with the need for protecting groups and subsequent deprotection steps, contributed to the long-standing neglect of sulfoximines in both academic and industrial settings.

One of the earliest oxidative approaches to sulfoximines involved the use of lead tetraacetate ($Pb(OAc)_4$). In these reactions, sulfoxides were subjected to oxidative conditions with lead tetraacetate, producing sulfoximines in moderate yields (**Figure 1.5-5, F**).[95] While effective, the method suffered from several drawbacks, including poor selectivity, stoichiometric use of toxic heavy-metal oxidants, and difficulty in handling. Environmental and safety concerns surrounding lead compounds further restricted the adoption of this strategy, and it was quickly overshadowed by other methodologies.

Efforts to circumvent these limitations led to the exploration of other strategies. One such method was electrochemical imination, in which *N*-phthalimido sulfoximines were electrolyzed at a platinum anode in methanol, using water as the proton source, to afford *NH*-sulfoximines in good yields (**Figure 1.5-5, F**).[96] This protocol, developed by Yudin and Siu, avoided the use of metal-based oxidants and hazardous reagents, offering a conceptually safer pathway. However, the requirement of specialized electrochemical setups limited its widespread application.

Transition-metal-catalyzed nitrene transfer represented another major advance. Richards and Ge reported a rhodium-catalyzed imination of sulfoxides using *O*-(2,4-dinitrophenyl)hydroxylamine (DPH) as the nitrogen source (**Figure 1.5-5, G**).[97] The reaction proceeded via a Rh–nitrene intermediate, enabling the stereospecific conversion of sulfoxides into *NH*-sulfoximines with retention of configuration at sulfur. Importantly, this strategy avoided the need for *N*-protection, demonstrated broad substrate scope, and tolerated diverse functional groups, including aryl, alkyl, and heteroaryl sulfoxides.

Further progress came from the use of hypervalent iodine reagents in combination with mild nitrogen sources. Luisi and Bull developed a direct metal-free *NH*-transfer from

sulfoxides using ammonium carbamate and iodobenzene diacetate (PIDA), delivering sulfoximines with complete retention of configuration (**Figure 1.5-5, H**).[98] Mechanistic studies indicated that reactive iminoiodinane or iodonitrene intermediates served as the active electrophiles (**Figure 1.5-6**).[98] This protocol was scalable, displayed excellent functional group tolerance, and was ultimately applied in the manufacturing of the ATR inhibitor AZD6738 (Ceralasertib).[85] The concept was later expanded to one-pot sequential *NH*/*O*-transfer to sulfides, enabling direct conversion of sulfides to sulfoximines in a single step.[102, 103]

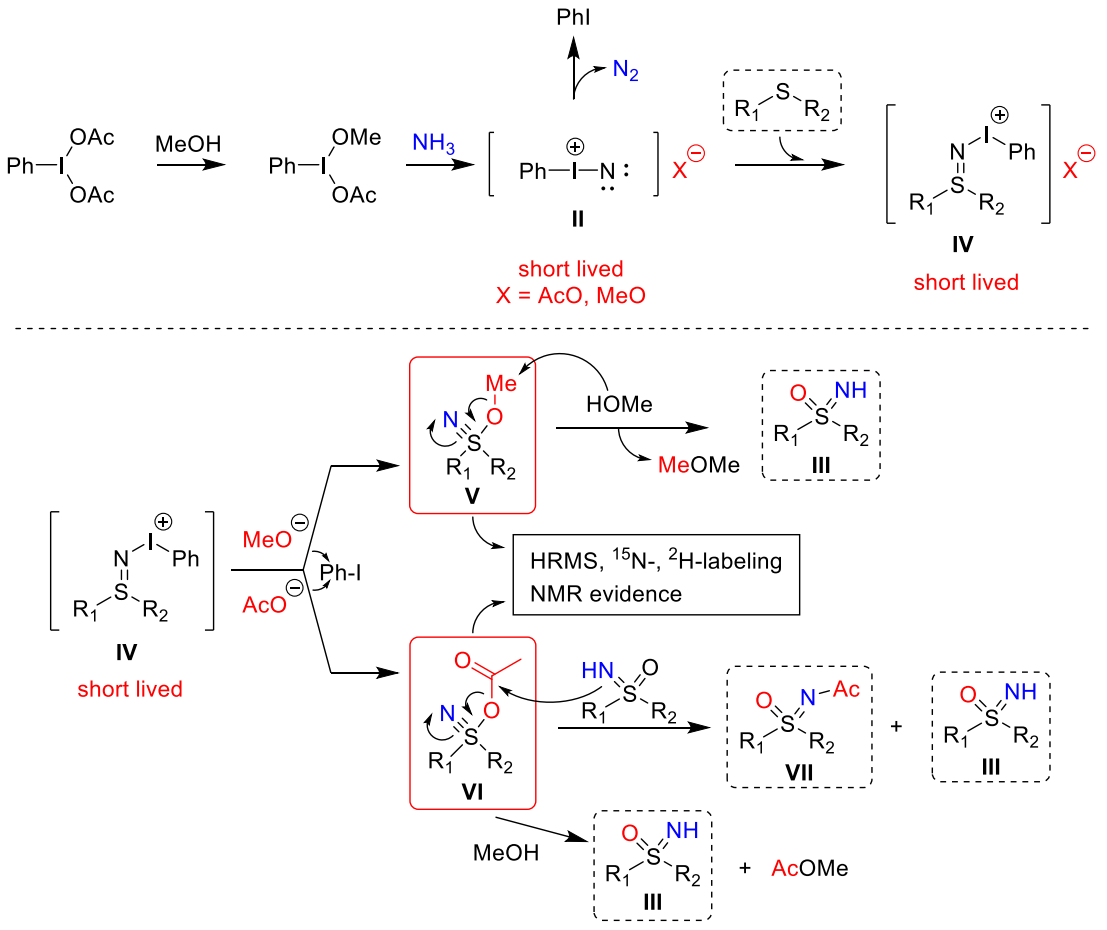

Figure 1.5-6. Mechanistic evidence for λ⁶-sulfanenitrile intermediates.[78] The short-lived iodonitrene **II** that reacts with the sulfide to generate the sulfilimine iodonium species **IV**. Futher attack of the methoxy or acetate anion to **IV** leads to **V** or **VI** respectively. Sulfanenitrile **V** may undergo nucleophilic attack producing dimethyl ether and the corresponding *NH*-sulfoximine **III**. Similarly, sulfanenitrile VI may behave as an acetylating agent reacting either with sulfoximine or methanol, leading to *N*-acyl sulfoximine **VII** and *NH*-sulfoximine **III**.[103]

In summary, classical synthetic routes to sulfoximines, whether via sulfilimine or sulfoxide intermediates, were restricted by instability, poor efficiency, and above all the hazardous nature of the nitrogen-transfer reagents. The exploration of electrochemical methods, transition-metal-catalyzed nitrene transfer (using DPH), and hypervalent iodine-mediated processes marked the transition toward modern, scalable, and safer methodologies. These advances transformed sulfoximines from chemical curiosities into synthetically viable motifs with clear utility in medicinal and agrochemical research.[98, 104-109]

1.6 Sulfoximines in β-lactam antibiotics

In the late 1970s, Pfizer reported work on the synthesis of the first sulfoximine derivatives on the penam scaffold featuring *N*-cyanamido (**13**) and *N*-phthalimido (**14**) substituted sulfoximines (**Figure 1.6-1**).[95, 110] Kemp and coworkers report that sulfoximine derivatives lacked antibacterial activity, likely as a consequence of the phthalimido protecting group in the case of **14** and chemical stability in the case of **13.**[95, 110]

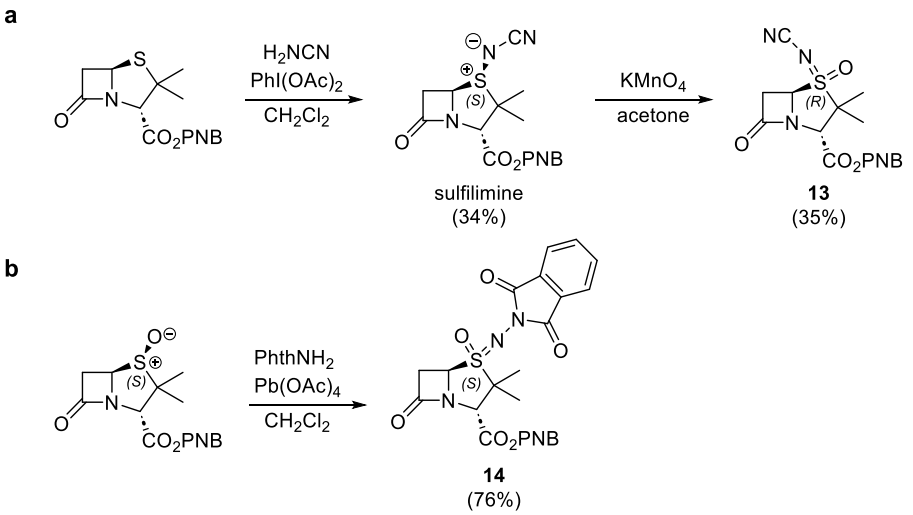

Figure 1.6-1. Reported synthesis of **a**) *N*-cyanamido sulfoximine (**13**) and **b**) *N*-phthalimido sulfoximine (**14**).[95, 110]

The lack of antibacterial activity, along with a lack of synthetic methodologies for sulfoximine diversification at the time, likely hindered further investigations of sulfoximine derivatives of sulbactam. Since the 1970s, advances in sulfoximine chemistry, however, may have greatly expanded their synthetic accessibility.[76, 111, 112] As medicinal chemistry increasingly demands functional groups that balance potency, safety, and pharmacokinetic performance, sulfoximines offer solutions not achievable with classical sulfones or sulfonamides. The continued exploration of sulfoximines is likely to yield both incremental and transformative advances in the design of next-generation therapeutics.

1.7 Objectives of the work described in this thesis

The overarching objective of this thesis is to explore sulfoximine substitution on the penam scaffold as a strategy to expand the chemical and biological properties of β-lactamase inhibitors. In particular, this work seeks to revisit sulbactam-derived scaffolds in light of modern sulfoximine chemistry, leveraging recent advances in nitrogen-transfer methodologies to access sulfoximine derivatives that were previously synthetically inaccessible. By replaying the sulfone motif of sulbactam with a sulfoximine, this thesis aims to systematically evaluate how this transformation influences stability, reactivity, and interactions with serine β-lactamases and bacterial targets.

A second key objective is to develop robust, scalable synthetic routes to penam sulfoximines and to characterize their biochemical and antibacterial activity, with a particular focus on clinically relevant enzymes and pathogens such as *Acinetobacter baumannii*. Through a combination of synthetic chemistry, enzymatic assays, and antibacterial testing, this work seeks to establish structure-activity relationships for

sulfoximine-containing penams and to assess their potential as a next-generation β-lactamase inhibitors or antibacterial agents. Collectively, these studies aim to provide fundamental insights into the utility of sulfoximines within β-lactam chemistry and to inform future inhibitor design against resistant Gram-negative bacteria.

Chapter 2 | Synthesis of Sulfoximine Derivatives of Sulbactam

2.1 Introduction

Pioneering studies on sulbactam sulfoximine derivatives were reported in the late 1970s, establishing that penam and cepham sulfoximines are, at least in principle, synthetically accessible.[110, 113] However, only a relatively limited number of penam/cepham sulfoximine derivatives were reported, bearing only cyanamido **13** or phthalimido **14** substituents at the sulfoximine nitrogen (**Figure 2.1-1**). This narrow scope likely reflects the restricted methodologies available at the time for sulfoximine synthesis and derivatization. Moreover, these early sulfoximine derivatives were noted to lack "useful" antibacterial activity, though no experimental details of the activity studies were provided. The absence of activity may stem from several factors, including reduced stability under physiological conditions due to high reactivity of the cyano group with nucleophiles such as water, or steric impediments introduced by the bulky *N*-substituents that hinder binding to SBLs and PBPs.

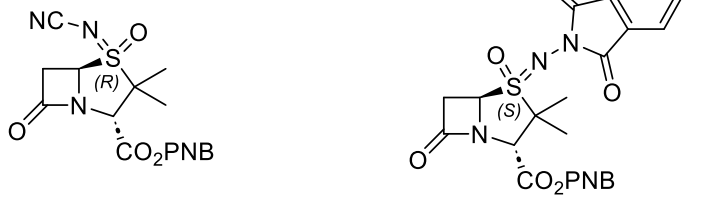

cyanamidosulfoximine (**13**) phthalimidosulfoximine (**14**)

Figure 2.1-1. Structures of previously synthesized penam sulfoximines **13** and **14**.[110, 113]

Despite these negative results, penam/cepham sulfoximine derivatives remain of significant interest, given the unique electronic and steric properties of the sulfoximine functional group, its capacity for diverse *N*-functionalization, and precedent as a bioisostere of sulfoxides, sulfones, and amides in bioactive molecules.[74, 81] It was envisaged that recent advances in synthetic methodology, particularly Rh(II)-catalyzed nitrene transfer reactions (**Section 1.5-3**, **Chapter 1**), would now enable direct and

efficient access to β-lactam sulfoximine derivatives, including those bearing free *NH* groups or readily modifiable substituents.[97, 98] These synthetic developments created new opportunities to systematically explore the chemistry and biological potential of penam-sulfoximines, a space that has remained uninvestigated since 1979.[110, 113]

This chapter describes studies leading to the synthesis of enantiopure (*S*)- and (*R*)-penam-sulfoximines using a Rh(II)-based catalytic system. It further describes the optimization and scope of the penam-sulfoximine formation reaction and its utility for preparation of *NH* penam sulfoximines. *NH* functionalization reactions at the sulfoximine nitrogen are subsequently described, including amide bond formation reactions, arylations, urea formation reactions, alkylation reactions, *N*-acyl carbonyl reductions, reductive aminations, and attempted Michael additions and Mitsunobu reactions. These studies establish both the opportunities and limitations of sulfoximine derivatizations of penams and provide a foundation for the future development of β-lactam sulfoximine derivatives as potential antibacterial agents. The initial target compounds were the (*S*)- and (*R*)-penam sulfoximine analogs of sulbactam (**6**) (**Figure 2.1-2**).

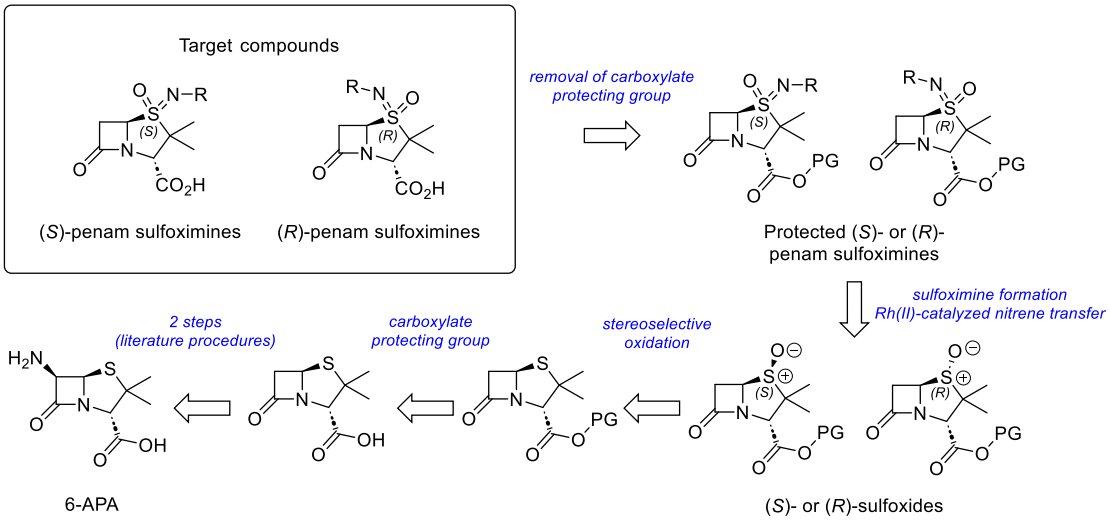

Figure 2.1-2. Retrosynthesis of target (*S*)- and (*R*)-penam sulfoximines.

2.2 Syntheses of penam (*S*)-sulfoximines

The penam (*S*)-sulfoxide **19** was synthesized as a single diastereomer in four steps from commercial 6-aminopenicillanic acid (6-APA, **15**) to assess its suitability as a starting material for the synthesis of the corresponding penam sulfoximine derivatives (**Scheme 2.2-1**). Following reported procedures, **15** was first converted into 6α-bromopenicillin[114] **16** which was subsequently protected with *para*-methoxybenzyl (PMB) bromide to afford the corresponding 6α-bromopenicillin ester **17**.[115] Reduction of the C-Br bond of **17** using tributylphosphane in methanol[116, 117] furnished the corresponding 6-dihydropenam **18**. In contrast to the literature, alternative reduction methods were not useful. Thus, reduction of **17** using zinc metal in acetic acid,[118] as well as the reduction of the corresponding 6,6-dibromopenam **24** with either magnesium metal in HCl[119, 120] or under radical conditions,[121, 122] failed to afford the desired product **18** in sufficient yield or purity. **18** was subsequently oxidized with *meta*-chloroperoxybenzoic acid (*m*CPBA) at -78 °C to yield (*S*)-sulfoxide **19** as a single isolated diastereomer.[110]

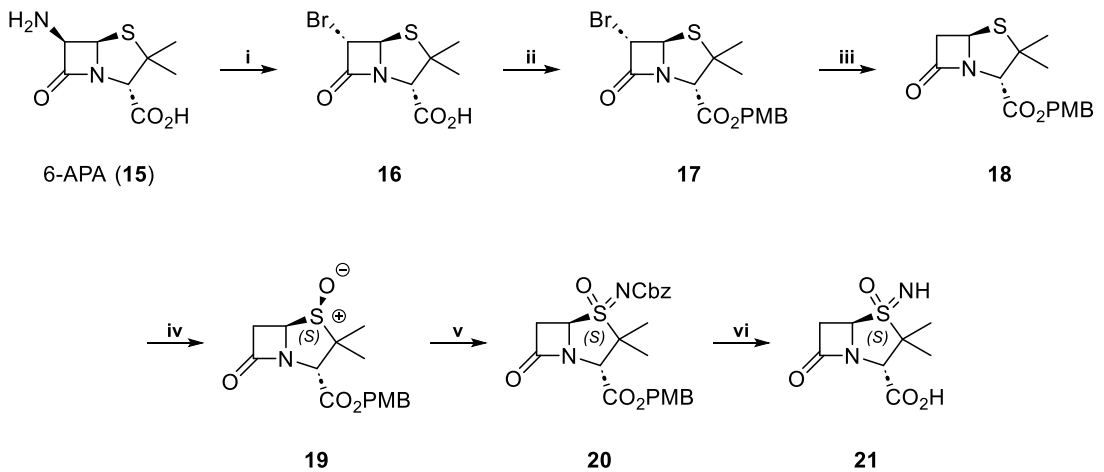

Scheme 2.2-1. Synthesis of penam (*S*)-sulfoximine **21**. Reagents and conditions: (i) HBr, $NaNO_2$, MeOH, H_2O, –15 °C to rt, 90%; (ii) PMB-Br, K_2CO_3, DMF, CH_2Cl_2, , 67–99%; (iii) P^nBu_3, MeOH, rt, 60–90%; (iv) *m*CPBA, CH_2Cl_2, –78 °C, 59–84%; (v) $CbzNH_2$, MgO, $PhI(OAc)_2$, $Rh_2(OAc)_4$ (5 mol%), dimethoxyethane, 40 °C, 64–95%; (vi) Pd/C, H_2, THF, rt, 70%.

Sulfoximine **20** was obtained under Rh(II)-catalyzed nitrene transfer conditions, and subsequent Pd/C-catalyzed hydrogenolysis afforded **21** without erosion of stereochemical integrity.

Performing the oxidation at higher temperatures, such as 0 °C and 20 °C, resulted in 8:1 and 4:1 mixtures of the (*S*):(*R*)-sulfoxides **19**:**25**, respectively. The stereochemical outcome of this reaction is proposed, at least in part, to results from the hydrogen bonding interaction between the **19** *C7* carbonyl and the peroxide of *m*CPBA forcing the sulfoxide to preferentially attack from the concave face (**Figure 2.2-2**). Notably, oxidation of **17** prior to bromine reduction, also provided the (*S*)-sulfoxide **18b** as a single diastereomer.

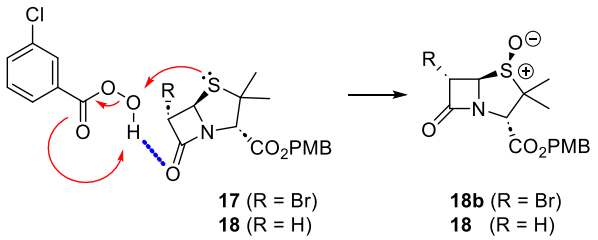

17 (R = Br)
18 (R = H)

18b (R = Br)
18 (R = H)

Figure 2.2-2. Stereoselective oxidation of **17** and **18** with *m*CPBA.

2.2.1 Syntheses of penam (*R*)-sulfoximines

The diastereomeric (*R*)-sulfoxide **25** was synthesized as a single isolated diastereomer in four steps from 6-APA (**15**). Thus, according to reported procedures, 6-APA (**15**) was converted into 6,6-dibromopenam **22** (**Scheme 2.2-2**).[123] Oxidation of **23** with *m*CPBA furnished the (*R*)-sulfoxide **24** as a single isolated diastereomer. The stereochemical outcome of this reaction is attributed to the relatively bulky bromine substituents at the *C6* position of **24**, which sterically directs *m*CPBA to preferentially approach from the less hindered convex face. Formation of sulfoximine **26** was achieved via Rh(II)-catalyzed nitrene transfer, albeit in lower yield, which is attributed to steric hinderance on the concave face of the molecule. Subsequent deprotection of

26 under hydrogenolysis conditions was unsuccessful, as will be discussed further in **Chapter 3**.

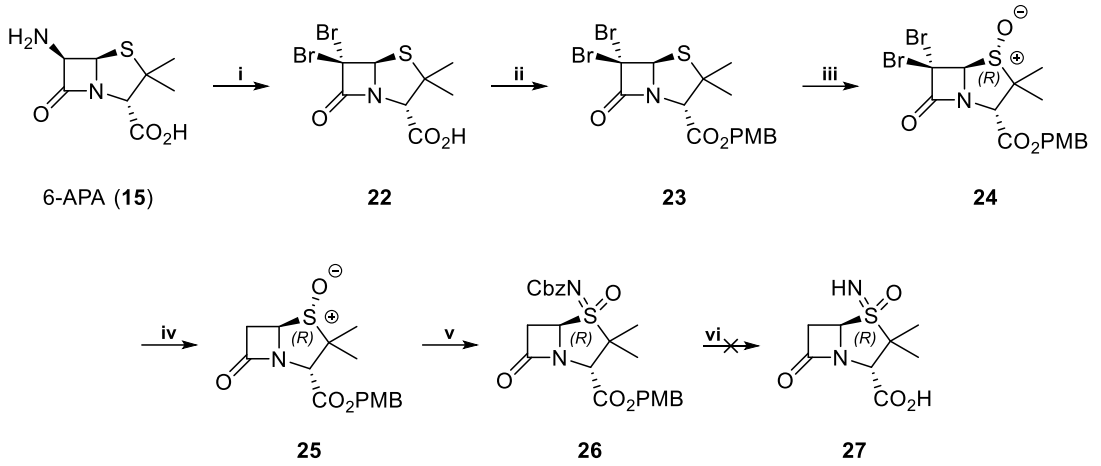

Scheme 2.2-2. Synthesis of penam (*R*)-sulfoximine **27**. Reagents and conditions: (i) Br_2, H_2SO_4, $NaNO_2$, CH_2Cl_2, H_2O, 0–10 °C to rt, 68%; (ii) PMB-Br, K_2CO_3, DMF, CH_2Cl_2, 40 °C, 90%; (iii) *m*CPBA, CH_2Cl_2, –78 °C, 80%; (iv) P^nBu_3, MeOH, rt, 99%; (v) H_2NCbz, MgO, $PhI(OAc)_2$, $Rh_2(OAc)_4$ (5 mol%), dimethoxyethane, 40 °C, 52%; (vi) Pd/C, H_2, THF, rt.

2.3.1 Optimization of the penam-sulfoximine formation reaction

The sulfoximine forming reaction was first evaluated with the commercially sourced (*S*)-sulfoxide **28** and benzyl carbamate as substrates employing conditions previously reported for synthesis of thietane 1-oxide-derived *N*-Boc sulfoximine (*i.e.* $BocNH_2$, MgO, diacetoxyiodobenzene ($PhI(OAc)_2$), and $Rh_2(OAc)_2$ in dichloromethane at 40 °C).[124] The desired sulfoximine **29** was obtained, however, the isolated chemical yield was relatively low (<50%) (**Scheme 2.3-1**).

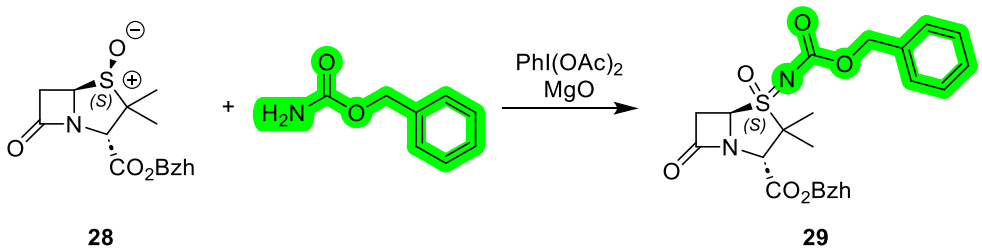

Scheme 2.3-1. Sulfoximine formation of **29**. Reagents and conditions: H_2NCbz, $PhI(OAc)_2$, MgO, $Rh_2(OAc)_4$, CH_2Cl_2, 40 °C, 16 h, 42%.

The sulfoximine forming reaction was then systematically optimized by evaluating the effects of solvent, reaction temperature, reagent concentration, and catalyst choice (**Table 2.3-2**). The results revealed that optimal turnover of sulfoxide **28** to give sulfoximine **29** can reproducibly be achieved using $Rh_2(OAc)_4$ as the catalyst in 1,2-dimethoxyethane (DME) (0.2 M) at 40 °C (**Table 2.3-2**, **entry xii**).

Entry	Estimated Conversion	Solvent	Temperature	Catalyst (5 mol%)	Concentration
i	52%	DCM	20 °C	$Rh_2(Oac)_4$	0.2 M
ii	27%	CH_3CN	20 °C	$Rh_2(Oac)_4$	0.2 M
iii	44%	1,4-Dioxane	20 °C	$Rh_2(Oac)_4$	0.2 M
iv	58%	THF	20 °C	$Rh_2(Oac)_4$	0.2 M
v	59%	DCE	20 °C	$Rh_2(Oac)_4$	0.2 M
vi	66%	Toluene	20 °C	$Rh_2(Oac)_4$	0.2 M
vii	75%	DME	20 °C	$Rh_2(Oac)_4$	0.2 M
viii	61%	Toluene	20 °C	$Rh_2(Oac)_4$	0.3 M
ix	74%	DME	20 °C	$Rh_2(Oac)_4$	0.3 M
x	80%	Toluene	40 °C	$Rh_2(Oac)_4$	0.2 M
xi	77%	Toluene	60 °C	$Rh_2(Oac)_4$	0.2 M
xii	87%	DME	40 °C	$Rh_2(Oac)_4$	0.2 M
xiii	69%	DME	60 °C	$Rh_2(Oac)_4$	0.2 M
xiv	19%	DME	40 °C	$Rh_2(O_2CCF_3)_4$	0.2 M
xv	5%	DME	40 °C	$Rh(C_8H_{12})_2\ BF_4$	0.2 M
xvi	54%	DME	40 °C	$Rh_2(esp)_2$	0.2 M
xvii	19%	DME	40 °C	$Rh_2(TPA)_4$	0.2 M

Table 2.3-2. Optimization of the penam sulfoximine-forming reaction. a) Benzyl carbamate (1.5 equiv.), PhI(Oac)2 (1.5 equiv.), MgO (2 equiv.). b) The percentage conversion was estimated by comparing the integrals of characteristic ^1H NMR signals of the starting material to those of the desired product in the crude reaction mixture.

2.3.2 Scope of the penam-sulfoximine forming reaction

The scope of the optimized sulfoximine forming reaction with respect to both the penam substrate and nitrene precursor was next investigated, with the aim of obtaining a set of structurally diverse penam sulfoximine derivatives for structure activity relationship studies. The results reveal that carbamates including the *tert*-butyl and methyl carbamate (**30a** and **30b**) were suitable nitrene precursors under the optimized conditions (**Figure 2.3-3**). The allyl carbamate was not an efficient substrate, likely due to catalyst poisoning and/or aziridine formation. It was envisaged that the sulfonamides (**30c**, **30d**) and sulfamates (**30e**) could substitute for carbamates in the sulfoximine formation reaction, substantially expanding the substrate scope of the accessible sulfoximines. Ureas, hydroxylamines, and hydrazines were not suitable nitrene precursors for sulfoximine formation with the penam substrate (**Figure 2.3-3**).

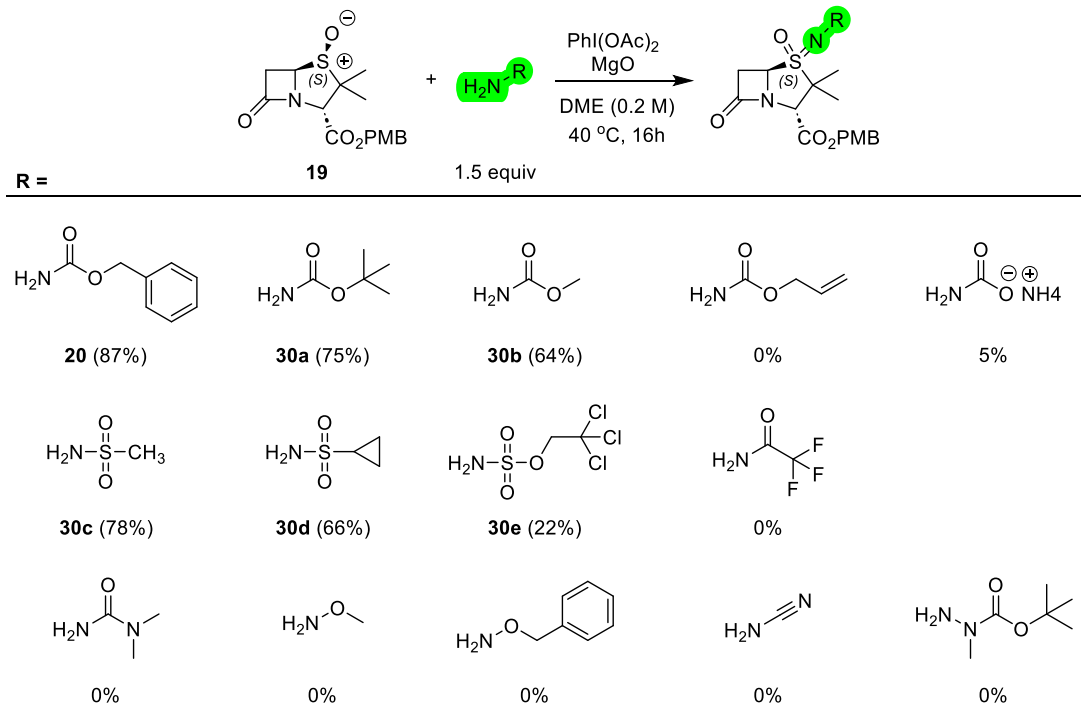

Figure 2.3-3. Substrate scope of the penam-sulfoximine formation reaction. The percentages represent isolated yield.

2.4 Synthesis of penam *NH*-sulfoximine 32

Penam sulfoximine **32** with an unprotected *NH* group was an attractive synthesis target because of its potential to serve as a starting material for subsequent sulfoximine *NH* functionalization and because its structure closely resembles that of sulbactam; thus it can serve as a model to investigate the effect of substituting one of the sulbactam sulfone oxo ligands by an imine ligand on inhibition potency and selectivity.

Synthesis of sulfoximine **32** from sulfoxide **19** was attempted in a single step using a reported protocol for the synthesis of tetrahydrothiophene 1-sulfoximine which employs *O*-(2,4-dinitrophenyl)hydroxylamine (DPH) as the nitrene precursor and $Rh_2(esp)_2$ as a catalyst.[125] Although ^{1}H NMR analysis of the crude reaction mixture revealed formation of sulfoximine **32** under these conditions, **32** could not be separated from DPH-derived byproducts. To circumvent the problems associated with the use of DPH for the synthesis of **32**, DPH was substituted by ammonium carbamate.[98] Sulfoximine **32** was obtained from **19** under the reported catalyst-free conditions, which employed $PhI(OAc)_2$ as a stoichiometric oxidant, in ~50% conversion as indicated by ^{1}H NMR analysis of the crude reaction mixture. However, conversion could not be improved and the unreacted starting material **19** could not be separated form sulfoximine **32** via silica column chromatography.

As sulfoximine **32** could not be synthesized from sulfoxide **19** in one step, an efficient two-step protocol to synthesize **32** was developed. The Cbz-protected sulfoximine **20** was subjected to hydrogenation using 10% (w/w) palladium on carbon (0.6 equiv.) as a catalyst; under these conditions, the Cbz group of **20** was selectively removed in the presence of the PMB ester to afford **32** in 52% yield following purification by column chromatography **(Figure 2.4-1**). The unreacted Cbz-protected sulfoximine **20** was recovered following purification with 40% yield.

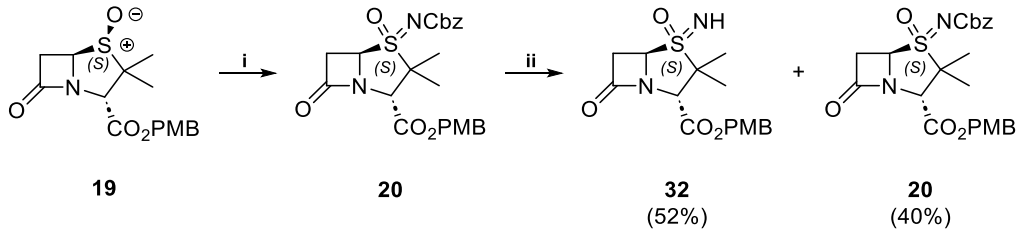

Figure 2.4-1. Synthesis of *NH*-sulfoximine **32** from sulfoxide **19**. Reagents and conditions: (i) $CbzNH_2$, MgO, $PhI(OAc)_2$, $Rh_2(OAc)_4$ (5 mol%), dimethoxyethane, 40 °C, 87%; (ii) H_2, Pd/C, THF, rt, 52%.

Crystallographic analysis of a single crystal of penam *NH*-sulfoximine **32** revealed retention of stereochemistry during sulfoximine formation (**Figure 2.4-2**).

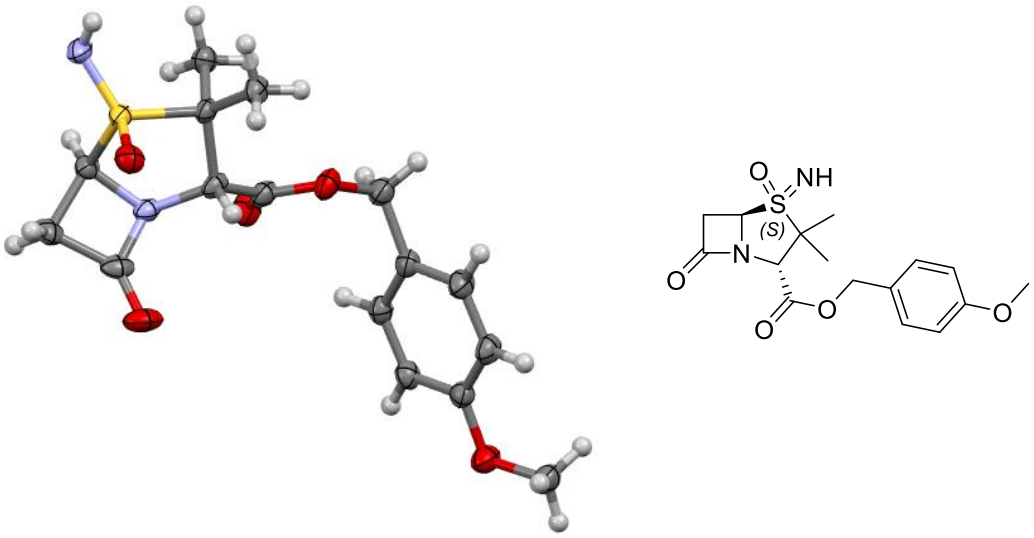

Figure 2.4-2. Crystal structure of penam (*S*)-sulfoximine **32**. Crystallographic analysis of a single crystal of 4-methoxybenzyl (*2S*,*4S*,*5R*)-4-imino-3,3-dimethyl-7-oxo-4λ^6-thia-1-azabicyclo[3.2.0]heptane-2-carboxylate 4-oxide (**32**) confirms its structural assignment based on ^{1}H and ^{13}C NMR, IR, MS, and $[\alpha]_D^{25}$ analysis. Analysis of the Flack parameter[126] supports the assignment of the sulfur-configuration as (*S*). Color code: white: hydrogen; gray: carbon; blue: nitrogen; red: oxygen; yellow: sulfur. Select crystallographic data are shown in **Appendix 7.1**.

2.5 Penam *NH* sulfoximine functionalization

Functionalized of the *NH* group of **32** was achieved using: (i) amide bond forming reactions with either acyl chlorides or carboxylic acids and 1-ethyl-3-(3-dimethylaminopropyl)carbodiimide hydrochloride (EDCI) as a coupling reagent,[127]

(ii) Cu(II)-catalyzed Chan-Evans-Lam type cross-coupling with boronic acids,[128-130] and (iii) urea formation with aryl and alkyl isocyanates.[131]

2.5.1 Amide bond forming reactions

Amide bond forming reactions with the penam *NH* sulfoximine **32** as the substrate proved to be a reliable and versatile transformation. Treatment of **32** with either acid chlorides (**33a-d**) or carboxylic acids (**33e-f**) furnished the corresponding sulfoximine amides in moderate to excellent yields (57-99%, **Figure 2.5-1**). When acid chlorides were employed, acylation in the presence of catalytic 4-(dimethylamino)pyridine (DMAP) (5 mol%) and triethylamine (TEA) gave the desired products **33a-d** in consistently high yields ranging from 77-99%. In contrast, coupling of carboxylic acids using 1-ethyl-3-(3-dimethylaminopropyl)carbodiimide hydrochloride (EDCI) and DMAP afforded amides **33e-f** in somewhat diminished yields (57-62%). The methodology tolerated both aliphatic and aromatic carboxylic acid substituents with minimal variation in efficiency across substrates. Vinyl-substituted acyl derivative **33c** was also accessible, highlighting the broad functional group compatibility of this approach (**Figure 2.5-1**).

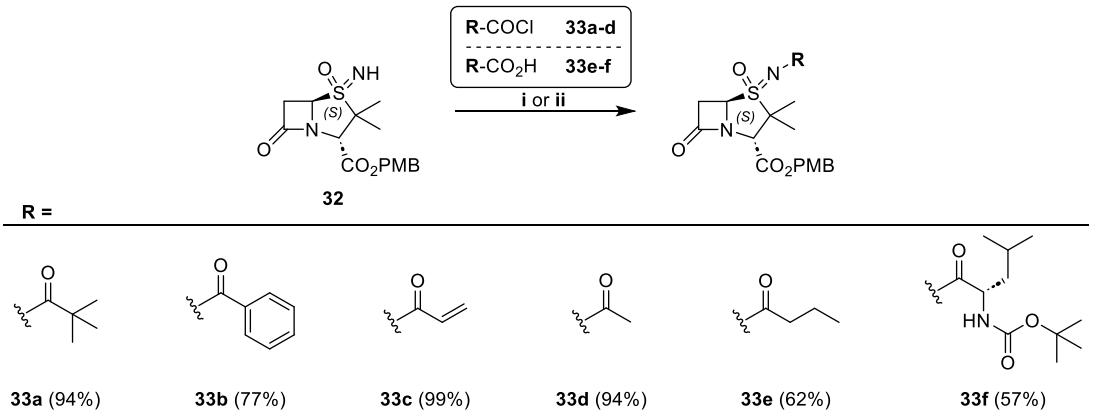

Figure 2.5-1. Amide bond forming reactions with *NH*-sulfoximine **32**. Reagents and conditions: (i) acid chloride (**33a-d**), 4-dimethylaminopyridine (DMAP)[132] (5 mol%), triethylamine, CH_2Cl_2, 0 °C to rt, 77–

99%; (ii), carboxylic acid (**33e-f**), 1-ethyl-3-(3-dimethylaminopropyl)carbodiimide hydrochloride (EDCI)[133], DMAP[134], CH_2Cl_2, 0 °C to rt, 57–62%.

These results establish that penam *NH*-sulfoximines undergo efficient amidation under standard amide bond forming conditions, enabling access to a diverse range of acylated derivatives. This transformation provided a robust platform for further exploration of structure-activity relationships in the sulfoximine series.

2.5.2 Arylation of 32

The *NH* group of sulfoximine **32** was subjected to Cu(II)-catalyzed Chan-Evans-Lam[128-130] coupling with aryl boronic acids under mild conditions in methanol at room temperature (**Figure 2.5-2**), as reported for non-penam types of sulfoximines.[135]

The reaction proceeded with only modest efficiency, with isolated yields ranging from 9-28%, but nonetheless provided access to a small library of *N*-aryl derivatives (**Figure 2.5-2**). A variety of electronically diverse aryl boronic acids **35a-g**, including electron-donating, electron-withdrawing, and halogen substituents, were tolerated. Despite the relatively low conversions, this study demonstrated the feasibility of *N*-arylation in the penam sulfoximine series. The ability to incorporate diverse aromatic groups onto the sulfoximine nitrogen offers an additional handle for structural diversification.

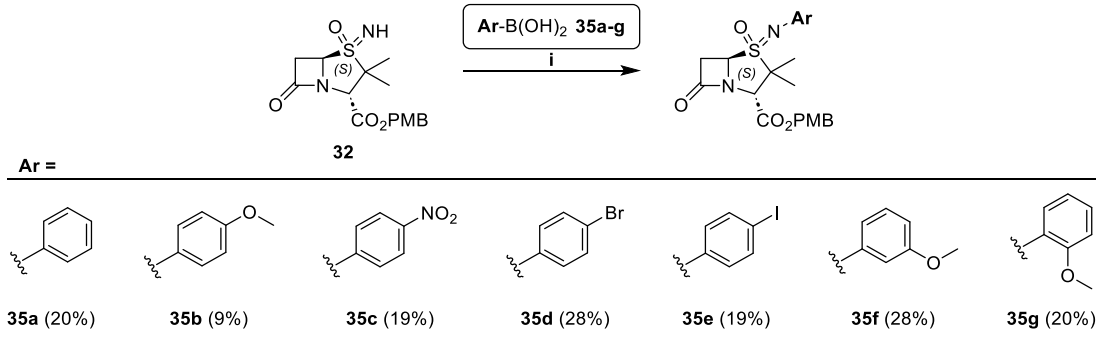

Figure 2.5-2. Arylation of *NH*-sulfoximine **32**. Reagents and conditions: (i) boronic acid (**35a-g**), $Cu(OAc)_2$ (10 mol%), MeOH, rt.

2.5.3 Urea formation

Sulfoximine **32** was employed in a urea formation reaction with a broad set of isocyanates (**36a-s**) in the presence of TEA and catalytic DMAP[132] (**Figure 2.5-3**). This transformation proceeded under mild conditions to afford the corresponding *N*-sulfoximine ureas in variable yields ranging from 9–67%. The scope included both aliphatic and aromatic isocyanates **36a-s** that a large set of urea-functionalized penam-sulfoximine derivatives can be accessed through this route, providing an additional avenue for modulation physiochemical and biological properties of the sulfoximine scaffold.

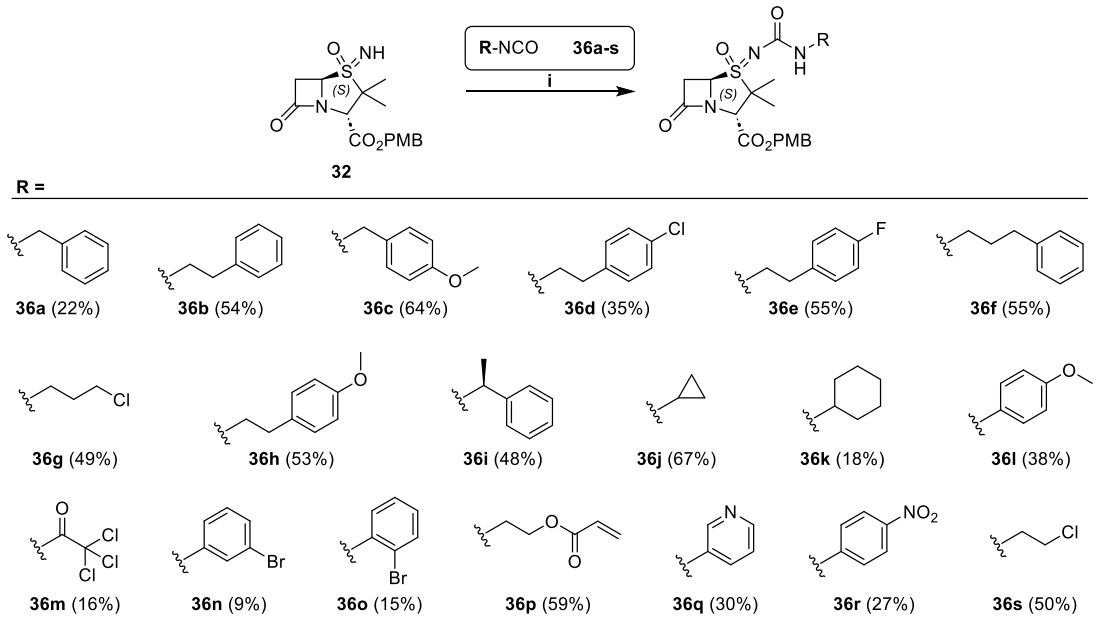

Figure 2.5-3. Scope of urea forming reactions with *NH*-sulfoximine **32**. Reagents and conditions: (i) R-NCO (**36a-s**), DMAP[132] (10 mol%), triethylamine, CH_2Cl_2, 0 °C to rt.

2.5.4 Investigations on *NH*-alkylation of penam-sulfoximine 32

Initial efforts to alkylate *NH* sulfoximine **32** focused on adapting literature procedures that had proven effective for simpler, non-penam sulfoximine derivatives. However, the reported conditions were incompatible with the penam core, which is highly sensitive to both bases and elevated temperatures. A range of alkylating reagents,

bases, temperatures, and solvents were screened in attempts to functionalize the *NH* group of sulfoximine **32** (**Figure 2.5-4**).

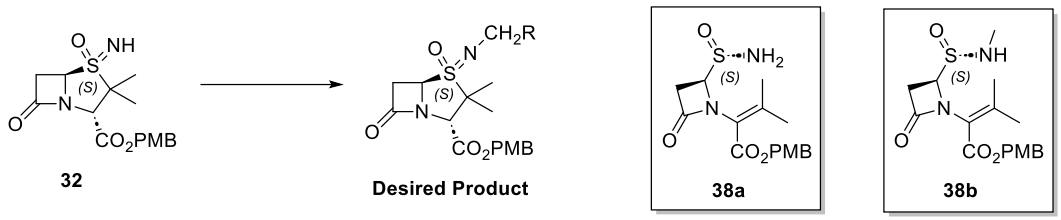

Entry	Alkylating Agent	Base	Temperature	Solvent	Result
i	CH_3I	K_2CO_3	0 – 25 °C	DMF	Degradation of **32**
ii	CH_3I	DIPEA	0 – 25 °C	THF	No reaction
iii	CH_3I	NaH	0 – 25 °C	THF	Degradation of **32**
iv	CH_3I	DBU	0 – 25 °C	THF	Degradation of **32**
v	CH_3I	TEA	25 – 40 °C	THF	No reaction
vi	$PhCH_2Br$	KO^{t}Bu	25 °C	THF	Conversion to **38a**
vii	$PhCH_2OTf$	DIPEA	20 °C	DCM	No reaction
viii	$PhCH_2OTf$	DIPEA	40 °C	DCM	No reaction
ix	Me_2SO_4	Barton's base[136]	25 °C	THF	Degradation of **32**
x	Me_2SO_4	Barton's base[136]	0 °C	THF	Degradation of **32**
xi	Me_2SO_4	DIPEA	25 °C	THF	No reaction
xii	Me_2SO_4	DIPEA	40 °C	THF	Degradation of **32**
xiii	Me_2SO_4	LHMDS	0 °C	THF	Conversion to **38a**
xiv	Me_2SO_4	KO^{t}Bu	0 °C	THF	Conversion to **38a**
xv	Me_2SO_4	LHMDS	-78 °C	THF	Conversion to **38a**
xvi	Me_2SO_4	KO^{t}Bu	-78 °C	THF	Conversion to **38a**
xvii	$(CH_3)_3SiCHN_2$	-	25 °C	THF	Conversion to **38b**

Figure 2.5-4. Investigations on *NH* alkylation of sulfoximine **32.**

The results revealed that standard alkylating agents including methyl iodide (CH_3I) and methyl sulfate (Me_2SO_4), also in combination with bases like potassium carbonate (K_2CO_3), sodium hydride (NaH), 1,8-diazabicylo(5,4,0)undec-7-ene (DBU), triethylamine (TEA), or *N*,*N*-diisopropylethylamine (DIPEA), either led to no reaction or decomposition of the starting material. Milder conditions using DIPEA or TEA with CH_3I showed no conversion, while stronger bases like NaH and DBU resulted in

degradation of **32**. Interestingly, in the presence of bulky, non-nucleophilic bases like potassium *tert*-butoxide (KO^{t}Bu) and lithium bis(trimethylsilyl)amide (LHMDS), **32** degraded to sulfinamide **35a**, as observed by ^{1}H NMR analyses (**Figure 2.5-5**). The ^{1}H NMR analysis was consistent with the formation of a single diastereomer of **35a**; note, however, that the configuration of the sulfinamide was tentatively assigned as (*S*), based on the configuration of the sulfur stereocenter of **32**, which was assigned by crystallography.

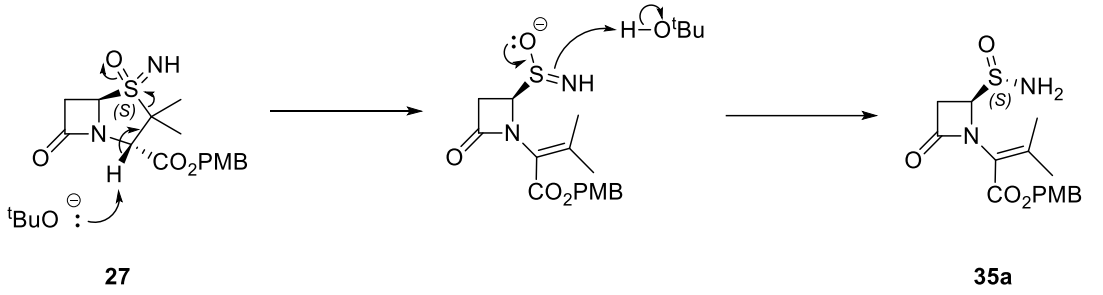

Figure 2.5-5. Proposed base-mediated degradation pathway of *NH* sulfoximine **27** to sulfinamide **35a**.

Interestingly, treatment of **32** with trimethylsilyl diazomethane under neutral conditions with no added base at room temperature resulted in the formation of the methylated sulfinamide **38b**. It is currently unclear whether methylation of the *NH* sulfoximine or ring opening of the thiazolidine ring occurs first.

2.5.5 Investigations on the reduction of penam *N*-acyl sulfoximine carbonyl

Since attempts for the direct alkylation of *NH* sulfoximine **32** were unsuccessful, an alternative approach in which the *N*-acyl sulfoximine carbonyl group would be reduced to a methylene group was explored (**Figure 2.5-6**). While this strategy has been reported for non-penam sulfoximines, the presence of the β-lactam raised concerns about chemoselectivity.[137]

A range of borane-based reducing agents was investigated, including BH_3·THF, BH_3·DMS, and catecholborane, across a range of temperatures. In all cases, the desired reduction product was not obtained. At low to ambient temperatures, the starting *N*-acyl sulfoximine (**28d**) did not react with BH_3·THF, while reactions with BH_3·DMS and catecholborane led to decomposition. Elevating the reaction temperature to 40 °C did not improve outcomes, and still resulted in no productive reaction. These studies indicate that reduction of the *N*-acyl sulfoximine motif in the penam framework is highly challenging under standard borane-mediated conditions. The incompatibility likely arises from competing reactivity at the strained β-lactam carbonyl and the overall instability of the penam scaffold under reducing conditions.

28d

Entry	Reducing Agent	Temperature	Solvent	Result
i	BH_3·THF	0 – 25 °C	THF	No reaction
ii	BH_3·THF	40 °C	THF	No reaction
iii	BH_3·DMS	0 – 25 °C	THF	Degradation of **28d**
iv	Catecholborane	0 – 25 °C	THF	Degradation of **28d**

Figure 2.5-6. Investigations on the attempted reduction of penam *N*-acyl sulfoximine carbonyl.

2.5.6 Investigations on reductive amination of the penam *NH*-sulfoximine 32

Attempts to functionalize the *NH* group of sulfoximine **32** through reductive amination were unsuccessful (**Figure 2.5-7**). Several aldehyde reactants were tested in combination with sodium triacetoxyborohydride (STAB) or sodium cyanoborohydride ($NaBH_3CN$) as reducing regents, under conditions commonly employed for reductive amination.[131, 138]

The lack of reactivity may be due to the failure of the sulfoximine *NH* to undergo condensation with the aldehyde to form the corresponding imine intermediate, a prerequisite for subsequent reduction. Although anhydrous solvents were employed to minimize water-promoted reversibility of imine formation, no evidence of imine intermediates or reduced products was detected. This observation suggests that the intrinsic acidity and reduced nucleophilicity of the sulfoximine *NH* prevents productive engagement in the condensation step even when employing reactive electron deficient aldehydes (*i.e.*, *para*-nitrobenzaldehyde).

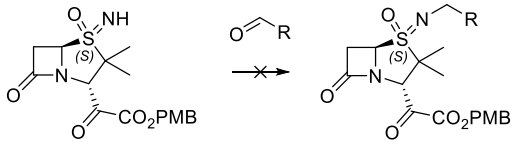

32

R group	Reaction Conditions	Result
	STAB (1.5 equiv.) in DCE 25 – 40 °C, 16 h	No reaction
	STAB (1.5 equiv.), AcOH (cat.) in DCE/THF 25 – 40 °C, 16 h	No reaction
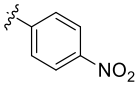	STAB (1.5 equiv.), AcOH (cat.) in DCE/THF 25 – 40 °C, 16 h	No reaction
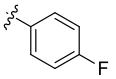	$NaBH_3CN$ (1.5 equiv.), AcOH (cat.) in DCE/THF 25 – 40 °C, 16 h	No reaction

Figure 2.5-7. Investigations on the reductive amination of sulfoximine **32**.

These findings indicate that reductive amination, a transformation that is well-precedented for amines, does not readily extend to penam *NH*-sulfoximines, further underscoring the challenges associated with derivatization of *NH*-sulfoximines in this reactive scaffold.

2.5.7 Investigations on Michael additions with the penam *NH*-sulfoximine 32

The 1,4-conjugate (Michael) addition of nitrogen nucleophiles to activated alkenes is a well-established method for C–N bond formation, particularly in the context of imides, sulfonamides, and related *NH* functionalities.[139] In these reactions, nucleophiles add to the β-position of an α,β-unsaturated carbonyl compound, typically following deprotonation of the *NH* or activation of the Michael acceptor by a Lewis acid.

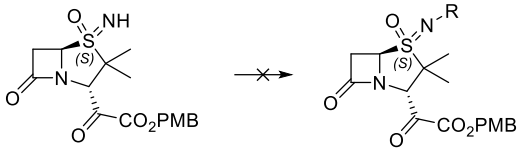

32

Substrate	Reaction Conditions	Result
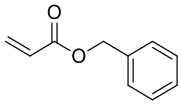	MeCN 25 – 40 °C, 16 h	No reaction
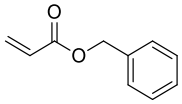	$AlCl_3$ (0.1 equiv.) in MeCN 25 – 40 °C, 16 h	No reaction
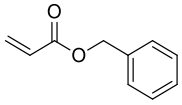	$BF_3 \cdot Et_2O$ (0.1 equiv.) in MeCN 25 – 40 °C, 16 h	No reaction
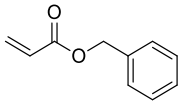	$ZnCl_2$ (0.1 equiv.) in MeCN 25 – 40 °C, 16 h	No reaction
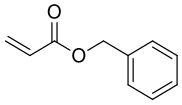	TEA (2 equiv.) in MeCN 25 – 40 °C, 16 h	No reaction
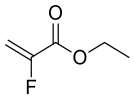	$AlCl_3$ (0.1 equiv.) in MeCN 25 – 40 °C, 16 h	No reaction
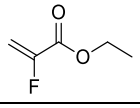	$BF_3 \cdot Et_2O$ (0.1 equiv.) in MeCN 25 – 40 °C, 16 h	No reaction
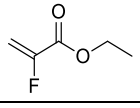	$ZnCl_2$ (0.1 equiv.) in MeCN 25 – 40 °C, 16 h	No reaction
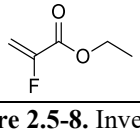	TEA (2 equiv.) in MeCN 25 – 40 °C, 16 h	No reaction

Figure 2.5-8. Investigations on the Michael addition of sulfoximine **32**.

To evaluate this strategy for sulfoximines, benzyl acrylate was first examined in acetonitrile under a range of activating conditions. The use of $BF_3 \cdot Et_2O$ (0.1 equiv.) was intended to enhance electrophilicity of the acrylate through carbonyl coordination,[140] while $AlCl_3$ (0.1 equiv.) was investigated as a stronger Lewis acid expected to provide greater activation. $ZnCl_2$ (0.1 equiv.) was tested as a milder Lewis acid that has precedent in promoting conjugate additions of weak nitrogen nucleophiles,[140] and triethylamine (2 equiv.) was employed to generate the deprotonated sulfoximine anion under basic conditions. Across these variations, reactions conducted at room temperature and at 40 °C failed to give the desired Michael adducts, instead returning unreacted starting material (**Figure 2.5-8**).

2.5.8 Investigations on Mitsunobu reactions with sulfoximine 32

The Mitsunobu reaction is a well-established method for converting alcohols into a wide range of derivatives through the nucleophilic substitution of an activated oxyphosphonium intermediate.[141] Classically, the reaction couples an acidic *NH* or *OH* nucleophile (*e.g.*, imides, sulfonamides, hydantoins, phenols, carboxylic acids) with an alcohol in the presence of a phosphine and an azo agent, *e.g.* diethyl azodicarboxylate (DEAD) or diisopropyl azodicarboxylate (DIAD). The success of this transformation relies on the relatively low pK_a of the nucleophile, which facilitates deprotonation and subsequent attack on the activated alcohol species. Given that sulfoximine N-H groups can possess acidity comparable to imides and sulfonamides, in principle they represent viable candidate for Mitsunobu-type functionalization.

To evaluate the Mitsunobu strategy, attempts were made to functionalize the penam-sulfoximine *NH* with both isopropyl alcohol and benzyl alcohol under standard Mitsunobu conditions.[141] A variety of reagent and solvent combinations were

examined, including DIAD and bis(4-chlorobenzyl) (*E*)-diazene-1,2-dicarboxylate (DCAD) as azo reagents; triphenylphosphine (PPh_3), tricyclohexylphosphine (PCy_3), and tributylphosphine (P_nBu_3) as phosphines, as well as; THF or acetonitrile as solvents. The reactions were initiated at 0 °C, warmed up to ambient temperature, and in some cases further heated to 40 °C. In addition, triethylamine was tested as an additive to promote sulfoximine *NH* deprotonation (**Figure 2.5-9**).

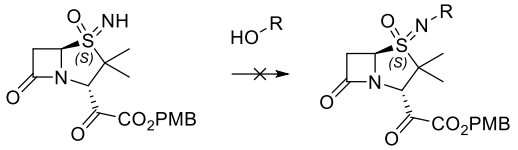

32

R group	Reaction Conditions	Result
	DIAD (1.1 equiv.), PPh_3 (1.1 equiv.) in THF 25 – 40 °C, 16 h	No reaction
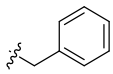	DIAD (1.1 equiv.), PPh_3 (1.1 equiv.) in MeCN 25 – 40 °C, 16 h	No reaction
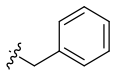	DCAD (1.1 equiv.), PPh_3 (1.1 equiv.) in MeCN 25 – 40 °C, 16 h	No reaction
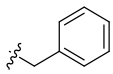	DIAD (1.1 equiv.), PCy_3 (1.1 equiv.) in MeCN 25 – 40 °C, 16 h	No reaction
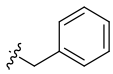	DIAD (1.1 equiv.), P_nBu_3 (1.1 equiv.) in MeCN 25 – 40 °C, 16 h	No reaction
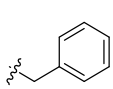	DIAD (1.1 equiv.), PPh_3 (1.1 equiv.), TEA (1 equiv.) in MeCN 25 – 40 °C, 16 h	No reaction

Figure 2.5-9. Investigations on Mitsunobu reactions with sulfoximine **32**.

The results revealed that, despite the broad range of conditions employed, no desired *N*-alkylated sulfoximine product was obtained. Instead, reactions either returned starting material or produced complex mixtures of by-products. These results suggest that, unlike related imide or sulfonamide substrates, sulfoximine *NH* groups, at least on the penam scaffold, do not undergo efficient Mitsunobu coupling, likely due to the lack of acidity of the *NH*-sulfoximine proton.

2.6 Summary

This chapter described the efficient synthesis of (*S*)- and (*R*)-penam sulfoximines via Rh(II)-catalyzed nitrene transfer and examined the scope of this methodology across a range of penam-sulfoximine derivatives. Access to the *NH* sulfoximines enabled systematic evaluation of its reactivity, revealing both successful and unsuccessful strategies for *N*-functionalization: amide bond formation, arylation, and urea formation were identified as reliable transformations, whereas reductive aminations, Michael additions, Mitsunobu[141] reactions, and direct alkylations were unsuccessful under the conditions tested. These findings underscore the distinct reactivity profile of the sulfoximine moiety within the penam framework, where conventional approaches to *NH* derivatization often prove ineffective.

Sulbactam sulfoximine derivatives bearing different sulfoximine *N*-substituents, including aryl, carbonyl, sulfonyl, formate, and formamide groups (**Figure 2.3-2**, **2.5-1**, **2.5-2**, **2.5-3**), were efficiently synthesized in 6-8 steps from commercial 6-APA (**Figure 2.2-1**), providing a diverse compound set for biochemical and biological testing.

Chapter 3 | Deprotection of Penam- and Cephem-sulfoximines

3.1 Introduction

Sulfoximines have recently emerged as valuable functional motifs in medicinal chemistry, offering a versatile alternative to sulfones by providing an additional stereogenic center, expanded hydrogen-bond capacity, and tunable polarity and stereoelectronic properties.[76, 77] When incorporated into β-lactam antibiotic scaffolds, sulfoximines present an opportunity to modulate physicochemical properties and potentially alter interactions with PBPs and/or SBLs. However, introduction and manipulation of sulfoximines within β-lactam frameworks pose significant synthetic challenges, arising from the inherent reactivity of the strained β-lactam ring and the sensitivity of the sulfur (VI) functionality to acidic, basic, and reductive conditions.

The *C2*-carboxylate of β-lactam antibiotics plays a pivotal role in both chemical reactivity and biological activity and is therefore a mandatory functional group in compounds intended for antibacterial evaluation.[10] During the synthesis of penam- and cephem-based sulfoximines, however, protection of this carboxylate is essential to enable multistep functionalization of the sulfur center. Conventional ester cleavage methods typically rely on strongly acidic, basic, or nucleophilic conditions, all of which readily promote β-lactam ring opening. In sulfoximine-containing systems, these challenges are further compounded by the potential for metal coordination ,redox processes, or catalyst poisoning, complicating the selective unveiling of the free acid at late stages of synthesis.

This chapter focuses on identifying carboxylate protecting groups and deprotection conditions compatible with β-lactam sulfoximines. Initial studies examine the penam (*S*)-sulfoximine series as a model system, systematically evaluating commonly employed *C2* protecting groups – including benzhydryl, *p*-nitrobenzyl, biphenyl methyl, and *p*-methoxybenzyl esters – under representative hydrogenolytic, acidic, and

basic deprotection conditions. These experiments were designed to probe the intrinsic stability of penam-sulfoximines toward ester cleavage and to establish conditions that enable selective liberation of the free carboxylic acid without compromising β-lactam integrity.

Building on these findings, the scope of the study was extended to (*R*)-configured penam-sulfoximines to assess the influence of sulfoximine stereochemistry on deprotection efficiency and stability. Finally, the cephem scaffold was investigated to determine whether reduced ring strain and altered electronics relative to penams could expand the accessible deprotection window. Multiple protecting groups and cleavage strategies were evaluated in the cephem series to define the structural and chemical limits of sulfoximine-containing β-lactams.

Collectively, this work establishes key structure-stability relationships governing the protection and deprotection of β-lactam sulfoximines. By directly comparing penam and cephem systems, this chapter reveals a pronounced divergence in chemical robustness between the two scaffolds and identifies protecting group strategies that enable reliable access to stable penam-sulfoximine free acids, while highlighting the intrinsic instability of the corresponding cephem analogues.

3.2 Deprotection of penam (*S*)-sulfoximines

With the *C2* carboxylate necessarily protected during sulfoximine installation, its selective deprotection represents a key late-stage transformation in the synthesis of penam sulfoximines. To identify protecting groups compatible with this scaffold, a series of commonly employed C2 esters were systematically evaluated using representative (S)-configured penam-sulfoximine substrates. Benzhydryl, *para*-nitrobenzyl (PNB), biphenyl methyl, and *para*-methoxybenzyl (PMB) esters were

examined under standard ester-cleavage conditions, including catalytic hydrogenolysis, acidolysis, and basic methanolysis. Reaction outcomes were assessed in terms of deprotection efficiency, substrate stability, and integrity of the β-lactam core, enabling direct comparison of protecting group performance across a consistent reaction framework.

3.2.1 Benzhydryl ester cleavage

Benzhydryl esters are commonly employed as protecting groups during synthesis of β-lactam antibiotics/SBL inhibitors because they can, in principle, be removed under different orthogonal conditions, including using catalytic hydrogenolysis with catalytic Pd, strong Brønsted acids in presence of arene scavengers, transfer hydrogenation in formic acid, or basic alcoholysis.[142-145] In the case of penam-sulfoximine derivatives, this strategy was expected to permit late-stage unveiling of the *C2* carboxylate under conditions that would avoid prolonged heating, aqueous workups, or basic alcoholysis. To evaluate this approach, four standard protocols for benzhydryl ester cleavage were trialed using representative penam-sulfoximine substrates. These conditions comprised: (i) catalytic hydrogenolysis using H_2 and Pd/C in methanol/THF (3 h),[142] (ii) acidolysis with trifluoroacetic acid (TFA) in presence of phenol at room temperature (30 min),[143] (iii) solvolysis in formic acid at 40-50 °C,[144] and (iv) basic methanolysis with 1 M NaOH in methanol at room temperature.[145]

Catalytic hydrogenolysis did not result in ester cleavage, and only starting material was recovered within 3 h. In contrast, exposure to acidic (TFA/phenol, formic acid) or basic (NaOH/MeOH) conditions led to rapid decomposition of the substrate (**Figure 3.2-1**). This degradation is most plausibly attributed to acid- or base-catalyzed hydrolysis of the β-lactam ring, which proceeds more rapidly than benzhydryl ester

cleavage under these conditions. As a result, no free acid product could be obtained in preparative yields.

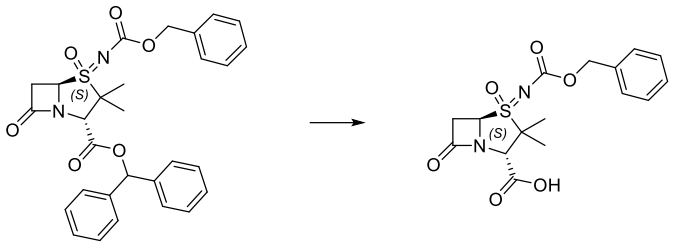

29

Entry	Conditions	Result
i	H_2, Pd/C (0.2 equiv.) in MeOH/THF; RT	Only SM after 3h
ii	TFA in phenol; RT	Degradation of **29**
iii	Formic acid; 40 °C	Degradation of **29**
iv	1 M NaOH in MeOH; RT	Degradation of **29**

Figure 3.2-1. Benzhydryl ester cleavage of **29**.

These results demonstrate that benzhydryl esters may be incompatible with penam-sulfoximine scaffolds, as the typical deprotection protocols are either ineffective or promote β-lactam degradation (**Figure 3.2-1**). Subsequent efforts therefore focused on alternative ester protecting groups amenable to removal under neutral or otherwise non-degrading conditions. However, it is possible that the result of the deprotection reaction is scale dependent and that benzhydryl esters are of use when performing the reaction not on a laboratory scale.

3.2.2 *p*-Nitrobenzyl ester cleavage

Next, the PNB ester **42a** was evaluated as a protecting group for the *C2* carboxylate. PNB esters are widely used in β-lactam antibiotics/SBL inhibitors because they can be selectively removed under mild reductive conditions, most commonly by catalytic hydrogenolysis, while remaining stable to a broad range of acidic and basic transformations.[146] Catalytic hydrogenolysis of the PNB group typically proceeds via

reduction of the nitro moiety to an aniline intermediate, followed by rapid benzylic cleavage.[147]

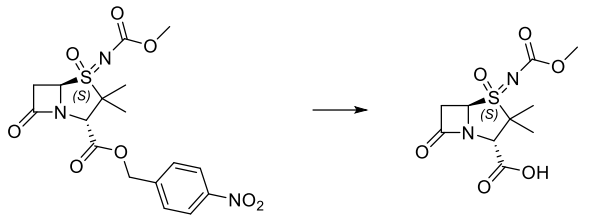

42a **31b**

Entry	Pd/C (equiv.)	Solvent	Result
i	0.2	THF	Full conversion to **31b** with slight degradation
ii	0.2	EtOAc	Full conversion to **31b** with slight degradation
iii	0.2	MeOH	Degradation of **31b**

Figure 3.2-2. *p*-Nitrobenzyl ester hydrogenation of **42a**.

Hydrogenolysis of sulfoximine **42a** was performed under an atmosphere of H_2 using Pd/C (0.2 equiv.) at room temperature in different solvents (**Figure 3.2-2**). In THF, full conversion to the desired free acid **31b** was achieved, though accompanied by trace levels of decomposition. A similar outcome was obtained in ethyl acetate, where **31b** formed cleanly with formation of trace decomposition by-products. In contrast, when methanol was employed as a solvent, extensive degradation occurred and no product was obtained.

The instability observed under methanolic conditions likely arises after PNB removal, as the liberated β-lactam sulfoximine acid is potentially unstable in protic, nucleophilic media. Following hydrogenolysis, methanol can cause β-lactam ring opening, while the *in-situ* formation of *p*-aminobenzyl species from nitro reduction may further accelerate decomposition through nucleophilic or base-catalyzed attack.

These results demonstrate that PNB esters are compatible with mild hydrogenation conditions, provided that aprotic solvents are used. THF and ethyl acetate represent

suitable media for selective deprotection, whereas protic solvents such as methanol lead to rapid degradation of the acid product **31b**.

3.2.3 Biphenyl methyl ester cleavage

The biphenyl methyl ester **46a** was next investigated as *C2* carboxylate protecting groups. The biphenyl methyl moiety was selected because, like PNB esters, it can be removed under hydrogenation conditions but is generally more resistant to side reactions during multi-step synthesis.

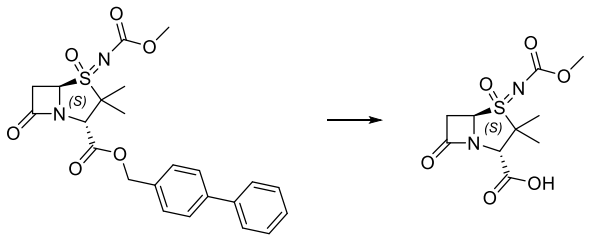

Entry	Pd/C (equiv.)	Solvent	Result
i	0.2	THF	Full conversion to **31b** after 16 h
ii	0.2	EtOAc	Full conversion to **31b** after 8 h
iii	0.2	MeOH	Full conversion to **31b** after 3 h with degradation

Figure 3.2-3. Biphenyl methyl ester hydrogenation of **46a**.

Hydrogenolysis of sulfoximine **46a** was performed under an atmosphere of H_2 using Pd/C (0.2 equiv.) at room temperature in various solvents (**Figure 3.2-3**). In all cases, conversion to the corresponding free acid **31b** was achieved as observed by ^{1}H NMR, though the rate and product purity, however, depended strongly on solvent. In THF, complete conversion was observed after 16 h, whereas in ethyl acetate, full deprotection of **46a** to give **31b** was achieved within 8 h. In methanol, cleavage of **46a** occurred rapidly (3 h) but was accompanied by trace levels of decomposition.

These results indicate that biphenyl methyl esters are a viable protecting group for penam-sulfoximine derivatives, permitting efficient deprotection under mild hydrogenation conditions. However, solvent polarity and nucleophilicity strongly influence both the reaction kinetics and product stability. Aprotic solvents such as THF and ethyl acetate afford cleaner reactions at slower rates, while methanol accelerates hydrogenolysis but promotes partial degradation, likely through nucleophilic opening of the β-lactam ring following ester cleavage.

3.2.4 *p*-Methoxybenzyl ester cleavage

The PMB ester **30b** was next evaluated as a protecting group for the *C2* carboxylate. PMB esters are frequently employed in β-lactam and peptide chemistry because they can be selectively removed under mild hydrogenolytic conditions. The electron-donating methoxy substituent stabilizes the benzylic cation formed during cleavage, facilitating smooth deprotection while minimizing side reactions.

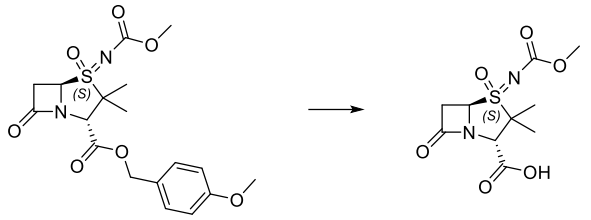

30b **31b**

Entry	Pd/C (equiv.)	Solvent	Result
i	0.2	THF	Full conversion to **31b** after 3 h
ii	0.2	EtOAc	Full conversion to **31b** after 3 h
iii	0.2	MeOH	Full conversion to **31b** after 3 h with degradation

Figure 3.2-4. *p*-Methoxybenzyl ester hydrogenation of **30b**.

Hydrogenolysis of sulfoximine **30b** was carried out under an atmosphere of H_2 using Pd/C (0.2 equiv.) at room temperature in THF (**Figure 3.2-4**). Under these conditions,

complete conversion to the free acid **31b** was achieved within 3 h with no detectable degradation. Analysis by ^{1}H NMR confirmed clean formation of the desired product, and no by-products were observed.

These results identify PMB esters as highly effective protecting groups for penam-sulfoximine derivatives. In contrast to benzhydryl, *p*-nitrobenzyl, and biphenyl methyl esters, the PMB ester was removed efficiently and selectively under mild hydrogenation conditions, yielding the desired carboxylic acid without compromising β-lactam integrity.

3.2.5 Summary of ester deprotection strategies

A comparative evaluation of benzhydryl, PNB, biphenyl methyl, and PMB esters as protecting groups for the *C2* carboxylate of penam-sulfoximines revealed marked differences in their suitability for penam-sulfoximine deprotection (**Figure 3.2-1 – 3.2-4**). The benzhydryl ester **29** proved unsuitable due to its resistance to hydrogenolysis and susceptibility to acid- and base-catalyzed degradation of the β-lactam ring. Similarly, the PNB ester **42a** underwent efficient hydrogenolysis in aprotic solvents but was prone to decomposition in methanol, likely due to β-lactam ring opening following generation of nucleophilic aniline byproducts. Biphenyl methyl ester **46a** displayed improved stability and clean hydrogenolysis in THF and ethyl acetate, although prolonged reaction times were required and minor degradation was observed in protic solvents.

In contrast, the PMB ester **30a** exhibited superior performance, undergoing complete and selective cleavage under mild hydrogenolytic conditions without compromising the integrity of the β-lactam. The electron-donating methoxy substituent is likely to

facilitate benzylic cleavage while avoiding undesired formation of byproducts like aniline that could cause degradation of the desired free acid.

Collectively, these results establish the PMB ester as the most effective protecting group for the *C2* carboxylate of penam-sulfoximines. This protecting group was therefore adopted for all subsequent analogs and late-stage transformations.

3.3 Penam-sulfoximine salts

The free acid forms of penam-sulfoximine derivatives were found to be relatively unstable. When stored at room temperature, these compounds degraded rapidly, and ^{1}H NMR analysis even revealed 20% degradation after one week of storage at –20 °C. The instability is likely a result of autocatalytic degradation of the β-lactam ring. The free carboxylate can protonate the β-lactam carbonyl, activating it to acid-catalyzed hydrolysis even under nominally mild storage conditions. This phenomenon has been observed previously for related β-lactam scaffolds and underscores the difficulty of handling the free acid form of such compounds.[148]

To improve stability, efforts were directed toward isolating the compounds as alkali metal salts. The free acids were dissolved in ethyl acetate and stirred with sodium 2-ethylhexanoate or potassium 2-ethylhexanoate for 15 minutes.[146] After solvent removal *in vacuo*, the salts were precipitated with diethyl ether and isolated by filtration, affording the corresponding sodium and potassium salts in good yield. Importantly, these salts exhibited markedly enhanced stability as also reported to be the case with sulbactam itself[38]: when stored at –10 °C, no significant degradation was detected by ^{1}H NMR analysis after more than six months.

These results demonstrate that conversion of penam-sulfoximine free acids into their corresponding sodium or potassium salts represents an effective strategy to mitigate

instability during storage and handling and provides a practical means of maintaining compound integrity for subsequent biological evaluation.

3.4 Deprotection of the penam (*R*)-sulfoximines

The deprotection of (*R*)-penam-sulfoximines was next investigated using the PMB-protected sulfoximine **26** as a representative substrate. Based on the success of PMB ester hydrogenolysis for the corresponding (*S*)-sulfoximine series, similar conditions were anticipated to afford the free *NH* sulfoximine **48** and, upon extended hydrogenation, the corresponding *C2* carboxylic acid **27**.

Initial hydrogenolysis was performed under an atmosphere of H_2 with Pd/C as a catalyst at room temperature, varying solvents and catalyst loadings (**Figure 3.4-1**). However, surprisingly, under standard conditions (0.2 equiv. Pd/C, THF), no reaction was observed after 3h, and only starting material was recovered. In ethyl acetate, partial conversion (20%) to the free *NH* sulfoximine **48** was obtained. The substrate was not soluble in methanol, precluding evaluation under these conditions.

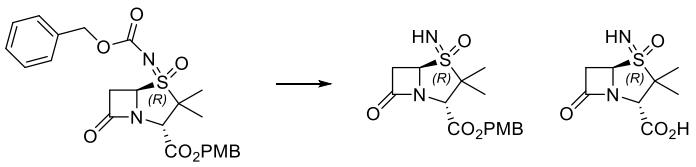

26 **48** **27**

Entry	Pd/C (equiv.)	Solvent	Result
i	0.2	THF	Only **26** after 3 h
ii	0.2	EtOAc	80% **26**, 20% **48** after 3 h
iii	0.2	MeOH	**26** not soluble in MeOH
iv	1.3	THF	85% **26**, 15% **48** after 8 h
v	1.3	EtOAc	45% **26**, 55% **48** after 8 h
vi	3.0	EtOAc	80% **26**, 20% **48** and degradation after 3 h

Figure 3.4-1. Hydrogenation of (*R*)-sulfoximine **26**. Percentages are estimated based on crude ^{1}H NMR mixtures comparing SM to products.

Higher catalyst loadings were investigated next because formation of the free *NH* sulfoximine **48** could potentially poison the catalyst through coordination to palladium. Increasing the catalyst loading to 1.3 equiv. in THF led to modest conversion (15%) to **48** after 8 h, whereas in ethyl acetate, conversion improved to approximately 55%. Further increasing Pd/C to 3.0 equiv. in ethyl acetate did not enhance the outcome and instead resulted in partial decomposition after 3 h (**Figure 3.4-1**).

These results indicate that deprotection of (*R*)-configured penam-sulfoximines proceeds significantly less efficiently than for the (*S*)-diastereomers under comparable conditions. The reduced reactivity may arise from stereoelectronic effects that alter accessibility of the sulfoximine substituent to the catalyst surface, or from coordination of the sulfoximine nitrogen to palladium, inhibiting hydrogen activation.

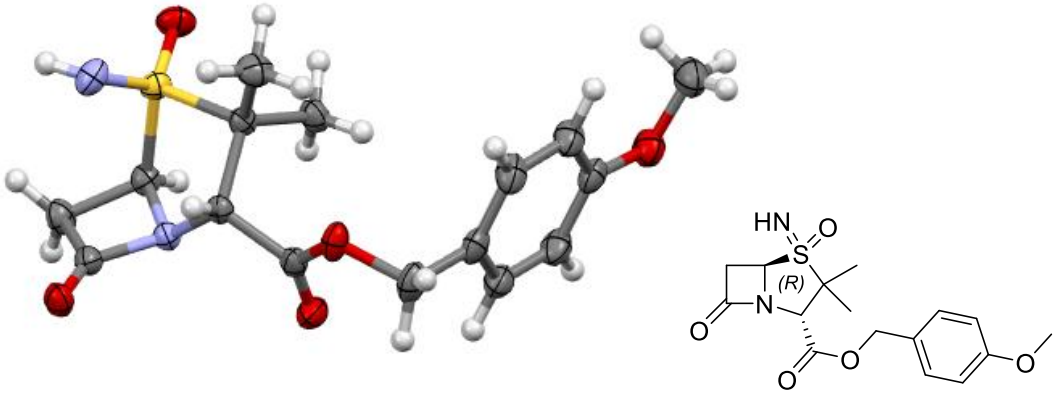

Figure 3.4-2. Crystal structure of penam (*R*)-sulfoximine **48**. Crystallographic analysis of a single crystal of 4-methoxybenzyl (*2S*,*4R*,*5R*)-4-imino-3,3-dimethyl-7-oxo-4λ^6-thia-1-azabicyclo[3.2.0]heptane-2-carboxylate 4-oxide (**48**) confirms its structural assignment based on ^{1}H and ^{13}C NMR, IR, MS, and $[\alpha]_D^{25}$ analysis. Analysis of the Flack parameter[126] supports the assignment of the sulfur-configuration as (*R*). Color code: white: hydrogen; gray: carbon; blue: nitrogen; red: oxygen; yellow: sulfur. Select crystallographic data are shown in the **Appendix 7.1**.

Single-crystal X-ray diffraction analysis of the free *NH* sulfoximine **48** was performed (**Figure 3.4-2**). The structure confirms the assigned absolute configuration and reveals a conformation in which the sulfoximine nitrogen is oriented toward the β-lactam core.

This spatial arrangement may facilitate coordination to transition metal catalysts following partial deprotection, providing structural support for the observed resistance to hydrogenolytic ester cleavage in the (*R*)-series.

Hydrogenation of select (*R*)-configured penam sulfoximines was investigated under standard conditions (H_2, Pd/C, THF, rt) using representative substrates **48**, **47**, and **49** (**Figure 3.4-3**). These compounds included both free *NH* sulfoximine **48**, and *N*-substituted analogues bearing methyl carbamate (**47**) or urea (**49**) substituents. In all cases, reactions performed in THF, ethyl acetate, or methanol with either 0.2 or 1.1 equiv. of Pd/C resulted in recovery of starting material accompanied by varying degrees of degradation after 3 h.

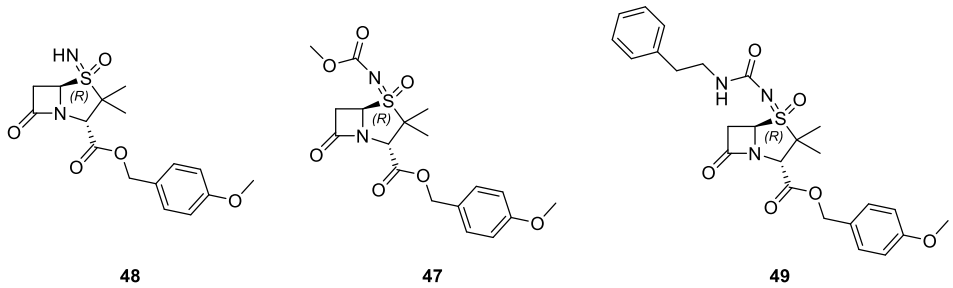

48 47 49

Entry	SM	Conditions	Result
i	**48**	Pd/C (1.1 equiv.) in THF	Only SM after 3 h
ii	**48**	Pd/C (1.1 equiv.) in EtOAc	Only SM with degradation after 3 h
iii	**48**	Pd/C (1.1 equiv.) in MeOH	Only SM with degradation after 3 h
iv	**47**	Pd/C (0.2 equiv.) in THF	Only SM with degradation after 3 h
v	**49**	Pd/C (0.2 equiv.) in THF	Only SM with degradation after 3 h

Figure 3.4-3. Hydrogenation of select (*R*)-penam sulfoximines**.**

The observation of unreacted starting material alongside decomposition products suggests that hydrogenolysis of the (*R*)-diastereomer proceeds more slowly than the rate of product degradation under the reaction conditions and/or that the decomposition product(s) poison the catalyst. Transient formation of the desired acid is therefore likely followed by rapid β-lactam ring opening or further breakdown mediated by the

catalyst or solvent. These results indicate that both the (*R*)-penam scaffold and the sulfoximine functionality confer substantial instability toward hydrogenation, preventing selective deprotection even under mild catalytic conditions. Notably, the (*S*)-configured diastereomer appears to be significantly more stable under comparable hydrogenation conditions, suggesting that subtle stereoelectronic or conformational factors influence the susceptibility of the β-lactam sulfoximine core to degradation.

3.5 Synthesis of cephem-sulfoximines

To further evaluate the generality of the sulfoximine derivatization strategy, the cephem scaffold was next explored. Compared to the [3,2,0] bicyclic ring system of penams, the 4:6 ring bicyclic system of cephems exhibits relatively reduced angular strain and greater thermodynamic stability.[148] This decreased ring strain was expected to confer enhanced resistance to β-lactam hydrolysis and to improve the overall chemical robustness of the sulfoximine derivatives during oxidation and deprotection steps. Consequently, the cephem series provided an attractive platform to test whether the synthetic sequence developed for penam-sulfoximines could be extended to a less strained β-lactam system.

Building on the success of the (*S*)-penam-sulfoximine series, the same synthetic strategy was next applied to the preparation of cephem-sulfoximine analogues. 7-Aminodesacetoxycephalosporanic acid (7-ADCA, **50**) was first converted into 7α-bromo cephalosporanic acid **51**[149] which was subsequently protected with *para*-methoxybenzyl (PMB) bromide to afford the corresponding ester **52**. Oxidation of **52** with *m*CPBA afforded a 5:1 mixture of (*S*):(*R*) sulfoxides, which were readily separated by silica gel chromatography to provide **53** and **57** in 51% and 9% overall yield, respectively (**Figure 3.5-1**).

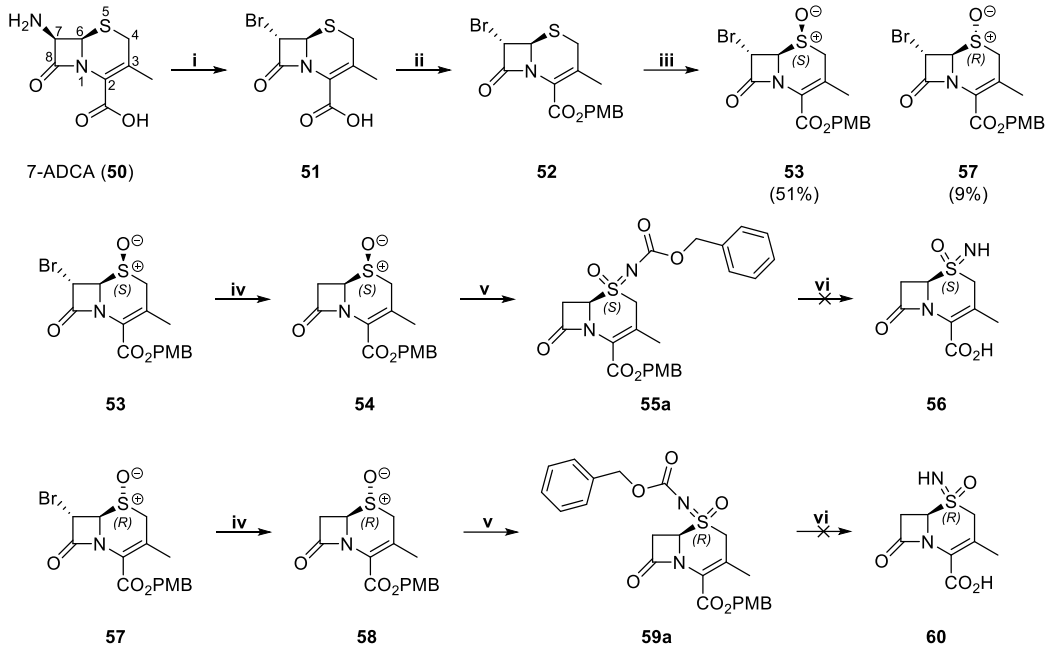

Figure 3.5-1. Synthesis of (*S*)- and (*R*)-cephem-sulfoximines **56** and **60**. Reagents and conditions: (i) HBr, $NaNO_2$, MeOH, H_2O, –15 °C to rt, 48%; (ii) PMB-Br, K_2CO_3, DMF, CH_2Cl_2, 40 °C, 64%; (iii) *m*CPBA, CH_2Cl_2, –78 °C, 60%%; (iv) P^nBu_3, MeOH, rt, 82%; (v) $CbzNH_2$, MgO, $PhI(OAc)_2$, $Rh_2(OAc)_4$ (5 mol%), dimethoxyethane, 40 °C, 72%; (vi) Pd/C, H_2, THF, rt, 0%.

Bromine reduction of **53** and **57** using tributylphosphane in methanol furnished the corresponding 6,6-dihydrocephems **54** and **58**, respectively. The (*S*)-sulfoxide **54** was subjected to $Rh_2(OAc)_4$-catalyzed nitrene transfer using benzyl carbamate as the nitrogen source, affording the corresponding (*S*)-sulfoximine **55a** in 72% yield. Similarly, (*R*)-sulfoxide **58** underwent the same transformation to produce (*R*)-sulfoximine **59a** in 36% yield. The lower yield for the (*R*)-isomer is likely due to steric hinderance at the sulfur center during nitrene transfer, as the sulfur approaches from the concave face of the cephem framework. Assignment of sulfoxide stereochemistry was confirmed by crystallographic analysis of a single crystal of cephem sulfoxide **54** (**Figure 3.5-2**).

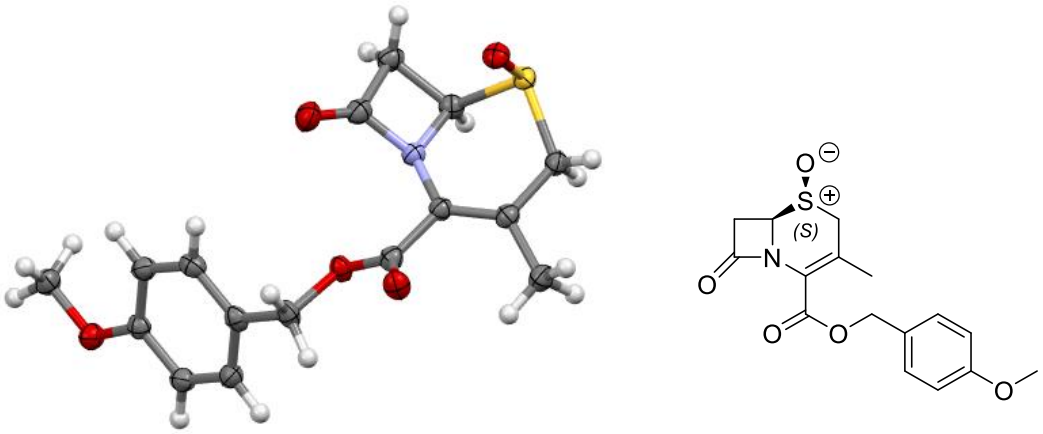

Figure 3.5-2. Crystal structure of cephem **54**. Crystallographic analysis of a single crystal of 4-methoxybenzyl (*6R*)-3-methyl-8-oxo-5-thia-1-azabicyclo[4.2.0]oct-2-ene-2-carboxylate 5-oxide **54** confirms its structural assignment based on ^{1}H and ^{13}C NMR, IR, MS, and $[\alpha]_D^{25}$ analysis. Analysis of the Flack parameter[126] supports the assignment of the sulfur-configuration as (*S*). Color code: white: hydrogen; gray: carbon; blue: nitrogen; red: oxygen; yellow: sulfur. Select crystallographic data are shown in the **Appendix 7.2**.

3.5.1 Deprotection of cephem-sulfoximines

Hydrogenation of the (*S*)-sulfoximine **55a** under standard conditions (H_2, Pd/C, THF, rt) did not yield the desired free acid **56** (**Figure 3.5-3**). Performing the reaction in alternative solvents such as ethyl acetate or methanol likewise failed to produce either the deprotected acid or the corresponding free *NH* sulfoximine. Increasing the catalyst loading from 0.2 to 1.1 equiv. and testing different hydrogenation catalysts (*i.e.*, Pd/C, Pt/C, and $Pd(OH)_2$) did not lead to product formation, and only unreacted starting material was recovered in all cases.

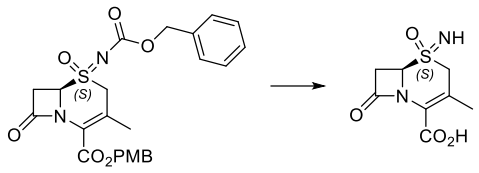

Entry	Catalyst (equiv.)	Solvent	Result
i	Pd/C (0.2)	THF	Only SM after 6h
ii	Pd/C (0.2)	EtOAc	Only SM after 6h
iii	Pd/C (0.2)	MeOH	Only SM + degradation after 6h
iv	Pd/C (1.1)	THF	Only SM after 6h
v	Pd/C (1.1)	EtOAc	Only SM after 6h
vi	Pd/C (1.1)	MeOH	Only SM + degradation after 6h
vii	Pt/C (1.1)	THF	Only SM after 6h
viii	$Pd(OH)_2$ (1.1)	THF	Only SM + degradation after 6h

Figure 3.5-3. Hydrogenation of (*S*)-cephem sulfoximine **55a**.

The resistance to hydrogenolysis is likely attributable to π-coordination of palladium to the *C2-C3* cephem alkene to the metal surface. This interaction might form a stable, non-productive complex that inhibits activation of the *p*-methoxybenzyl group toward reduction. In some cases, partial decomposition was observed, which may reflect a faster rate of product degradation relative to the slower rate of hydrogenolytic cleavage under reaction conditions. Thus, even if transient formation of the desired acid occurs, it is likely unstable in the presence of the catalyst or the solvent medium. As a result, hydrogenation of both the protecting group and the sulfoximine moiety is effectively suppressed, and the overall transformation remains non-productive even under forcing conditions.

These results establish a concise route to both (*S*)- and (*R*)-configured cephem-sulfoximines from 7-ADCA via selective oxidation and nitrene transfer, while underscoring the intrinsic limitations of PMB deprotection within the cephem-sulfoximine series due to metal-olefin interactions and product instability under hydrogenation conditions.

3.5.2 Evaluation of alternative protecting groups for cephem-sulfoximines

Given the limited success of *p*-methoxybenzyl (PMB) ester deprotection in the cephem-sulfoximine series, alternative protecting groups were next explored to identify conditions compatible with both the β-lactam and sulfoximine functionalities. To streamline the synthetic sequence, the phenylacetylamide (PenG) side chain was introduced at the amine position to allow direct comparison of multiple *C2*-protecting groups without the need for extensive side-chain manipulations (**Scheme 3.5-4**).

The synthesis proceeded through the corresponding *C2* esters of 7-aminodesacetoxycephalosporanic acid (7-ADCA, **50**) bearing *p*-nitrobenzyl (PNB, **62**), methyl (**65**), trimethylsilyl ethyl (TMSE, **68**), allyl (Alloc, **71**), or 9-fluorenylmethyl (Fmoc, **74**) groups. Oxidation of the corresponding sulfides with *m*-chloroperbenzoic acid (*m*CPBA) followed by $Rh(OAc)_2$-catalyzed nitrene transfer was used to assess the compatibility of each protecting group under sulfoximine-forming conditions.

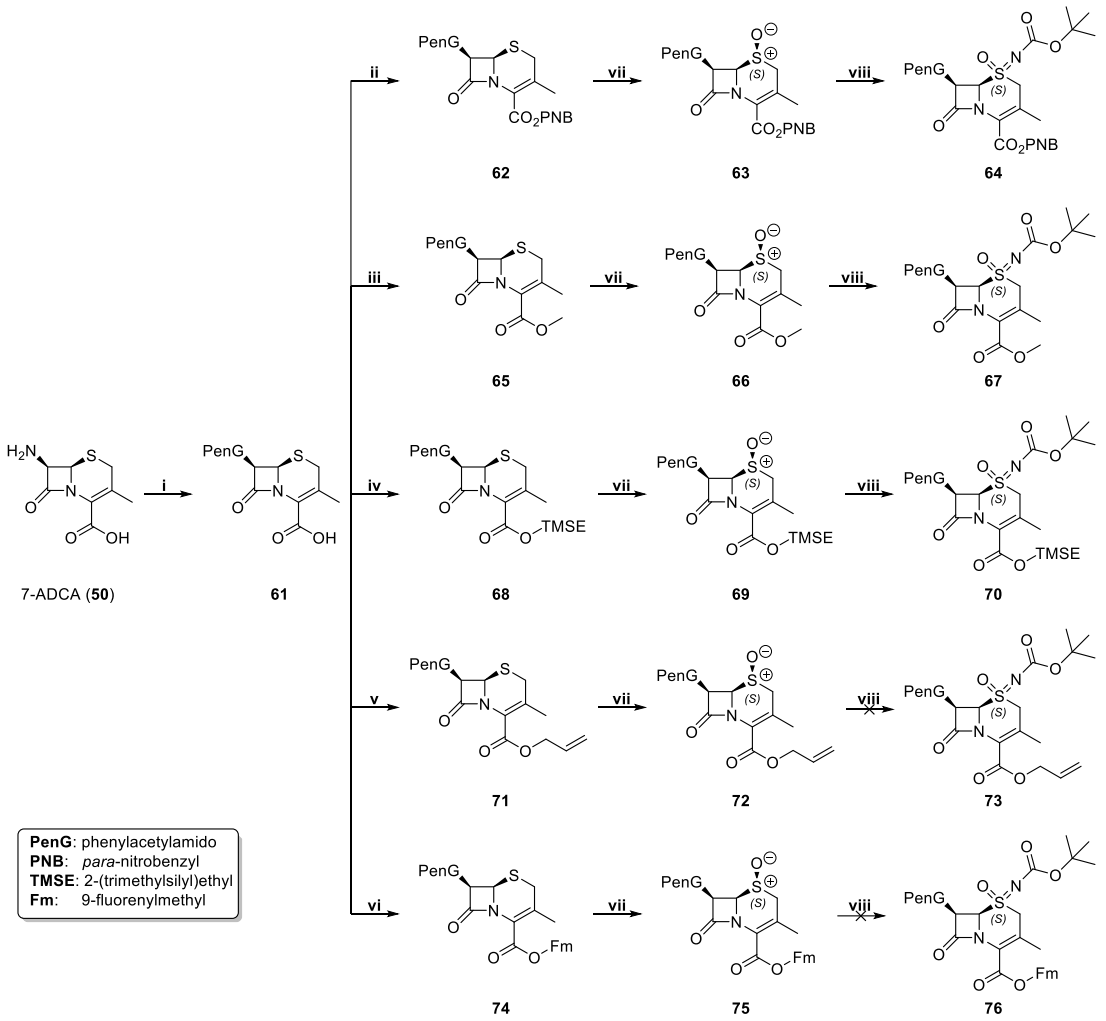

Scheme 3.5-4. Synthesis of cephem-sulfoximines. Reagents and conditions: (i) phenylacetyl chloride, $NaHCO_3$, acetone, H_2O, rt, 90%; (ii) PNB-Br, K_2CO_3, DMF, CH_2Cl_2, 40 °C, 69%; (iii) CH_3I, K_2CO_3, DMF, CH_2Cl_2, 35 °C, 84%; (iv) TMSE-OH, *N*,*N*'-dicyclohexylcarbodiimide (DCC), 4-dimethylaminopyridine (DMAP)[132], CH_2Cl_2, 0 °C, 84%; (v) 3-bromoprop-1-ene, K_2CO_3, DMF, CH_2Cl_2, 40 °C, 49%; (vi) Fm-OH, 1-ethyl-3-(3-dimethylaminopropyl)carbodiimide (EDC), DMAP[132], CH_2Cl_2, 0 °C; 82%; (vii) *m*CPBA, CH_2Cl_2, –78 °C, 31-83%; (viii) $CbzNH_2$, MgO, $PhI(OAc)_2$, $Rh_2(OAc)_4$ (5 mol%), dimethoxyethane, 40 °C, 33-46%.

Sulfoximine formation did not proceed for PNB-protected sulfoxide **63**, likely due to poor solubility of the substrate under reaction conditions. Similarly, attempts using the Alloc-protected sulfoxide **72** failed to yield the corresponding sulfoximine, might indicate coordination of the rhodium catalyst to the accessible alkene double bond, thereby preventing productive nitrene transfer. In contrast, reaction of the Fmoc-protected sulfoxide **75** led to detectable formation of the desired sulfoximine, but in

very low yield (<5%), and isolation of the product from reaction byproducts was not possible. These results indicate that sulfoximine formation in the cephem series is highly sensitive to both substrate solubility and functional-group compatibility with the rhodium catalyst. Electron-rich or π-coordinating protecting groups tend to inhibit nitrene insertion, whereas bulky or poorly soluble esters further limit conversion. Collectively, these observations underscore the narrow operational window for achieving efficient sulfoximine formation within the cephem framework and emphasize the need for neutral, non-coordinating protecting groups to ensure both solubility and catalyst accessibility.

3.5.3 Deprotection of cephem-sulfoximines

Deprotection of the methyl ester was investigated using cephem-sulfoximine **67** as a model substrate (**Figure 3.5-5**). Methyl esters are employed in β-lactam chemistry due to their ease of introduction and potential for mild cleavage via nucleophilic or reductive conditions. However, the cephem scaffold presents additional challenges for ester hydrolysis, as the β-lactam ring is highly sensitive to nucleophilic or basic environments. Several conventional methyl ester cleavage methods (including aqueous saponification, acid-catalyzed hydrolysis, and enzymatic esterases) were considered but ultimately excluded, as they require non-anhydrous or protic conditions that risk rapid β-lactam degradation. To preserve the integrity of the cephem core, only strictly anhydrous deprotection strategies were pursued, employing nucleophilic (KOTMS) and reductive (LiI) reagents under aprotic conditions.

A range of classical deprotection conditions was screened, including potassium trimethylsilanolate (KOTMS)[150] and lithium iodide (LiI)[151] in various solvents (THF,

ether, ethyl acetate, and acetonitrile) and temperatures (0 °C to rt). In all cases, extensive degradation of **67** was observed, with no recovery of the desired free acid.

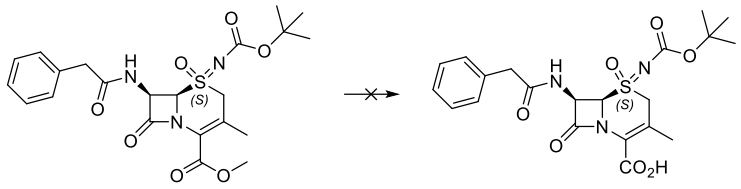

67 **77**

Entry	Conditions	Result
i	KOTMS, THF, rt	Degradation of **67**
ii	KOTMS, ether, rt	Degradation of **67**
iii	KOTMS, THF, 0 °C	Degradation of **67**
iv	KOTMS, ether, 0 °C	Degradation of **67**
v	LiI, EtOAc, rt	Degradation of **67**
vi	LiI, THF, rt	Degradation of **67**
vii	LiI, MeCN, rt	Degradation of **67**
viii	LiI, EtOAc, 0 °C	Degradation of **67**
ix	LiI, THF, 0 °C	Degradation of **67**
x	LiI, MeCN, 0 °C	Degradation of **67**

Figure 3.5-5. Deprotection of cephem-sulfoximines **67**.

The consistent observation of decomposition under both alkoxide- and iodide-mediated conditions suggests that methyl ester cleavage is accompanied by rapid β-lactam ring opening. In the presence of strong nucleophiles or halides, the cephem nucleus is likely activated toward intramolecular rearrangement or fragmentation through the polarized *C2-C3* alkene. Additionally, the highly electrophilic β-lactam carbonyl may undergo direct attack under these conditions, leading to irreversible breakdown of the bicyclic core.

These findings demonstrate that conventional nucleophilic and reductive protection strategies are incompatible with cephem-sulfoximines and highlight the need for neutral or non-ionic methods capable of selectively cleaving the ester without compromising the β-lactam framework.

To further evaluate mild, anhydrous strategies for unveiling the *C2* carboxylate, deprotection of the TMSE-protected cephem-sulfoximine **70** was investigated (**Figure 3.5-6**). TMSE esters are typically cleaved under fluoride-mediated β-elimination using reagents such as TBAF, KF, or CsF, which are compatible with neutral, aprotic media and therefore represent one of the few potentially β-lactam-tolerant options for ester removal.[152]

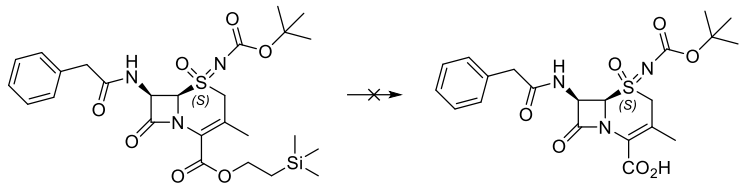

70 **77**

Entry	Conditions	Result
i	TBAF, THF, 0 °C to rt	Degradation of **70**
ii	TBAF, THF, -78 °C to rt	Degradation of **70**
iii	KF, THF, 0 °C to rt	Degradation of **70**
iv	KF, THF, -78 °C to rt	Degradation of **70**
v	CsF, THF, 0 °C to rt	Degradation of **70**
vi	CsF, THF, -78 °C to rt	Degradation of **70**

Figure 3.5-6. Deprotection of cephem-sulfoximines **70**.

A range of fluoride sources and temperatures was screened, including TBAF, KF, and CsF in anhydrous THF from -78 °C to room temperature. In all cases, rapid degradation of **70** was observed, and no trace of the desired free acid product could be detected by ^{1}H NMR. Lowering the temperature did not improve substrate stability, indicating that decomposition occurs independently of the specific fluoride reagent or reaction rate. Given that the free acid was not observed under any of the deprotection strategies evaluated throughout this study – including hydrogenolysis, basic, reductive, and fluoride-mediated conditions – it is likely that the deprotected cephem-sulfoximine is intrinsically unstable under the reaction environments required for ester cleavage. The

instability may arise from the inherent lability of the β-lactam sulfoximine core once the *C2* carboxylate is unmasked, suggesting that the fully deprotected species cannot be isolated under standard synthetic conditions.

3.6 Summary

This chapter investigated the protection and deprotection of the *C2* carboxylate in penam- and cephem-based sulfoximines, with the goal of identifying conditions compatible with the β-lactam sulfoximine framework. Systematic evaluation of commonly employed ester protecting groups revealed pronounced differences in stability and deprotection behavior across scaffolds and sulfoximine stereochemistry.

In the penam (*S*)-sulfoximine series, PMB esters enabled rapid and selective hydrogenolytic cleavage under mild conditions, providing reliable access to the corresponding free acids. Conversion of these acids to their alkali metal salts was essential to ensure long-term stability. In contrast, benzhydryl, PNB, and biphenyl methyl esters displayed inferior performance due to incomplete deprotection, prolonged reaction times, and/or product degradation.

Deprotection of (*R*)-configured penam-sulfoximines proved markedly less efficient, highlighting a pronounced stereochemical dependence that limits the applicability of late-stage hydrogenolysis in this series. Extension of the strategy to the cephem scaffold demonstrated that, although sulfoximine installation is feasible, deprotection of the *C2* carboxylate is not achievable without degradation, indicating an intrinsic stability limitation of cephem-sulfoximines.

Collectively, these findings define the chemical boundaries of β-lactam sulfoximine deprotection and establish PMB-protected penam (*S*)-sulfoximines as a robust platform for subsequent synthetic and biological studies.

Chapter 4: Biological Activity of Penam-sulfoximines and Insights in their Inhibition Mechanism

4.1 Introduction

The emergence and global dissemination of multidrug-resistant Gram-negative pathogens has intensified the need for new β-lactamase inhibitors capable of restoring the efficacy of β-lactam antibiotics against resistant strains.[4] Among these pathogens, *Acinetobacter baumannii* represents a particularly challenging clinical threat due to its ability to express multiple β-lactamases, including class A, C, and D SBLs, often in combination with MBLs.[63, 70] Recently, the sulbactam, and durlobactam combination was approved for *A. baumannii* treatment, in which sulbactam serves as both antibiotic and SBL inhibitor and durlobactam as a SBL inhibitor (**Chapter 1**, **Section 1.4**). Although the sulbactam/durlobactam combination has improved options for treatment of *A. baumannii* infections, limitations in potency, spectrum of SBLs inhibition, and stability motivate the development of improved inhibitor scaffolds.[61]

Penam-sulfoximines have emerged as a promising class of SBL inhibitors that enable systematic structural diversification and modulation of covalent reactivity while retaining key features of clinically validated penam-based SBL inhibitors.

In this chapter, the biological activity and inhibition mechanism of a series of penam-sulfoximine derivatives are systematically evaluated. Biochemical inhibition assays with representative isolated SBLs from class A, C, and D and stability studies combined with mass spectrometric and crystallographic analyses inform of the scope and inhibition mechanisms of penam-sulfoximine derivatives. Antimicrobial susceptibility testing against clinically isolated *A. baumannii* strains demonstrates the clinical potential of penam-sulfoximine derivatives in combination with durlobactam. Together, this approach aims to define the structural and physicochemical features required for effective SBL inhibition and helps to identify penam-sulfoximines capable of translating potent enzyme inhibition into meaningful antibacterial activity.

4.2 Inhibition of SBL by penam-sulfoximine derivatives

The inhibitory activity of the selected penam-sulfoximine derivatives on catalysis by representative isolated recombinant SBLs from Ambler classes A (TEM-116[153]), C (AmpC[154]), and D (OXA-10[155], OXA-48[156]) was evaluated using reported fluorescence-based inhibition assays.[39, 157] These assays employ cephalosporin-derived FC-5 as a fluorogenic substrate to quantify SBL activity.[157] In its intact form, FC-5 exhibits minimal intrinsic fluorescence, however, upon SBL-catalyzed hydrolysis of the FC-5 β-lactam ring, FC-5 fragments to release 7-hydroxycoumarin, a strongly fluorescent molecule which is monitored using a plate reader (**Figure 4.2-1**).[158] Inhibition of SBL catalysis therefore manifests as a concentration-dependent suppression of fluorescence development, enabling quantification of inhibitor potency.

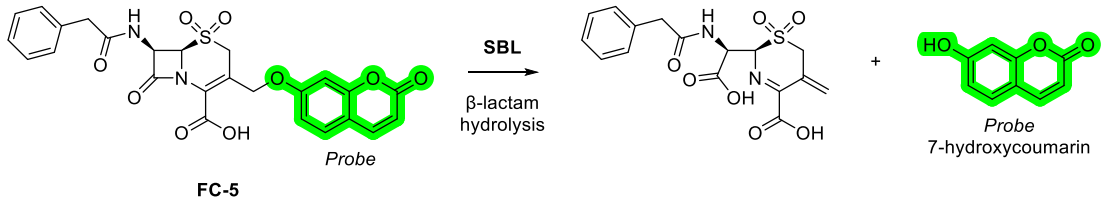

Figure 4.2-1. SBL-catalyzed hydrolysis of FC-5 produces fluorescent 7-hydroxycoumarin.

SBLs were incubated at room temperature in reaction buffer (50 mM phosphate buffer, pH 7.5, with 0.01% (v/v) Triton X-100) in the presence of varying concentrations of penam-sulfoximine derivative for 10 min. For OXA-10 and OXA-48, the reaction buffer was supplemented with sodium bicarbonate (50 mM) to maintain the carbamylated, catalytically active form of the enzyme.[39, 157] Reactions were initiated by addition of the reported fluorogenic substrate FC-5 (5 μM)[157] and florescence was monitored immediately (λ_{ex} = 380 nm, λ_{ex} = 460 nm) over 30-45 min using either a BMG LABTECH Clariostar or a Pherastar plate reader. Sulbactam (**6**) and Avibactam (**9**) were included as reference inhibitors (**Figure 4.2-2**).

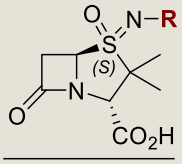 R =	pIC$_{50}$ AmpC	pIC$_{50}$ TEM-116	pIC$_{50}$ OXA-10	pIC$_{50}$ OXA-48	pIC$_{50}$ OXA-10 ($NaHCO_3$)	pIC$_{50}$ OXA-48 ($NaHCO_3$)
Sulbactam (**6**)	4.6 ± 0.1	6.5 ± 0.1	4.6 ± 0.1	ND	4.0 ± 0.1	ND
Avibactam (**9**)	7.1 ± 0.1	>8.0	4.8 ± 0.1	6.1 ± 0.1	4.8 ± 0.1	6.0 ± 0.1
21 	4.6 ± 0.1	5.9 ± 0.1	4.1 ± 0.1	ND	<4.0	ND
31a 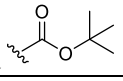	4.5 ± 0.1	6.2 ± 0.1	4.6 ± 0.1	4.6 ± 0.1	5.0 ± 0.1	5.0 ± 0.1
31b 	5.4 ± 0.1	5.4 ± 0.1	<4.0	ND	5.4 ± 0.1	5.2 ± 0.1
34a 	4.7 ± 0.1	5.2 ± 0.1	4.2 ± 0.1	ND	4.3 ± 0.1	4.0 ± 0.1
34b 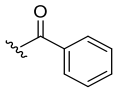	5.4 ± 0.1	6.7 ± 0.1	<4.0	ND	5.4 ± 0.1	5.5 ± 0.1
34c 	<4.0	5.2 ± 0.1	<4.0	ND	5.1 ± 0.1	4.8 ± 0.1
37a 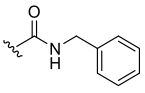	6.5 ± 0.1	7.5 ± 0.1	5.7 ± 0.1	5.6 ± 0.1	5.8 ± 0.1	5.6 ± 0.1
37b 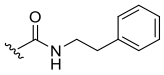	7.1 ± 0.1	>8.0	6.0 ± 0.1	5.9 ± 0.1	6.0 ± 0.1	5.9 ± 0.1
37c 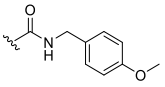	6.5 ± 0.1	7.5 ± 0.1	5.6 ± 0.1	5.7 ± 0.1	5.5 ± 0.1	5.7 ± 0.1
37d 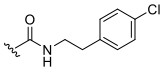	6.5 ± 0.1	7.7 ± 0.1	5.7 ± 0.1	5.6 ± 0.1	5.6 ± 0.1	5.5 ± 0.1
37e 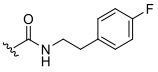	6.8 ± 0.1	7.8 ± 0.1	5.7 ± 0.1	5.7 ± 0.1	5.8 ± 0.1	5.8 ± 0.1
37f 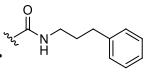	6.7 ± 0.1	7.8 ± 0.1	5.6 ± 0.1	5.7 ± 0.1	5.8 ± 0.1	5.6 ± 0.1
37g 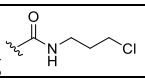	5.9 ± 0.1	7.2 ± 0.1	5.4 ± 0.1	5.6 ± 0.1	5.2 ± 0.1	5.6 ± 0.1
37h 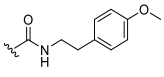	6.4 ± 0.1	7.6 ± 0.1	5.6 ± 0.1	5.7 ± 0.1	5.6 ± 0.1	5.7 ± 0.1
37i 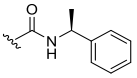	5.8 ± 0.1	7.1 ± 0.1	5.8 ± 0.1	6.0 ± 0.1	5.8 ± 0.1	5.9 ± 0.1
37j 	5.8 ± 0.1	7.0 ± 0.1	5.5 ± 0.1	5.4 ± 0.1	5.5 ± 0.1	5.4 ± 0.1

Figure 4.2-2. Inhibition of isolated recombinant SBLs by selected penam-sulfoximines. pIC$_{50}$ color representation: 4.0–4.9 (red), 5.0–5.9 (yellow), ≥ 6.0 (green). Sulfoximines were employed as sodium salts. Results are means of 2 independent repeats performed in technical quadruplicates. Representative dose response curves are shown in **Figure 4.2-3 – 4.2-5**.

The unsubstituted penam-sulfoximine **21** inhibited SBL catalysis with potency comparable to that of sulbactam (**6**), with both compounds displaying more potent inhibition of TEM-116 than of AmpC or OXA-10. The majority of the *N*-substituted sulbactam-derived sulfoximines exhibited inhibition profiles broadly similar to sulbactam (**6**). In contrast, urea-type sulfoximine derivatives **37a**-**37j** were generally ~30- to 300-fold more potent inhibitors of class A, C, and D SBLs relative to sulbactam. Notably, sulfoximine **37b** inhibited the tested SBLs with comparable or improved potency relative to avibactam (**9**), Specifically, **37b** exhibited pIC_{50} values of 7.1 (AmpC), >8.0 (TEM-116), 6.0 (OXA-10), and 5.7 (OXA-48), compared with corresponding values of 7.1 (AmpC), >8.0 (TEM-116), 4.8 (OXA-10), and 6.1 (OXA-48) for avibactam. In all cases, inhibition was concentration-dependent and yielded well-defined sigmoidal dose-response curves, enabling reliable determination of pIC_{50} values. Representative dose-response curves for selected inhibitors across class A, C, and D SBLs are shown in **Figures 4.2-3** – **4.2-5**.

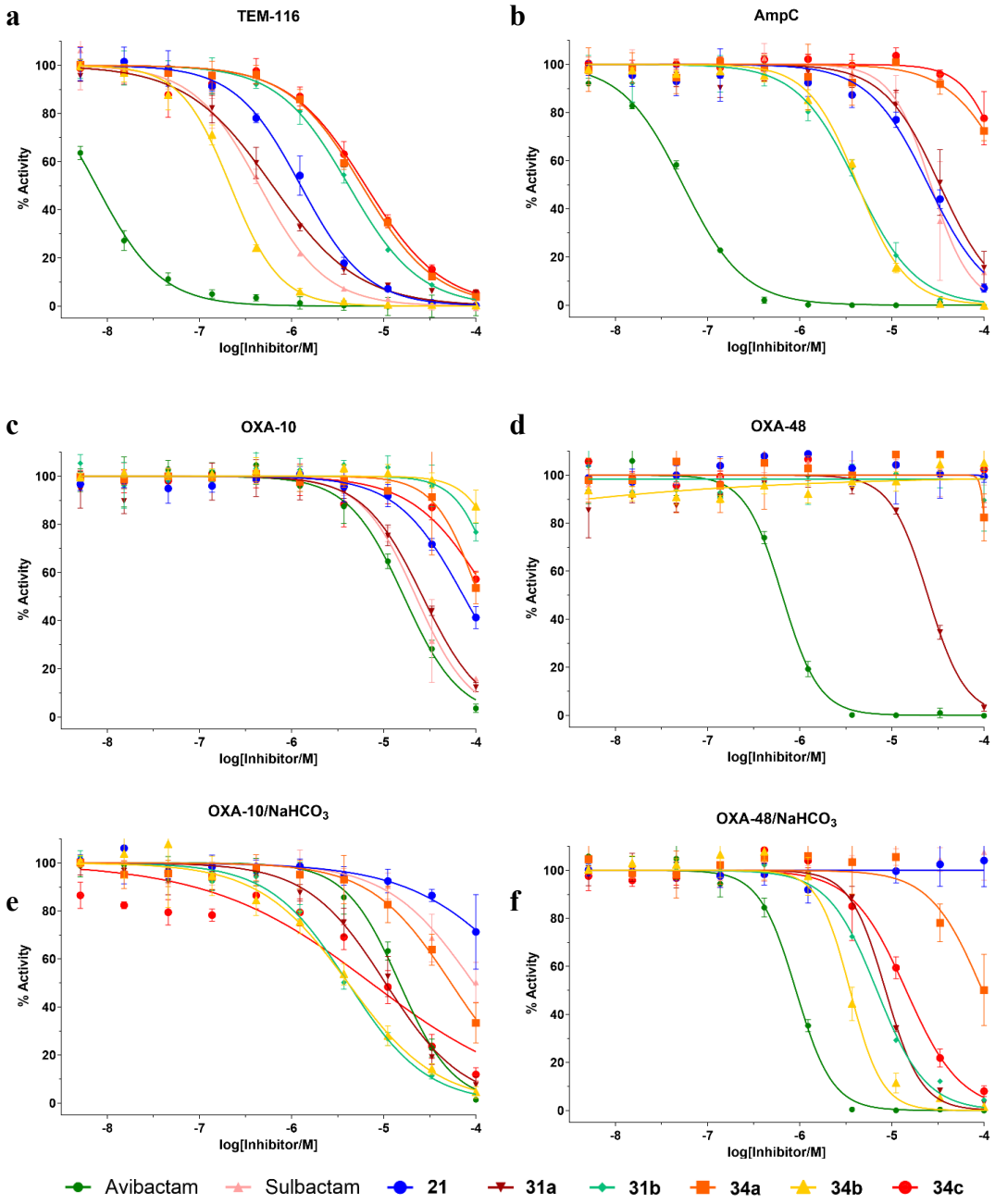

Figure 4.2-3. Dose response curves for selected penam sulfoximines for inhibition of a representative set of SBLs. (**a-f**) Dose response curves for sulfoximines **21** (blue circles), **31a** (brown inverse triangles), **31b** (turquoise diamonds), **34a** (orange squares), **34b** (yellow triangles), **34c** (red circles): **a**) TEM-116 (5 nM), **b**) AmpC (2.5 nM), **c**) OXA-10 (1.25 nM), **d**) OXA-48 (6.25 nM), **e**) OXA-10/$NaHCO_3$ (1.25 nM), and **f**) OXA-48/$NaHCO_3$ (6.25 nM) using Avibactam (green circles) and Sulbactam (pink triangles) as positive inhibition controls. Conditions: 50 mM phosphate buffer, pH 7.4, 0.01%$_{v/v}$ Triton-X, 5 μM FC-5.[159] (**e-f**) $NaHCO_3$ (50 mM) was added to the buffer. See the Methods Section for assay details.

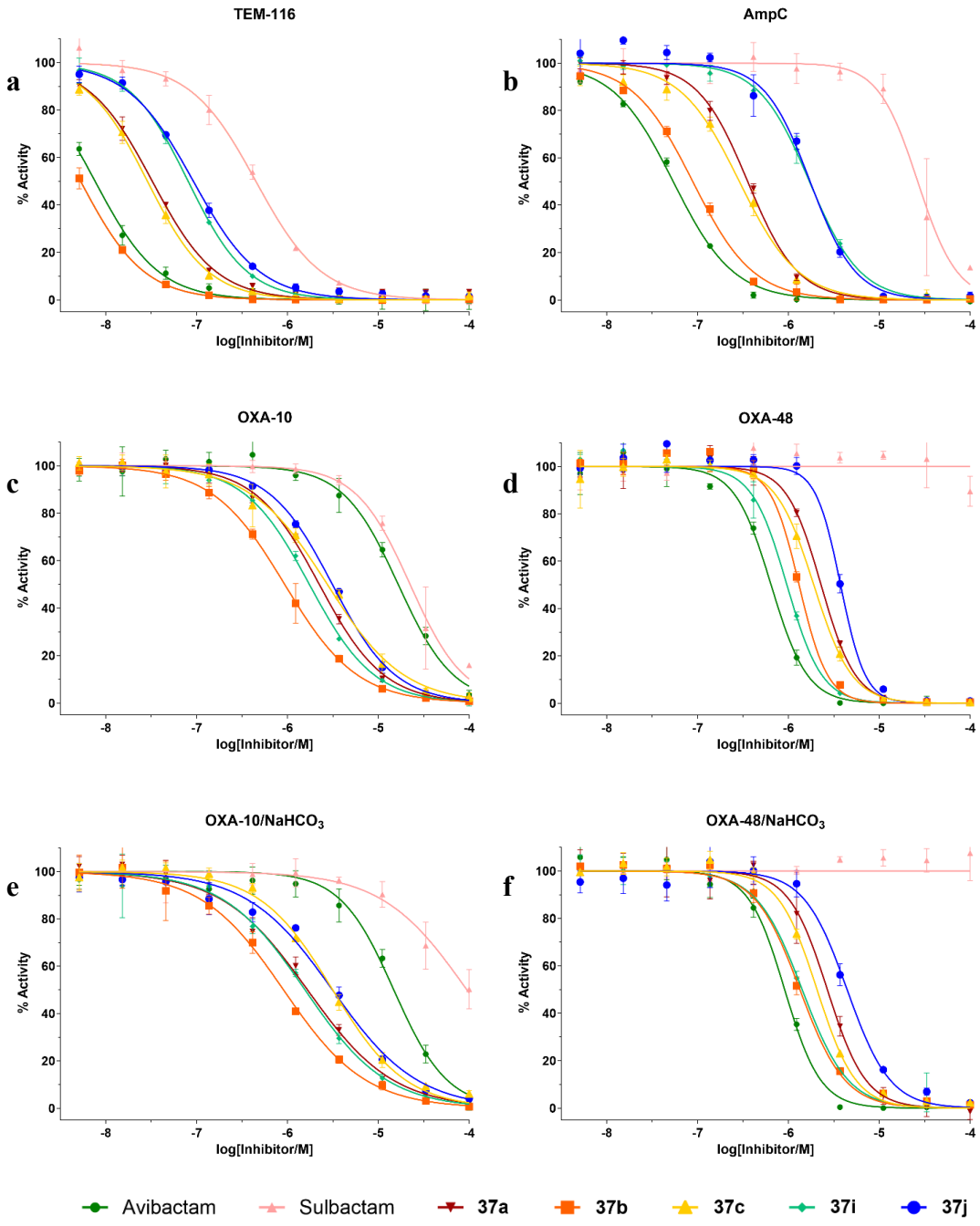

Figure 4.2-4. Dose response curves for selected penam sulfoximines for inhibition of a representative set of SBLs. (**a-f**) Dose response curves for sulfoximines **37a** (burgundy inverse triangles), **37b** (orange squares), **37c** (yellow triangles), **37i** (turquoise diamonds), **37j** (blue circles): **a**) TEM-116 (5 nM), **b**) AmpC (2.5 nM), **c**) OXA-10 (1.25 nM), **d**) OXA-48 (6.25 nM), **e**) OXA-10/$NaHCO_3$ (1.25 nM), and **f**) OXA-48/$NaHCO_3$ (6.25 nM) using Avibactam (green circles) and Sulbactam (pink triangles) as positive inhibition controls. Conditions: 50 mM phosphate buffer, pH 7.4, 0.01%$_{v/v}$ Triton-X, 5 µM FC-5.[159] (**e-f**) $NaHCO_3$ (50 mM) was added to the buffer. See the Methods Section for assay details.

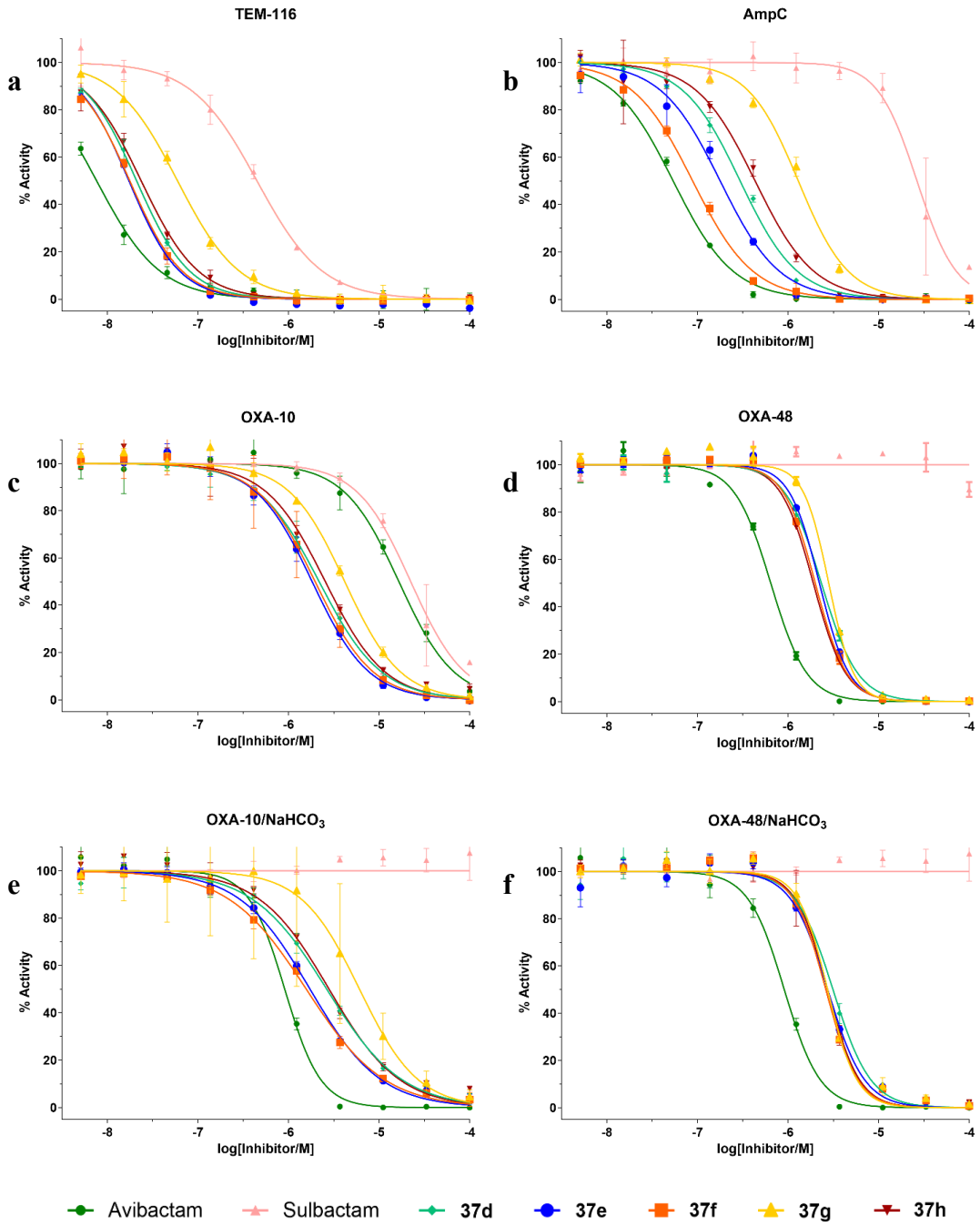

Figure 4.2-5. Dose response curves for selected penam sulfoximines for inhibition of a representative set of SBLs. (**a-f**)Dose response curves for sulfoximines **37d** (turquoise diamonds), **37e** (blue circles), **37f** (orange squares), **37g** (yellow triangles), **37h** (burgundy inverse triangles): **a**) TEM-116 (5 nM), **b**) AmpC (2.5 nM), **c**, OXA-10 (1.25 nM), **d**, OXA-48 (6.25 nM), **e**, OXA-10/$NaHCO_3$ (1.25 nM), and **f**) OXA-48/$NaHCO_3$ (6.25 nM) using Avibactam (green circles) and Sulbactam (pink triangles) as positive inhibitor controls. Conditions: 50 mM phosphate buffer, pH 7.4, 0.01%$_{v/v}$ Triton-X, 5 µM FC-5.[159] (**e-f**) $NaHCO_3$ (50 mM) was added to the buffer. See the Methods Section for assay details.

4.3 Covalent reaction of penam-sulfoximines with SBLs

To gain mechanistic insight into the mode of SBL inhibition by penam-sulfoximines, the potential covalent reactions of selected derivatives with isolated recombinant AmpC and OXA-10 were investigated using protein-observed solid-phase extraction mass spectrometry (SPE-MS).[39] This approach enables direct detection of enzyme-bound inhibitor adducts and provides information on the integrity and relative stability of acyl-enzyme complexes (AECs) as previously employed to study sulbactam (**6**), tazobactam (**7**), and enmetazobactam (**8**).[39]

SPE-MS assays were performed and analyzed as described,[39] using an Agilent RapidFire365 system coupled to an Agilent 6550 Accurate Mass QTOF spectrometer. Prior to analysis, SBL solutions were buffer-exchanged into 50 mM Tris (pH 7.5). Substrate or inhibitor (10 μM) was added to the SBL solution (1 μM), and after the indicated incubation time, a 50 μL aliquot was injected onto a C4 SPE cartridge, washed, then eluted into the mass spectrometer for analysis.

Across all tested sulfoximine derivatives, the dominant observed mass shifts corresponded to formation of intact covalent adducts, consistent with acylation of the nucleophilic serine residue by the full penam-sulfoximine scaffold (**Figure 4.3-1**). Extensive fragmentation of the inhibitor scaffold was not observed under the SPE-MS conditions employed, indicating that covalent inhibition proceeds primarily via formation of relatively stable AEC-derived species. This observation parallels findings reported for enmetazobactam, where intact *trans*-enamine adducts (**Chapter 1**, **Figure 1.3-3**) were shown to dominate under mild MS conditions and to represent the biologically relevant inhibitory species.[39]

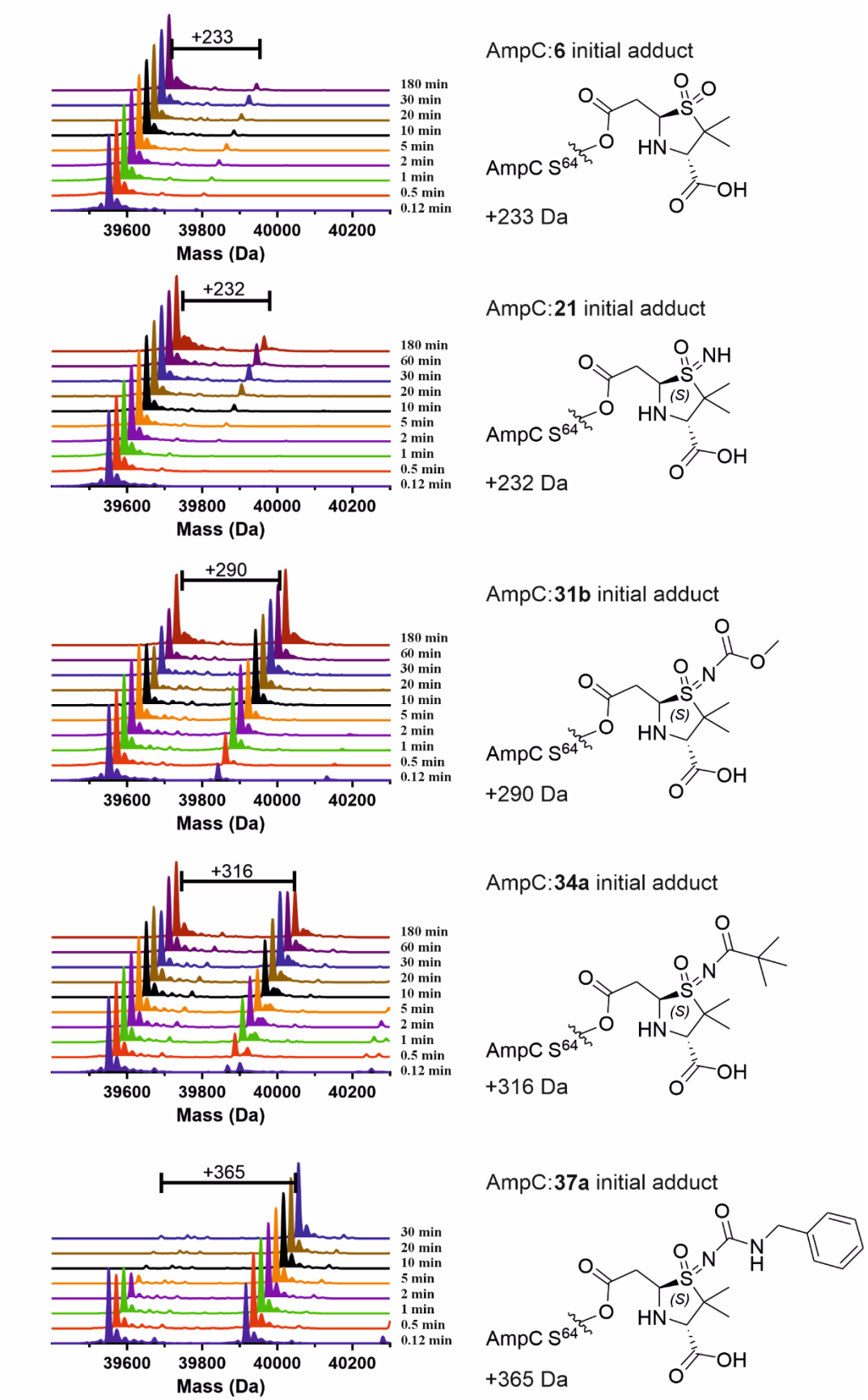

Figure 4.3-1. Mass spectrometric investigations on the covalent reaction of selected penam-sulfoximines derivatives with AmpC. See **Appendix 7.3** for complete data.

Analysis of the SPE-MS data revealed that the nature of the sulfoximine *N*-substituent strongly influences the efficiency of covalent AEC formation with AmpC. Carbamate-type (**31b**), amide- type (**34a**), and urea-type (**37a**) sulfoximines all formed readily detectable intact covalent adducts, whereas the unsubstituted sulfoximine **21** exhibited minimal AEC formation within 3 h (**Figure 4.3-1**). This reduced reactivity likely reflects inefficient acylation and/or rapid hydrolysis of the AEC, consistent with the weaker inhibition observed for this compound in biochemical assays (**Figure 4.2-2**) and with prior observations for sulbactam (**6**) against AmpC.[39]

Notably, the efficiency and persistence of intact AEC formation correlated with inhibitor potency, with more active compounds exhibiting more rapid and extensive formation of covalent adducts. These results support a model in which productive SBL inhibition by penam-sulfoximines arises primarily from formation of intact, hydrolytically stable AEC-derived species, rather than from extensive scaffold fragmentation. Minor lower-abundance mass shifts were occasionally detected; however, analogous to observations reported for penam-sulfones, such species are likely promoted by denaturing or acidic MS conditions and are unlikely to represent dominant solution-phase intermediates under physiological conditions.

Closer inspection of the time-resolved SPE-MS data revealed pronounced differences in the stability of the OXA-10 AECs formed by closely related urea-substituted penam-sufloximines. For compound **37b**, the intact covalent adduct corresponding to a +379 Da mass shift persisted overt the full 24 h incubation period, with little to no detectable regeneration of free OXA-10 observed (**Figure 4.3-2**). This behavior is indicative of a highly stable AEC, consistent with efficient and sustained inhibition of the enzyme.

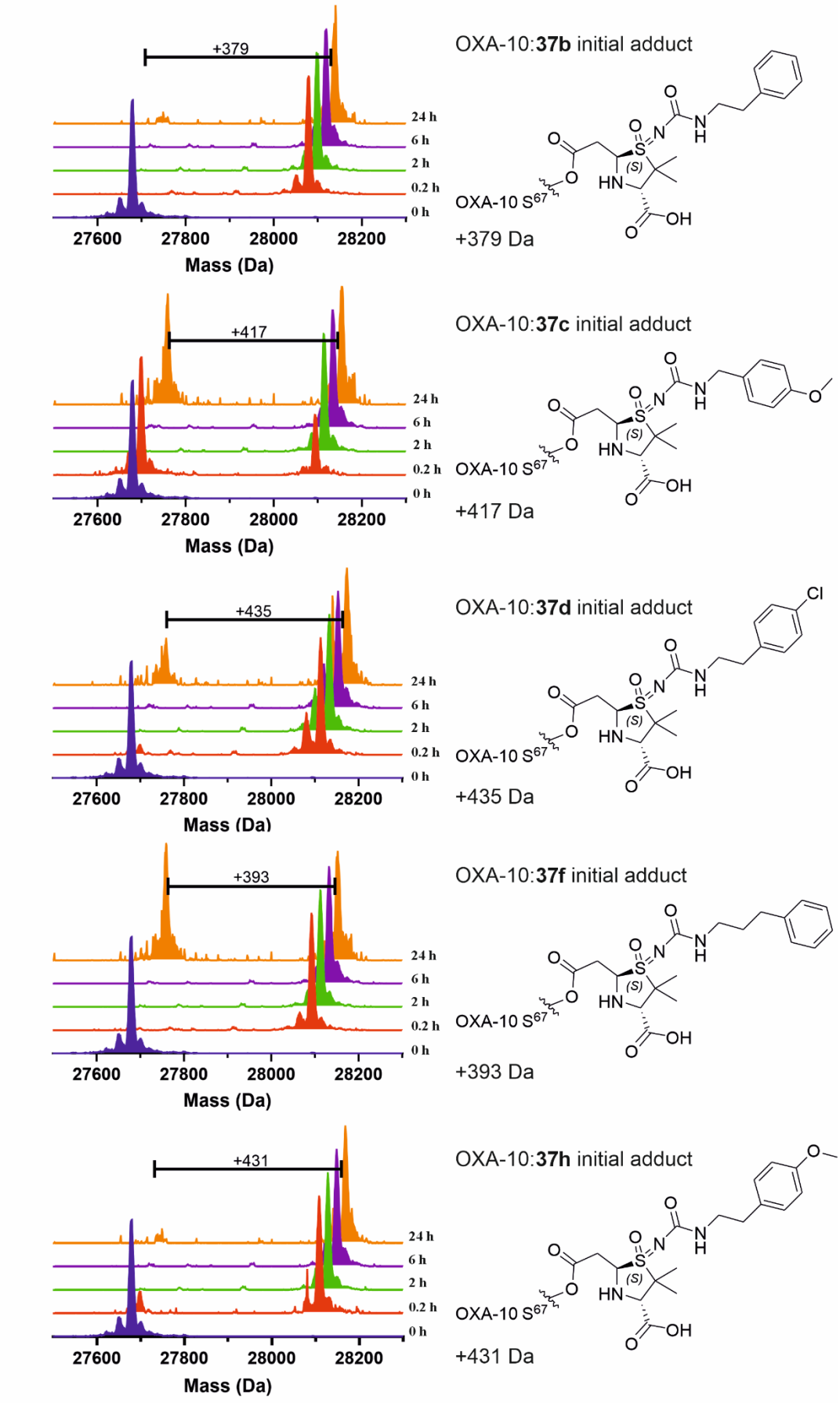

Figure 4.3-2 Mass spectrometric investigations on the covalent reaction of selected penam-sulfoximines derivatives with OXA-10. See **Appendix 7.4** for complete data.

By contrast, subtle modifications to the urea *N*-substituent resulted in marked changes in AEC stability. Extension of the linker by a single methylene unit, as in **37f**, led to partial recovery of unmodified OXA-10 over extended incubation, indicating increased susceptibility of the AEC to hydrolysis. Similarly, incorporation of a *para*-chloro substituent on the phenyl ring (**37d**) resulted in reduced persistence of the intact adduct relative to **37b**, despite formation of the expected initial covalent species. These observations demonstrate that relatively small differences in sulfoximine substitution can modulate AEC stability and lifetime for OXA-10.

Collectively, these data highlight AEC stability – rather than initial acylation efficiency alone – as a key determinant of sustained inhibition of OXA-10 by penam sulfoximines and underscore the sensitivity of class D SBL inhibition to subtle structure-activity relationships.

4.4 Crystal structure of the AmpC:37a adduct

To investigate the mode of SBL inhibition by penam-sulfoximines, crystallographic studies were carried out to determine the structure of AmpC in complex with **37a**. AmpC was crystallized using a modification of a reported protocol.[39] Briefly, AmpC (25 mg/mL in 50 mM Tris, pH 7.5) was mixed with precipitant solution (1.6 M potassium phosphate, pH 8.8) containing 1,000-fold diluted seed crystals and crystallized using the hanging drop vapor diffusion method over a reservoir of 500 µL precipitant solution. Crystals were subsequently soaked in a solution containing **37a** (10 mM) and glycerol (20% w/v) for 10 min at room temperature prior to rapid freezing in liquid nitrogen. X-ray diffraction data were collected at beamline i03 at Diamond Light Source using automatic data collection. The structure was solved in the C121

space group at 1.43 Å resolution (PDB ID: 9I5D), using a previously reported AmpC structure as search model (PDB ID: 2BLS) (**Figure 4.4-1**).[160]

Inspection of the AmpC:**37a** complex reveals that the covalently bound sulfoximine is well accommodated within the active site and engages in several stabilizing interactions (**Figure 4.4-1, a**). The acylated β-lactam carbonyl engages in a hydrogen-bond interaction with the backbone amide of A318, while the carboxylate group forms a h-bond with the amide side chain of Q120. In addition, the sulfinamide oxygen forms a h-bond interaction with the backbone amide of G320, contributing to stabilization of the acyl-enzyme complex (AEC) within the active site. These interactions may contribute to precise positioning of **37a** for nucleophilic attack and may facilitate subsequent fragmentation to the *trans*-enamine adduct (**Figure 4.4-2**).

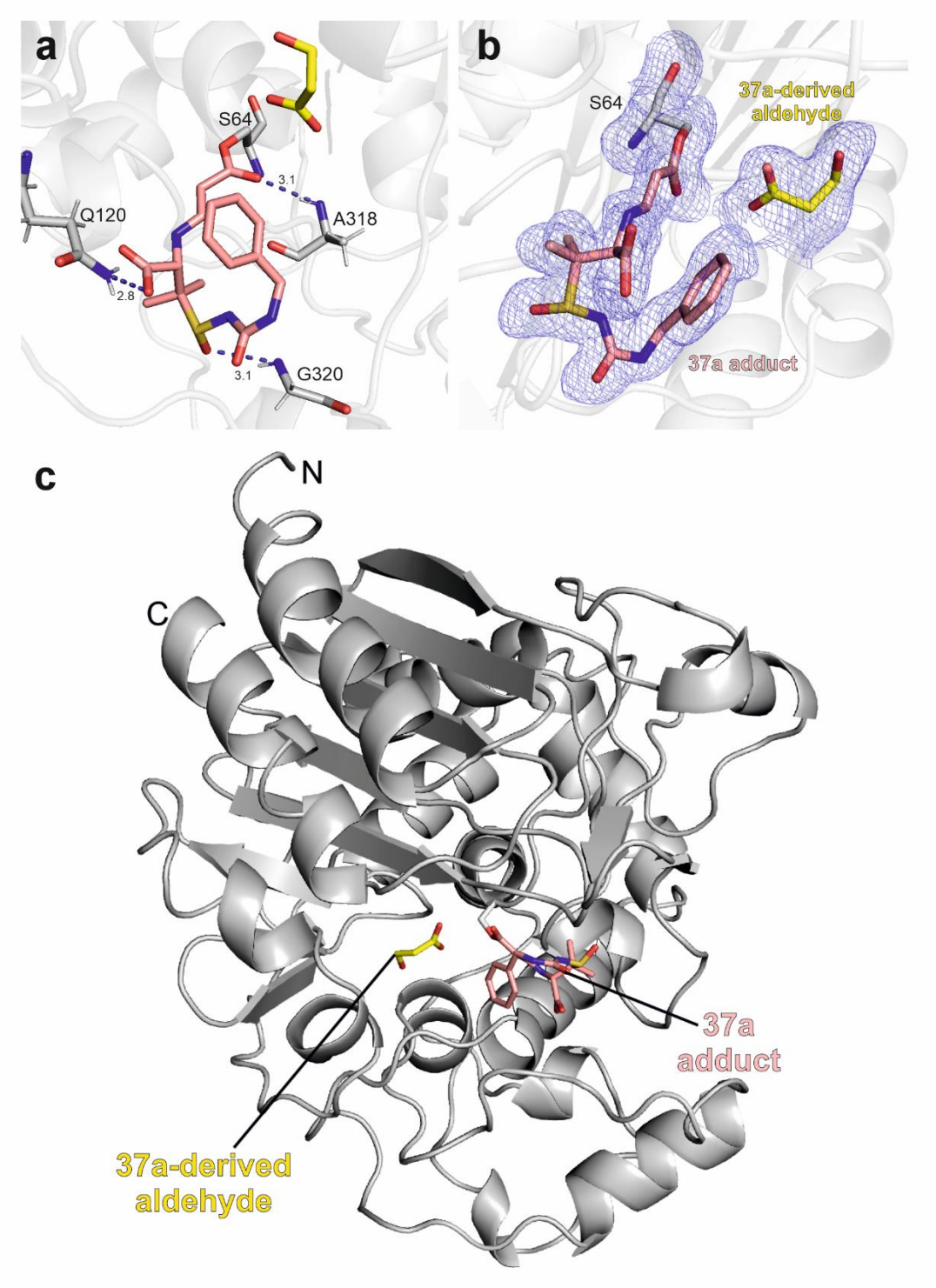

Figure 4.4-1. Crystal structure of penam-sulfoximine **37a** covalently reacted with the nucleophilic serine of AmpC. **a**) View from a crystal structure of *E. coli* AmpC incubated with **37a** for 10 min (PDB: 9I5D, 1.43 Å resolution). **b**) Polder map showing electron density of the AmpC: **37a** adduct and, likely the **37a**-derived aldehyde. Contour level 1.0 σ. **c**, Zoomed out view of **a**. Distances shown in **a** are in Å.

Analysis of the electron density maps confirmed formation of a covalent AEC via nucleophilic attack of the active-site Ser64 on the β-lactam of **37a**. The electron density further revealed fragmentation of the thiazolidine sulfoximine ring to generate a *trans*-enamine sulfinamide species bound to AmpC (**Figure 4.4-2**). Notably, the absolute configuration at the sulfoximine sulfur atom was retained upon fragmentation, consistent with retention of configuration at the sulfoximine sulfur atom during acylation and subsequent rearrangement.

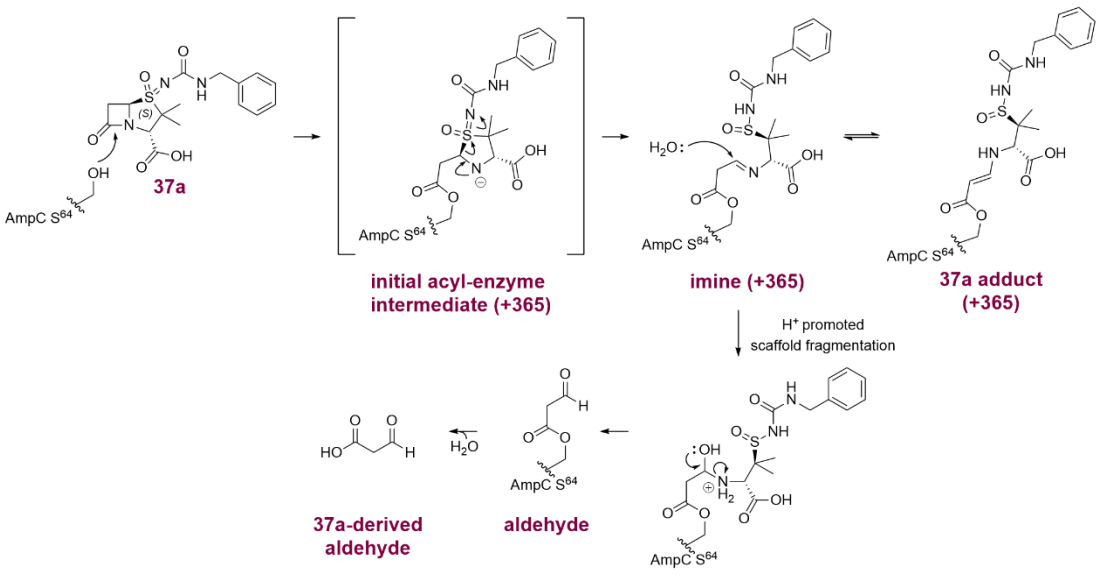

Figure 4.4-2. Outline mechanism for the covalent reaction of penam sulfoximine **37a** with nucleophilic S64 of AmpC.

Additional electron density was observed within the active site that may correspond to a low-occupancy hydrolysis product of the *trans*-enamine adduct, tentatively assigned as a **37a**-derived aldehyde. The presence of this species suggests that hydrolysis of the AmpC-bound *trans*-enamine adduct occurs, albeit slowly relative to the initial covalent acylation step. This interpretation is supported by SPE-MS analyses (**Figure 4.3-1**), which indicate low-level formation of an AmpC:**37a**-deverived aldehyde adduct compared to the dominant covalent AEC species. Together with mass spectrometric data, these observations support a reaction pathway analogous to those reported for

sulbactam and enmetazobactam, in which formation of a *trans*-enamine AEC represents the principal inhibitory species.[39]

The observed binding mode and stabilizing interactions in the AmpC:**37a** complex provide a structural rationale for the efficient formation and persistence of intact AECs observed by SPE-MS, reinforcing the central role of AEC stability in productive SBL inhibition.

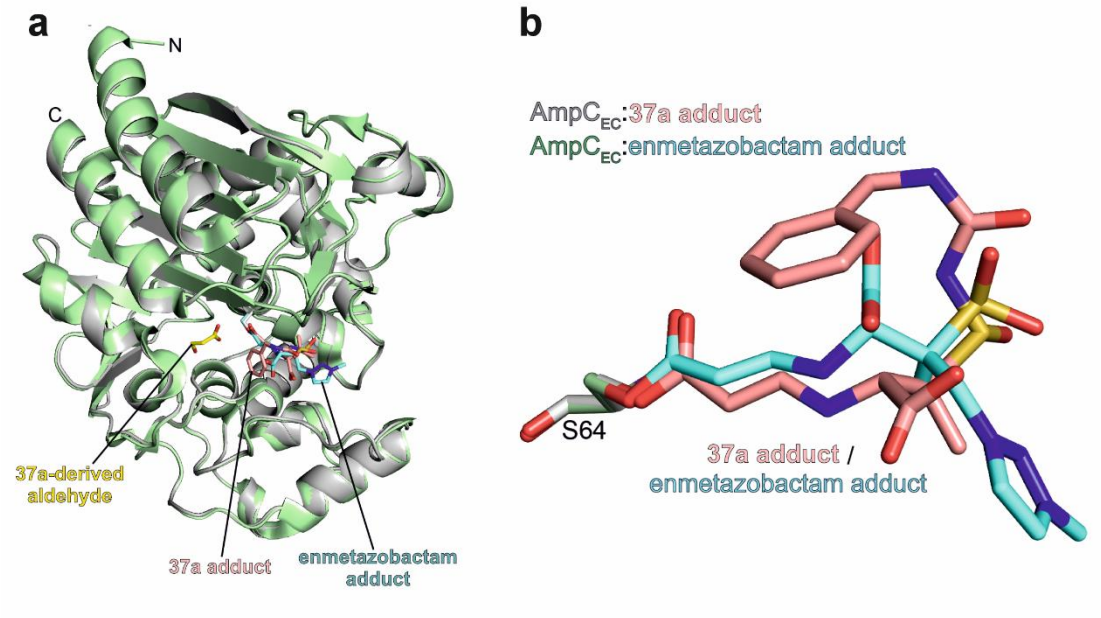

Figure 4.4-3. a) Overlay of the AmpC:**37a** adduct crystal structure (gray) with a reported AmpC:enmetazobactam complex crystal structure (green, PDB:6T35)[39] revealing similar overall AmpC folds (RMSD = 0.257 Å). **b**) Zoomed in overlay.

4.5 Stability of penam-sulfoximines

The hydrolytic stability of selected penam-sulfoximines was evaluated in phosphate buffer to assess their suitability for cellular inhibition assays. Compounds were incubated in phosphate buffer (50 mM, pH 7.4 or 6.0) at ambient temperature, with sulbactam included as a reference control. Stability was monitored by ^{1}H NMR analysis, with integrals of the characteristic H-5 and H-6 resonances quantified relative

to an internal standard to determine the percentage of intact β-lactam remaining over time (**Figure 4.5-1**).

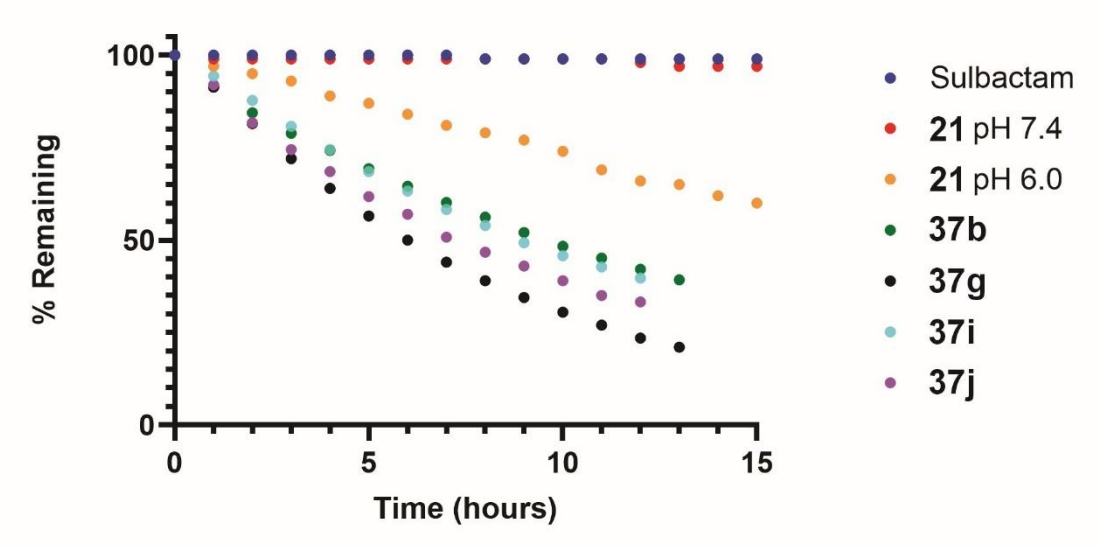

Figure 4.5-1. Stability of selected penam-sulfoximines in phosphate buffer.

Sulbactam and the unsubstituted sulfoximine **21** displayed high hydrolytic stability at pH 7.4, with minimal degradation observed over the duration of the experiment and estimated half-lives exceeding 15 h with over 95% remaining at the 15 h time point. Compound **21** exhibited a clear pH dependence, with accelerated degradation at pH 6.0 and an estimated half-life of approximately 16 h, indicating increased susceptibility to hydrolysis under mildly acidic conditions.

In comparison, urea-substituted sulfoximines showed substantially reduced stability. Compound **37b** exhibited moderate stability with an estimated half-life of 9 h at pH 7.4, whereas **37i** and **37j** degraded more rapidly, with half-lives of approximately 8-9 h and 6-7 h, respectively. The least stable compound, **37g**, displayed rapid hydrolysis with an estimated half-life of 5-6 h under the same conditions. These results indicate that urea substitution at the sulfoximine nitrogen generally compromises β-lactam

stability, with relatively small structural variations leading to pronounced differences in degradation rate.

Collectively, these data demonstrate that chemical stability is a key differentiating factor within the penam-sulfoximine series and likely contributes to the limited cellular activity observed for many urea-substituted derivatives despite their favorable biochemical potency. In contrast, the superior stability of compound **21** is consistent with its retained antibacterial activity in cellular assays, under scoring the importance of balancing β-lactamase inhibition with hydrolytic stability for effective antibacterial performance.

4.6 Penam sulfoximine derivatives inhibit clinically relevant *A. baumannii* strains

Since sulbactam (**6**) possess intrinsic antibacterial activity against *A. baumannii* (**Chapter 1**, **Section 1.4**), antimicrobial susceptibility testing (AST) was performed to evaluate whether penam-sulfoximines retain or improve upon this activity, both as single agents and in combination with the SBL inhibitor durlobactam (**11**)[61]. A panel of clinically isolated *A. baumannii* strains expressing diverse β-lactamases was examined, including strains harboring OXA-23, OXA-64, OXA-51, TEM-1, and NDM-1.

In the absence of durlobactam, penam-sulfoximine **21** displayed measurable intrinsic antibacterial activity (MICs < 4 μg/mL) against multiple *A. baumannii* strains and consistently outperformed sulbactam and durlobactam when tested individually (**Figure 4.6-1**). This observation indicates that **21** retains effective engagement of PBPs while exhibiting enhanced resilience toward SBL-mediated inactivation relative to sulbactam.

	A. Baumannii strain	β-Lactamases present	meropenem (μg/mL)	**6** (μg/mL)	**11** (μg/mL)	**21** (μg/mL)	**6 / 11** (μg/mL)	**21 / 11** (μg/mL)
Control strains	NCTC13304	TEM-1, OXA-23, OXA-66	>16	16	>16	>16	0.5/4	0.5/4
	ATCC19606	None	1	8-16	>16	8	1/4	1/4
	ATCC27853[c]	None	0.5	NA	NA	NA	NA	NA
SBL	KA1	OXA-23, OXA-144	>16	>16	>16	>16	1-2/4	1/4
	KA3	OXA-23, OXA-66	>16	>16	>16	>16	2-4/4	2/4
	KA4	OXA-23, OXA-64	>16	16	>16	8-16	1/4	0.5/4
	ACB 105	OXA-72, OXA-65, TEM-1A	>16	>16	>16	16	2/4	1/4
	ACB110	OXA-72, OXA-65, TEM-1A	>16	8	>16	8	2/4	1/4
	ACB120	OXA-72, OXA-65, TEM-1A	>16	16	>16	8	1-2/4	1/4
	ACB129	OXA-72, OXA-65, TEM-1A	>16	>16	>16	>16	1-2/4	1/4
	ACB37	OXA-72, OXA-64, OXA-23	>16	16	>16	2	1/4	0.5/4
	ACB41	OXA-72, OXA-64, OXA-23	>16	16	>16	4	2/4	1/4
	ACB42	OXA-231, OXA-51	>16	8	>16	4	2/4	1/4
	ACB71	OXA-72, OXA-65, TEM-1A	>16	16	>16	8-16	2/4	1/4
	ACB73	OXA-231, OXA-51	>16	8	>16	4	1/4	1/4
	ACB85	OXA-72, OXA-65, TEM-1A	>16	8-16	>16	8	2/4	0.5/4
	ACB96	OXA-72, OXA-65, TEM-1A	>16	8	>16	8-16	2/4	1/4
	ACB103	OXA-72, OXA-65, TEM-1A	>16	16	>16	16	2/4	1/4
	ACB117	OXA-72, OXA-65, TEM-1A	>16	4-8	>16	4	1/4	0.5/4
	ACB118	OXA-72, OXA-64, OXA-23	>16	8-16	>16	2	1/4	0.5/4
	ACB128	OXA-72, OXA-64, OXA-23	>16	16	>16	2	1/4	1/4
MBL	KA10	NDM-1, OXA-98	>16	>16	>16	8-16	8-16/4	4/4
	BRA5	IMP-1	>16	16	>16	8-16	2/4	1/4
	BRA8[a]	IMP-1	>16	4	>16	4	1-2/4	1/4
	BRA9[b]	IMP-1	>16	1	8	0.25-0.5	0.25/4	0.25/4

Figure 4.6-1. Effects of penam-sulfoximine **21**/durlobactam (**11**) combinations on clinically isolated *A. baumannii* strains with sulbactam (**6**) for comparison. [a] denotes *A. nosocomiales*. [b] denotes *A. bereziniae*. [c] denotes *P. aeruginosa*. Sulbactam/durlobactam (CLSI Breakpoint): 4/4 – susceptible (green), 8/4 – intermediate (yellow), 16/4 – resistant (red). NCTC13304 (QC range CLSI): 0.5/4 – 2/4.[161] AST was performed in independent duplicates for all compounds. See **Chapter 6.1.6** for assay details.

Across a broad set of SBL-producing clinical isolates, the **21**/durlobactam combination showed antibacterial activity that was comparable to, and in several cases superior to, the clinically used sulbactam/durlobactam regimen. Improved activity was particularly evident against strains expressing OXA-72, OXA-65, and TEM-1A (*e.g.* ACB71), where lower MIC values were consistently observed for the **21**/durlobactam

combination. Notably, enhanced efficacy was also observed against the highly resistant KA10 strain, which expresses SBL OXA-98 and the MBL NDM-1. While this strain exhibited poor susceptibility to sulbactam/durlobactam, the **21**/durlobactam combination achieved 2- to 4-fold reduction in MIC, demonstrating improved antibacterial activity in a background that includes both SBL- and MBL-mediated resistance mechanisms.

The superior standalone activity of **21**, together with its enhanced performance when paired with durlobactam, suggests that **21** achieves more effective PBP inhibition while also displaying improved tolerance to SBL-mediated degradation. The ability **21**/durlobactam combination to retain activity against highly resistant clinical isolates, including those harboring both OXA-type enzymes and NDM-1, highlights its potential as a promising candidate for development of improved treatments for multi-drug resistant *A. baumannii* infections.

To further delineate the structural features required for antibacterial activity, additional penam-sulfoximine derivatives (**34b, 37b, 37e,** and **37f**) were evaluated in combination with durlobactam against the same panel of clinically isolated *A. baumannii* strains (**Figure 4.6-2**). In contrast to **21**, none of these analogues displayed measurable antibacterial activity when combined with durlobactam, with MIC values remaining >16 μg/mL across both SBL- and MBL-producing strains. These results indicate that the enhanced activity observed for **21** is not a general feature of the penam-sulfoximine scaffold, but instead depends on specific structural and physicochemical properties.

	A. Baumannii strain	β-Lactamases present	meropenem (μg/mL)	**34b** / durlobactam (μg/mL)	**37b** / durlobactam (μg/mL)	**37e** / durlobactam (μg/mL)	**37f** / durlobactam (μg/mL)
Control strains	NCTC13304	TEM-1, OXA-23, OXA-66	>16	>16/4	>16/4	>16/4	>16/4
	ATCC25922[d]	None	<0.125	<0.125/4	<0.125/4	<0.125/4	<0.125/4
	ATCC27853[c]	None	0.5	NA	NA	NA	NA
SBL	KA1	OXA-23, OXA-144	>16	>16/4	>16/4	>16/4	>16/4
	KA3	OXA-23, OXA-66	>16	>16/4	>16/4	>16/4	>16/4
	KA4	OXA-23, OXA-64	>16	>16/4	>16/4	>16/4	>16/4
	ACB 105	OXA-72, OXA-65, TEM-1A	>16	>16/4	>16/4	>16/4	>16/4
	ACB110	OXA-72, OXA-65, TEM-1A	>16	>16/4	>16/4	>16/4	>16/4
	ACB120	OXA-72, OXA-65, TEM-1A	>16	>16/4	>16/4	>16/4	>16/4
	ACB129	OXA-72, OXA-65, TEM-1A	>16	>16/4	>16/4	>16/4	>16/4
	ACB37	OXA-72, OXA-64, OXA-23	>16	>16/4	>16/4	>16/4	>16/4
	ACB41	OXA-72, OXA-64, OXA-23	>16	>16/4	>16/4	>16/4	>16/4
	ACB42	OXA-231, OXA-51	>16	>16/4	>16/4	>16/4	>16/4
	ACB71	OXA-72, OXA-65, TEM-1A	>16	>16/4	>16/4	>16/4	>16/4
	ACB73	OXA-231, OXA-51	>16	>16/4	>16/4	>16/4	>16/4
	ACB85	OXA-72, OXA-65, TEM-1A	>16	>16/4	>16/4	>16/4	>16/4
	ACB96	OXA-72, OXA-65, TEM-1A	>16	>16/4	>16/4	>16/4	>16/4
	ACB103	OXA-72, OXA-65, TEM-1A	>16	>16/4	>16/4	>16/4	>16/4
	ACB117	OXA-72, OXA-65, TEM-1A	>16	>16/4	>16/4	>16/4	>16/4
	ACB118	OXA-72, OXA-64, OXA-23	>16	>16/4	>16/4	>16/4	>16/4
	ACB128	OXA-72, OXA-64, OXA-23	>16	>16/4	>16/4	>16/4	>16/4
MBL	KA10	NDM-1, OXA-98	>16	>16/4	>16/4	>16/4	>16/4
	BRA5	IMP-1	>16	>16/4	>16/4	>16/4	>16/4
	BRA8[a]	IMP-1	>16	>16/4	>16/4	>16/4	>16/4
	BRA9[b]	IMP-1	>16	>16/4	>16/4	>16/4	>16/4

Figure 4.6-2. Effects of select penam-sulfoximines/durlobactam combinations on clinically isolated *A. baumannii* strains. [a] denotes *A. nosocomiales*. [b] denotes *A. bereziniae*. [c] denotes *P. aeruginosa*. [d] denotes *E. coli*. Sulbactam/durlobactam (CLSI Breakpoint): 4/4 – susceptible (green), 8/4 – intermediate (yellow), 16/4 – resistant (red). NCTC13304 (QC range CLSI): 0.5/4 – 2/4.[161] AST was performed in independent duplicates for all compounds. See **Chapter 6.1.6** for assay details.

The lack of activity observed for the other sulfoximines likely reflects a combination of insufficient engagement of *A. baumannii* PBPs and unfavorable cellular accumulation, potentially due to reduced penetration and/or increased efflux. In

addition, compound stability appears to be a critical differentiating factor and likely contributes to the lack of antibacterial activity in cellular assays (**Figure 4.5-1**).

Taken together, these data suggests that the superior performance of **21** arises from a favorable combination of intrinsic antibacterial activity and sufficient chemical stability under physiological conditions. The absence of activity for related sulfoximines underscores the sensitivity of antibacterial efficacy to subtle structural modifications within this scaffold and highlights the importance of balancing β-lactamase inhibition and stability.

4.7 Summary

This chapter describes the biological activity and inhibition mechanism of a series of penam-sulfoximine derivatives. Collectively, these studies establish clear structure–activity relationships within this scaffold and identify key features required for productive inhibition of SBLs *in vitro* and antibacterial efficacy against clinically isolated *A. baumannii* strains.

Biochemical inhibition assays demonstrated that while unsubstituted and many *N*-substituted penam-sulfoximines exhibit inhibition profiles overall similar to sulbactam, urea-substituted derivatives display markedly enhanced potency against class A, C, and D SBLs, in several cases approaching or exceeding the potency of avibactam (**9**), a DBO-based SBL inhibitor much more recently developed compared to sulbactam. SPE-MS analyses revealed that these potency differences correlate with the efficiency of covalent AEC formation, with more potent inhibitors exhibiting more rapid and complete formation of intact AECs. In contrast, unsubstituted sulfoximine **21** showed limited AEC formation, consistent with weaker inhibition and/or rapid adduct hydrolysis and reported data for sulbactam.

Crystallographic analysis of the AmpC:**37a** complex provided direct structural insight into the covalent inhibition mechanism of penam-sulfoximines. The structure confirmed formation of a covalent AEC via nucleophilic attack of the active-site serine, followed by fragmentation to a *trans*-enamine sulfinamide species. The observed binding mode and stabilizing interactions are similar to those reported for clinically used sulbactam and enmetazobactam, an observation supporting a conserved mechanistic pathway for this inhibitor class.

Despite their favorable biochemical potency, many urea-substituted penam-sulfoximines exhibited reduced hydrolytic stability in aqueous buffer, which likely limits their suitability for cellular applications. Consistent with this observation, only the unsubstituted sulfoximine **21** displayed measurable intrinsic antibacterial activity against clinically isolated *A. baumannii* strains, both as a single agent and in combination with durlobactam. Notably, the **21**/durlobactam combination demonstrated antibacterial activity comparable to, and in several cases superior to, the clinically used sulbactam/durlobactam combination across a broad panel of multidrug-resistant clinical isolates, including strains harboring both SBLs and MBLs.

Overall, these findings highlight the delicate balance between SBL inhibition, chemical stability, and cellular activity within the penam-sulfoximine scaffold. While urea substitution enhances biochemical potency, compromised stability and/or cellular accumulation limit antibacterial efficacy. In contrast, **21** achieves an optimal balance of intrinsic PBP inhibition, resistance to SBL-mediated degradation, and chemical stability, underpinning its superior cellular performance compared to the other tested penam sulfoximines. These results provide a framework for the design of next-generation penam-based inhibitors that integrate potent enzyme inhibition with favorable physicochemical properties required for antibacterial activity.

Chapter 5 | Summary and future work

5.1 Summary

This chapter integrates the chemical, biochemical, and microbiological findings described in **Chapters 2 – 4** of this thesis and outlines future directions for the development of sulfoximine-containing β-lactams. The key synthetic advances, structure–reactivity relationships, and biological insights established in **Chapters 2 – 4** are first summarized, with emphasis on how chemical stability and sulfoximine substitution govern biological performance. On the basis of these findings, future work is proposed to address remaining limitations, advance promising lead compounds, and extend the sulfoximine strategy to additional clinically relevant β-lactam scaffolds.

Chapter 2 demonstrates that penam-sulfoximines derived from sulbactam are synthetically accessible in enantiopure form using modern Rh(II)-catalyzed nitrene transfer chemistry, and defines the scope and limitations of sulfoximine *N*-functionalization within the chemically sensitive penam framework.

Enantiopure (*S*)- and (*R*)-penam sulfoxides were reproducibly prepared from commercial 6-APA (**15**) (**Scheme 2.2-1**). For the (*S*)-series, stereoselective oxidation of the reduced 6-dihydropenam **18** with *m*CPBA at -78 °C afforded the (*S*)-sulfoxide **19** as a single diastereomer, whereas higher temperatures resulted in erosion of diastereoselectivity. In contrast, the (*R*)-sulfoxide **25** was accessed selectively via oxidation of a 6,6-dibromoinated precursor **23**, where steric shielding by bromine substituents enforced oxidant approach from the convex face (**Scheme 2.2-2**). These routes provided reliable access to both sulfoxide stereoisomers, establishing well-defined substrates for sulfoximine formation.

Rh(II)-catalyzed sulfoximine formation on the penam scaffold was shown to be feasible but highly sensitive to reaction conditions. Systematic optimization revealed that $Rh_2(OAc)_4$ in 1,2-dimethoxyethane at 40 °C gave the highest and most

reproducible conversions, reaching ~85–90% conversion by crude ^{1}H NMR analysis (**Table 2.3-1**).

Direct access to the *NH*-penam sulfoximine **32** proved challenging. A reliable two-step strategy was developed, in which *Cbz*-protected sulfoximines were first generated in high yield and then selectively deprotected by hydrogenolysis, affording the *NH*-sulfoximine in ~50% isolated yield (**Figure 2.4-1**).

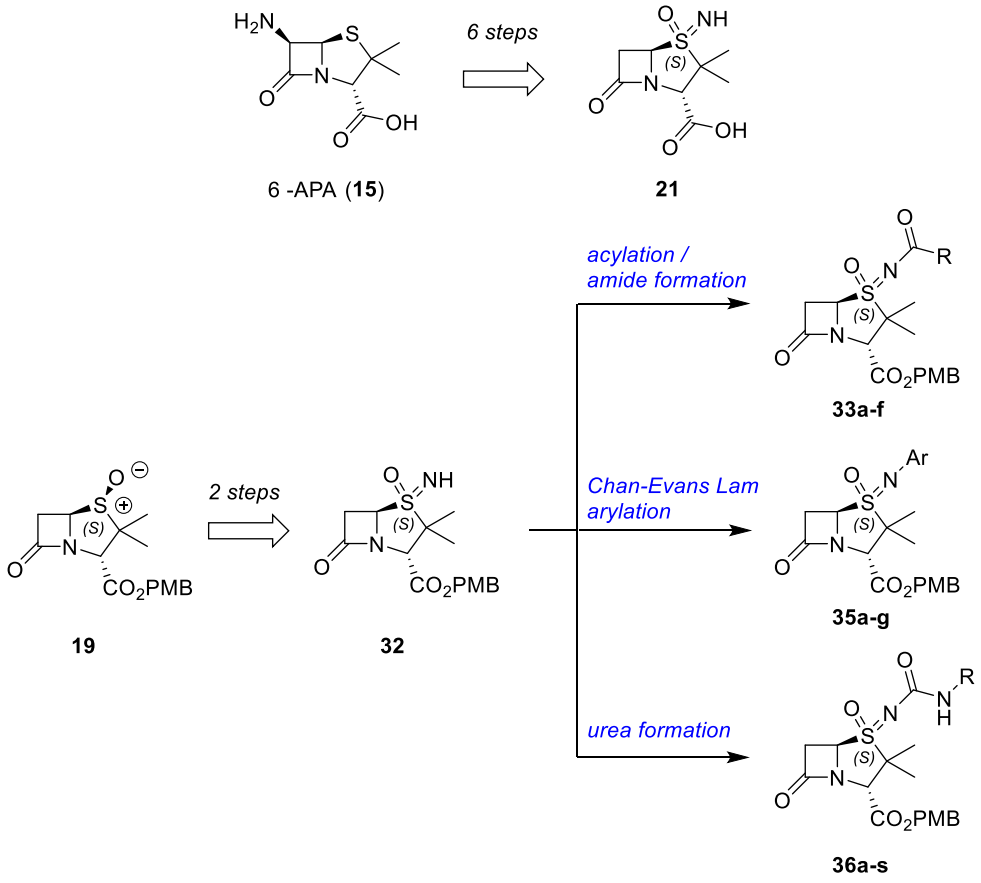

Figure 5.1-1. Summary of successful penam-sulfoximine *NH* functionalization.

The *NH*-sulfoximine **32** was then used to systematically evaluate *N*-functionalization strategies. Amide bond formation proved highly reliable: acyl chlorides furnished *N*-acyl sulfoximines in consistently high yields (77–99%), while carbodiimide-mediated coupling with carboxylic acids gave moderate yields (57–62%) (**Figure 5.1-1**). Urea formation with aryl and alkyl isocyanates was also successful, providing a broad series

of urea-functionalized sulfoximines in yields up to 67%. In contrast, Cu(II)-mediated Chan–Evans–Lam arylation was feasible but inefficient, affording *N*-aryl sulfoximines in low yields (9–28%).

Multiple alternative *N*-functionalization strategies were shown to be incompatible with the penam-sulfoximine scaffold. Direct *N*-alkylation using standard alkylating agents either failed to react or caused rapid degradation, often via base-mediated ring opening to sulfinamide species (**Figures 2.5-4** and **2.5-5**). Reductive amination, borane-mediated reduction of *N*-acyl sulfoximines, Michael additions to activated alkenes, and Mitsunobu reactions all failed under a wide range of conditions (**Figures 2.5-6 – 2.5-9**). These negative results demonstrate that, despite superficial similarity to sulfonamides or imides, penam *NH*-sulfoximines possess a distinct reactivity profile that severely limits the applicability of common nitrogen-functionalization chemistry. Overall, the results described in **Chapter 2** establish that sulbactam-derived penam sulfoximines can be prepared stereoselectively and diversified at the sulfoximine nitrogen, but only through a restricted set of chemically compatible transformations. The compound set generated – comprising *NH*, amide-, aryl-, and urea-substituted sulfoximines prepared in 6–8 steps from 6-APA – provided the structurally defined library required for subsequent biological evaluation.

Chapter 3 establishes the chemical boundaries governing carboxylate deprotection in sulfoximine-containing β-lactams and demonstrates that deprotection success is strongly dependent on both scaffold type and sulfoximine stereochemistry. Through systematic evaluation of protecting groups and cleavage conditions, this chapter identifies strategies that enable reliable access to penam-sulfoximine free acids while revealing intrinsic instability in the corresponding cephem series.

In the (*S*)-penam-sulfoximine series, commonly used *C2* protecting groups displayed markedly different behavior under standard deprotection conditions. Benzhydryl esters proved unsuitable: catalytic hydrogenolysis failed to effect cleavage, while acidic or basic conditions led exclusively to rapid β-lactam degradation, preventing isolation of the free acid (**Figure 3.2-1**). PNB esters underwent efficient hydrogenolysis in aprotic solvents such as THF and ethyl acetate, affording the desired free acid; however, reactions conducted in methanol resulted in extensive decomposition, indicating that the liberated acid is unstable in protic, nucleophilic media (**Figure 3.2-2**). Biphenyl methyl esters were similarly cleaved under hydrogenation conditions, though deprotection required longer reaction times and was accompanied by minor degradation in protic solvents (**Figure 3.2-3**). In contrast, PMB esters exhibited consistently superior performance. Hydrogenolysis of PMB-protected penam-sulfoximines proceeded rapidly and cleanly under mild conditions in aprotic solvents, affording the corresponding free acids without detectable β-lactam ring opening (**Figure 3.2-4**). These results establish PMB as the optimal *C2* protecting group for (*S*)-penam sulfoximines and rationalize its adoption for all subsequent late-stage transformations.

Despite successful deprotection, the free acid forms of penam-sulfoximines were found to be intrinsically unstable. Even under frozen storage conditions, measurable degradation was observed by ^{1}H NMR, consistent with autocatalytic β-lactam hydrolysis promoted by intramolecular protonation from the carboxylate. Conversion of the (*S*) free acids into their sodium or potassium salts using 2-ethylhexanoate counterions dramatically improved stability, with no detectable degradation observed after prolonged storage at sub-zero temperatures. This transformation proved essential for compound handling and downstream biological evaluation.

Deprotection of (*R*)-configured penam-sulfoximines was significantly less successful than for the (*S*)-diastereomers. Under conditions that cleanly deprotected the corresponding (*S*)-diastereomers, (*R*)-penam sulfoximines showed minimal conversion, even at elevated catalyst loadings, and were prone to decomposition (**Figure 3.4-1**). Partial formation of the free *NH* (*R*)-sulfoximine **48** was observed in some cases, but further hydrogenolysis to the free acid could not be achieved reproducibly. Crystallographic analysis revealed a conformation in which the sulfoximine nitrogen is oriented toward the β-lactam core, providing a plausible structural basis for catalyst inhibition or steric shielding during hydrogenation (**Figure 3.4-2**).

Notably, in the (*R*)-configured sulfoximine **48**, the *NH* is positioned such that it may participate in a hydrogen-bonding network bridging a bound water molecule to the β-lactam carbonyl. This geometry could facilitate water activation and lower the energetic barrier for β-lactam hydrolysis, providing a structural rationale for the enhanced chemical lability observed for (*R*)-configured free acids.[162] These findings demonstrate a pronounced stereochemical dependence in penam-sulfoximine deprotection that limits the synthetic accessibility of (*R*)-configured free acids.

Extension of the deprotection strategy to the cephem scaffold revealed more severe limitations. Although both (*S*)- and (*R*)-cephem-sulfoximines could be synthesized efficiently via oxidation and Rh(II)-catalyzed nitrene transfer, hydrogenolytic removal of PMB esters consistently failed, regardless of solvent, catalyst, or loading (**Figure 3.5-3**). Alternative protecting groups, including PNB, allyl, Fmoc, methyl, and TMSE esters, were also incompatible: either sulfoximine formation was inhibited during synthesis or deprotection led exclusively to degradation (**Figures 5.3-5 – 5.3-6**). Nucleophilic, reductive, and fluoride-mediated ester cleavage strategies uniformly

resulted in rapid β-lactam breakdown, indicating that the deprotected cephem-sulfoximine acid is intrinsically unstable under all conditions tested.

Collectively, the results described in **Chapter 3** demonstrate that penam- and cephem-sulfoximines differ fundamentally in their chemical robustness. While PMB-protected (*S*)-penam-sulfoximines can be reliably deprotected and stabilized as alkali metal salts, (*R*)-penam analogues and all cephem-sulfoximines exhibit deprotection behavior dominated by degradation. These findings define a clear synthetic boundary for β-lactam sulfoximines and establish the (*S*)-penam scaffold as the only viable platform for late-stage deprotection and biological evaluation.

The results of **Chapter 4** establish clear structure–activity relationships within the penam-sulfoximine scaffold and identifies the key determinants governing productive SBL inhibition and antibacterial efficacy. Through a combination of biochemical inhibition assays, stability studies, mass spectrometric analyses, crystallography, and antimicrobial susceptibility testing, this chapter demonstrates that sulfoximine *N*-substitution strongly modulates enzyme inhibition potency, AEC stability, and cellular activity.

Biochemical inhibition assays against representative class A (TEM-116), class C (AmpC), and class D (OXA-10 and OXA-48) SBLs revealed that the unsubstituted penam-sulfoximine **21** exhibits inhibitory activity broadly comparable to sulbactam (**6**) across all enzyme classes (**Figure 4.2-2**). In contrast, urea-substituted penam-sulfoximines showed markedly enhanced potency, with several derivatives achieving pIC_{50} values approaching or exceeding those of avibactam (**9**), a clinically advanced diazabicyclooctane inhibitor. These data demonstrate that substitution at the sulfoximine nitrogen can substantially enhance SBL inhibition without abolishing recognition of the penam core by the enzyme active site.

SPE-MS analysis provided mechanistic insight into these potency differences. Urea-substituted sulfoximines formed intact covalent AECs more rapidly and completely than the unsubstituted analogue, consistent with their enhanced inhibitory activity. In contrast, sulfoximine **21** displayed limited accumulation of intact AECs, suggesting either slower acylation or more rapid adduct hydrolysis, behavior closely resembling that reported for sulbactam. These findings establish AEC formation efficiency as a key mechanistic determinant of enzyme inhibition potency within the penam-sulfoximine series (**Figures 4.3-1 – 4.3-2**).

Crystallographic analysis of the AmpC:**37a** complex confirmed that penam-sulfoximines inhibit SBLs via a conserved covalent mechanism (**Figure 4.4-1**). The structure revealed nucleophilic attack of the active-site serine on the β-lactam carbonyl, followed by fragmentation to a *trans*-enamine sulfinamide species. The observed binding mode and stabilizing interactions closely resemble those reported for sulbactam and enmetazobactam, supporting a shared mechanistic pathway and demonstrating that sulfoximine substitution does not disrupt productive engagement of the penam scaffold within the enzyme active site (**Figures 4.4-2** and **4.4-3**).

Despite their favorable biochemical potency, urea-substituted penam-sulfoximines exhibited reduced hydrolytic stability in aqueous buffer. Whereas sulbactam and the unsubstituted sulfoximine **21** remained largely intact at pH 7.4 over the duration of the assay, urea-substituted derivatives showed substantially shorter half-lives, with degradation rates strongly dependent on substituent identity (**Figure 4.5-1**). This instability likely limits effective intracellular exposure and provides a mechanistic explanation for the disconnect observed between biochemical potency and cellular activity for many *N*-substituted sulfoximines.

Antimicrobial susceptibility testing against a panel of clinically isolated *Acinetobacter baumannii* strains revealed that only the unsubstituted penam-sulfoximine **21** displayed measurable intrinsic antibacterial activity, both as a single agent and in combination with durlobactam (**Figure 4.6-1**). Notably, the **21**/durlobactam combination demonstrated antibacterial efficacy comparable to, and in several cases exceeding, that of the clinically used sulbactam/durlobactam regimen, including against strains harboring both SBLs and MBLs. In contrast, urea-substituted sulfoximines showed little or no cellular activity, consistent with their reduced chemical stability and likely compromised accumulation (**Figure 4.6-2**).

Collectively, the results of **Chapter 4** demonstrate that effective antibacterial activity within the penam-sulfoximine series requires a delicate balance between SBL inhibition potency, AEC stability, chemical robustness, and cellular compatibility. While urea substitution enhances biochemical inhibition, compromised stability limits translation to cellular efficacy. In contrast, the unsubstituted sulfoximine **21** achieves a productive balance of intrinsic antibacterial activity, resistance to SBL-mediated degradation, and chemical stability, underpinning its superior performance in cellular assays. Although penam-sulfoximines were initially evaluated as SBL inhibitors, the cellular activity of compound **21** is best explained by PBP inhibition, distinguishing it mechanistically from the more potent but less stable *N*-substituted analogues. These findings define key design principles for next-generation penam-based inhibitors that integrate potent enzyme inhibition with the physicochemical properties required for antibacterial activity.

5.2 Future work

Although the penam-sulfoximines synthesized in this work display potent inhibition of clinically relevant SBLs, most of these compounds exhibit insufficient stability under physiological conditions to be viable SBL inhibitors.[163] However, rapid degradation of most sulfoximine-containing penams under physiological conditions limits their applicability in biological settings, with the notable exception of the free *NH* sulfoximine **21**, which demonstrated enhanced stability relative to its *N*-substituted derivatives. These observations highlight the need to balance chemical stability with inhibitory potency in further development of sulfoximine-containing β-lactams.

Future synthetic efforts should therefore focus on modifying the sulfoximine-containing penam scaffold to improve chemical stability while preserving biological activity. In particular, removal of the carbonyl group α to the sulfoximine nitrogen represents a promising strategy. This electron-withdrawing carbonyl is likely to increase the electrophilicity of the β-lactam ring, rendering the scaffold more susceptible to hydrolysis under physiological conditions. Attenuation of this effect may reduce β-lactam ring opening and improve overall stability. However, the synthesis of such analogues presents significant challenges as discussed in **Chapter 2**.

Penam-sulfoximine **21** represents a viable lead for further biological evaluation against *A. baumannii*. Unlike the less stable *N*-substituted sulfoximines, **21** acts as a PBP inhibitor and retains sufficient stability to warrant progression beyond enzyme-level studies. Evaluation of **21** against a panel of *A. baumannii* clinical isolates, including strains harboring the most prevalent resistance determinants such as OXA-23, chromosomal AmpC, and OXA-51, will be critical to determine whether PBP inhibition translates into meaningful whole-cell antibacterial activity in resistant backgrounds.[26]

Further studies should also examine the frequency and mechanisms of resistance to compound **21**. While resistance to PBP-targeting agents can arise through alterations in target PBPs or changes in cell wall metabolism, such pathways are often constrained by essentiality and fitness costs.[164] Given that resistance in *A. baumannii* is more commonly driven by acquisition or overexpression of β-lactamases, resistance emerging specifically against the sulfoximine scaffold may occur at low frequency; however, this hypothesis requires experimental validation through serial passaging and frequency-of-resistance assays.[26, 165]

Finally, advancement of compound **21** into preliminary ADME characterization is an essential step toward its *in vivo* evaluation. Assessment of metabolic stability in mouse liver microsomes, aqueous solubility, and cytotoxicity will help define the pharmacokinetic liabilities of the scaffold and guide optimization efforts.[166, 167] Compounds exhibiting acceptable *in vitro* profiles could then be progressed to murine infection models to evaluate *in vivo* efficacy and exposure–response relationships.[168, 169]

Encouraged by the potent activity observed for the sulbactam-derived penam-sulfoximine series, extension of the sulfoximine replacement strategy to other clinically relevant β-lactam scaffolds was pursued. Tazobactam represents a particularly attractive target for such modification, as it is a widely used penam-based β-lactamase inhibitor whose sulfone functionality is central to its mechanism of action. Replacement of the sulfone moiety with a sulfoximine therefore offers the potential to modulate chemical stability and reactivity while preserving the core penam framework. On this basis, synthesis of tazobactam-derived sulfoximines was undertaken to evaluate the generality of sulfoximine substitution across clinically important β-lactam scaffolds.

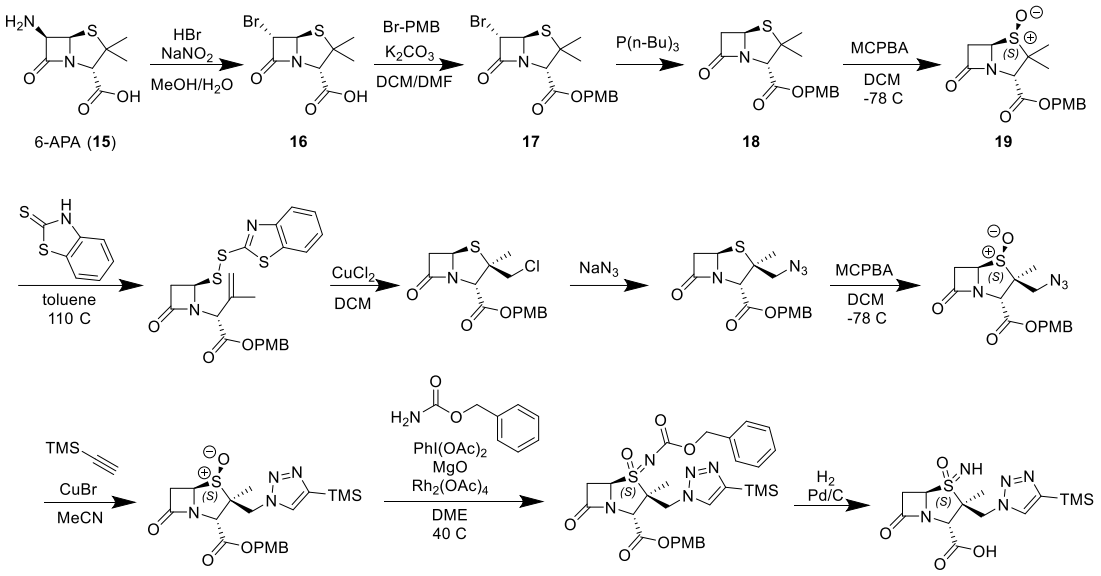

Figure 5.2-1. 11-step synthesis of tazobactam-derived (*S*)-penam sulfoximine. This synthetic work was carried out by Ben Spivey and is described in detail in his Part II master's thesis.

Initial efforts to extend the sulfoximine replacement strategy to the tazobactam scaffold were undertaken by Ben Spivey, a Part II student whom I supervised during the 2024–2025 academic year. An 11-step synthetic route to a tazobactam-derived penam-sulfoximine was designed and successfully executed, and this work is described in detail in the corresponding master's thesis (**Figure 5.2-1**). Although installation of the sulfoximine moiety was achieved, isolation of the fully deprotected target compound proved unsuccessful due to substantial instability during the final deprotection steps, precluding further biological evaluation.

Subsequently, an alternative and more concise strategy for introduction of the triazole moiety was developed (**Figure 5.2-2**). Rather than installing the triazole at an early stage, sulfoxide **19** was directly reacted with 2-trimethylsilyl triazole, enabling late-stage functionalization to afford intermediate **78**. Oxidation of **78** with *m*CPBA proceeded smoothly to give the corresponding sulfoxide **79**. Notably, Rh(II)-catalyzed nitrene transfer from **79** resulted in formation of the desired sulfoximine, with product **80** detected by mass spectrometry.

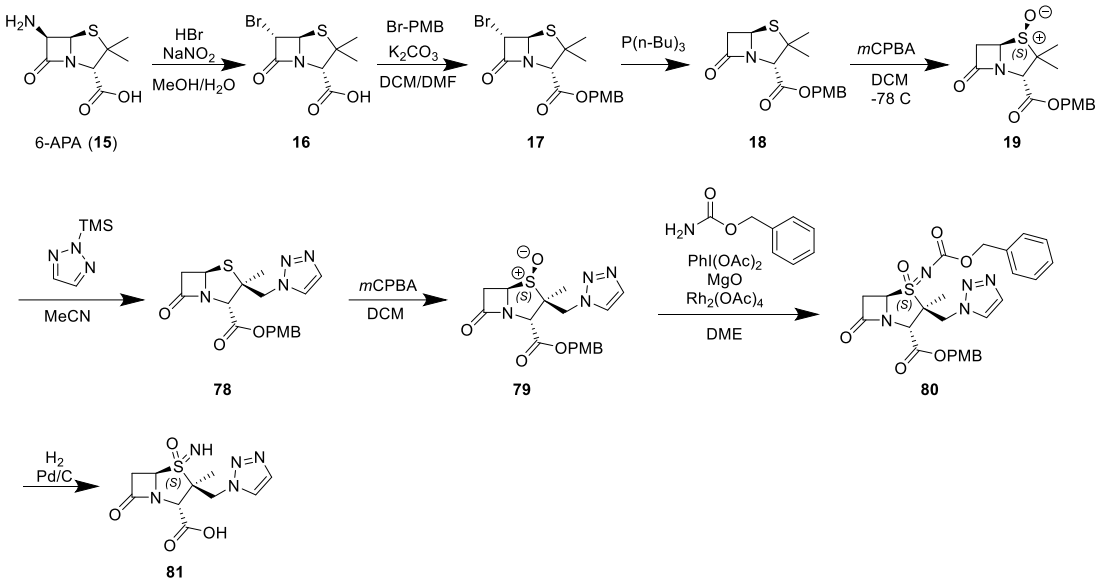

Figure 5.2-2. Proposed 8-step synthesis of tazobactam-derived (*S*)-penam sulfoximine **81**.

Despite successful sulfoximine formation, attempts to isolate compound **80** were unsuccessful due to rapid degradation during purification, particularly upon exposure to silica gel. This behavior mirrors the instability observed for other highly functionalized sulfoximine β-lactams and suggests that the tazobactam-derived sulfoximine lies near the stability limit of the scaffold under standard chromatographic conditions.

Future work will therefore focus on mitigating degradation during purification to enable isolation and full characterization of tazobactam-derived sulfoximines. Given the pronounced sensitivity of these compounds to silica gel, alternative purification strategies will be explored, including chromatography on neutral alumina and deacidification of silica through the addition of basic modifiers such as triethylamine to the elution solvent. Implementation of these approaches may allow isolation of the sulfoximine products without compromising structural integrity and facilitate subsequent evaluation of their chemical and biological properties.

Chapter 6 | Materials and Methods

6.1 Biochemical procedures

6.1.1 Enzyme production

Recombinant *E. Coli* AmpC, TEM-116, OXA-10, and OXA-48 were produced and purified (>90% by SDS-PAGE and MS) as reported.[170, 171]

6.1.2 SBL inhibition studies

The effects of penam-sulfoximine derivatives on AmpC (0.5 nM), TEM-116 (1 nM), OXA-10 (0.25 nM) and OXA-48 (12.5 nM) catalysis were determined as reported.[157] In brief, SBLs were incubated at room temperature in reaction buffer (50 mM phosphate buffer (pH 7.5), 0.01% (v/v) Triton X-100) with inhibitor for 10 min; for OXA-10 and OXA-48, the reaction buffer was supplemented with sodium bicarbonate (50 mM). Reactions were initiated by the addition of the reported fluorogenic substrate FC-5 (5 μM)[157] and immediately monitored by assessing fluorescence intensity at λ_{ex} = 380 nm and λ_{ex} = 460 nm over a period of 30-45 min using a BMG LABTECH Clariostar or a Pherastar plate reader. Initial reaction rates were determined, and analyzed by nonlinear regression using Prism 5 (GraphPad) to determine IC_{50} values (in independent duplicates each consisting of technical quadruplicates).

6.1.3 SPE-MS assays

SPE-MS assays were performed and analyzed as described,[39] using an Agilent RapidFire365 system coupled to an Agilent 6550 Accurate Mass QTOF spectrometer. SBL solutions were buffer exchanged into 50 mM Tris (pH 7.5) prior to analysis. Substrate/inhibitor (10 μM) was added to the SBL solution (1 μM). After the indicated time, 50 μL of the solution was injected onto a C4 SPE cartridge, washed, then eluted into the mass spectrometer.

6.1.4 AmpC crystallization and data collection

AmpC was crystallized using a modification of a reported protocol[39]: AmpC (25 mg/mL, in: 50 mM Tris, pH 7.5) was added to precipitant solution 1.6M potassium phosphate (pH 8.8)) containing 1,000-fold diluted seeds crystals and allowed to crystallize using the hanging drop method, over a well of 500 µL precipitant solution. Crystals were transferred to a solution containing **37a** (10 mM) and glycerol (20% w/v) and were incubated at room temperature for 10 min prior to rapid freezing in liquid nitrogen and storage under cryogenic conditions. Data were collected at beamline i03 at Diamond Light Source, employing automatic data collection.

6.1.5 Crystallographic data processing

Crystallographic data were indexed and integrated with DIALS using xia2,[39] and scaled using Aimless. The complex structure was solved by molecular replacement using Phaser,[172] and a reported apo structure of AmpC as a search model (PDB ID: 6T35).[39] Alternating cycles of refinement using REFMAC[173] and manual model building using COOT[174] were performed iteratively. Processing and refinement statistics are in **Appendix 7.5**. The wwPDB pdb extract tool was used to prepare coordinate and structure factor files in mmCIF format ready for deposition.[175]

6.1.6 Antimicrobial susceptibility testing

Antimicrobial susceptibility testing (AST) was performed by the Muller Hinton (Millipore, USA) agar dilution method according to the Clinical Laboratory Standards Institute (CLSI) guideline. MICs were interpreted using CLSI breakpoints[176] for all antimicrobial agents except those for which CLSI breakpoints are not available. Bacterial inocula were prepared from fresh overnight cultures and adjusted to a

turbidity equivalent to a 0.5 McFarland standard (approximately 1 x 10^8 CFU/mL), followed by dilution to achieve a final inoculum of ~1 x 10^4 CFU per spot on agar plates, as recommended by CLSI. Plates were incubated at 35–37°C for 16–20 h prior to MIC determination. Meropenem was used as a control for carbapenemase-producing bacteria. Quality control testing was performed according to CLSI using *P. aeruginosa* ATCC 27853, and *A. baumannii* NCTC 13304 strains1. *A. baumannii* ATCC 19606 was used as a meropenem susceptible control. The MIC quality control range was 0.125 to 16 μg/mL for meropenem, sulbactam, durlobactam, avibactam and **21**; and 0.125/4 to 16/4 μg/mL for sulbactam/durlobactam, **17**/durlobactam, sulbactam/avibactam and **21**/avibactam. AST was performed in independent duplicates for all compounds.

6.2 Chemical synthesis

6.2.1 General synthetic information

Reagents were from commercial suppliers (Sigma-Aldrich, Inc.; Fluorochem Ltd; Alfa Aesar; Tokyo Chemical Industry) and were used as received. Anhydrous solvents were from Sigma-Aldrich, Inc. and kept under an atmosphere of N_2. All reactions were carried out under an atmosphere of N_2 unless stated otherwise. Purifications were performed with an automated Biotage Selekt purification machine using Biotage® Sfär Silica D Duo or Biotage® Sfär C18 D Duo Ultra flash chromatography cartridges. The cartridge size and solvent gradients used are specified in the individual experimental procedures. High-Performance Liquid Chromatography (HPLC) was performed with an automated ACCQ Prep HP 150 machine using XBridge® Prep C18 5μm OBD™ 19 x 250 mm column. HPLC grade solvents were used for purifications, reaction work-ups, and extractions.

Thin-layer chromatography (TLC) was carried out using Merck silica gel 60 F_{254} TLC plates and visualized under UV light. Melting points (m.p.) were determined using a Stuart SMP-40 automated melting point apparatus with starting temperature of 50 °C, a ramp rate of 3 °C/min, and a final temperature of 250 °C. High-resolution mass spectrometry (HRMS) was performed using electrospray ionization (ESI) mass spectrometry (MS) operated in the positive or negative ionization modes using a Thermo Scientific Exactive mass spectrometer (ThermoFisher Scientific); data are presented as a mass-to-charge ratio (m/z). Nuclear magnetic resonance (NMR) spectra were recorded using a Bruker AV600 (600 MHz) or a Bruker AV400 (400 MHz), as stated in the individual experimental procedures. For ^{1}H NMR, chemical shifts are reported in parts per million (ppm) downfield from tetramethylsilane and are referenced to residual protium in the NMR solvent (*i.e.* $CDCl_3$: $\delta = 7.26$ ppm; CD_3OD-*d*$_4$: $\delta = 3.31$ ppm; DMSO-*d*$_6$: $\delta = 2.50$ ppm; CD_3CN: $\delta = 1.94$ ppm). For ^{13}C NMR, chemical shifts are reported in the scale relative to the NMR solvent (i.e., $CDCl_3$: $\delta =$ 77.06 ppm; CD_3OD-*d*$_4$: $\delta = 49.00$ ppm; DMSO-*d*$_6$: $\delta = 39.52$ ppm; CD_3CN: $\delta = 118.26$ and 1.32 ppm). Coupling constants are recorded to the nearest 0.1 Hz. Infrared (IR) spectroscopy was performed using a Bruker Tensor-27 Fourier transform infrared (FT-IR) spectrometer. Optical rotation (α) measurements were performed using a Unipol (Schmidt Haensch) polarimeter operated at 25 °C and using a wavelength (λ) of 589 nm (sodium D-lines).

6.3 General synthetic procedures

6.3.1 General Procedure A for ester synthesis

To a solution of a carboxylic acid (1.0 equiv.) in anhydrous 1:1 (v/v) dichloromethane/*N*,*N*-dimethylformamide (0.5 M) was added carefully potassium carbonate (0.9 equiv.), followed by a commercially-sourced alkyl bromide (1.1 equiv.), at ambient temperature and atmosphere. The reaction mixture was stirred at 38 °C for 1 h, then poured onto water and extracted three times with dichloromethane. The combined organic extracts were sequentially washed with water, a saturated aqueous $NaHCO_3$ solution, and brine, then dried over anhydrous Na_2SO_4, filtered, and evaporated. The crude residue was purified by flash column chromatography to afford the desired esters.[177]

6.3.2 General Procedure B for sulfoxide synthesis

To a solution of an ester (1.0 equiv.) in dichloromethane (0.1 M) was added dropwise a solution of *meta*-chloroperoxybenzoic acid (mCPBA) (0.98 equiv.) in dichloromethane at -78 °C under an ambient atmosphere. The reaction mixture was stirred for 16 h while it was slowly warmed from -78 °C to ambient temperature. The resultant suspension was sequentially washed with a 10% (v/v) aqueous $Na_2S_2O_3$ solution, a saturated aqueous $NaHCO_3$ solution, and brine, then was dried over anhydrous Na_2SO_4 and evaporated. The crude residue was purified by flash column chromatography to afford the desired sulfoxide.[95]

6.3.3 General Procedure C for sulfoximine synthesis

The sulfoximine forming reaction was optimized based on reported conditions (**Chapter 2**, **Section 2.3.1**).[178] To a solution of a sulfoxide ester (1.0 equiv.) in

anhydrous 1,2-dimethoxyethane (0.2 M) was sequentially added an amine (1.5 equiv.), (diacetoxyiodo)benzene (1.5 equiv.), magnesium oxide (2.0 equiv.), and rhodium (II) acetate dimer (0.05 equiv.) The reaction mixture was stirred at 40 °C for 16 h under a nitrogen atmosphere before being filtered using Celite®; the Celite® pad was eluted with dichloromethane. The combined filtrates were concentrated and purified by flash column chromatography to afford the desired sulfoximine.

6.3.4 General Procedure D for hydrogenation of esters

A round bottom flask was charged with a sulfoximine ester (1.0 equiv.) and 10% (w/w) Pd/C (0.2 – 1.0 equiv.) in an anhydrous solvent (0.1 M). The reaction mixture was evacuated and backfilled with hydrogen gas three times using a Schlenk line. The reaction mixture was stirred at ambient temperature for 3 – 9 h under a hydrogen atmosphere, then filtered using Celite®; the Celite® pad was eluted with dichloromethane, which was then removed *in vacuo*. The residue was redissolved in ethyl acetate before addition of sodium 2-ethylhexanoate (1.0 equiv.). The resultant mixture was stirred for 15 min before being evaporated. The product was precipitated by the addition of diethyl ether to the crude residue. The diethyl ether was separated and the solid was purified by trituration using diethyl ether. Filtration afforded the desired carboxylate sodium salt.

6.3.5 General Procedure E for sulfoximine amide bond forming reactions

A reported procedure was followed with modifications:[137] To a solution of a sulfoximine ester (1.0 equiv.), 4-dimethylaminopyridine (DMAP)[132] (0.05 equiv.), and triethylamine (1.5 equiv.) in dichloromethane (0.125 M) was added dropwise an acyl chloride (1.0 equiv.) at 0 °C under an ambient atmosphere. The reaction mixture was

allowed to slowly warm up to ambient temperature over 4 h, then evaporated and partitioned between ethyl acetate and water. The organic phase was sequentially washed with water and brine, dried over anhydrous Na_2SO_4, then evaporated. The crude residue was purified by flash column chromatography to afford the desired *N*-acylated sulfoximine.

6.3.6 General Procedure F for sulfoximine amide bond forming reactions

A reported procedure was followed with modifications:[127] To a solution of 1-ethyl-3-(3-dimethylaminopropyl)carbodiimide hydrochloride (EDCI)[133] (3 equiv.) and 4-dimethylaminopyridine (DMAP)[134] (2.2 equiv.) in dichloromethane (0.2 M) was added a carboxylic acid (1.1 equiv.) at 0 °C under an ambient atmosphere. The mixture was stirred for 5 min at 0 °C before addition of a sulfoximine ester (1.0 equiv.). The resultant reaction mixture was allowed to slowly warm to ambient temperature, then evaporated and partitioned between ethyl acetate and water. The organic phase was sequentially washed with water and brine, dried over anhydrous Na_2SO_4, then evaporated. The crude residue was purified by flash column chromatography to afford the desired *N*-acylated sulfoximine.

6.3.7 General Procedure G for sulfoximine arylation

A reported procedure was followed with modifications:[179] To a solution of a sulfoximine ester (1.0 equiv.) in anhydrous methanol (0.2 M) was added copper (II) acetate (0.1 equiv.) and an aryl boronic acid (2.3 equiv.) under a nitrogen atmosphere. The reaction mixture was stirred at ambient temperature for 16 h, then filtered and concentrated. The crude residue was purified by flash column chromatography to afford the desired *N*-arylated sulfoximine.

6.3.8 General Procedure H for sulfoximine urea formation

A reported procedure was followed with modifications:[131] To a solution of a sulfoximine ester (1.0 equiv.), 4-dimethylaminopyridine (DMAP)[132] (0.1 equiv.), and triethylamine (1.5 equiv.) in dichloroethane (0.2 M) was added dropwise an isocyanate (1.6 equiv.) at 0 °C under an ambient atmosphere. The reaction mixture was allowed to slowly warm up to ambient temperature over 4 h, then evaporated and partitioned between ethyl acetate and water. The organic phase was sequentially washed with water and brine, dried over anhydrous Na_2SO_4, and evaporated *in vacuo*. The crude residue was purified by flash column chromatography to afford the desired urea.

6.4 Compound synthesis

(*2S,6S*)-6-Bromo-3,3-dimethyl-7-oxo-4-thia-1-azabicyclo[3.2.0]heptane-2-carboxylic acid (16).

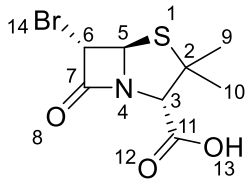

A reported procedure was followed with modifications:[114] To a solution of HBr (27.3 g, 18.3 mL, 48% (w/w), 3.5 equiv., 162 mmol) in methanol (70 mL) and deionized water (27.2 mL) at -10 °C was added (+)-6-aminopenicillanic acid **16** (10.0 g, 1.0 equiv., 46 mmol) followed by the dropwise addition of an aqueous solution of sodium nitrite (4.79 g, 1.5 equiv., 69 mmol in 13.2 mL water) over 30 min. The reaction mixture was stirred for an additional 30 min at ambient temperature before the addition of NaCl (4.8 g). The reaction mixture was extracted with dichloromethane. The combined organic extracts were washed with brine, dried over anhydrous Na_2SO_4, and concentrated under reduced pressure. The crude material was purified using silica column chromatography (330 g Sfär cartridge; 200 mL/min; initially 100% (v/v) cyclohexane (3 CV), followed by a linear gradient (15 CV): 0–35% (v/v) ethyl acetate in cyclohexane) to give acid

16 (11.7 g, 41 mmol, 90%).[114] The analytical data for **16** are consistent with those reported.[114]

Amorphous solid. **^{1}H NMR** (600 MHz, 300 K, $CDCl_3$): δ = 5.40 (d, *J* = 1.4 Hz, 1H, *H6*), 4.82 (d, *J* = 1.4 Hz, 1H, *H5*), 4.58 (s, 1H, *H3*), 1.65 (s, 3H, *H10*), 1.57 ppm (s, 3H, *H9*). **^{13}C NMR** (151 MHz, 300 K, $CDCl_3$): δ = 171.1, 167.6, 70.5, 69.8, 65.1, 49.3, 33.7, 26.1 ppm. **HRMS** (ESI): *m/z* calculated for $C_8H_9BrNO_3S$ $(M–H)^-$ = 277.9491, found 277.9492. **IR** (film): $\tilde{\nu}$ = 2984, 1791, 1460, 1394, 1374, 1334, 1297, 1215, 1151, 1091, 1025 cm^{-1}. $[\alpha]_D^{25}$ = + 170.9 (c = 0.79, $CHCl_3$).

4-Methoxybenzyl (*2S*,*6S*)-6-bromo-3,3-dimethyl-7-oxo-4-thia-1-azabicyclo[3.2.0]heptane-2-carboxylate (17).

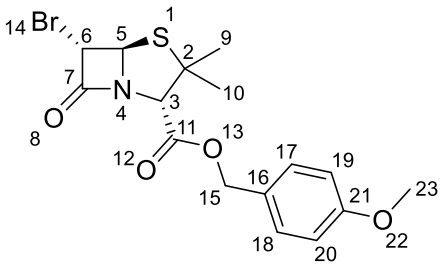

Following General Procedure A, ester **17** (3.73 g, 9.3 mmol, 67%) was obtained by reaction of acid **16** (3.89 g, 1.0 equiv., 14 mmol) and 1-(bromomethyl)-4-nitrobenzene (2.17 g, 1.0 equiv., 14 mmol), followed by column chromatography (50 g Sfär cartridge; 120 mL/min; initially 100% (v/v) cyclohexane (3 CV), followed by a linear gradient (15 CV): 0–10% (v/v) ethyl acetate in cyclohexane). The melting point for **17** was consistent with that reported, while ^{1}H NMR did not match those reported.[115] Previous ^{1}H NMR data were reported at 90 MHz.

White solid. **MP**: 73 – 75 °C (lit. 73 – 74 °C). **^{1}H NMR** (500 MHz, 300 K, $CDCl_3$): δ = 7.34 – 7.27 (m, 2H, *H17*, *H18*), 6.93 – 6.84 (m, 2H, *H19*, *H20*), 5.40 (d, *J* = 1.4 Hz, 1H, *H6*), 5.13 (s, 2H, *H15*), 4.79 (d, *J* = 1.4 Hz, 1H, *H5*), 4.54 (s, 1H, *H3*), 3.82 (s, 3H, *H23*), 1.58 (s, 3H, *H10*), 1.37 ppm (s, 3H, *H9*). **^{13}C NMR** (126 MHz, 300 K, $CDCl_3$): δ = 167.4, 167.0, 160.1, 130.7, 126.9, 114.2, 70.6, 70.0, 67.5, 65.2, 55.4, 49.6, 34.2, 25.8 ppm. **HRMS** (ESI): *m/z* calculated for $C_{16}H_{18}BrNO_4SNa$ $(M+Na)^+$ = 422.0032,

found 422.0032. **IR** (film): ṽ = 3775, 3663, 2961, 1791, 1745, 1659, 1613, 1549, 1517, 1463, 1302, 1252, 1205, 1176, 1033 cm^{-1}. $[\alpha]_D^{25}$ = + 118.2 (c = 1.3, $CHCl_3$).

4-Methoxybenzyl (*2S*)-3,3-dimethyl-7-oxo-4-thia-1-azabicyclo[3.2.0]heptane-2-carboxylate (18).

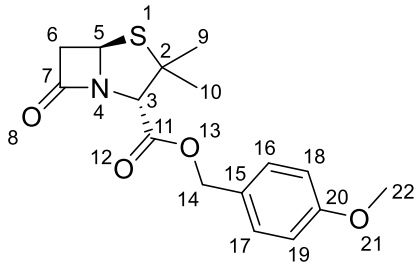

To a solution of **17** (33.3 g, 1.0 equiv., 83 mmol) in methanol (166 mL) was added tributylphosphine (16.8 g, 21 mL, 1.0 equiv., 83 mmol) dropwise. The reaction mixture was stirred for 1 h at ambient temperature before being evaporated. The crude material was purified using silica column chromatography (330 g Sfär cartridge; 200 mL/min; initially 100% (v/v) cyclohexane (3 CV), followed by a linear gradient (15 CV): 0–35% (v/v) dichloromethane in cyclohexane) affording ester **18** (24.1 g, 75 mmol, 90%). The analytical data for **18** are consistent with those reported.[180]

Amorphous solid. **^{1}H NMR** (600 MHz, 300 K, $CDCl_3$): δ = 7.33 – 7.28 (m, 2H, *H16*, *H17*), 6.92 – 6.86 (m, 2H, *H18*, *H19*), 5.27 (dd, *J* = 4.2, 1.8 Hz, 1H, *H5*), 5.15, 5.10 (2H, ABq, *J* = 11.8 Hz, *H14*), 4.46 (s, 1H, *H3*), 3.82 (s, 3H, *H22*), 3.54 (dd, *J* = 15.9, 4.2 Hz, 1H, *H6*), 3.05 (dd, *J* = 15.9, 1.8 Hz, 1H, *H6*), 1.62 (s, 3H, *H10*), 1.37 ppm (s, 3H, *H9*). **^{13}C NMR** (151 MHz, 300 K, $CDCl_3$): δ = 172.3, 168.0, 159.9, 130.5, 127.1, 114.0, 70.2, 67.2, 65.8, 60.6, 55.3, 46.5, 31.8, 26.7 ppm. **HRMS** (ESI): *m/z* calculated for $C_{16}H_{19}NO_4SNa$ $(M+Na)^+$ = 344.0927, found 344.0926. **IR** (film): ṽ = 3847, 3790, 3697, 3663, 3640, 2971, 2359, 1783, 1691, 1659, 1613, 1549, 1517, 1463, 1303, 1251, 1206, 1176, 1034 cm^{-1}. $[\alpha]_D^{25}$ = + 161.2 (c = 0.26, $CHCl_3$).

4-Methoxybenzyl (*2S*,*5R*,*6S*)-6-bromo-3,3-dimethyl-7-oxo-4-thia-1-azabicyclo[3.2.0]heptane-2-carboxylate 4-oxide (18b).

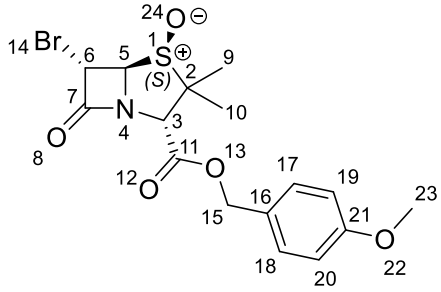

Following General Procedure B, sulfoxide **18b** (2.96 g, 7.1 mmol, 86%) was obtained from sulfide **17** (3.33 g, 1.0 equiv., 8.3 mmol), following column chromatography (50 g Sfär cartridge; 120 mL/min; initially 100% (v/v) cyclohexane (3 CV), followed by a linear gradient (15 CV): 0–35% (v/v) ethyl acetate in cyclohexane). The melting point and ^{1}H NMR for **18b** were not consistent with that reported.[115] Previous ^{1}H NMR data were reported at 90 MHz.

White Solid. **MP**: 120 – 122 °C (lit. 137 – 139 °C). **^{1}H NMR** (600 MHz, 300 K, $CDCl_3$): δ = 7.34 – 7.29 (m, 2H, *H17*, *H18*), 6.92 – 6.87 (m, 2H, *H19*, *H20*), 5.25, 5.11 (2H, ABq, *J* = 11.7 Hz, *H15*), 5.07 (d, *J* = 1.6 Hz, 1H, *H6*), 5.01 (d, *J* = 1.6 Hz, 1H, *H5*), 4.52 (s, 1H, *H3*), 3.81 (s, 3H, *H23*), 1.62 (s, 3H, *H10*), 1.06 ppm (s, 3H, *H9*). **^{13}C NMR** (151 MHz, 300 K, $CDCl_3$): δ = 167.3, 166.0, 160.2, 130.9, 126.9, 114.3, 79.4, 73.8, 68.0, 65.6, 55.4, 38.8, 20.0, 18.2 ppm. **HRMS**: Compound did not ionise using different mass spectrometry techniques (ESI, APCI, and EI). **IR** (film): $\tilde{\nu}$ = 2980, 1798, 1752, 1613, 1517, 1463, 1252, 1210, 1056 cm^{-1}. $[\alpha]_D^{25}$ = + 193.1 (c = 0.47, $CHCl_3$).

4-Methoxybenzyl (*2S*)-3,3-dimethyl-7-oxo-4-thia-1-azabicyclo[3.2.0]heptane-2-carboxylate 4-oxide (19).

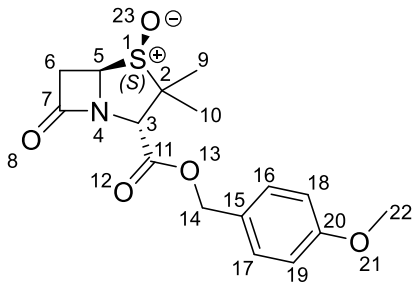

Following General Procedure B, sulfoxide **19** (3.61 g, 10.7 mmol, 74%) was obtained from sulfide **18** (4.64 g, 14 mmol), following column chromatography (50 g Sfär cartridge; 120 mL/min; initially 100% (v/v) cyclohexane (3 CV), followed by a linear gradient (15 CV): 0–

80% (v/v) ethyl acetate in cyclohexane). The analytical data for **19** are consistent with those reported.[180]

White Solid. **MP**: 150 – 152 °C. **^{1}H NMR** (600 MHz, 300 K, $CDCl_3$): δ = 7.36 – 7.29 (m, 2H, *H16*, *H17*), 6.95 – 6.85 (m, 2H, *H18*, *H19*), 5.24, 5.09 (2H, ABq, *J* = 11.8 Hz, *H14*), 4.92 (dd, *J* = 3.6, 2.9 Hz, 1H, *H5*), 4.52 (s, 1H, *H3*), 3.82 (s, 3H, *H22*), 3.39 – 3.30 (m, 2H, *H6*), 1.64 (s, 3H, *H10*), 1.08 ppm (s, 3H, *H9*). **^{13}C NMR** (151 MHz, 300 K, $CDCl_3$): δ = 170.7, 168.4, 160.2, 130.8, 127.1, 114.2, 74.1, 71.1, 67.8, 65.7, 55.5, 36.2, 20.3, 18.6 ppm. **HRMS** (ESI): *m/z* calculated for $C_{16}H_{20}NO_5S$ $(M+H)^+$ = 338.1057, found 338.1057. **IR** (film): ṽ = 3847, 3789, 3697, 3662, 1788, 1754, 1691, 1659, 1613, 1549, 1516, 1467, 1252, 1207, 1057 cm^{-1}. $\boldsymbol{[\alpha]_D^{25}}$ = + 189.2 (c = 0.27, $CHCl_3$).

4-Methoxybenzyl (*2S*,*4S*,*5R*)-4-(((benzyloxy)carbonyl)imino)-3,3-dimethyl-7-oxo-4λ^6-thia-1-azabicyclo[3.2.0]heptane-2-carboxylate 4-oxide (20).

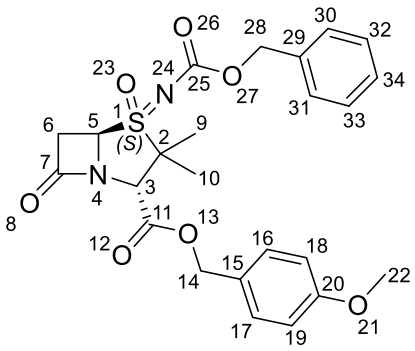

Following General Procedure C, sulfoximine **20** (2.5 g, 5.1 mmol, 87%) was obtained by reaction of sulfoxide **19** (2.0 g, 1.0 equiv., 5.9 mmol) and benzyl carbamate (1.34 g, 1.5 equiv., 8.9 mmol), following column chromatography (25 g Sfär cartridge; 80 mL/min; initially 100% (v/v) cyclohexane (3 CV), followed by a linear gradient (15 CV): 0–30% (v/v) ethyl acetate in cyclohexane).

Amorphous solid. **^{1}H NMR** (600 MHz, 300 K, $CDCl_3$): δ = 7.38 – 7.32 (m, 5H, *H30*, *H31*, *H32*, *H33*, *H34*), 7.31 – 7.28 (m, 2H, *H16*, *H17*), 6.92 – 6.87 (m, 2H, *H18*, *H19*), 5.23, 5.11 (2H, ABq, *J* = 11.7 Hz, *H14*), 5.15 (d, *J* = 12.0 Hz, 1H, *H28*), 5.08 (d, *J* = 12.0 Hz, 1H, *H28*), 4.87 (dd, *J* = 3.9, 2.4 Hz, 1H, *H5*), 4.41 (s, 1H, *H3*), 3.82 (s, 3H, *H22*), 3.51 – 3.43 (m, 2H, *H6*), 1.67 (s, 3H, *H10*), 1.27 ppm (s, 3H, *H9*). **^{13}C NMR**

(151 MHz, 300 K, $CDCl_3$): δ = 170.7, 166.7, 160.4, 159.0, 135.6, 130.9, 128.8, 128.7, 128.6(8), 126.5, 114.3, 69.1, 68.4, 67.8, 67.0, 63.8, 55.5, 39.5, 21.1, 18.8 ppm. **HRMS** (ESI): *m/z* calculated for $C_{24}H_{26}N_2O_7SNa$ $(M+Na)^+$ = 509.1353, found 509.1355. **IR** (film): $\tilde{\nu}$ = 3790, 3662, 2980, 1804, 1755, 1665, 1613, 1549, 1516, 1463, 1380, 1266 cm^{-1}. $[\alpha]_D^{25}$ = + 85.0 (c = 1.1, $CHCl_3$).

Sodium (*2S*,*4S*,*5R*)-4-imino-3,3-dimethyl-7-oxo-4λ⁶-thia-1-azabicyclo[3.2.0]heptane-2-carboxylate 4-oxide (21).

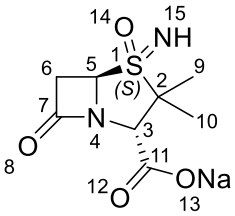

Following General Procedure D, acid **21** (20 mg, 86 µmol, 56%) was obtained by reaction of ester **20** (75 mg, 1.0 equiv., 0.15 mmol) with 10% (w/w) Pd/C (1.0 equiv.) in anhydrous THF stirring for 6 h under hydrogen atmosphere. The reaction mixture was filtered using Celite® and the Celite® pad was rinsed with DCM. The product was eluted with anhydrous methanol, which was then removed *in vacuo*. The residue was redissolved in anhydrous methanol before the addition of sodium 2-ethylhexanoate (1.0 equiv.). The resultant mixture was stirred for 15 min before being evaporated *in vacuo*. The product was precipitated by the addition of diethyl ether to the crude residue. Filtration afforded the carboxylate sodium salt.

White solid. **MP**: decomposition > 100 °C. **^{1}H NMR** (600 MHz, 300 K, MeOD-d_4): δ = 4.72 (dd, *J* = 4.4, 1.6 Hz, 1H, *H5*), 4.13 (s, 1H, *H3*), 3.46 (dd, *J* = 15.9, 4.3 Hz, 1H, *H6*), 3.16 (dd, *J* = 15.9, 1.7 Hz, 1H, *H6*), 1.55 (s, 3H, *H10*), 1.40 ppm (s, 3H, *H9*). **^{13}C NMR** (151 MHz, 300 K, MeOD-d_4): δ = 174.0, 173.9, 68.2, 67.2, 64.3, 37.4, 21.9, 19.1 ppm. **HRMS** (ESI): *m/z* calculated for $C_8H_{10}N_2O_4S$ $(M-H)^-$ = 231.0445, found 231.0449. **IR** (film): $\tilde{\nu}$ = 3658, 3207, 2981, 2889, 2664, 2361, 2341, 1781, 1620, 1473, 1462, 1383, 1251, 1152, 1073 cm^{-1}. $[\alpha]_D^{25}$ = + 148.3 (c = 0.12, MeOH).

(*2S*,*5R)*-6,6-Dibromo-3,3-dimethyl-7-oxo-4-thia-1-azabicyclo[3.2.0]heptane-2-carboxylic acid (22).

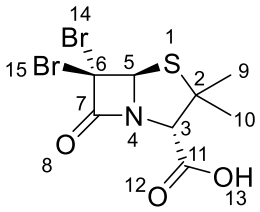

A reported procedure was followed with modifications:[123] To a solution of bromine (66.5 g, 21.4 mL, 3.0 equiv. 416 mmol), H_2SO_4 (20.4 g, 160 mL, 1.3 M, 1.5 equiv., 208 mmol), and sodium nitrite (14.4 g, 1.5 equiv., 208 mmol) in dichloromethane (277 mL) at 0 °C was added (+)-6-aminopenicillanic acid (30.0 g, 1.0 equiv., 139 mmol) portion wise over 30 min while maintaining reaction temperature between 0-10 °C. The resultant dark red solution was stirred for 5 hours, then quenched with 1M aqueous $NaHSO_3$ solution dropwise over a period of 20 min until the color became light yellow. The organic layer was separated, and the aqueous layer was extracted with additional DCM. The combined organic extracts were washed with brine, dried over anhydrous sodium sulfate, and concentrated under reduced pressure. The crude material was purified using silica column chromatography (330 g Sfär cartridge; 200 mL/min; initially 100% (v/v) cyclohexane (3 CV), followed by a linear gradient (15 CV): 0–35% (v/v) ethyl acetate in cyclohexane) to give acid **22** (34.0 g, 95 mmol, 68%). The analytical data for **22** are consistent with those reported.[123]

Brown solid. **MP**: 144 – 146 °C. **^{1}H NMR** (600 MHz, 300 K, $CDCl_3$): δ = 5.79 (s, 1H, *H5*), 4.58 (s, 1H, *H3*), 1.66 (s, 3H, *H10*), 1.56 ppm (s, 3H, *H9*). **^{13}C NMR** (151 MHz, 300 K, $CDCl_3$): δ = 169.3, 164.7, 80.8, 69.4, 64.6, 58.5, 33.5, 26.2 ppm. **HRMS** (ESI): *m/z* calculated for $C_8H_{10}Br_2NO_3S$ $(M+H)^+$ = 355.8597, found 355.8610. **IR** (film): $\tilde{\nu}$ = 3789, 3661, 3638, 2981, 2890, 1799, 1587, 1549, 1514, 1462, 1381, 1252, 1156 cm^{-1}. $[\alpha]_D^{25}$ = + 144.1 (c = 0.12, $CHCl_3$).

4-Methoxybenzyl (*2S*,*5R*)-6,6-dibromo-3,3-dimethyl-7-oxo-4-thia-1-azabicyclo[3.2.0]heptane-2-carboxylate (23).

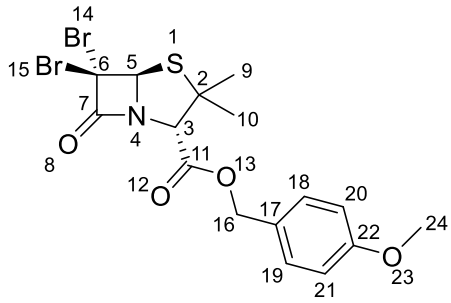

Following General Procedure A, ester **23** (7.57 g, 15.8 mmol, 91%) was obtained by reaction of acid **22** (6.27 g, 1.0 equiv., 17.5 mmol) and 1-(bromomethyl)-4-methoxybenzene (3.51 g, 1.0 equiv., 17.5 mmol), following column chromatography (25 g Sfär cartridge; 80 mL/min; initially 100% (v/v) cyclohexane (3 CV), followed by a linear gradient (15 CV): 0–70% (v/v) dichloromethane in cyclohexane). The analytical data for **23** are consistent with those reported.[181]

Liquid. **^{1}H NMR** (600 MHz, 300 K, $CDCl_3$): δ = 7.33 – 7.28 (m, 2H, *H18*, *H19*), 6.93 – 6.87 (m, 2H, *H20*, *H21*), 5.79 (s, 1H, *H5*), 5.18 – 5.10 (m, 2H, *H16*), 4.53 (s, 1H, *H3*), 3.82 (s, 3H, *H24*), 1.58 (s, 3H, *H10*), 1.36 ppm (s, 3H, *H9*). **^{13}C NMR** (151 MHz, 300 K, $CDCl_3$): δ = 166.7, 164.6, 160.2, 130.8, 126.8, 114.2, 80.9, 69.8, 67.7, 64.9, 58.8, 55.5, 33.7, 25.9 ppm. **HRMS**: Compound did not ionize using different mass spectrometry techniques (ESI, APCI, and EI). **IR** (film): $\tilde{\nu}$ = 3662, 2981, 2890, 1801, 1745, 1613, 1517, 1463, 1382, 1304, 1252, 1205, 1176, 1035 cm^{-1}. $[\alpha]_D^{25}$ = + 145.5 (c = 0.53, $CHCl_3$).

4-Methoxybenzyl (*2S*,*5R*)-6,6-dibromo-3,3-dimethyl-7-oxo-4-thia-1-azabicyclo[3.2.0]heptane-2-carboxylate 4-oxide (24).

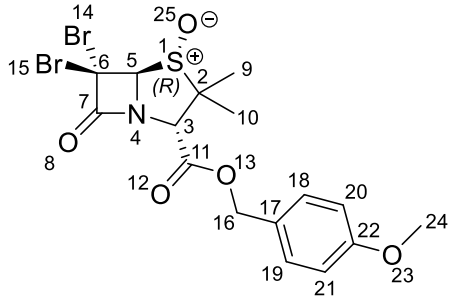

Following General Procedure B, sulfoxide **24** (16.0 g, 32 mmol, 80%) was obtained from sulfide **23** (21.3 g, 1.0 equiv., 40 mmol), following column chromatography (25 g Sfär cartridge; 80 mL/min; initially 100% (v/v) cyclohexane (3 CV), followed by a linear gradient (15 CV): 0–25% (v/v) ethyl acetate in cyclohexane). The previous report of **24** did not provide NMR/MS data.[180]

Amorphous solid. **^{1}H NMR** (600 MHz, 300 K, $CDCl_3$): δ = 7.35 – 7.30 (m, 2H, *H18*, *H19*), 6.93 – 6.88 (m, 2H, *H20*, *H21*), 5.28 (s, 1H, *H5*), 5.21, 5.14 (2H, ABq, *J* = 11.7 Hz, *H16*), 4.56 (s, 1H, *H3*), 3.82 (s, 3H, *H24*), 1.53 (s, 3H, *H10*), 1.31 ppm (s, 3H, *H9*). **^{13}C NMR** (151 MHz, 300 K, $CDCl_3$): δ = 166.2, 162.4, 160.3, 130.9, 126.5, 114.3, 93.0, 72.5, 68.3, 67.0, 55.5, 48.0, 24.8, 16.9 ppm. **HRMS** (ESI): *m/z* calculated for $C_{16}H_{18}Br_2NO_5S$ $(M+H)^+$ = 493.9267, found 493.9268. **IR** (film): ṽ = 3847, 3775, 3661, 3642, 2980, 2890, 1807, 1753, 1659, 1613, 1549, 1517, 1463, 1382, 1305, 1252, 1177, 1072 cm^{-1}. $[\alpha]_D^{25}$ = + 90.8 (c = 0.45, $CHCl_3$).

4-Methoxybenzyl (*2S*,*5R*)-3,3-dimethyl-7-oxo-4-thia-1-azabicyclo[3.2.0]heptane-2-carboxylate 4-oxide (25).

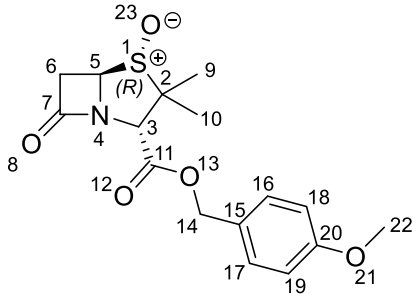

To a solution of sulfoxide **24** (16.0 g, 1.0 equiv., 32.3 mmol) in methanol (162 mL) was added tributylphosphine (13.1 g, 16 mL, 2.0 equiv., 64.6 mmol) dropwise. The reaction mixture was stirred for 1 h at ambient temperature before being concentrated. The crude material was purified using column chromatography (25 g Sfär cartridge; 80 mL/min; initially 100% (v/v) cyclohexane (3 CV), followed by a linear gradient (15 CV): 0–100% (v/v) ethyl acetate in cyclohexane) to give sulfoxide **25** (10.8 g, 32.3 mmol, 99%). The analytical data for **25** are consistent with those reported.[180]

White solid. **MP**: 103 – 105 °C. **^{1}H NMR** (400 MHz, 300 K, $CDCl_3$): δ = 7.36 – 7.28 (m, 2H, *H16*, *H17*), 6.94 – 6.86 (m, 2H, *H18*, *H19*), 5.22, 5.11 (2H, ABq, *J* = 11.8 Hz, *H14*), 4.59 (dd, *J* = 4.5, 1.9 Hz, 1H, *H5*), 4.38 (s, 1H, *H3*), 3.82 (s, 3H, *H22*), 3.59 (dd, *J* = 16.4, 4.5 Hz, 1H, *H6*), 3.35 (dd, *J* = 16.4, 1.9 Hz, 1H, *H6*), 1.54 (s, 3H, *H10*), 1.24 ppm (s, 3H, *H9*). **^{13}C NMR** (101 MHz, 300 K, $CDCl_3$): δ = 169.2, 167.4, 160.2, 130.9,

126.8, 114.3, 72.6, 70.9, 68.0, 64.1, 55.5, 40.9, 24.5, 15.6 ppm. **HRMS** (ESI): *m/z* calculated for $C_{16}H_{17}NO_5S$ $(M–H)^-$ = 336.0911, found 336.0902. **IR** (film): $\tilde{\nu}$ = 3697, 3020, 1788, 1751, 1614, 1517, 1466, 1304, 1252, 1188, 1064 cm^{-1}. $[\alpha]_D^{25}$ = + 145.8 (c = 0.17, $CHCl_3$).

4-Methoxybenzyl (*2S*,*4R*,*5R*)-4-(((benzyloxy)carbonyl)imino)-3,3-dimethyl-7-oxo-4λ⁶-thia-1-azabicyclo[3.2.0]heptane-2-carboxylate 4-oxide (26).

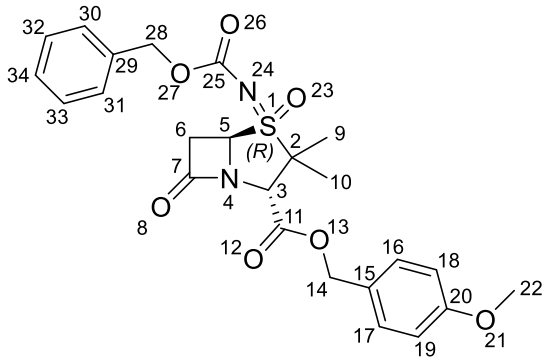

Following General Procedure C, sulfoximine **26** (68 mg, 0.14 mmol, 52%) was obtained from sulfoxide **25** (90 mg, 1.0 equiv., 0.27 mmol) and benzyl carbamate (61 mg, 1.5 equiv., 0.40 mmol), following column chromatography (10 g Sfär cartridge; 40 mL/min; initially 100% (v/v) cyclohexane (3 CV), followed by a linear gradient (15 CV): 0–45% (v/v) ethyl acetate in cyclohexane).

Amorphous solid. **^{1}H NMR** (600 MHz, 300 K, $CDCl_3$): δ = 7.41 – 7.32 (m, 5H, *H30*, *H31*, *H32*, *H33*, *H34*), 7.31 – 7.28 (m, 2H, *H16*, *H17*), 6.92 – 6.85 (m, 2H, *H18*, *H19*), 5.23, 5.10 (2H, ABq, *J* = 12.0 Hz, *H14*), 5.13 (s, 2H, *H28*), 4.88 (dd, *J* = 4.2, 2.1 Hz, 1H, *H5*), 4.49 (s, 1H, *H3*), 3.82 (s, 3H, *H22*), 3.55 – 3.45 (m, 2H, *H6*), 1.60 (s, 3H, *H10*), 1.32 ppm (s, 3H, *H9*). **^{13}C NMR** (151 MHz, 300 K, $CDCl_3$): δ = 169.7, 166.5, 160.3, 158.64 135.9, 130.9, 128.7, 128.4(3), 128.4, 126.6, 114.3, 68.8, 68.4, 68.3, 67.4, 64.1, 55.5, 41.4, 20.9, 19.2 ppm. **HRMS** (ESI): *m/z* calculated for $C_{24}H_{24}N_2O_7S$ $(M–H)^-$ = 485.1388, found 485.1393. **IR** (film): $\tilde{\nu}$ = 2959, 1804, 1613, 1517, 1262, 1096 cm^{-1}. $[\alpha]_D^{25}$ = – 23.7 (c = 0.25, $CHCl_3$).

Benzhydryl (*2S,4S,5R*)-4-(((benzyloxy)carbonyl)imino)-3,3-dimethyl-7-oxo-4λ⁶-thia-1-azabicyclo[3.2.0]heptane-2-carboxylate 4-oxide (29).

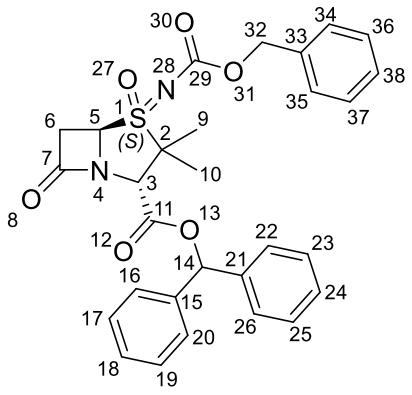

Following General Procedure C, sulfoximine **29** (139 mg, 87%) was obtained by reaction of commercial benzhydryl (*2S*)-3,3-dimethyl-7-oxo-4-thia-1-azabicyclo[3.2.0]heptane-2-carboxylate 4-oxide (115 mg, 1.0 equiv., 0.30 mmol) and benzyl carbamate (68 mg, 1.5 equiv., 0.45 mmol), following column chromatography (10 g Sfär cartridge; 40 mL/min; initially 100% (v/v) cyclohexane (3 CV), followed by a linear gradient (15 CV): 0–50% (v/v) ethyl acetate in cyclohexane).

Amorphous solid. **^{1}H NMR** (600 MHz, 300 K, $CDCl_3$): δ = 7.39 – 7.31 (m, 15H, *H16*, *H17*, *H18*, *H19*, *H20*, *H22*, *H23*, *H24*, *H25*, *H26*, *H34*, *H35*, *H36*, *H37*, *H38*), 6.98 (s, 1H, *H14*), 5.14 (d, *J* = 12.0 Hz, 1H, *H32*), 5.07 (d, *J* = 12.0 Hz, 1H, *H32*), 4.87 (dd, *J* = 3.8, 2.5 Hz, 1H, *H5*), 4.52 (s, 1H, *H3*), 3.54 – 3.45 (m, 2H, *H6*), 1.72 (s, 3H, *H10*), 1.14 ppm (s, 3H, *H9*). **^{13}C NMR** (151 MHz, 300 K, $CDCl_3$): δ = 170.5, 165.8, 158.9, 138.7, 138.5, 135.4, 128.8, 128.7(9), 128.7, 128.6, 128.5(4), 128.5(2), 128.5, 127.7, 126.9, 79.3, 68.9, 67.8, 66.8, 63.6, 39.3, 20.6, 18.7 ppm. **HRMS** (ESI): *m/z* calculated for $C_{29}H_{27}N_2O_6S$ $(M–H)^-$ = 531.1595, found 531.1593. **IR** (film): ṽ = 3691, 3676, 3649, 3630, 3032, 2946, 2898, 2833, 1804, 1760, 1718, 1671, 1616, 1541, 1498, 1457, 1418, 1374, 1265, 1217, 1184, 1099, 1028 cm^{-1}. $[\alpha]_D^{25}$ = + 109.6 (c = 0.67, $CHCl_3$).

4-Methoxybenzyl (*2S*,*4S*,*5R*)-4-((*tert*-butoxycarbonyl)imino)-3,3-dimethyl-7-oxo-4λ^6-thia-1-azabicyclo[3.2.0]heptane-2-carboxylate 4-oxide (30a).

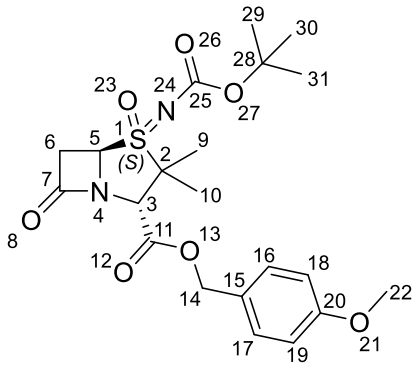

Following General Procedure C, sulfoximine **30a** (190 mg, 0.42 mmol, 75%) was obtained by reaction of sulfoxide **19** (190 mg, 1.0 equiv., 0.56 mmol) and *tert*-butyl carbamate (99 mg, 1.5 equiv., 0.85 mmol), following column chromatography (10 g Sfär cartridge; 40 mL/min; initially 100% (v/v) cyclohexane (3 CV), followed by a linear gradient (15 CV): 0–35% (v/v) ethyl acetate in cyclohexane).

Amorphous solid. **^{1}H NMR** (600 MHz, 300 K, $CDCl_3$): δ = 7.33 – 7.28 (m, 2H, *H16*, *H17*), 6.92 – 6.87 (m, 2H, *H18*, *H19*), 5.23, 5.12 (2H, ABq, *J* = 11.7 Hz, *H14*), 4.89 (dd, *J* = 4.2, 2.1 Hz, 1H, *H5*), 4.41 (s, 1H, *H3*), 3.82 (s, 3H, *H22*), 3.66 – 3.55 (m, 2H, *H6*), 1.69 (s, 3H, *H10*), 1.47 (s, 9H, *H29*, *H30*, *H31*), 1.29 ppm (s, 3H, *H9*). **^{13}C NMR** (151 MHz, 300 K, $CDCl_3$): δ = 170.9, 166.8, 160.3, 158.3, 130.9, 126.6, 114.3, 82.1, 68.3, 67.8, 66.7, 63.9, 55.5, 39.7, 28.2, 21.1, 19.1 ppm. **HRMS** (ESI): *m/z* calculated for $C_{21}H_{27}N_2O_7S$ $(M–H)^-$ = 451.1544, found 451.1547. **IR** (film): $\tilde{\nu}$ = 3775, 3662, 2980, 1804, 1756, 1724, 1659, 1613, 1549, 1517, 1463, 1370, 1290, 1254, 1160 cm^{-1}. $[\alpha]_D^{25}$ = + 96.4 (c = 0.5, $CHCl_3$).

4-Methoxybenzyl (*2S*,*4S*,*5R*)-4-((methoxycarbonyl)imino)-3,3-dimethyl-7-oxo-4λ^6-thia-1-azabicyclo[3.2.0]heptane-2-carboxylate 4-oxide (30b).

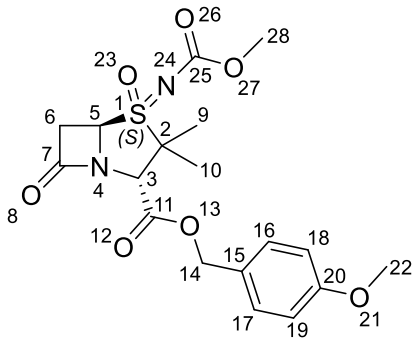

Following General Procedure C, sulfoximine **30b** (250 mg, 0.61 mmol, 64%) was obtained by reaction of sulfoxide **19** (320 mg, 1.0 equiv., 0.95 mmol) and methyl carbamate (107 mg, 1.5 equiv., 1.4 mmol), following column chromatography (10

g Sfär cartridge; 40 mL/min; initially 100% (v/v) cyclohexane (3 CV), followed by a linear gradient (15 CV): 0–45% (v/v) ethyl acetate in cyclohexane).

Amorphous solid. **^{1}H NMR** (600 MHz, 300 K, $CDCl_3$): δ = 7.33 – 7.28 (m, 2H, *H16*, *H17*), 6.93 – 6.87 (m, 2H, *H18*, *H19*), 5.24, 5.12 (2H, ABq, *J* = 11.7 Hz, *H14*), 4.91 (dd, *J* = 4.3, 2.0 Hz, 1H, *H5*), 4.43 (s, 1H, *H3*), 3.82 (s, 3H, *H22*), 3.73 (s, 3H, *H28*), 3.69 – 3.57 (m, 2H, *H6*), 1.68 (s, 3H, *H10*), 1.28 ppm (s, 3H, *H9*). **^{13}C NMR** (151 MHz, 300 K, $CDCl_3$): δ = 170.7, 166.7, 160.4, 160.3, 130.9, 126.5, 114.3, 68.4, 67.8, 66.9, 63.8, 55.5, 54.1, 39.6, 29.9, 21.1, 18.9 ppm. **HRMS** (ESI): *m/z* calculated for $C_{18}H_{22}N_2O_7SNa$ $(M+Na)^+$ = 433.1040, found 433.1037. **IR** (film): $\tilde{\nu}$ = 3775, 3697, 3662, 3641, 2927, 1804, 1756, 1665, 1612, 1549, 1516, 1463, 1442, 1380, 1276 cm^{-1}. $[\alpha]_D^{25}$ = + 82.2 (c = 0.29, $CHCl_3$).

4-Methoxybenzyl (*2S*,*4S*,*5R*)-3,3-dimethyl-4-((methylsulfonyl)imino)-7-oxo-4λ^6-thia-1-azabicyclo[3.2.0]heptane-2-carboxylate 4-oxide (30c).

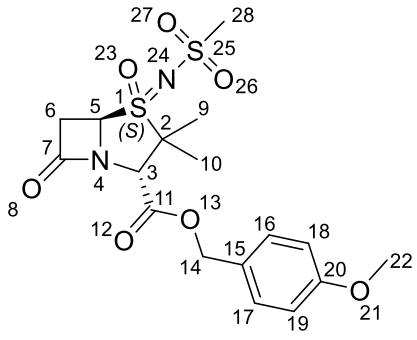

Following General Procedure C, sulfoximine **30c** (250 mg, 0.58 mmol, 78%) was obtained by reaction of sulfoxide **19** (250 mg, 1.0 equiv., 0.74 mmol) and methane sulfonamide (105 mg, 1.6 equiv., 1.1 mmol), following column chromatography (10 g Sfär cartridge; 40 mL/min; initially 100% (v/v) cyclohexane (3 CV), followed by a linear gradient (15 CV): 0–45% (v/v) ethyl acetate in cyclohexane).

Amorphous solid. **^{1}H NMR** (600 MHz, 300 K, $CDCl_3$): δ = 7.33 – 7.28 (m, 2H, *H16*, *H17*), 6.93 – 6.88 (m, 2H, *H18*, *H19*), 5.25, 5.13 (2H, ABq, *J* = 11.7 Hz, *H14*), 5.05 (dd, *J* = 4.4, 1.8 Hz, 1H, *H5*), 4.39 (s, 1H, *H3*), 3.82 (s, 3H, *H22*), 3.66 (dd, *J* = 16.8, 4.5, 1H, *H6*), 3.50 (dd, *J* = 16.8, 1.8 Hz, 1H, *H6*), 3.14 (s, 3H, *H28*), 1.66 (s, 3H, *H10*), 1.32 ppm (s, 3H, *H9*). **^{13}C NMR** (151 MHz, 300 K, $CDCl_3$): δ = 170.3, 166.3, 160.4,

131.0, 126.4, 114.4, 68.9, 68.5, 68.1, 62.9, 55.5, 45.3, 39.5, 21.1, 18.6 ppm. **HRMS** (ESI): *m/z* calculated for $C_{17}H_{22}N_2O_7S_2Na$ $(M+Na)^+$ = 453.0761, found 453.0760. **IR** (film): $\tilde{\nu}$ = 3789, 3697, 3662, 3640, 2981, 1805, 1756, 1691, 1659, 1613, 1549, 1516, 1467, 1318, 1250, 1190, 1144, 1065 cm^{-1}. $[\alpha]_D^{25}$ = + 99.7 (c = 0.47, $CHCl_3$).

4-Methoxybenzyl (*2S*,*4S*,*5R*)-4-((cyclopropylsulfonyl)imino)-3,3-dimethyl-7-oxo-4λ^6-thia-1-azabicyclo[3.2.0]heptane-2-carboxylate 4-oxide (30d).

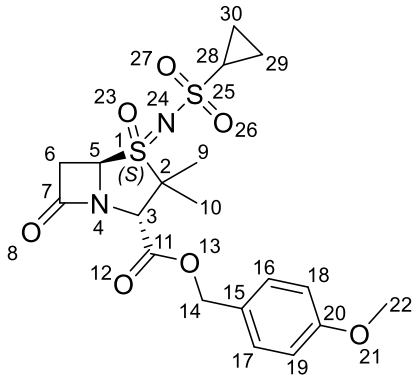

Following General Procedure C, sulfoximine **30d** (134 mg, 0.29 mmol, 66%) was obtained by reaction of sulfoxide **19** (150 mg, 1.0 equiv., 0.45 mmol) and cyclopropane sulfonamide (80 mg, 1.5 equiv., 0.67 mmol), following column chromatography (10 g Sfär cartridge; 40 mL/min; initially 100% (v/v) cyclohexane (3 CV), followed by a linear gradient (15 CV): 0–35% (v/v) ethyl acetate in cyclohexane).

Amorphous solid. **^{1}H NMR** (600 MHz, 300 K, $CDCl_3$): δ = 7.33 – 7.28 (m, 2H, *H16*, *H17*), 6.93 – 6.87 (m, 2H, *H18*, *H19*), 5.24, 5.17 (2H, ABq, *J* = 11.7 Hz, *H14*), 5.04 (dd, *J* = 4.4, 1.8 Hz, 1H, *H5*), 4.38 (s, 1H, *H3*), 3.82 (s, 3H, *H22*), 3.64 (dd, *J* = 16.8, 4.4 Hz, 1H, *H6*), 3.46 (dd, *J* = 16.7, 1.8 Hz, 1H, *H6*), 2.63 (m, 1H, *H28*), 1.67 (s, 3H, *H10*), 1.32 (s, 3H, H9), 1.30 – 1.18 (m, 2H, *H30*), 1.10 – 0.99 ppm (m, 2H, *H29*). **^{13}C NMR** (151 MHz, 300 K, $CDCl_3$): δ = 170.4, 166.4, 160.4, 131.0, 126.5, 114.4, 68.9, 68.5, 68.1, 63.0, 55.5, 39.5, 34.4, 21.2, 18.6, 6.7, 6.5 ppm. **HRMS** (ESI): *m/z* calculated for $C_{19}H_{24}N_2O_7S_2Na$ $(M+Na)^+$ = 479.0917, found 479.0919. **IR** (film): $\tilde{\nu}$ = 3847, 3790, 3697, 3683, 3662, 3639, 2969, 1805, 1756, 1711, 1691, 1659, 1641, 1613, 1549, 1516, 1467, 1443, 1326, 1303, 1248, 1190, 1141, 1069 cm^{-1}. $[\alpha]_D^{25}$ = + 96.3 (c = 0.38, $CHCl_3$).

4-Methoxybenzyl (*2S*,*4S*,*5R*)-3,3-dimethyl-7-oxo-4-(((2,2,2-trichloroethoxy)sulfonyl)imino)-4λ^6-thia-1-azabicyclo[3.2.0]heptane-2-carboxylate 4-oxide (30e).

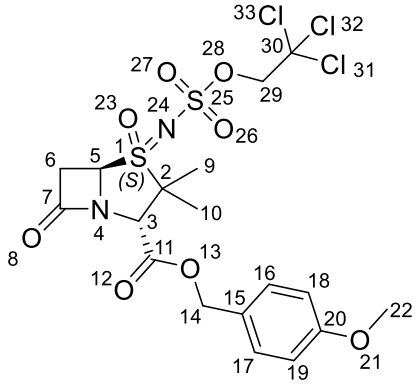

Following General Procedure C, sulfoximine **30e** (56 mg, 0.45 mmol, 22%) was obtained by reaction of sulfoxide **19** (150 mg, 1.0 equiv., 0.45 mmol) and 2,2,2-trichloroethyl sulfamate (152 mg, 1.5 equiv., 0.67 mmol), following column chromatography (10 g Sfär cartridge; 40 mL/min; initially 100% (v/v) cyclohexane (3 CV), followed by a linear gradient (15 CV): 0–20% (v/v) ethyl acetate in cyclohexane).

^{1}H NMR (400 MHz, 300 K, $CDCl_3$): δ = 7.35 – 7.27 (m, 2H, *H16*, *H17*), 6.93 – 6.85 (m, 2H, *H18*, *H19*), 5.52 (dd, *J* = 3.7, 1.4 Hz, 1H, *H5*), 5.16, 5.11 (2H, ABq, *J* = 11.8 Hz, *H14*), 4.76 (d, *J* = 10.9 Hz, 1H, *H29*), 4.71 (d, *J* = 10.8 Hz, 1H, *H29*), 4.39 (s, 1H, *H3*), 3.82 (s, 3H, *H22*), 3.65 (dd, *J* = 15.9, 1.5 Hz, 1H, *H6*), 3.56 (dd, *J* = 15.9, 3.7 Hz, 1H, *H6*), 1.64 (s, 3H, *H10*), 1.44 ppm (s, 3H, *H9*). **^{13}C NMR** (151 MHz, 300 K, $CDCl_3$): δ = 166.3, 164.1, 160.2, 130.7, 126.7, 114.3, 92.7, 79.4, 68.3, 61.3, 58.5, 55.4, 53.3, 45.7, 23.0, 22.1 ppm. **HRMS** (ESI): *m/z* calculated for $C_{18}H_{20}Cl_3N_2O_8S_2$ $(M–H)^-$ = 560.9732, found 560.9741. **IR** (film): $\tilde{\nu}$ = 3811, 3659, 3199, 2981, 2888, 2665, 2360, 1786, 1613, 1549, 1515, 1473, 1462, 1383, 1252, 1152, 1073 cm^{-1}. $[\alpha]_D^{25}$ = – 18.3 (c = 0.12, $CHCl_3$).

Sodium (*2S,4S,5R*)-4-((*tert*-butoxycarbonyl)imino)-3,3-dimethyl-7-oxo-4λ^6-thia-1-azabicyclo[3.2.0]heptane-2-carboxylate 4-oxide (31a).

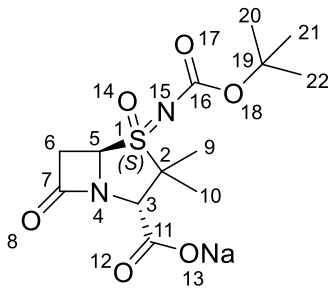

Following General Procedure D, acid **31a** (277 mg, 0.84 mmol, 70%) was obtained by reaction of ester **30a** (573 mg, 1.0 equiv., 1.2 mmol) with 10% (w/w) Pd/C (0.2 equiv.) in anhydrous THF stirring for 3 h under hydrogen atmosphere. The reaction mixture was filtered using Celite®; the Celite® pad was rinsed with DCM, which was then removed *in vacuo*. The residue was redissolved in ethyl acetate before the addition of sodium 2-ethylhexanoate (1.0 equiv.). The resultant mixture was stirred for 15 min before being evaporated *in vacuo*. The product was precipitated by the addition of diethyl ether to the crude residue. Filtration afforded the carboxylate sodium salt.

Yellow solid. **MP**: decomposition > 100 °C. **^{1}H NMR** (500 MHz, 300 K, DMSO-d_6): δ = 5.20 (dd, *J* = 4.3, 1.5 Hz, 1H, *H5*), 3.73 (s, 1H, *H3*), 3.64 (dd, *J* = 16.0, 4.3 Hz, 1H, *H6*), 3.12 (dd, *J* = 16.0, 1.6 Hz, 1H, *H6*), 1.56 (s, 3H, *H10*), 1.38 (s, 9H, *H20*, *H21*, *H22*), 1.34 ppm (s, 3H, *H9*). **^{13}C NMR** (126 MHz, 300 K, DMSO-d_6): δ = 171.7, 167.4, 157.6, 80.0, 67.5, 65.9, 65.8, 37.8, 27.8, 20.8, 18.8 ppm. **HRMS** (ESI): *m/z* calculated for $C_{13}H_{19}N_2O_6S$ $(M–H)^-$ = 331.0969, found 331.0962. **IR** (film): $\tilde{\nu}$ = 3450, 1784, 1624, 1370, 1287, 1256, 1158 cm^{-1}. $[\alpha]_D^{25}$ = + 72.6 (c = 0.52, CH_3CN).

Sodium (*2S*,*4S*,*5R*)-4-((methoxycarbonyl)imino)-3,3-dimethyl-7-oxo-4l6-thia-1-azabicyclo[3.2.0]heptane-2-carboxylate 4-oxide (31b).

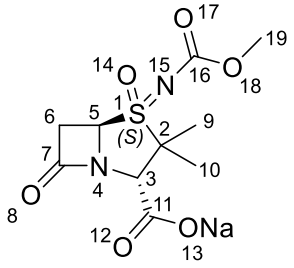

Following General Procedure D, acid **31b** (90 mg, 0.31 mmol, 50%) was obtained by reaction of ester **30b** (257 mg, 1.0 equiv., 0.63 mmol) with 10% (w/w) Pd/C (0.2 equiv.) in THF stirring for 3 h under hydrogen atmosphere. The reaction mixture was filtered using Celite®; the Celite® pad was rinsed with DCM, which was then removed *in vacuo*. The residue was redissolved in ethyl acetate before the addition

of sodium 2-ethylhexanoate (1.0 equiv.). The resultant mixture was stirred for 15 min before being evaporated *in vacuo*. The product was precipitated by the addition of diethyl ether to the crude residue. Filtration afforded the carboxylate sodium salt.

White solid. **MP**: decomposition > 100 °C. **^{1}H NMR** (500 MHz, 300 K, MeOD-d_4): δ = 5.14 (dd, J = 4.4, 1.6 Hz, 1H, *H5*), 4.13 (s, 1H, *H3*), 3.70 (s, 3H, *H19*), 3.66 (dd, J = 16.3, 4.4 Hz, 1H, *H6*), 3.37 (dd, J = 16.3, 1.7 Hz, 1H, *H6*), 1.70 (s, 3H, *H10*), 1.48 ppm (s, 3H, *H9*). **^{13}C NMR** (126 MHz, MeOD-d_4): δ = 173.2, 172.8, 161.9, 69.1, 68.0, 67.3, 54.3, 39.2, 21.6, 19.3 ppm. **HRMS** (ESI): *m/z* calculated for $C_{10}H_{13}N_2O_6S$ $(M–H)^-$ = 289.0500, found 289.0513. **IR** (film): $\tilde{\nu}$ = 3791, 3659, 3439, 2981, 2888, 2665, 2361, 2342, 1787, 1709, 1630, 1549, 1530, 1472, 1462, 1383, 1265, 1252, 1152, 1073, 1033 cm^{-1}. $[\alpha]_D^{25}$ = + 105.7 (c = 0.44, MeOH).

4-Methoxybenzyl (*2S*,*4S*,*5R*)-4-imino-3,3-dimethyl-7-oxo-4λ^6-thia-1-azabicyclo[3.2.0]heptane-2-carboxylate 4-oxide (32).

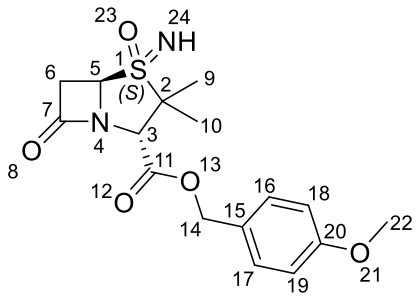

To a solution of sulfoximine **20** (600 mg, 1.0 equiv., 1.23 mmol) in anhydrous THF (6 mL) was added 10% wt Pd/C (79 mg, 0.6 equiv., 0.74 mmol). Using a Schlenk line, the reaction mixture was evacuated and backfilled with hydrogen gas 3 times. The reaction mixture was stirred at ambient temperature for 3 h under a hydrogen atmosphere before being filtered over celite, washed with dichloromethane, and evaporated *in vacuo*. The crude material was purified using silica column chromatography (25 g Sfär cartridge; 80 mL/min; initially 100% (v/v) cyclohexane (3 CV), followed by a linear gradient (15 CV): 0–100% (v/v) ethyl acetate in cyclohexane) to give *NH*-sulfoximine **32** (220 mg, 0.62 mmol, 51%).

White solid. **MP**: 113 – 115 °C. **^{1}H NMR** (600 MHz, 300 K, $CDCl_3$): δ = 7.34 – 7.28 (m, 2H, *H16*, *H17*), 6.93 – 6.87 (m, 2H, *H18*, *H19*), 5.24, 5.09 (2H, ABq, *J* = 11.5 Hz, *H14*), 4.63 (dd, *J* = 4.5, 2.0 Hz, 1H, *H5*), 4.44 (s, 1H, *H3*), 3.82 (s, 3H, *H22*), 3.43 (dd, *J* = 16.0, 4.5 Hz, 1H, *H6*), 3.37 (dd, *J* = 16.0, 2.0 Hz, 1H, *H6*), 2.71 (s, 1H, *H24*), 1.49 (s, 3H, *H10*), 1.23 ppm (s, 3H, H9*).* **^{13}C NMR** (151 MHz, 300 K, $CDCl_3$): δ = 171.1, 167.4, 160.1, 130.7, 126.7, 114.1, 67.8, 65.6, 64.1, 62.9, 55.3, 37.8, 21.3, 18.4 ppm. **HRMS** (ESI): *m/z* calculated for $C_{16}H_{21}N_2O_5S$ $(M+H)^+$ = 353.1166, found 353.1166. **IR** (film): ṽ = 3847, 3812, 3790, 3697, 3683, 3662, 3640, 2980, 1798, 1755, 1711, 1691, 1659, 1641, 1612, 1549, 1516, 1467, 1443, 1251 cm^{-1}. $\boldsymbol{[\alpha]_D^{25}}$ = + 73.2 (c = 0.35, $CHCl_3$).

4-Methoxybenzyl (*2S*,*4S*,*5R*)-3,3-dimethyl-7-oxo-4-(pivaloylimino)-4λ^6-thia-1-azabicyclo[3.2.0]heptane-2-carboxylate 4-oxide (33a).

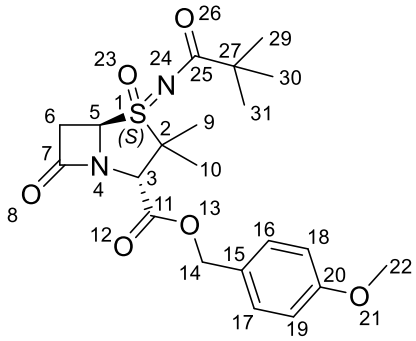

Following General Procedure E, *N*-acyl sulfoximine **33a** (58 mg, 0.13 mmol, 94%) was obtained by reaction of *NH*-sulfoximine **32** (50 mg, 1.0 equiv., 0.14 mmol) and pivaloyl chloride (17 mg, 1.0 equiv., 0.14 mmol), following column chromatography (5 g Sfär cartridge; 20 mL/min; initially 100% (v/v) cyclohexane (3 CV), followed by a linear gradient (15 CV): 0–40% (v/v) ethyl acetate in cyclohexane). Amorphous solid. **^{1}H NMR** (600 MHz, 300 K, $CDCl_3$): δ = 7.35 – 7.27 (m, 2H, *H16*, *H17*), 6.93 – 6.87 (m, 2H, *H18*, *H19*), 5.27, 5.10 (2H, ABq, *J* = 11.7 Hz, *H14*), 4.82 (dd, *J* = 4.1, 2.3 Hz, 1H, *H5*), 4.41 (s, 1H, *H3*), 3.82 (s, 3H, *H22*), 3.70 – 3.60 (m, 2H, *H6*), 1.66 (s, 3H, *H10*), 1.20 (s, 3H, *H9*), 1.18 ppm (s, 9H, *H29*, *H30*, *H31*). **^{13}C NMR** (151 MHz, 300 K, $CDCl_3$): δ = 189.5, 171.4, 166.9, 160.3, 131.0, 126.7, 114.3, 68.2, 67.6, 67.0, 63.7, 55.5, 41.5, 39.8, 27.6, 21.1, 18.9 ppm. **HRMS** (ESI): *m/z* calculated

for $C_{21}H_{28}N_2O_6SNa$ $(M+Na)^+$ = 459.1560, found 459.1556. **IR** (film): $\tilde{\nu}$ = 3775, 3697, 3662, 2960, 1804, 1756, 1691, 1659, 1641, 1549, 1516, 1463, 1292, 1218, 1190 cm^{-1}. $[\alpha]_D^{25}$ = + 88.1 (c = 0.31, $CHCl_3$).

4-Methoxybenzyl (*2S*,*4S*,*5R*)-4-(benzoylimino)-3,3-dimethyl-7-oxo-4λ⁶-thia-1-azabicyclo[3.2.0]heptane-2-carboxylate 4-oxide (33b).

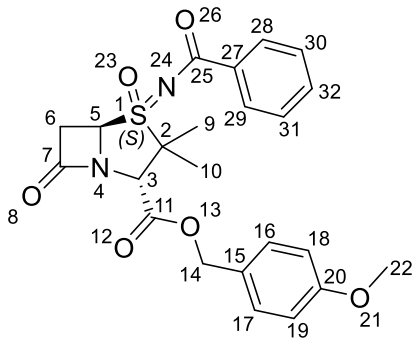

Following General Procedure E, *N*-acyl sulfoximine **33b** (50 mg, 0.11 mmol, 77%) was obtained by reaction of *NH*-sulfoximine **32** (50 mg, 1.0 equiv., 0.14 mmol) and benzoyl chloride (20 mg, 1.0 equiv., 0.14 mmol), following column chromatography (5 g Sfär cartridge; 20 mL/min; initially 100% (v/v) cyclohexane (3 CV), followed by a linear gradient (15 CV): 0–35% (v/v) ethyl acetate in cyclohexane). Amorphous solid. **^{1}H NMR** (600 MHz, 300 K, $CDCl_3$): δ = 8.09 (m, 2H, *H28*, *H29*), 7.54 (t, *J* = 7.5 Hz, 1H, *H32*), 7.42 (m, 2H, *H30*, *H31*), 7.32 (m, 2H, *H16*, *H17*), 6.90 (m, 2H, *H18*, *H19*), 5.28, 5.12 (2H, ABq, *J* = 11.7 Hz, *H14*), 5.00 (dd, *J* = 4.0, 2.6 Hz, 1H, *H5*), 4.48 (s, 1H, *H3*), 3.82 (s, 3H, *H22*), 3.79 – 3.72 (m, 2H, *H6*), 1.76 (s, 3H, *H10*), 1.30 ppm (s, 3H, *H9*). **^{13}C NMR** (151 MHz, 300 K, $CDCl_3$): δ = 175.2, 171.2, 166.9, 160.3, 134.1, 133.1, 131.0, 129.8, 128.4, 126.6, 114.3, 68.3, 67.9, 67.3, 63.7, 55.5, 40.0, 21.2, 19.1 ppm. **HRMS** (ESI): *m/z* calculated for $C_{23}H_{24}N_2O_6SNa$ $(M+Na)^+$ = 479.1247, found 479.1245. **IR** (film): $\tilde{\nu}$ = 3775, 3696, 3662, 2980, 1804, 1756, 1691, 1659, 1631, 1549, 1516, 1451, 1315, 1287, 1219, 1177, 1124, 1028 cm^{-1}. $[\alpha]_D^{25}$ = + 81.6 (c = 0.41, $CHCl_3$).

4-Methoxybenzyl (*2S*,*4S*,*5R*)-4-(acryloylimino)-3,3-dimethyl-7-oxo-4λ⁶-thia-1-azabicyclo[3.2.0]heptane-2-carboxylate 4-oxide (33c).

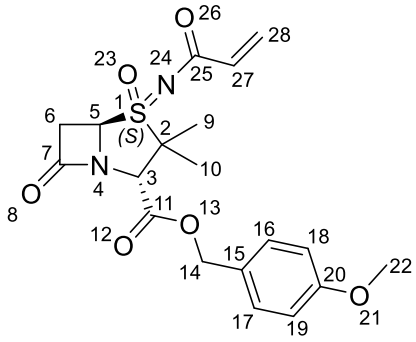

Following General Procedure E, *N*-acyl sulfoximine **33c** (57 mg, 0.14 mmol, 99%) was obtained by reaction of *NH*-sulfoximine **32** (50 mg, 1.0 equiv., 0.14 mmol) and acryloyl chloride (13 mg, 1 equiv., 0.14 mmol), following column chromatography (5 g Sfär cartridge; 20 mL/min; initially 100% (v/v) cyclohexane (3 CV), followed by a linear gradient (15 CV): 0–40% (v/v) ethyl acetate in cyclohexane). Amorphous solid. **^{1}H NMR** (400 MHz, 300 K, $CDCl_3$): δ = 7.36 – 7.27 (m, 2H, *H16*, *H17*), 6.94 – 6.86 (m, 2H, *H18*, *H19*), 6.38 (dd, *J* = 17.2, 1.6 Hz, 1H, *H28*), 6.20 (dd, *J* = 17.2, 10.1 Hz, 1H, *H27*), 5.80 (dd, *J* = 10.2, 1.7 Hz, 1H, *H28*), 5.26, 5.11 (2H, ABq, *J* = 11.7 Hz, *H14*), 4.91 (t, *J* = 3.2 Hz, 1H, *H5*), 4.43 (s, 1H, H3), 3.82 (s, 3H, *H22*), 3.68 (d, *J* = 3.2 Hz, 2H, *H6*), 1.69 (s, 3H, *H10*), 1.24 ppm (s, 3H, *H9*). **^{13}C NMR** (151 MHz, 300 K, $CDCl_3$): δ = 174.8, 171.2, 166.8, 160.3, 133.3, 131.0, 130.2, 126.6, 114.3, 68.3, 67.8, 67.2, 63.7, 55.5, 39.8, 21.0, 18.9 ppm. **HRMS** (ESI): *m/z* calculated for $C_{19}H_{22}N_2O_6SNa$ $(M+Na)^+$ = 429.1091, found 429.1090. **IR** (film): $\tilde{\nu}$ = 3847, 3812, 3789, 3697, 3683, 3662, 3637, 2980, 1804, 1756, 1711, 1691, 1659, 1642, 1612, 1549, 1515, 1482, 1463, 1296, 1217, 1070 cm^{-1}. $[\alpha]_D^{25}$ = + 101.3 (c = 0.2, $CHCl_3$).

4-Methoxybenzyl (*2S*,*4S*,*5R*)-4-(acetylimino)-3,3-dimethyl-7-oxo-4λ^6-thia-1-azabicyclo[3.2.0]heptane-2-carboxylate 4-oxide (33d).

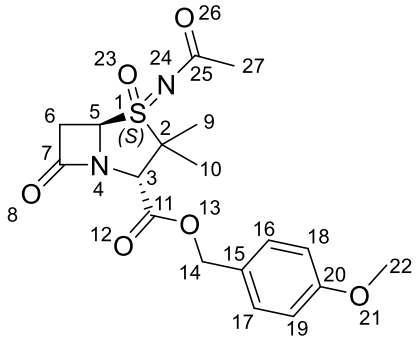

Following General Procedure E, *N*-acyl sulfoximine **33d** (210 mg, 0.53 μmol, 94%) was obtained by reaction of *NH*-sulfoximine **32** (200 mg, 1.0 equiv., 0.57 mmol) and acetyl chloride (67 mg, 1.0 equiv., 0.14 mmol), following column

chromatography (5 g Sfär cartridge; 20 mL/min; initially 100% (v/v) cyclohexane (3 CV), followed by a linear gradient (15 CV): 0–50% (v/v) ethyl acetate in cyclohexane). **^{1}H NMR** (600 MHz, 300 K, $CDCl_3$): δ = 7.34 – 7.28 (m, 2H, *H16*, *H17*), 6.93 – 6.87 (m, 2H, *H18*, *H19*), 5.25, 5.11 (2H, ABq, *J* = 11.7 Hz, *H14*), 4.87 (dd, *J* = 4.0, 2.5 Hz, 1H, *H5*), 4.41 (s, 1H, *H3*), 3.82 (s, 3H, *H22*), 3.68 – 3.58 (m, 2H, *H6*), 2.13 (s, 3H, *H27*), 1.66 (s, 3H, *H10*), 1.22 ppm (s, 3H, *H9*). **^{13}C NMR** (151 MHz, 300 K, $CDCl_3$): δ = 181.1, 171.2, 166.9, 160.3, 130.9, 126.6, 114.3, 68.3, 67.6, 67.1, 63.7, 55.5, 39.7, 26.1, 21.0, 18.8 ppm. **HRMS** (ESI): *m/z* calculated for $C_{18}H_{21}N_2O_6S$ $(M–H)^-$ = 393.1126, found 393.1121. **IR** (film): $\tilde{\nu}$ = 3657, 2981, 2889, 2359, 1801, 1756, 1637, 1516, 1463, 1381, 1254, 1176, 1034 cm^{-1}. $[\alpha]_D^{25}$ = + 67.0 (c = 0.21, $CHCl_3$).

4-Methoxybenzyl (*2S*,*4S*,*5R*)-4-(butyrylimino)-3,3-dimethyl-7-oxo-4λ^6-thia-1-azabicyclo[3.2.0]heptane-2-carboxylate 4-oxide (33e).

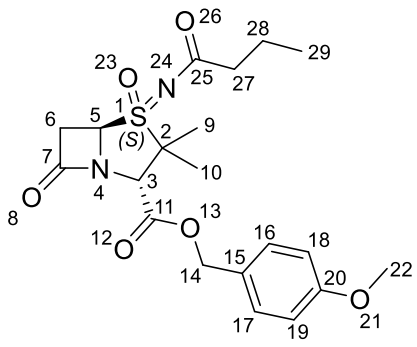

Following General Procedure F, *N*-acyl sulfoximine **33e** (74 mg, 0.18 mmol, 62%) was obtained from *NH*-sulfoximine **32** (100 mg, 1.0 equiv., 0.28 mmol) and butyric acid (28 mg, 1.1 equiv., 0.31 mmol), following column chromatography (10 g Sfär cartridge; 40 mL/min; initially 100% (v/v) cyclohexane (3 CV), followed by a linear gradient (15 CV): 0–40% (v/v) ethyl acetate in cyclohexane).

Amorphous solid. **^{1}H NMR** (600 MHz, 300 K, $CDCl_3$): δ = 7.34 – 7.28 (m, 2H, *H16*, *H17*), 6.92 – 6.87 (m, 2H, *H18*, *H19*), 5.25, 5.11 (2H, ABq, *J* = 11.7 Hz, *H14*), 4.85 (dd, *J* = 3.9, 2.6 Hz, 1H, *H5*), 4.41 (s, 1H, *H3*), 3.82 (s, 3H, *H22*), 3.64 (dd, *J* = 3.3, 2.3 Hz, 2H, *H6*), 2.36 (td, *J* = 7.3, 1.1 Hz, 2H, *H27*), 1.66 (s, 3H, *H10*), 1.63 (h, *J* = 7.3 Hz, 2H, *H28*), 1.22 (s, 3H, *H9*), 0.93 ppm (t, *J* = 7.4 Hz, 3H, *H29*). **^{13}C NMR** (151 MHz, 300 K, $CDCl_3$): δ = 183.8, 171.3, 166.9, 160.3, 130.9, 126.7, 114.3, 68.3, 67.6,

67.2, 63.7, 55.5, 41.0, 39.8, 21.0, 19.0, 18.9, 13.9 ppm. **HRMS** (ESI): *m/z* calculated for $C_{20}H_{27}N_2O_6S$ $(M+H)^+$ = 423.1584, found 423.1584. **IR** (film): ṽ = 3847, 3775, 3697, 3662, 3639, 2980, 1804, 1756, 1691, 1641, 1549, 1517, 1463, 1380, 1253, 1217, 1081 cm^{-1}. $[\alpha]_D^{25}$ = + 127.4 (c = 0.45, $CHCl_3$).

4-Methoxybenzyl (*2S*,*4S*,*5R*)-4-(((*tert*-butoxycarbonyl)-*L*-leucyl)imino)-3,3-dimethyl-7-oxo-4λ⁶-thia-1-azabicyclo[3.2.0]heptane-2-carboxylate 4-oxide (33f).

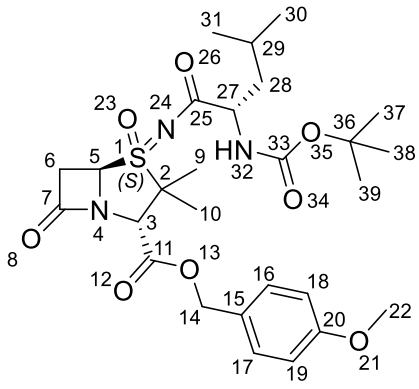

Following General Procedure F, *N*-acyl sulfoximine **33f** (46 mg, 81 µmol, 57%) was obtained from *NH*-sulfoximine **32** (50 mg, 1.0 equiv., 0.14 mmol) and (*tert*-butoxycarbonyl)-*L*-leucine (33 mg, 1.0 equiv., 0.14 mmol), following column chromatography (5 g Sfär cartridge; 20 mL/min; initially 100% (v/v) cyclohexane (3 CV), followed by a linear gradient (15 CV): 0–30% (v/v) ethyl acetate in cyclohexane).

Amorphous solid. **^{1}H NMR** (600 MHz, 300 K, $CDCl_3$): δ = 7.34 – 7.28 (m, 2H, *H16*, *H17*), 6.93 – 6.87 (m, 2H, *H18*, *H19*), 5.26, 5.11 (2H, ABq, *J* = 11.7 Hz, *H14*), 4.89 (m, 2H, *H5*), 4.41 (s, 1H, *H3*), 4.28 (m, 1H, *H27*), 3.82 (s, 3H, *H22*), 3.68 – 3.58 (m, 2H, *H6*), 1.76 – 1.68 (m, 1H, *H29*), 1.66 (m, 4H, *H10*, *H28*), 1.43 (m, 10H, *H28*, *H37*, *H38*, *H39*), 1.23 (s, 3H, *H9*), 0.94 ppm (dd, *J* = 6.5, 4.0 Hz, 6H, *H30*, *H31*). **^{13}C NMR** (151 MHz, 300 K, $CDCl_3$): δ = 183.0, 171.1, 166.7, 160.4, 155.7, 131.0, 126.6, 114.3, 79.7, 68.3, 67.9, 67.1, 63.7, 55.5, 55.1, 42.3, 39.7, 28.5, 25.1, 23.2, 22.1, 21.1, 18.8 ppm. **HRMS** (ESI): *m/z* calculated for $C_{27}H_{38}N_3O_8S$ $(M–H)^–$ = 566.2531, found 566.2527. **IR** (film): ṽ = 3788, 3682, 3662, 3636, 2980, 1805, 1756, 1711, 1658, 1642, 1548, 1517, 1467, 1369, 1252 cm^{-1}. $[\alpha]_D^{25}$ = + 78.5 (c = 0.27, $CHCl_3$).

Sodium (*2S*,*4S*,*5R*)-3,3-dimethyl-7-oxo-4-(pivaloylimino)-4λ⁶-thia-1-azabicyclo[3.2.0]heptane-2-carboxylate 4-oxide (34a).

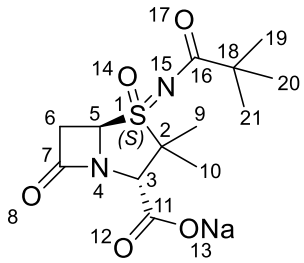

Following General Procedure D, acid **34a** (11 mg, 35 µmol, 63%) was obtained from ester **33a** (24 mg, 1.0 equiv., 55 µmol) with 10% (w/w) Pd/C (0.2 equiv.) in anhydrous methanol stirring for 3 h under hydrogen atmosphere. The reaction mixture was filtered using Celite®; the Celite® pad was rinsed with DCM, which was then removed *in vacuo*. The residue was redissolved in anhydrous methanol before the addition of sodium 2-ethylhexanoate (1.0 equiv.). The resultant mixture was stirred for 15 min before being evaporated *in vacuo*. The product was precipitated by the addition of pentane to the crude residue. Filtration afforded the carboxylate sodium salt.

White solid. **MP**: decomposition > 100 °C. **^{1}H NMR** (500 MHz, 300 K, MeOD-d_4): δ = 5.18 (dd, *J* = 4.5, 1.7 Hz, 1H, *H5*), 4.38 (s, 1H, *H3*), 3.72 (dd, *J* = 16.6, 4.5 Hz, 1H, *H6*), 3.46 (dd, *J* = 16.5, 1.7 Hz, 1H, *H6*), 1.72 (s, 3H, *H10*), 1.48 (s, 3H, *H9*), 1.20 ppm (s, 9H, *H19*, *H20*, *H21*). **^{13}C NMR** (126 MHz, 300 K, MeOD-d_4): δ = 191.3, 173.4, 170.2, 68.7, 68.0, 65.1, 42.2, 39.8, 28.0, 21.3, 19.0 ppm. **HRMS** (ESI): *m/z* calculated for $C_{13}H_{19}N_2O_5S$ $(M–H)^-$ = 315.1020, found 315.1035. **IR** (film): $\tilde{\nu}$ = 2979, 1795, 1636, 1480, 1394, 1293, 1205, 1084, 1029 cm^{-1}. $[\alpha]_D^{25}$ = + 128.7 (c = 0.81, MeOH).

Sodium (*2S*,*4S*,*5R*)-4-(benzoylimino)-3,3-dimethyl-7-oxo-4λ⁶-thia-1-azabicyclo[3.2.0]heptane-2-carboxylate 4-oxide (34b).

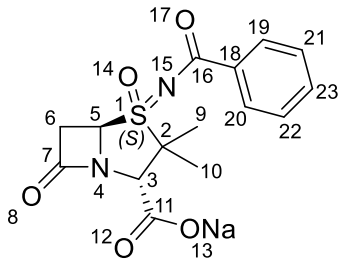

Following General Procedure D, acid **34b** (11 mg, 33 µmol, 75%) was obtained from ester **33b** (20 mg, 1.0 equiv., 44 µmol) with 10% (w/w) Pd/C (0.2 equiv.) in anhydrous THF stirring for 3 h under hydrogen

atmosphere. The reaction mixture was filtered using Celite®; the Celite® pad was rinsed with DCM, which was then removed *in vacuo*. The residue was redissolved in ethyl acetate before the addition of sodium 2-ethylhexanoate (1.0 equiv.). The resultant mixture was stirred for 15 min before being evaporated *in vacuo*. The product was precipitated by the addition of diethyl ether to the crude residue. Filtration afforded the carboxylate sodium salt.

White solid. **MP**: decomposition > 100 °C. **^{1}H NMR** (500 MHz, 300 K, MeOD-d_4): δ = 8.15 – 8.10 (m, 2H, *H19*, *H20*), 7.63 – 7.54 (m, 1H, *H23*), 7.48 (t, *J* = 7.8 Hz, 2H, *H21*, *H22*), 5.35 (dd, *J* = 4.5, 1.7 Hz, 1H, *H5*), 4.41 (s, 1H, *H3*), 3.81 (dd, *J* = 16.5, 4.5 Hz, 1H, *H6*), 3.59 (dd, *J* = 16.5, 1.7 Hz, 1H, *H6*), 1.85 (s, 3H, *H10*), 1.59 ppm (s, 3H, *H9*). **^{13}C NMR** (126 MHz, 300 K, MeOD-d_4): δ = 177.1, 173.5, 172.9, 135.7, 133.9, 130.5, 129.3, 69.4, 68.3, 67.4, 39.6, 21.8, 19.6 ppm. **HRMS** (ESI): *m/z* calculated for $C_{15}H_{15}N_2O_5SNa$ $(M+Na)^+$ = 335.0707, found 335.0712. **IR** (film): ṽ = 3750, 3347, 1792, 1627, 1318, 1290, 1215, 1027 cm^{-1}. $[\alpha]_D^{25}$ = + 59.0 (c = 0.1, MeOH).

Sodium (*2S*,*4S*,*5R*)-3,3-dimethyl-7-oxo-4-(propionylimino)-4λ^6-thia-1-azabicyclo[3.2.0]heptane-2-carboxylate 4-oxide (34c).

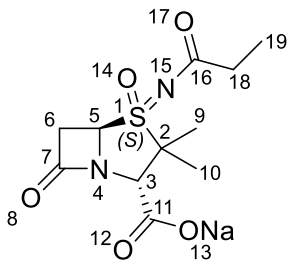

Following General Procedure D, acid **34c** (21 mg, 73 µmol, 63%) was obtained from ester **33c** (47 mg, 1.0 equiv., 0.12 mmol) with 10% (w/w) Pd/C (0.2 equiv.) in anhydrous THF stirring for 3 h under hydrogen atmosphere. The reaction mixture was filtered using Celite®; the Celite® pad was rinsed with DCM, which was then removed *in vacuo*. The residue was redissolved in ethyl acetate before the addition of sodium 2-ethylhexanoate (1.0 equiv.). The resultant mixture was stirred for 15 min before being evaporated *in vacuo*. The product was precipitated by the addition of diethyl ether to the crude residue. Filtration afforded the carboxylate sodium salt.

White solid. **MP**: decomposition > 100 °C. **^{1}H NMR** (500 MHz, 300 K, MeOD-*d*$_4$): δ = 5.24 (dd, *J* = 4.6, 1.8 Hz, 1H, *H5*), 4.39 (s, 1H, *H3*), 3.73 (dd, *J* = 16.6, 4.5 Hz, 1H, *H6*), 3.46 (dd, *J* = 16.6, 1.8 Hz, 1H, *H6*), 2.42 (qd, *J* = 7.5, 3.0 Hz, 2H, *H18*), 1.72 (s, 3H, *H10*), 1.48 (s, 3H, *H9*), 1.12 ppm (t, *J* = 7.5 Hz, 3H, *H19*). **^{13}C NMR** (126 MHz, 300 K, MeOD-*d*$_4$): δ = 186.5, 173.3, 170.0, 68.6, 68.1, 65.0, 39.8, 32.9, 21.2, 18.8, 10.0 ppm. **HRMS** (ESI): *m/z* calculated for $C_{11}H_{15}N_2O_5S$ $(M–H)^-$ = 287.0707, found 287.0705. **IR** (film): ṽ = 3480, 2988, 2941, 1797, 1637, 1465, 1373, 1289, 1216, 1135, 1079, cm^{-1}. $[\alpha]_D^{25}$ = + 105.7 (c = 0.64, MeOH).

4-Methoxybenzyl (*2S*,*4S*,*5R*)-3,3-dimethyl-7-oxo-4-(phenylimino)-4λ^6-thia-1-azabicyclo[3.2.0]heptane-2-carboxylate 4-oxide (35a).

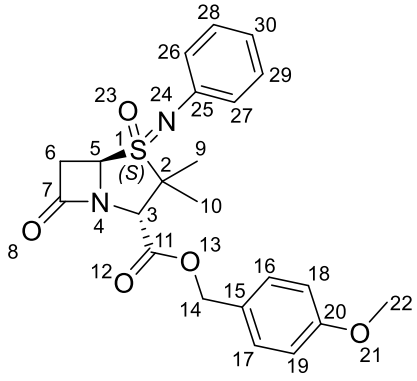

Following General Procedure G, *N*-aryl sulfoximine **35a** (12 mg, 28 μmol, 20%) was obtained from *NH*-sulfoximine **32** (50 mg, 1.0 equiv., 0.14 mmol) and phenylboronic acid (40 mg, 2.3 equiv., 0.33 mmol), following column chromatography (5 g Sfär cartridge; 20 mL/min; initially 100% (v/v) cyclohexane (3 CV), followed by a linear gradient (15 CV): 0–25% (v/v) ethyl acetate in cyclohexane).

Amorphous solid. **^{1}H NMR** (600 MHz, 300K, $CDCl_3$): δ = 7.30 (m, 2H, *H16*, *H17*), 7.23 – 7.17 (m, 2H, *H26*, *H27*), 7.07 – 7.03 (m, 2H, *H28*, *H29*), 6.98 (t, *J* = 7.3 Hz, 1H, *H30*), 6.91 – 6.86 (m, 2H, *H18*, *H19*), 5.25, 5.09 (2H, ABq, *J* = 11.7 Hz, *H14*), 4.73 (m, 1H, *H5*), 4.48 (s, 1H, *H3*), 3.81 (s, 3H, *H22*), 3.50 – 3.47 (m, 2H, *H6*), 1.61 (s, 3H, *H10*), 1.31 ppm (s, 3H, *H9*). **^{13}C NMR** (151 MHz, 300 K, $CDCl_3$): δ = 170.8, 167.2, 160.3, 143.4, 130.9, 129.5, 126.8, 123.2, 122.9, 114.3, 68.0, 67.9, 64.4, 64.2, 55.5, 38.7, 21.3, 20.8 ppm. **HRMS** (ESI): *m/z* calculated for $C_{22}H_{25}N_2O_5S$ $(M+H)^+$ =

429.1479, found 429.1479. **IR** (film): ṽ = 3896, 3847, 3828, 3811, 3775, 3717, 3697, 3683, 3662, 3641, 3573, 2958, 1802, 1755, 1711, 1691, 1659, 1641, 1594, 1549, 1515, 1493, 1463, 1443, 1306, 1272, 1200, 1050 cm^{-1}. $[\alpha]_D^{25}$ = + 4.6 (c = 0.25, $CHCl_3$).

4-Methoxybenzyl (*2S*,*4S*,*5R*)-4-((4-methoxyphenyl)imino)-3,3-dimethyl-7-oxo-4λ⁶-thia-1-azabicyclo[3.2.0]heptane-2-carboxylate 4-oxide (35b).

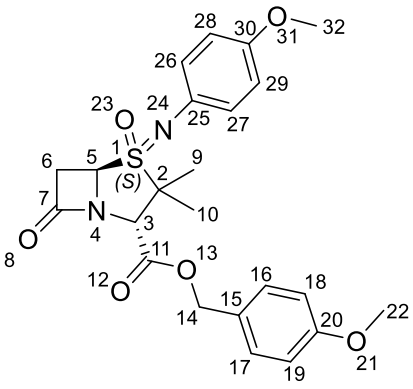

Following General Procedure G, *N*-aryl sulfoximine **35b** (6 mg, 13 μmol, 9%) was obtained from *NH*-sulfoximine **32** (50 mg, 1.0 equiv., 0.14 mmol) and (4-methoxyphenyl)boronic acid (32 mg, 1.5 equiv., 0.21 mmol), following column chromatography (5 g Sfär cartridge; 20 mL/min; initially 100% (v/v) cyclohexane (3 CV), followed by a linear gradient (15 CV): 0–30% (v/v) ethyl acetate in cyclohexane).

Amorphous solid. **^{1}H NMR** (400 MHz, 300 K, $CDCl_3$): δ = 7.34 – 7.27 (m, 2H, *H16*, *H17*), 7.04 – 6.95 (m, 2H, *H26*, *H27*), 6.94 – 6.84 (m, 2H, *H18*, *H19*), 6.80 – 6.71 (m, 2H, *H28*, *H29*), 5.24, 5.08 (2H, ABq, *J* = 11.7 Hz, *H14*), 4.71 (dd, *J* = 3.6, 2.7 Hz, 1H, *H5*), 4.46 (s, 1H, *H3*), 3.81 (s, 3H, *H22*), 3.75 (s, 3H, *H32*), 3.49 – 3.43 (m, 2H, *H6*), 1.57 (s, 3H, *H10*), 1.30 ppm (s, 3H, *H9*). **^{13}C NMR** (151 MHz, 300 K, $CDCl_3$): δ = 170.9, 167.3, 160.3, 155.7, 136.2, 130.9, 126.8, 124.2, 114.7, 114.3, 68.0, 67.7, 64.5, 63.9, 55.6, 55.5, 38.6, 21.2, 20.9 ppm. **HRMS** (ESI): *m/z* calculated for $C_{23}H_{27}N_2O_6S$ $(M+H)^+$ = 459.1584, found 459.1585. **IR** (film): ṽ = 3896, 3847, 3812, 3790, 3697, 3683, 3663, 3638, 2960, 1798, 1755, 1711, 1691, 1659, 1641, 1612, 1548, 1504, 1467, 1443, 1245, 1050 cm^{-1}. $[\alpha]_D^{25}$ = + 2.1 (c = 0.33, $CHCl_3$).

4-Methoxybenzyl (*2S*,*4S*,*5R*)-3,3-dimethyl-4-((4-nitrophenyl)imino)-7-oxo-4λ⁶-thia-1-azabicyclo[3.2.0]heptane-2-carboxylate 4-oxide (35c).

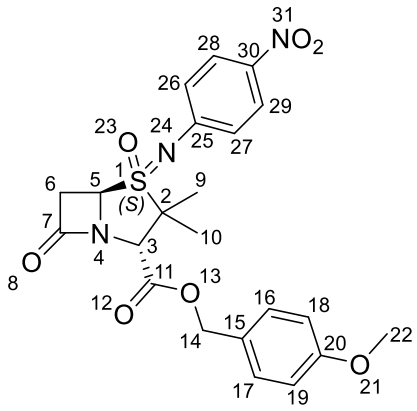

Following General Procedure G, *N*-aryl sulfoximine **35c** (13 mg, 27 μmol, 19%) was obtained from *NH*-sulfoximine **32** (50 mg, 1.0 equiv., 0.14 mmol) and (4-nitrophenyl)boronic acid (35 mg, 1.5 equiv., 0.21 mmol), following column chromatography (5 g Sfär cartridge; 20 mL/min; initially 100% (v/v) dichloromethane (3 CV), followed by a linear gradient (15 CV): 0–10% (v/v) ethyl acetate in dichloromethane).

Amorphous solid. **^{1}H NMR** (600 MHz, 300 K, $CDCl_3$): δ = 8.11 – 8.06 (m, 2H, *H28*, *H29*), 7.33 – 7.28 (m, 2H, *H16*, *H17*), 7.14 – 7.09 (m, 2H, *H26*, *H27*), 6.93 – 6.86 (m, 2H, *H18*, *H19*), 5.26, 5.10 (2H, ABq, *J* = 11.7 Hz, *H14*), 4.78 (dd, *J* = 4.3, 1.9 Hz, 1H, *H5*), 4.51 (s, 1H, *H3*), 3.81 (s, 3H, *H22*), 3.57 (dd, *J* = 16.2, 4.3 Hz, 1H, *H6*), 3.51 (dd, *J* = 16.2, 1.9 Hz, 1H, *H6*), 1.64 (s, 3H, *H10*), 1.30 ppm (s, 3H, *H9*). **^{13}C NMR** (151 MHz, 300 K, $CDCl_3$): δ = 170.1, 166.8, 160.4, 150.9, 142.8, 131.0, 126.6, 125.5, 122.7, 114.3, 68.9, 68.3, 64.9, 64.0, 55.5, 38.9, 21.3, 20.7 ppm. **HRMS** (ESI): *m/z* calculated for $C_{22}H_{22}N_3O_7S$ $(M–H)^-$ = 472.1184, found 472.1182. **IR** (film): ṽ = 3847, 3811, 3790, 3697, 3683, 3663, 3638, 2927, 1805, 1756, 1726, 1711, 1691, 1659, 1641, 1587, 1549, 1513, 1493, 1467, 1452, 1304, 1216 cm^{-1}. $[\alpha]_D^{25}$ = – 18.2 (c = 0.13, $CHCl_3$).

4-Methoxybenzyl (*2S*,*4S*,*5R*)-4-((4-bromophenyl)imino)-3,3-dimethyl-7-oxo-4λ^{6}-thia-1-azabicyclo[3.2.0]heptane-2-carboxylate 4-oxide (35d).

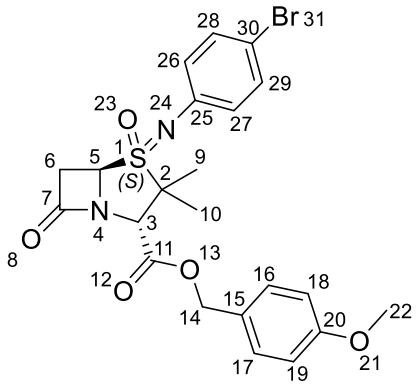

Following General Procedure G, *N*-aryl sulfoximine **35d** (20 mg, 39 μmol, 28%) was obtained from *NH*-sulfoximine **32** (50 mg, 1.0 equiv., 0.14 mmol) and (4-bromophenyl)boronic acid (65 mg, 2.3 equiv., 0.33 mmol), following column chromatography (5 g Sfär cartridge; 20 mL/min; initially 100% (v/v) dichloromethane (3 CV), followed by a linear gradient (15 CV): 0–8% (v/v) ethyl acetate in dichloromethane).

Amorphous solid. **^{1}H NMR** (400 MHz, 300 K, $CDCl_3$): δ = 7.33 – 7.28 (m, 4H, *H16*, *H17*, *H28*, *H29*), 6.96 – 6.91 (m, 2H, *H26*, *H27*), 6.89 (m, 2H, *H18*, *H19*), 5.25, 5.08 (2H, ABq, *J* = 11.7 Hz, *H14*), 4.72 (dd, *J* = 4.0, 2.3 Hz, 1H, *H5*), 4.47 (s, 1H, *H3*), 3.81 (s, 3H, *H22*), 3.56 – 3.41 (m, 2H, *H6*), 1.59 (s, 3H, *H10*), 1.29 ppm (s, 3H, *H9*). **^{13}C NMR** (101 MHz, 300 K, $CDCl_3$): δ = 170.6, 167.1, 160.3, 142.6, 132.4, 130.9, 126.7, 124.8, 115.6, 114.3, 68.2, 68.1, 64.3, 64.2(5), 55.4, 38.7, 21.2, 20.8 ppm. **HRMS** (ESI): *m/z* calculated for $C_{22}H_{22}BrN_2O_5S$ $(M–H)^-$ = 505.0438, found 505.0458. **IR** (film): $\tilde{\nu}$ = 3847, 3789, 3697, 3662, 3637, 2980, 1802, 1755, 1691, 1659, 1613, 1583, 1548, 1516, 1485, 1463, 1306, 1258, 1203, 1042 cm^{-1}. $[\alpha]_D^{25}$ = – 10.9 (c = 0.83, $CHCl_3$).

4-Methoxybenzyl (*2S*,*4S*,*5R*)-4-((4-iodophenyl)imino)-3,3-dimethyl-7-oxo-4λ^6-thia-1-azabicyclo[3.2.0]heptane-2-carboxylate 4-oxide (35e).

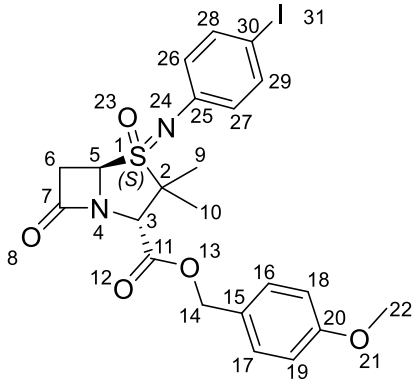

Following General Procedure G, *N*-aryl sulfoximine **35e** (15 mg, 27 μmol, 19%) was obtained from *NH*-sulfoximine **32** (50 mg, 1.0 equiv., 0.14 mmol) and (4-iodophenyl)boronic acid (81 mg, 2.3 equiv., 0.33 mmol), following column chromatography (5 g Sfär cartridge; 20 mL/min;

initially 100% (v/v) dichloromethane (3 CV), followed by a linear gradient (15 CV): 0–5% (v/v) ethyl acetate in dichloromethane).

Amorphous solid. **^{1}H NMR** (500 MHz, 300 K, $CDCl_3$): δ = 7.51 – 7.46 (m, 2H, *H28*, *H29*), 7.32 – 7.28 (m, 2H, *H16*, *H17*), 6.90 – 6.87 (m, 2H, *H18*, *H19*), 6.86 – 6.79 (m, 2H, *H26*, *H27*), 5.25, 5.08 (2H, ABq, *J* = 11.7 Hz, *H14*), 4.72 (dd, *J* = 4.1, 2.1 Hz, 1H, *H5*), 4.47 (s, 1H, *H3*), 3.81 (s, 3H, *H22*), 3.54 – 3.42 (m, 2H, *H6*), 1.59 (s, 3H, *H10*), 1.28 ppm (s, 3H, *H9*). **^{13}C NMR** (126 MHz, 300 K, $CDCl_3$): δ = 170.6, 167.1, 160.3, 143.4, 138.4, 130.9, 126.7, 125.2, 114.3, 85.9, 68.2, 68.1, 64.3 (2C), 55.5, 38.7, 21.2, 20.9 ppm. **HRMS** (ESI): *m/z* calculated for $C_{22}H_{24}IN_2O_5S$ $(M+H)^+$ = 555.0445, found 555.0447. **IR** (film): $\tilde{\nu}$ = 3847, 3827, 3811, 3790, 3697, 3683, 3662, 3637, 2981, 1803, 1755, 1711, 1691, 1659, 1641, 1612, 1549, 1515, 1483, 1463, 1443, 1306, 1255, 1202, 1040 cm^{-1}. $[\alpha]_D^{25}$ = – 17.9 (c = 0.25, $CHCl_3$).

4-Methoxybenzyl (*2S*,*4S*,*5R*)-4-((3-methoxyphenyl)imino)-3,3-dimethyl-7-oxo-4λ^6-thia-1-azabicyclo[3.2.0]heptane-2-carboxylate 4-oxide (35f).

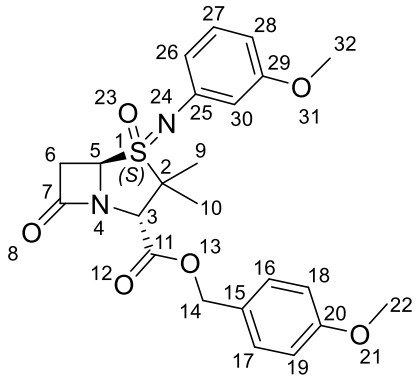

Following General Procedure G, *N*-aryl sulfoximine **35f** (18 mg, 39 μmol, 28%) was obtained from *NH*-sulfoximine **32** (50 mg, 1.0 equiv., 0.14 mmol) and (3-methoxyphenyl)boronic acid (50 mg, 2.3 equiv., 0.33 mmol), following column chromatography (5 g Sfär cartridge; 20 mL/min; initially 100% (v/v) dichloromethane (3 CV), followed by a linear gradient (15 CV): 0–5% (v/v) ethyl acetate in dichloromethane).

Amorphous solid. **^{1}H NMR** (600 MHz, 300 K, $CDCl_3$): δ = 7.33 – 7.27 (m, 2H, *H16*, *H17*), 7.10 (t, *J* = 8.1 Hz, 1H, *H27*), 6.92 – 6.86 (m, 2H, *H18*, *H19*), 6.66 (m, 1H, *H26*), 6.61 (t, *J* = 2.3 Hz, 1H, *H30*), 6.55 (m, 1H, *H28*), 5.25, 5.08 (2H, ABq, *J* = 11.7 Hz,

H14), 4.73 (dd, *J* = 3.7, 2.5 Hz, 1H, *H5*), 4.47 (s, 1H, *H3*), 3.81 (s, 3H, *H22*), 3.76 (s, 3H, *H32*), 3.53 – 3.44 (m, 2H, *H6*), 1.62 (s, 3H, *H10*), 1.30 ppm (s, 3H, *H9*). **^{13}C NMR** (151 MHz, 300 K, $CDCl_3$): δ = 170.8, 167.2, 160.6, 160.3, 144.6, 130.9, 130.0, 126.8, 115.5, 114.3, 109.0, 108.7, 68.0 (2C), 64.4, 64.2, 55.4, 55.4, 38.8, 21.3, 20.8 ppm. **HRMS** (ESI): *m/z* calculated for $C_{23}H_{27}N_2O_6S$ $(M+H)^+$ = 459.1584, found 459.1584. **IR** (film): ṽ = 3859, 3847, 3811, 3775, 3740, 3696, 3683, 3663, 3642, 2980, 1803, 1755, 1711, 1691, 1659, 1641, 1598, 1549, 1515, 1483, 1468, 1451, 1248, 1054 cm^{-1}. $[\alpha]_D^{25}$ = + 3.8 (c = 0.11, $CHCl_3$).

4-Methoxybenzyl (*2S*,*4S*,*5R*)-4-((2-methoxyphenyl)imino)-3,3-dimethyl-7-oxo-4λ^6-thia-1-azabicyclo[3.2.0]heptane-2-carboxylate 4-oxide (35g).

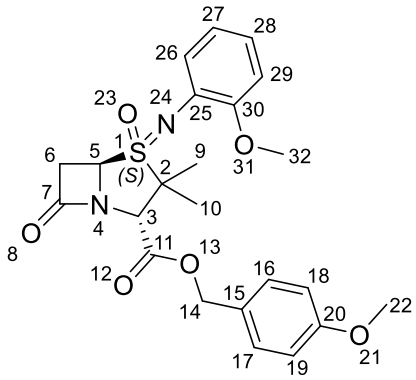

Following General Procedure G, *N*-aryl sulfoximine **35g** (13 mg, 28 μmol, 20%) was obtained from *NH*-sulfoximine **32** (50 mg, 1.0 equiv., 0.14 mmol) and (2-methoxyphenyl)boronic acid (50 mg, 2.3 equiv., 0.33 mmol), following column chromatography (5 g Sfär cartridge; 20 mL/min; initially 100% (v/v) dichloromethane (3 CV), followed by a linear gradient (15 CV): 0–5% (v/v) ethyl acetate in dichloromethane).

Amorphous solid. **^{1}H NMR** (400 MHz, 300 K, $CDCl_3$): δ = 7.36 – 7.27 (m, 2H, *H16*, *H17*), 7.04 (dd, *J* = 7.7, 1.7 Hz, 1H, *H26*), 6.98 (td, *J* = 7.7, 1.7 Hz, 1H, *H28*), 6.93 – 6.88 (m, 2H, *H18*, *H19*), 6.88 – 6.82 (m, 2H, *H27*, *H29*), 5.25, 5.10 (2H, ABq, *J* = 11.7 Hz, *H14*), 4.77 (dd, *J* = 3.9, 2.4 Hz, 1H, *H5*), 4.41 (s, 1H, *H3*), 3.82 (s, 3H, *H22*), 3.80 (s, 3H, *H32*), 3.56 – 3.42 (m, 2H, *H6*), 1.58 (s, 3H, *H10*), 1.37 ppm (s, 3H, *H9*). **^{13}C NMR** (151 MHz, 300 K, $CDCl_3$): δ = 172.0, 167.7, 160.2, 151.7, 131.3, 130.8, 126.9, 126.1, 123.8, 121.6, 114.3, 111.3, 68.0, 66.0, 65.5, 63.2, 56.0, 55.5, 39.4, 21.5, 18.9

ppm. **HRMS** (ESI): *m/z* calculated for $C_{23}H_{27}N_2O_6S$ $(M+H)^+$ = 459.1584, found 459.1585. **IR** (film): $\tilde{\nu}$ = 3869, 3847, 3811, 3785, 3742, 3696, 3662, 3637, 2970, 1803, 1760, 1711, 1691, 1659, 1641, 1598, 1548, 1504, 1473, 1463, 1442, 1247, 1050 cm^{-1}. $[\alpha]_D^{25}$ = + 4.8 (c = 0.12, $CHCl_3$).

4-Methoxybenzyl (*2S*,*4S*,*5R*)-4-((benzylcarbamoyl)imino)-3,3-dimethyl-7-oxo-4λ⁶-thia-1-azabicyclo[3.2.0]heptane-2-carboxylate 4-oxide (36a).

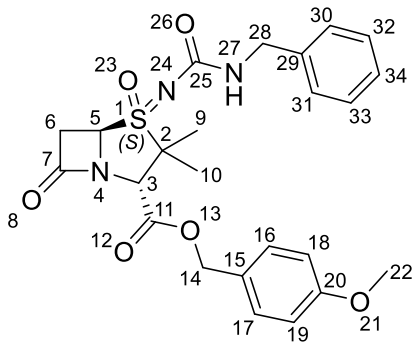

Following General Procedure H, urea **36a** (15 mg, 31 µmol, 22%) was obtained from *NH*-sulfoximine **32** (50 mg, 1.0 equiv., 0.14 mmol) and (isocyanatomethyl)benzene (30 mg, 1.6 equiv., 0.23 mmol), following column chromatography (5 g Sfär cartridge; 20 mL/min; initially 100% (v/v) cyclohexane (3 CV), followed by a linear gradient (15 CV): 0–45% (v/v) ethyl acetate in cyclohexane).

Amorphous solid. **^{1}H NMR** (500 MHz, 300 K, $CDCl_3$): δ 7.35 – 7.23 (m, 7H, *H16*, *H17*, *H30*, *H31*, *H32*, *H33*, *H34*), 6.93 – 6.86 (m, 2H, *H18*, *H19*), 5.34 (t, *J* = 6.0 Hz, 1H, *H27*), 5.24, 5.11 (2H, ABq, *J* = 11.7 Hz, *H14*), 4.97 (dd, *J* = 4.0, 2.4 Hz, 1H, *H5*), 4.45 – 4.37 (m, 2H, *H3*, *H28*), 4.33 (dd, *J* = 14.8, 5.1 Hz, 1H, *H28*), 3.82 (s, 3H, *H22*), 3.71 – 3.59 (m, 2H, *H6*), 1.64 (s, 3H, *H10*), 1.23 ppm (s, 3H, *H9*). **^{13}C NMR** (126 MHz, 300 K, $CDCl_3$): δ = 171.6, 167.1, 160.3, 160.1, 138.3, 130.9, 128.9, 127.8, 127.7, 126.7, 114.3, 68.2, 67.3, 67.2, 63.7, 55.5, 45.1, 39.8, 21.2, 18.9 ppm. **HRMS** (ESI): *m/z* calculated for $C_{24}H_{26}N_3O_6S$ $(M–H)^-$ = 484.1548, found 484.1562. **IR** (film): $\tilde{\nu}$ = 3697, 3034, 2926, 1800, 1756, 1640, 1517, 1453, 1249, 1131, 1031 cm^{-1}. $[\alpha]_D^{25}$ = + 117.1 (c = 0.11, $CHCl_3$).

4-Methoxybenzyl (*2S*,*4S*,*5R*)-3,3-dimethyl-7-oxo-4-((phenethylcarbamoyl)imino)-4λ⁶-thia-1-azabicyclo[3.2.0]heptane-2-carboxylate 4-oxide (36b).

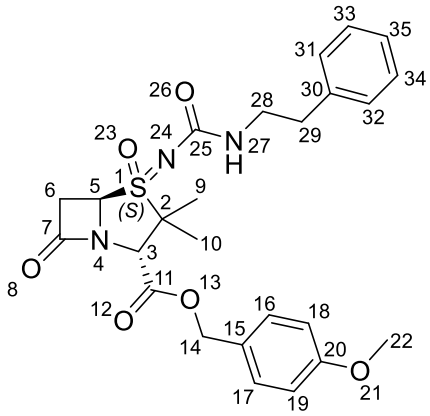

Following General Procedure H, urea **36b** (77 mg, 0.15 mmol, 54%) was obtained from *NH*-sulfoximine **32** (100 mg, 1.0 equiv., 0.28 mmol) and (2-isocyanatoethyl)benzene (67 mg, 1.6 equiv., 0.45 mmol), following column chromatography (5 g Sfär cartridge; 20 mL/min; initially 100% (v/v) cyclohexane (3 CV), followed by a linear gradient (15 CV): 0–50% (v/v) ethyl acetate in cyclohexane).

Amorphous solid. **^{1}H NMR** (600 MHz, 300 K, $CDCl_3$): δ = 7.34 – 7.27 (m, 4H, *H16*, *H17*, *H33*, *H34*), 7.25 – 7.14 (m, 3H, *H31*, *H32*, *H35*), 6.94 – 6.87 (m, 2H, *H18*, *H19*), 5.24, 5.11 (2H, ABq, *J* = 11.8 Hz, *H14*), 5.05 (t, *J* = 6.1 Hz, 1H, *H27*), 4.91 (dd, *J* = 4.3, 2.1 Hz, 1H, *H5*), 4.38 (s, 1H, *H3*), 3.82 (s, 3H, *H22*), 3.63 (m, 2H, *H6*), 3.53 – 3.37 (m, 2H, *H28*), 2.85 – 2.74 (m, 2H, *H29*), 1.62 (s, 3H, *H10*), 1.20 ppm (s, 3H, *H9*). **^{13}C NMR** (151 MHz, 300 K, $CDCl_3$): δ = 171.6, 167.1, 160.3, 160.1, 138.9, 130.9, 128.9, 128.8, 126.7, 126.6, 114.3, 68.2, 67.1, 67.1, 63.8, 55.5, 42.0, 39.7, 36.1, 21.1, 18.9 ppm. **HRMS** (ESI): *m/z* calculated for $C_{25}H_{28}N_3O_6S$ $(M–H)^-$ = 498.1704, found 498.1709. **IR** (film): ṽ = 3649, 3401, 2981, 1800, 1755, 1637, 1517, 1462, 1394, 1251, 1086 cm^{-1}. $[\alpha]_D^{25}$ = + 42.8 (c = 0.18, $CHCl_3$).

4-Methoxybenzyl (*2S*,*4S*,*5R*)-4-(((4-methoxybenzyl)carbamoyl)imino)-3,3-dimethyl-7-oxo-4λ⁶-thia-1-azabicyclo[3.2.0]heptane-2-carboxylate 4-oxide (36c).

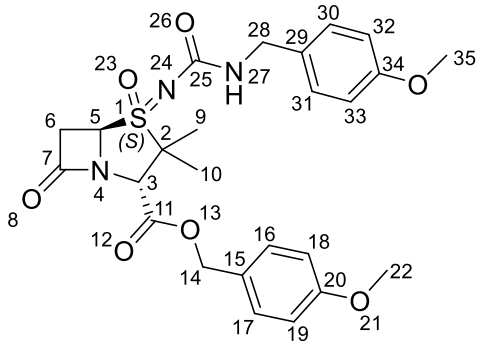

Following General Procedure H, urea **36c** (70 mg, 0.14 mmol, 64%) was obtained from *NH*-sulfoximine **32** (75 mg, 1.0 equiv., 0.21 mmol) and 1-(isocyanatomethyl)-4-methoxybenzene (56 mg, 1.6 equiv., 0.34 mmol), following column chromatography (5 g Sfär cartridge; 20 mL/min; initially 100% (v/v) cyclohexane (3 CV), followed by a linear gradient (15 CV): 0–50% (v/v) ethyl acetate in cyclohexane).

Amorphous solid. **^{1}H NMR** (600 MHz, 300 K, $CDCl_3$): δ = 7.33 – 7.28 (m, 2H, *H16*, *H17*), 7.22 – 7.15 (m, 2H, *H30*, *H31*), 6.92 – 6.88 (m, 2H, *H18*, *H19*), 6.87 – 6.83 (m, 2H, *H32*, *H33*), 5.27 (t, *J* = 5.8 Hz, 1H, *H27*), 5.24, 5.11 (2H, ABq, *J* = 11.7 Hz, *H14*), 4.96 (dd, *J* = 4.2, 2.3 Hz, 1H, *H5*), 4.39 (s, 1H, *H3*), 4.33 (dd, *J* = 14.4, 5.9 Hz, 1H, *H28*), 4.26 (dd, *J* = 14.5, 5.5 Hz, 1H, *H28*), 3.82 (s, 3H, *H22*), 3.79 (s, 3H, *H35*), 3.69 – 3.60 (m, 2H, *H6*), 1.63 (s, 3H, *H10*), 1.22 ppm (s, 3H, *H9*). **^{13}C NMR** (151 MHz, 300 K, $CDCl_3$): δ = 171.6, 167.1, 160.3, 160.0, 159.2, 130.9, 130.4, 129.1, 126.7, 114.3, 114.2, 68.2, 67.3, 67.2, 63.8, 55.5 (2C), 44.5, 39.8, 21.2, 18.9 ppm. **HRMS** (ESI): *m/z* calculated for $C_{25}H_{28}N_3O_7S$ $(M–H)^-$ = 514.1653, found 514.1664. **IR** (film): ṽ = 3656, 2980, 1799, 1755, 1636, 1516, 1463, 1383, 1250, 1176, 1074 cm^{-1}. $[\alpha]_D^{25}$ = + 44.8 (c = 0.49, $CHCl_3$).

4-Methoxybenzyl (*2S*,*4S*,*5R*)-4-(((4-chlorophenethyl)carbamoyl)imino)-3,3-dimethyl-7-oxo-4λ^6-thia-1-azabicyclo[3.2.0]heptane-2-carboxylate 4-oxide (36d).

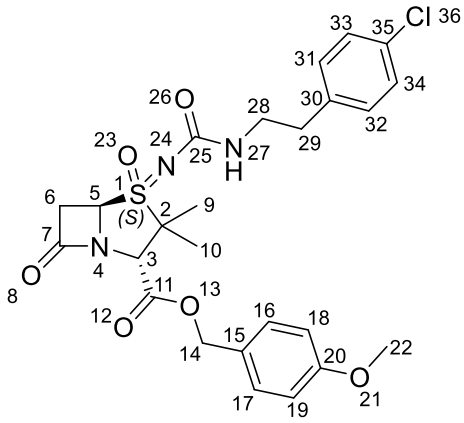

Following General Procedure H, urea **36d** (40 mg, 0.11 mmol, 35%) was obtained from *NH*-sulfoximine **32** (75 mg, 1.0 equiv., 0.21 mmol) and 1-chloro-4-(2-isocyanatoethyl)benzene (62 mg, 1.6 equiv., 0.34 mmol), following column chromatography (5 g Sfär cartridge; 20 mL/min; initially 100% (v/v) cyclohexane (3 CV), followed by a linear gradient (15 CV): 0–50% (v/v) ethyl acetate in cyclohexane).

Amorphous solid. **^{1}H NMR** (600 MHz, 300 K, $CDCl_3$): δ = 7.33 – 7.28 (m, 2H, *H16*, *H17*), 7.28 – 7.23 (m, 2H, *H33*, *H34*), 7.14 – 7.06 (m, 2H, *H31*, *H32*), 6.92 – 6.87 (m, 2H, *H18*, *H19*), 5.24, 5.11 (2H, ABq, *J* = 11.7 Hz, *H14*), 5.05 (t, *J* = 6.1 Hz, 1H, *H27*), 4.91 (dd, *J* = 4.3, 2.1 Hz, 1H, *H5*), 4.38 (s, 1H, *H3*), 3.81 (s, 3H, *H22*), 3.64 (dd, *J* = 16.7, 4.3 Hz, 1H, *H6*), 3.59 (dd, *J* = 16.6, 2.1 Hz, 1H, *H6*), 3.50 – 3.31 (m, 2H, *H28*), 2.82 – 2.72 (m, 2H, *H29*), 1.62 (s, 3H, *H10*), 1.20 ppm (s, 3H, *H9*). **^{13}C NMR** (151 MHz, 300 K, $CDCl_3$): δ = 171.5, 167.0, 160.3, 160.1, 137.4, 132.5, 130.9, 130.3, 128.9, 126.7, 114.3, 68.2, 67.3, 67.1, 63.7, 55.4, 41.9, 39.7, 35.5, 21.1, 18.9 ppm. **HRMS** (ESI): *m/z* calculated for $C_{25}H_{27}ClN_3O_6S$ $(M–H)^-$ = 532.1315, found 532.1318. **IR** (film): $\tilde{\nu}$ = 3396, 2980, 2888, 1800, 1755, 1636, 1517, 1463, 1394, 1251, 1090, 1033 cm^{-1}. $[\alpha]_D^{25}$ = + 47.6 (c = 0.94, $CHCl_3$).

4-Methoxybenzyl (*2S*,*4S*,*5R*)-4-(((4-fluorophenethyl)carbamoyl)imino)-3,3-dimethyl-7-oxo-4λ^6-thia-1-azabicyclo[3.2.0]heptane-2-carboxylate 4-oxide (36e).

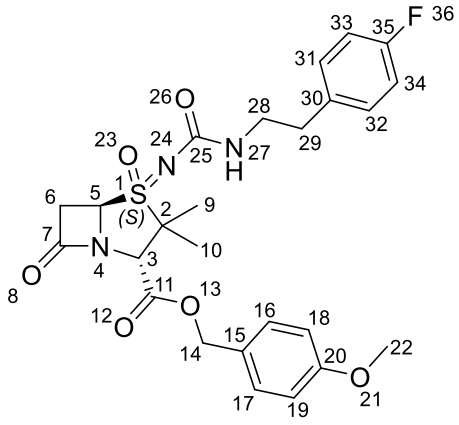

Following General Procedure H, urea **36e** (60 mg, 0.12 mmol, 55%) was obtained from *NH*-sulfoximine **32** (75 mg, 1.0 equiv., 0.21 mmol) and 1-fluoro-4-(2-isocyanatoethyl)benzene (56 mg, 1.6 equiv., 0.34 mmol), following column chromatography (5 g Sfär cartridge; 20 mL/min; initially 100% (v/v) cyclohexane (3 CV), followed by a linear gradient (15 CV): 0–55% (v/v) ethyl acetate in cyclohexane).

Amorphous solid. **^{1}H NMR** (600 MHz, 300 K, $CDCl_3$): δ = 7.33 – 7.28 (m, 2H, *H16*, *H17*), 7.17 – 7.11 (m, 2H, *H31*, *H32*), 7.02 – 6.95 (m, 2H, *H33*, *H34*), 6.92 – 6.87 (m, 2H, *H18*, *H19*), 5.24, 5.11 (2H, ABq, *J* = 11.7 Hz, *H14*), 5.04 (t, *J* = 6.1 Hz, 1H, *H27*), 4.92 (dd, *J* = 4.2, 2.1 Hz, 1H, *H5*), 4.39 (s, 1H, *H3*), 3.82 (s, 3H, *H22*), 3.65 (dd, *J* = 16.7, 4.3 Hz, 1H, *H6*), 3.60 (dd, *J* = 16.6, 2.1 Hz, 1H, *H6*), 3.51 – 3.31 (m, 2H, *H28*), 2.83 – 2.72 (m, 2H, *H29*), 1.63 (s, 3H, *H10*), 1.20 ppm (s, 3H, *H9*). **^{19}F NMR** (565 MHz, 300 K, $CDCl_3$): δ = -116.56 – -116.67 ppm (m). **^{13}C NMR** (151 MHz, 300 K, $CDCl_3$): δ = 171.5, 167.0, 161.8 (d, *J* = 244.6 Hz), 160.3, 160.1, 134.5 (d, *J* = 3.2 Hz), 130.9, 130.3 (d, *J* = 8.0 Hz), 126.7, 115.6 (d, *J* = 21.3 Hz), 114.3, 68.2, 67.3, 67.2, 63.8, 55.5, 42.1, 39.7, 35.4, 21.1, 18.9 ppm. **HRMS** (ESI): *m/z* calculated for $C_{25}H_{27}FN_3O_6S$ $(M–H)^-$ = 516.1610, found 516.1613. **IR** (film): $\tilde{\nu}$ = 2980, 1800, 1755, 1636, 1515, 1462, 1394, 1250, 1072, 1033 cm^{-1}. $[\alpha]_D^{25}$ = + 55.2 (c = 0.19, $CHCl_3$).

4-Methoxybenzyl (*2S*,*4S*,*5R*)-3,3-dimethyl-7-oxo-4-(((3-phenylpropyl)carbamoyl)imino)-4λ^6-thia-1-azabicyclo[3.2.0]heptane-2-carboxylate 4-oxide (36f).

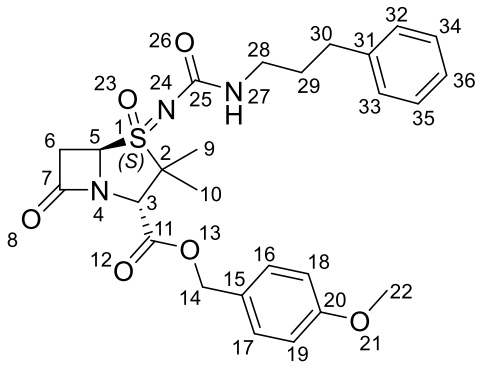

Following General Procedure H, urea **36f** (60 mg, 0.12 mmol, 55%) was obtained from *NH*-sulfoximine **32** (75 mg, 1.0 equiv., 0.21 mmol) and (3-isocyanatopropyl)benzene (55 mg, 1.6 equiv., 0.34 mmol), following column chromatography (5 g Sfär cartridge; 20 mL/min; initially 100% (v/v) cyclohexane (3 CV), followed by a linear gradient (15 CV): 0–50% (v/v) ethyl acetate in cyclohexane).

Amorphous solid. **^{1}H NMR** (400 MHz, 300 K, $CDCl_3$): δ 7.35 – 7.28 (m, 2H, *H16*, *H17*), 7.28 – 7.24 (m, 2H, *H34*, *H35*), 7.23 – 7.12 (m, 3H, *H32*, *H33*, *H36*), 6.94 – 6.86 (m, 2H, *H18*, *H19*), 5.24, 5.11 (2H, ABq, *J* = 11.7 Hz, *H14*), 5.06 (t, *J* = 5.9 Hz, 1H, *H27*), 4.93 (dd, *J* = 4.1, 2.3 Hz, 1H, *H5*), 4.39 (s, 1H, *H3*), 3.82 (s, 3H, *H22*), 3.70 – 3.55 (m, 2H, *H6*), 3.31 – 3.10 (m, 2H, *H28*), 2.68 – 2.60 (m, 2H, *H30*), 1.83 (p, *J* = 7.3 Hz, 2H, *H29*), 1.63 (s, 3H, *H10*), 1.22 ppm (s, 3H, *H9*). **^{13}C NMR** (151 MHz, 300 K, $CDCl_3$): δ = 171.5, 166.9, 160.2, 160.1, 141.3, 130.8, 128.5, 128.3, 126.6, 126.0, 114.2, 68.1, 67.1, 67.0, 63.6, 55.3, 40.5, 39.6, 33.2, 31.4, 21.0, 18.8 ppm. **HRMS** (ESI): *m/z* calculated for $C_{26}H_{30}N_3O_6S$ $(M–H)^-$ = 512.1861, found 512.1879. **IR** (film): $\tilde{\nu}$ = 3358, 2980, 2361, 1799, 1615, 1517, 1458, 1382, 1251, 1176, 1079, 1034 cm^{-1}. $[\alpha]_D^{25}$ = + 19.2 (c = 0.33, $CHCl_3$).

4-Methoxybenzyl (*2S*,*4S*,*5R*)-4-(((3-chloropropyl)carbamoyl)imino)-3,3-dimethyl-7-oxo-4λ^{6}-thia-1-azabicyclo[3.2.0]heptane-2-carboxylate 4-oxide (36g).

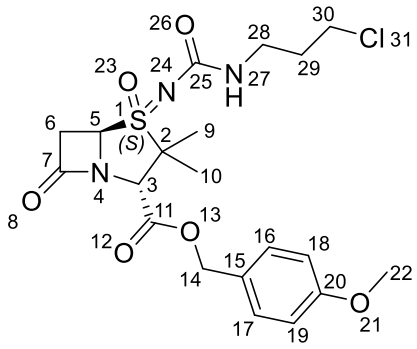

Following General Procedure H, urea **36g** (49 mg, 0.10 mmol, 49%) was obtained from *NH*-sulfoximine **32** (75 mg, 1.0 equiv., 0.21 mmol) and 1-chloro-3-isocyanatopropane (41 mg, 1.6 equiv., 0.34 mmol), following column chromatography (5 g Sfär cartridge; 20 mL/min; initially 100% (v/v) cyclohexane (3 CV), followed by a linear gradient (15 CV): 0–55% (v/v) ethyl acetate in cyclohexane).

Amorphous solid. **^{1}H NMR** (600 MHz, 300 K, $CDCl_3$): δ = 7.33 – 7.28 (m, 2H, *H16*, *H17*), 6.92 – 6.87 (m, 2H, *H18*, *H19*), 5.24, 5.11 (2H, ABq, *J* = 11.8 Hz, *H14*), 5.19 (t, *J* = 6.3 Hz, 1H, *H27*), 4.93 (dd, *J* = 4.3, 2.0 Hz, 1H, *H5*), 4.39 (s, 1H, *H3*), 3.82 (s, 3H, *H22*), 3.68 – 3.54 (m, 4H, *H6*, *H30*), 3.42 – 3.26 (m, 2H, *H28*), 1.97 (m, 2H, *H29*), 1.63 (s, 3H, *H10*), 1.22 ppm (s, 3H, *H9*). **^{13}C NMR** (151 MHz, 300 K, $CDCl_3$): δ = 171.5, 167.0, 160.4, 160.3, 130.9, 126.7, 114.3, 68.2, 67.3, 67.2, 63.7, 55.5, 42.5, 39.7, 38.3, 32.4, 21.2, 18.9 ppm. **HRMS** (ESI): *m/z* calculated for $C_{20}H_{25}ClN_3O_6S$ $(M–H)^-$ = 470.1158, found 470.1162. **IR** (film): $\tilde{\nu}$ = 2980, 1799, 1755, 1637, 1517, 1462, 1394, 1251, 1176, 1083, 1033 cm^{-1}. $[\alpha]_D^{25}$ = + 54.0 (c = 0.5, $CHCl_3$).

4-Methoxybenzyl (*2S*,*4S*,*5R*)-4-(((4-methoxyphenethyl)carbamoyl)imino)-3,3-dimethyl-7-oxo-4λ^6-thia-1-azabicyclo[3.2.0]heptane-2-carboxylate 4-oxide (36h).

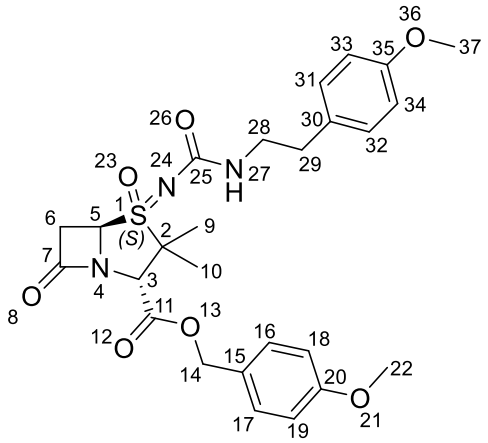

Following General Procedure H, urea **36h** (60 mg, 0.11 mmol, 53%) was obtained from *NH*-sulfoximine **32** (75 mg, 1.0 equiv., 0.21 mmol) and 1-(2-isocyanatoethyl)-4-methoxybenzene (60 mg, 1.6 equiv., 0.34 mmol), following column chromatography (5 g Sfär cartridge; 20 mL/min; initially 100% (v/v) cyclohexane

(3 CV), followed by a linear gradient (15 CV): 0–55% (v/v) ethyl acetate in cyclohexane).

Amorphous solid. **^{1}H NMR** (600 MHz, 300 K, $CDCl_3$): δ = 7.33 – 7.28 (m, 2H, *H16*, *H17*), 7.13 – 7.05 (m, 2H, *H31*, *H32*), 6.92 – 6.87 (m, 2H, *H18*, *H19*), 6.87 – 6.81 (m, 2H, *H33*, *H34*), 5.24, 5.11 (2H, ABq, *J* = 11.7 Hz, *H14*), 5.04 (t, *J* = 6.0 Hz, 1H, *H27*), 4.92 (dd, *J* = 4.2, 2.2 Hz, 1H, *H5*), 4.38 (s, 1H, *H3*), 3.82 (s, 3H, *H22*), 3.79 (s, 3H, *H37*), 3.68 – 3.57 (m, 2H, *H6*), 3.50 – 3.40 (m, 1H, *H28*), 3.40 – 3.31 (m, 1H, *H28*), 2.80 – 2.69 (m, 2H, *H29*), 1.62 (s, 3H, *H10*), 1.20 ppm (s, 3H, *H9*). **^{13}C NMR** (151 MHz, 300 K, $CDCl_3$) δ 171.6, 167.1, 160.3, 160.1, 158.4, 130.9, 130.9, 129.9, 126.7, 114.3, 114.2, 68.2, 67.2, 67.1, 63.8, 55.4(6), 55.4, 42.2, 39.7, 35.2, 21.1, 18.9 ppm. **HRMS** (ESI): *m/z* calculated for $C_{26}H_{30}N_3O_7S$ $(M–H)^-$ = 528.1810, found 528.1799. **IR** (film): $\tilde{\nu}$ = 3649, 2980, 2889, 1799, 1755, 1615, 1515, 1463, 1382, 1250, 1177, 1073 cm^{-1}. $[\alpha]_D^{25}$ = + 37.3 (c = 0.22, $CHCl_3$).

4-Methoxybenzyl (*2S*,*4S*,*5R*)-3,3-dimethyl-7-oxo-4-((((*S*)-1-phenylethyl)carbamoyl)imino)-4λ^6-thia-1-azabicyclo[3.2.0]heptane-2-carboxylate 4-oxide (36i).

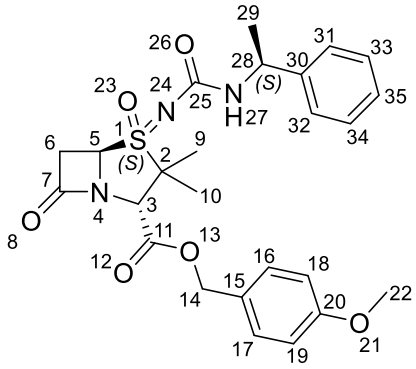

Following General Procedure H, urea **36i** (48 mg, 96 µmol, 48%) was obtained from *NH*-sulfoximine **32** (75 mg, 1.0 equiv., 0.21 mmol) and (*S*)-(1-isocyanatoethyl)benzene (50 mg, 1.6 equiv., 0.34 mmol), following column chromatography (5 g Sfär cartridge; 20 mL/min; initially 100% (v/v) cyclohexane (3 CV), followed by a linear gradient (15 CV): 0–50% (v/v) ethyl acetate in cyclohexane).

Amorphous solid. **^{1}H NMR** (600 MHz, 300 K, $CDCl_3$): δ = 7.37 – 7.27 (m, 7H, *H16*, *H17*, *H31*, *H32*, *H33*, *H34*, *H35*), 6.92 – 6.86 (m, 2H, *H18*, *H19*), 5.32 (d, *J* = 8.1 Hz, 1H, *H27*), 5.23, 5.11 (2H, ABq, *J* = 11.7 Hz, *H14*), 4.94 – 4.85 (m, 2H, *H3*, *H28*), 4.38 (s, 1H, *H3*), 3.81 (s, 3H, *H22*), 3.65 – 3.57 (m, 2H, *H6*), 1.63 (s, 3H, *H10*), 1.48 (d, *J* = 6.9 Hz, 3H, *H29*), 1.20 ppm (s, 3H, *H9*). **^{13}C NMR** (151 MHz, 300 K, $CDCl_3$): δ = 171.6, 167.1, 160.3, 159.2, 143.6, 130.9, 128.9, 127.5, 126.7, 126.1, 114.3, 68.2, 67.3, 67.2, 63.7, 55.5, 50.6, 39.8, 22.8, 21.2, 18.9 ppm. **HRMS** (ESI): *m/z* calculated for $C_{25}H_{28}N_3O_6S$ $(M–H)^-$ = 498.1704, found 498.1710. **IR** (film): ṽ = 3657, 2980, 1800, 1756, 1635, 1517, 1462, 1381, 1250, 1176, 1079, 1032 cm^{-1}. $[\alpha]_D^{25}$ = + 26.1 (c = 0.23, $CHCl_3$).

4-Methoxybenzyl (*2S*,*4S*,*5R*)-4-((cyclopropylcarbamoyl)imino)-3,3-dimethyl-7-oxo-4λ^6-thia-1-azabicyclo[3.2.0]heptane-2-carboxylate 4-oxide (36j).

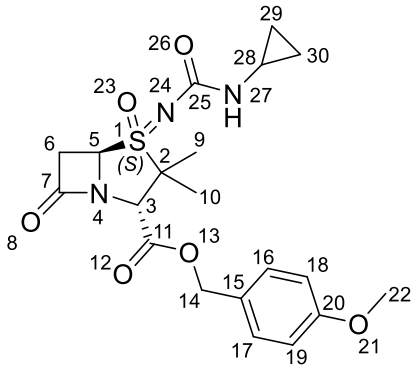

Following General Procedure H, urea **36j** (62 mg, 0.14 mmol, 67%) was obtained from *NH*-sulfoximine **32** (75 mg, 1.0 equiv., 0.21 mmol) and isocyanatocyclopropane (28 mg, 1.6 equiv., 0.34 mmol), following column chromatography (5 g Sfär cartridge; 20 mL/min; initially 100% (v/v) cyclohexane (3 CV), followed by a linear gradient (15 CV): 0–75% (v/v) ethyl acetate in cyclohexane).

Amorphous solid. **^{1}H NMR** (500 MHz, 300 K, $CDCl_3$): δ = 7.34 – 7.27 (m, 2H, *H16*, *H17*), 6.93 – 6.86 (m, 2H, *H18*, *H19*), 5.27 – 5.21 (m, 2H, *H14*, *H27*), 5.11 (d, *J* = 11.7 Hz, 1H, *H14*), 4.95 (dd, *J* = 4.2, 2.3 Hz, 1H, *H5*), 4.38 (s, 1H, *H3*), 3.82 (s, 3H, *H22*), 3.64 (m, 2H, *H6*), 2.59 (h, *J* = 3.1 Hz, 1H, *H28*), 1.62 (s, 3H, *H10*), 1.21 (s, 3H, *H9*), 0.73 (m, 2H, *H29*, *H30*), 0.57 – 0.46 ppm (m, 2H, *H29*, *H30*). **^{13}C NMR** (126 MHz,

300 K, $CDCl_3$): δ = 171.6, 167.1, 161.4, 160.3, 130.9, 126.7, 114.3, 68.2, 67.2, 67.2, 63.7, 55.5, 39.8, 23.3, 21.2, 18.9, 6.8(4), 6.8 ppm. **HRMS** (ESI): *m/z* calculated for $C_{20}H_{24}N_3O_6S$ $(M–H)^-$ = 434.1391, found 434.1387. **IR** (film): ṽ = 3658, 2980, 1800, 1755, 1636, 1517, 1463, 1382, 1250, 1176, 1084 cm^{-1}. $[\alpha]_D^{25}$ = + 48.2 (c = 0.25, $CHCl_3$).

4-Methoxybenzyl (*2S*,*4S*,*5R*)-4-((cyclohexylcarbamoyl)imino)-3,3-dimethyl-7-oxo-4λ^6-thia-1-azabicyclo[3.2.0]heptane-2-carboxylate 4-oxide (36k).

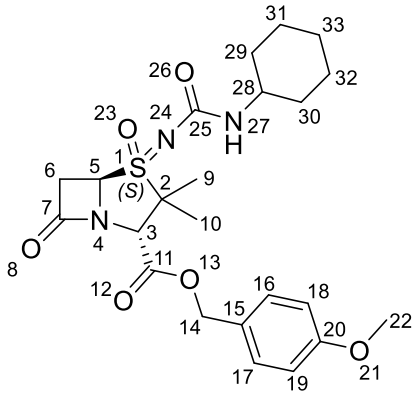

Following General Procedure H, urea **36k** (12 mg, 25 μmol, 18%) was obtained from *NH*-sulfoximine **32** (50 mg, 1.0 equiv., 0.14 mmol) and isocyanatocyclohexane (28 mg, 1.6 equiv., 0.23 mmol), following column chromatography (5 g Sfär cartridge; 20 mL/min; initially 100% (v/v) cyclohexane (3 CV), followed by a linear gradient (15 CV): 0–40% (v/v) ethyl acetate in cyclohexane).

Amorphous solid. **^{1}H NMR** (600 MHz, 300 K, $CDCl_3$): δ = 7.33 – 7.28 (m, 2H, *H16*, *H17*), 6.92 – 6.87 (m, 2H, *H18*, *H19*), 5.24, 5.11 (2H, ABq, *J* = 11.7 Hz, *H14*), 4.98 – 4.92 (m, 2H, *H5*, *H27*), 4.38 (s, 1H, *H3*), 3.82 (s, 3H, *H22*), 3.68 – 3.57 (m, 2H, *H6*), 3.56 – 3.47 (m, 1H, *H28*), 1.96 – 1.87 (m, 2H, *H29*, *H30*), 1.73 – 1.65 (m, 2H, *H31*, *H32*), 1.63 (s, 3H, *H10*), 1.62 – 1.56 (m, 1H, *H33*), 1.38 – 1.28 (m, 2H, H31, *H32*), 1.23 (s, 3H, *H9*), 1.19 – 1.07 ppm (m, 3H, *H29*, *H30*, *H33*). **^{13}C NMR** (151 MHz, 300 K, $CDCl_3$): δ = 171.7, 167.1, 160.3, 159.4, 130.9, 126.7, 114.3, 68.2, 67.2(1), 67.2, 63.8, 55.5, 49.9, 39.8, 33.6, 25.6, 25.0, 21.2, 18.9 ppm. **HRMS** (ESI): *m/z* calculated for $C_{23}H_{30}N_3O_6S$ $(M–H)^-$ = 476.1861, found 476.1858. **IR** (film): ṽ = 3401, 2932,

2854, 1800, 1756, 1629, 1517, 1464, 1253, 1069, 1033 cm^{-1}. $[\alpha]_D^{25}$ = + 45.0 (c = 0.08, $CHCl_3$).

4-Methoxybenzyl (*2S*,*4S*,*5R*)-4-(((4-methoxyphenyl)carbamoyl)imino)-3,3-dimethyl-7-oxo-4λ^6 -thia-1-azabicyclo[3.2.0]heptane-2-carboxylate 4-oxide (36l).

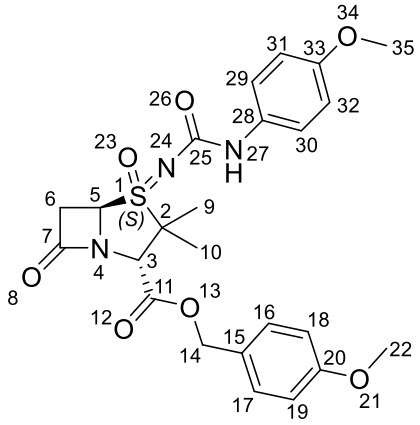

Following General Procedure H, urea **36l** (27 mg, 53 µmol, 38%) was obtained from *NH*-sulfoximine **32** (50 mg, 1.0 equiv., 0.14 mmol) and 1-isocyanato-4-methoxybenzene (34 mg, 1.6 equiv., 0.23 mmol), following column chromatography (5 g Sfär cartridge; 20 mL/min; initially 100% (v/v) cyclohexane (3 CV), followed by a linear gradient (15 CV): 0–40% (v/v) ethyl acetate in cyclohexane).

Amorphous solid. **^{1}H NMR** (600 MHz, 300 K, $CDCl_3$): δ = 7.34 – 7.29 (m, 2H, *H16*, *H17*), 7.27 (m, 2H, *H29*, *H30*), 6.93 – 6.87 (m, 2H, *H18*, *H19*), 6.86 – 6.81 (m, 2H, *H31*, *H32*), 6.77 (s, 1H, *H27*), 5.25, 5.12 (2H, ABq, *J* = 11.7 Hz, *H14*), 5.00 (dd, *J* = 4.1, 2.3 Hz, 1H, *H5*), 4.42 (s, 1H, *H3*), 3.82 (s, 3H, *H22*), 3.77 (s, 3H, *H35*), 3.70 – 3.62 (m, 2H, *H6*), 1.68 (s, 3H, *H10*), 1.27 ppm (s, 3H, *H9*). **^{13}C NMR** (151 MHz, 300 K, $CDCl_3$): δ = 171.4, 167.0, 160.3, 158.2, 156.4, 131.2, 130.9, 126.7, 121.5, 114.4, 114.3, 68.3, 67.5, 67.3, 63.8, 55.7, 55.5, 39.9, 21.2, 19.0 ppm. **HRMS** (ESI): *m/z* calculated for $C_{24}H_{26}N_3O_7S$ $(M–H)^-$ = 500.1497, found 500.1505. **IR** (film): ṽ = 2980, 1800, 1755, 1614, 1517, 1463, 1381, 1250, 1177, 1091, 1034 cm^{-1}. $[\alpha]_D^{25}$ = + 30.0 (c = 0.12, $CHCl_3$).

4-Methoxybenzyl (*2S*,*4S*,*5R*)-3,3-dimethyl-7-oxo-4-(((2,2,2-trichloroacetyl)carbamoyl)imino)-4λ^6-thia-1-azabicyclo[3.2.0]heptane-2-carboxylate 4-oxide (36m).

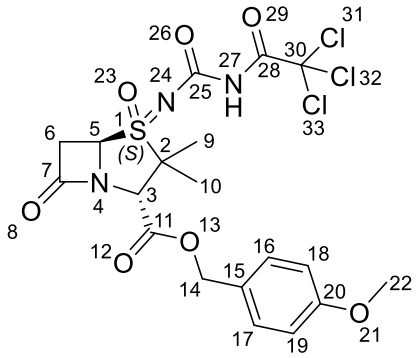

Following General Procedure H, urea **36m** (18 mg, 33 µmol, 16%) was obtained from *NH*-sulfoximine **32** (75 mg, 1.0 equiv., 0.21 mmol) and 2,2,2-trichloroacetyl isocyanate (64 mg, 1.6 equiv., 0.34 mmol), following column chromatography (5 g Sfär cartridge; 20 mL/min; initially 100% (v/v) cyclohexane (3 CV), followed by a linear gradient (15 CV): 0–40% (v/v) ethyl acetate in cyclohexane).

Amorphous solid. **^{1}H NMR** (600 MHz, 300 K, $CDCl_3$): δ = 8.46 (s, 1H, *H27*), 7.34 – 7.29 (m, 2H, *H16*, *H17*), 6.93 – 6.87 (m, 2H, *H18*, *H19*), 5.27, 5.12 (2H, ABq, *J* = 11.7 Hz, *H14*), 5.03 (dd, *J* = 4.3, 2.0 Hz, 1H, *H5*), 4.45 (s, 1H, *H3*), 3.82 (s, 3H, *H22*), 3.75 – 3.64 (m, 2H, *H6*), 1.70 (s, 3H, *H10*), 1.28 ppm (s, 3H, *H9*). **^{13}C NMR** (151 MHz, 300 K, $CDCl_3$) δ 170.4, 166.4, 160.4, 158.1, 155.6, 131.0, 126.5, 114.4, 92.2, 68.5, 68.4(6), 67.5, 63.6, 55.5, 39.9, 21.0, 18.8 ppm. **HRMS** (ESI): *m/z* calculated for $C_{19}H_{19}Cl_3N_3O_7S$ $(M–H)^-$ = 538.0015, found 538.0016. **IR** (film): ṽ = 3658, 2980, 1802, 1760, 1663, 1614, 1517, 1475, 1381, 1262, 1175, 1074 cm^{-1}. $[\alpha]_D^{25}$ = + 29.0 (c = 0.21, $CHCl_3$).

4-Methoxybenzyl (*2S*,*4S*,*5R*)-4-(((3-bromophenyl)carbamoyl)imino)-3,3-dimethyl-7-oxo-4λ^6-thia-1-azabicyclo[3.2.0]heptane-2-carboxylate 4-oxide (36n).

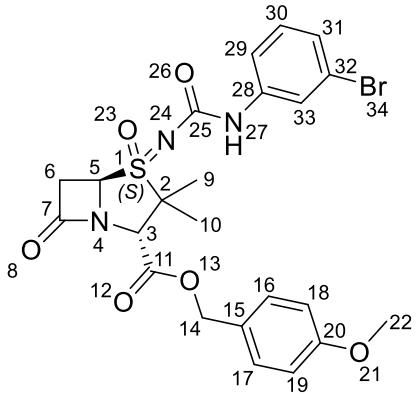

Following General Procedure H, urea **36n** (10 mg, 18 µmol, 9%) was obtained from *NH*-sulfoximine **32** (75 mg, 1.0 equiv., 0.21 mmol) and 1-bromo-3-isocyanatobenzene (67 mg, 1.6 equiv., 0.34 mmol), following column chromatography (5 g Sfär cartridge; 20 mL/min; initially 100% (v/v)

cyclohexane (3 CV), followed by a linear gradient (15 CV): 0–30% (v/v) ethyl acetate in cyclohexane).

Amorphous solid. **^{1}H NMR** (600 MHz, 300 K, $CDCl_3$): δ = 7.67 – 7.64 (m, 1H, *H29*), 7.34 – 7.29 (m, 2H, *H16*, *H17*), 7.26 (m, 1H, *H30*), 7.21 – 7.16 (m, 1H, *H31*), 7.16 – 7.12 (m, 1H, *H33*), 6.93 – 6.88 (m, 2H, *H18*, *H19*), 6.85 (s, 1H, *H27*), 5.26, 5.13 (2H, ABq, *J* = 11.7 Hz, *H14*), 5.00 (dd, *J* = 4.3, 2.1 Hz, 1H, *H5*), 4.43 (s, 1H, *H3*), 3.82 (s, 3H, *H22*), 3.74 – 3.62 (m, 2H, *H6*), 1.68 (s, 3H, *H10*), 1.27 ppm (s, 3H, *H9*). **^{13}C NMR** (151 MHz, 300 K, $CDCl_3$): δ = 171.2, 166.9, 160.3, 157.8, 139.7, 130.9, 130.4, 126.8, 126.6, 122.9, 122.0, 117.6, 114.3, 68.3, 67.8, 67.3, 63.7, 55.5, 39.9, 21.2, 19.0 ppm. **HRMS** (ESI): *m/z* calculated for $C_{23}H_{23}BrN_3O_6S$ $(M–H)^-$ = 548.0496, found 548.0503. **IR** (film): $\tilde{\nu}$ = 3657, 2980, 2362, 1801, 1758, 1654, 1587, 1518, 1463, 1381, 1261, 1174, 1080 cm^{-1}. $[\alpha]_D^{25}$ = + 18.9 (c = 0.15, $CHCl_3$).

4-Methoxybenzyl (*2S*,*4S*,*5R*)-4-(((2-bromophenyl)carbamoyl)imino)-3,3-dimethyl-7-oxo-4λ^6-thia-1-azabicyclo[3.2.0]heptane-2-carboxylate 4-oxide (36o).

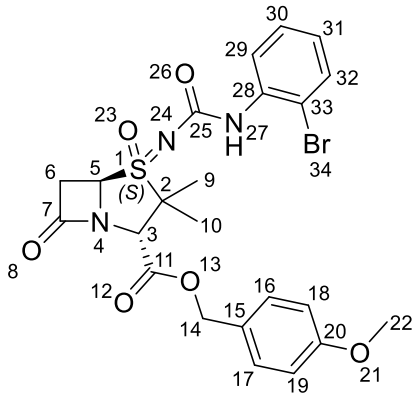

Following General Procedure H, urea **36o** (17 mg, 31 μmol, 15%) was obtained from *NH*-sulfoximine **32** (75 mg, 1.0 equiv., 0.21 mmol) and 1-bromo-2-isocyanatobenzene (67 mg, 1.6 equiv., 0.34 mmol), following column chromatography (5 g Sfär cartridge; 20 mL/min; initially 100% (v/v) cyclohexane (3 CV), followed by a linear gradient (15 CV): 0–30% (v/v) ethyl acetate in cyclohexane).

Amorphous solid. **^{1}H NMR** (600 MHz, 300 K, $CDCl_3$): δ = 8.14 (d, *J* = 8.3 Hz, 1H, *H32*), 7.53 – 7.47 (m, 1H, *H29*), 7.41 – 7.34 (m, 1H, *H27*), 7.34 – 7.30 (m, 2H, *H16*, *H17*), 7.30 – 7.27 (m, 1H, *H31*), 6.95 – 6.88 (m, 3H, *H18*, *H19*, *H30*), 5.27, 5.12 (2H,

ABq, *J* = 11.7 Hz, *H14*), 5.01 (dd, *J* = 4.1, 2.2 Hz, 1H, *H5*), 4.44 (s, 1H, *H3*), 3.82 (s, 3H, *H22*), 3.73 – 3.63 (m, 2H, *H6*), 1.71 (s, 3H, *H10*), 1.29 ppm (s, 3H, *H9*). **^{13}C NMR** (151 MHz, 300 K, $CDCl_3$): δ = 171.2, 166.9, 160.3, 158.00, 136.3, 132.5, 131.0, 128.5, 126.6, 124.6, 121.0, 114.3, 113.0, 68.3, 67.8, 67.2, 63.8, 55.5, 39.8, 21.2, 19.0 ppm. **HRMS** (ESI): *m/z* calculated for $C_{23}H_{23}BrN_3O_6S$ $(M–H)^-$ = 548.0496, found 548.0518. **IR** (film): ṽ = 2980, 1802, 1755, 1655, 1590, 1518, 1463, 1434, 1381, 1253, 1218, 1082 cm^{-1}. $[\alpha]_D^{25}$ = + 31.4 (c = 0.22, $CHCl_3$).

4-Methoxybenzyl (*2S*,*4S*,*5R*)-4-(((2-(acryloyloxy)ethyl)carbamoyl)imino)-3,3-dimethyl-7-oxo-4λ^6-thia-1-azabicyclo[3.2.0]heptane-2-carboxylate 4-oxide (36p).

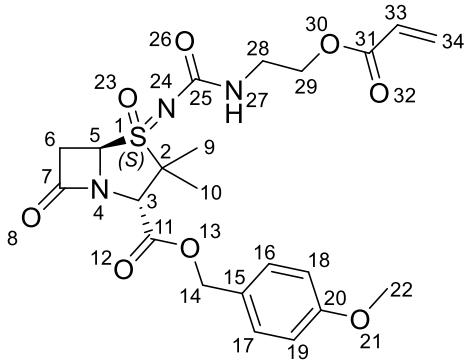

Following General Procedure H, urea **36p** (62 mg, 0.21 mmol, 59%) was obtained from *NH*-sulfoximine **32** (75 mg, 1.0 equiv., 0.21 mmol) and 2-isocyanatoethyl acrylate (48 mg, 1.6 equiv., 0.34 mmol), following column chromatography (5 g Sfär cartridge; 20 mL/min; initially 100% (v/v) cyclohexane (3 CV), followed by a linear gradient (15 CV): 0–80% (v/v) ethyl acetate in cyclohexane). Amorphous solid. **^{1}H NMR** (600 MHz, 300 K, $CDCl_3$): δ = 7.34 – 7.28 (m, 2H, *H16*, *H17*), 6.92 – 6.87 (m, 2H, *H18*, *H19*), 6.42 (dd, *J* = 17.4, 1.3 Hz, 1H, *H34*), 6.12 (dd, *J* = 17.3, 10.4 Hz, 1H, *H33*), 5.86 (dd, *J* = 10.5, 1.4 Hz, 1H, *H34*), 5.33 (t, *J* = 6.0 Hz, 1H, *H27*), 5.24, 5.11 (2H, ABq, *J* = 11.7 Hz, *H14*), 4.94 (dd, *J* = 4.4, 2.1 Hz, 1H, *H5*), 4.39 (s, 1H, *H3*), 4.24 (m, 2H, *H29*), 3.82 (s, 3H, *H22*), 3.68 – 3.56 (m, 2H, *H6*), 3.53 – 3.45 (m, 2H, *H28*), 1.64 (s, 3H, *H10*), 1.23 ppm (s, 3H, *H9*). **^{13}C NMR** (151 MHz, 300 K, $CDCl_3$): δ = 171.5, 167.0, 166.2, 160.3(1), 160.3, 131.6, 130.9, 128.2, 126.7, 114.3, 68.2, 67.3, 67.2, 63.8, 63.6, 55.5, 40.1, 39.7, 21.1, 18.9 ppm. **HRMS** (ESI): *m/z* calculated for $C_{22}H_{26}N_3O_8S$ $(M–H)^-$ = 492.1446, found 492.1461. **IR** (film): ṽ = 3657,

2981, 1801, 1755, 1725, 1638, 1518, 1463, 1382, 1253, 1079 cm^{-1}. $[\alpha]_D^{25}$ = + 30.5 (c = 0.19, $CHCl_3$).

4-Methoxybenzyl (*2S*,*4S*,*5R*)-3,3-dimethyl-7-oxo-4-((pyridin-3-ylcarbamoyl)imino)-4λ⁶-thia-1-azabicyclo[3.2.0]heptane-2-carboxylate 4-oxide (36q).

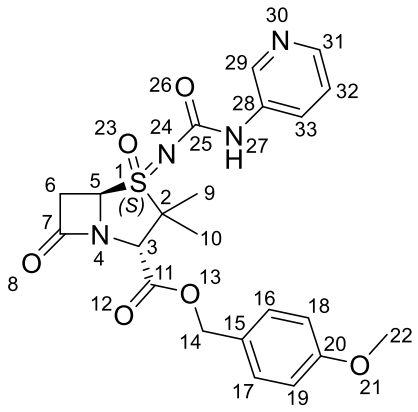

Following General Procedure H, urea **36q** (30 mg, 64 µmol, 30%) was obtained from *NH*-sulfoximine **32** (75 mg, 1.0 equiv., 0.21 mmol) and 3-isocyanatopyridine (41 mg, 1.6 equiv., 0.34 mmol), following column chromatography (5 g Sfär cartridge; 20 mL/min; initially 100% (v/v) cyclohexane (3 CV), followed by a linear gradient (15 CV): 0–100% (v/v) ethyl acetate in cyclohexane).

Amorphous solid. **^{1}H NMR** (600 MHz, 300 K, $CDCl_3$): δ = 8.44 (s, 1H, *H29*), 8.31 (dd, *J* = 4.8, 1.4 Hz, 1H, *H31*), 8.02 (s, 1H, *H33*), 7.34 – 7.28 (m, 2H, *H16*, *H17*), 7.25 – 7.22 (m, 1H, *H32*), 6.93 – 6.88 (m, 3H, *H18*, *H19*, *H27*), 5.26, 5.13 (2H, ABq, *J* = 11.7 Hz, *H14*), 5.00 (dd, *J* = 4.3, 2.1 Hz, 1H, *H5*), 4.44 (s, 1H, *H3*), 3.82 (s, 3H, *H22*), 3.73 – 3.62 (m, 2H, *H6*), 1.69 (s, 3H, *H10*), 1.28 ppm (s, 3H, *H9*). **^{13}C NMR** (151 MHz, 300 K, $CDCl_3$): δ = 171.1, 166.8, 160.4, 156.3, 145.0, 140.6, 135.2, 131.0, 126.6, 126.3, 123.8, 114.3, 68.4, 67.8, 67.3, 63.7, 55.5, 39.9, 21.2, 19.0 ppm. **HRMS** (ESI): *m/z* calculated for $C_{22}H_{23}N_4O_6S$ $(M–H)^-$ = 471.1344, found 471.1328. **IR** (film): ṽ = 3657, 2980, 1801, 1755, 1647, 1518, 1462, 1382, 1262, 1089 cm^{-1}. $[\alpha]_D^{25}$ = + 24.2 (c = 0.12, $CHCl_3$).

4-Methoxybenzyl (*2S*,*4S*,*5R)*-3,3-dimethyl-4-(((4-nitrophenyl)carbamoyl)imino)-7-oxo-4λ⁶-thia-1-azabicyclo[3.2.0]heptane-2-carboxylate 4-oxide (36r).

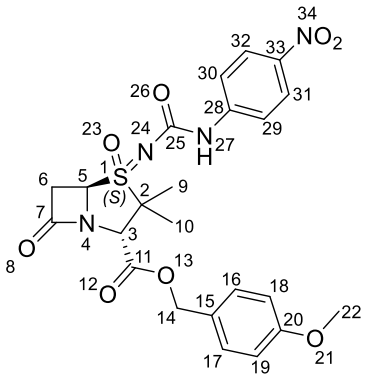

Following General Procedure H, urea **36r** (30 mg, 58 µmol, 27%) was obtained from *NH*-sulfoximine **32** (75 mg, 1.0 equiv., 0.21 mmol) and 1-isocyanato-4-nitrobenzene (56 mg, 1.6 equiv., 0.34 mmol), following column chromatography (5 g Sfär cartridge; 20 mL/min; initially 100% (v/v) cyclohexane (3 CV), followed by a linear gradient (15 CV): 0–50% (v/v) ethyl acetate in cyclohexane). Amorphous solid. **^{1}H NMR** (600 MHz, 300 K, $CDCl_3$): δ = 8.32 – 8.29 (m, 1H, *H32*), 7.93 – 7.88 (m, 1H, *H31*), 7.81 – 7.68 (m, 1H, *H30*), 7.45 (m, 1H, *H29*), 7.35 – 7.29 (m, 2H, *H16*, *H17*), 7.09 – 7.05 (m, 1H, *H27*), 6.93 – 6.88 (m, 2H, *H18*, *H19*), 5.26, 5.13 (2H, ABq, *J* = 11.7 Hz, *H14*), 5.02 (dd, *J* = 4.4, 2.0 Hz, 1H, *H5*), 4.44 (s, 1H, *H3*), 3.82 (s, 3H, *H22*), 3.72 (dd, *J* = 16.7, 4.3 Hz, 1H, *H6*), 3.67 (dd, *J* = 16.7, 2.0 Hz, 1H, *H6*), 1.70 (s, 3H, *H10*), 1.29 ppm (s, 3H, *H9*). **^{13}C NMR** (151 MHz, 300 K, $CDCl_3$): δ = 171.0, 166.8, 160.4, 148.9, 139.7, 131.0, 123.0, 126.6, 124.6, 118.3, 114.3, 68.4, 67.9, 67.4, 63.7, 55.5, 39.9, 21.2, 19.0 ppm. **HRMS** (ESI): *m/z* calculated for $C_{23}H_{23}N_4O_8S$ $(M–H)^-$ = 515.1242, found 515.1247. **IR** (film): ṽ = 3655, 2980, 1801, 1756, 1615, 1534, 1462, 1382, 1352, 1260, 1175, 1074 cm^{-1}. $[\alpha]_D^{25}$ = + 65.2 (c = 0.19, $CHCl_3$).

4-Methoxybenzyl (*2S*,*4S*,*5R*)-4-(((2-chloroethyl)carbamoyl)imino)-3,3-dimethyl-7-oxo-4λ^6-thia-1-azabicyclo[3.2.0]heptane-2-carboxylate 4-oxide (36s).

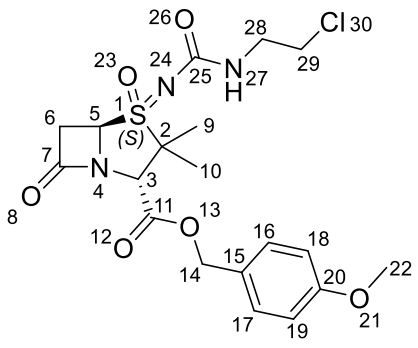

Following General Procedure G, urea **36s** (49 mg, 0.11 mmol, 50%) was obtained from *NH*-sulfoximine **32** (75 mg, 1.0 equiv., 0.21 mmol) and 1-chloro-2-isocyanatoethane (36 mg, 1.6 equiv., 0.34 mmol), following column chromatography (5

g Sfär cartridge; 20 mL/min; initially 100% (v/v) cyclohexane (3 CV), followed by a linear gradient (15 CV): 0–50% (v/v) ethyl acetate in cyclohexane).

Amorphous solid. **^{1}H NMR** (500 MHz, 300 K, $CDCl_3$): δ = 7.34 – 7.28 (m, 2H, *H16*, *H17*), 6.93 – 6.87 (m, 2H, *H18*, *H19*), 5.46 (t, *J* = 6.0 Hz, 1H, *H27*), 5.24, 5.11 (2H, ABq, *J* = 11.7 Hz, *H14*), 4.93 (dd, *J* = 4.2, 2.1 Hz, 1H, *H5*), 4.40 (s, 1H, *H3*), 3.82 (s, 3H, *H22*), 3.69 – 3.44 (m, 6H, *H6*, *H28*, *H29*), 1.64 (s, 3H, *H10*), 1.23 ppm (s, 3H, *H9*). **^{13}C NMR** (126 MHz, 300 K, $CDCl_3$): δ = 171.4, 167.0, 160.3, 160.2, 130.9, 126.6, 114.3, 68.2, 67.4, 67.1, 63.7, 55.5, 44.2, 42.7, 39.7, 21.1, 18.9 ppm. **HRMS** (ESI): *m/z* calculated for $C_{19}H_{23}ClN_3O_6S$ $(M–H)^-$ = 456.1002, found 456.0992. **IR** (film): ṽ = 3657, 2980, 1800, 1755, 1637, 1517, 1463, 1382, 1251, 1176, 1075 cm^{-1}. $[\alpha]_D^{25}$ = + 37.1 (c = 0.56, $CHCl_3$).

Sodium (*2S*,*4S*,*5R*)-4-((benzylcarbamoyl)imino)-3,3-dimethyl-7-oxo-4λ^6-thia-1-azabicyclo[3.2.0]heptane-2-carboxylate 4-oxide (37a).

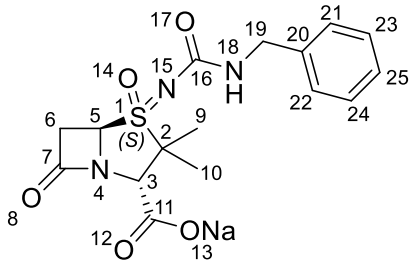

Following General Procedure D, acid **37a** (7 mg, 19 µmol, 62%) was obtained from ester **36a** (15 mg, 1.0 equiv., 31 µmol) with 10% (w/w) Pd/C (0.2 equiv.) in anhydrous THF stirring for 3 h under hydrogen atmosphere. The reaction mixture was filtered using Celite®; the Celite® pad was rinsed with DCM, which was then removed *in vacuo*. The residue was redissolved in ethyl acetate before the addition of sodium 2-ethylhexanoate (1.0 equiv.). The resultant mixture was stirred for 15 min before being evaporated *in vacuo*. The product was precipitated by the addition of diethyl ether to the crude residue. Filtration afforded the carboxylate sodium salt.

White solid. **MP**: decomposition > 100 °C. **^{1}H NMR** (500 MHz, 300 K, MeOD-d_4): δ = 7.35 – 7.26 (m, 4H, *H21*, *H22*, *H23*, *H34*), 7.26 – 7.19 (m, 1H, *H25*), 5.17 (dd, *J* =

4.5, 1.7 Hz, 1H, *H5*), 4.35 – 4.24 (m, 3H, *H3*, *H19*), 3.68 (dd, *J* = 16.5, 4.5 Hz, 1H, *H6*), 3.43 (dd, *J* = 16.5, 1.7 Hz, 1H, *H6*), 1.71 (s, 3H, *H10*), 1.49 ppm (s, 3H, *H9*). **^{13}C NMR** (126 MHz, 300 K, MeOD-*d*$_4$): δ = 173.7, 170.6, 162.8, 140.6, 129.5, 128.3, 128.1, 68.3, 68.1, 65.3, 45.2, 39.7, 21.4, 19.1 ppm. **HRMS** (ESI): *m/z* calculated for $C_{16}H_{17}N_3O_5S$ $(M–H)^-$ = 364.0973, found 364.0973. **IR** (film): ṽ = 3792, 3379, 2849, 2362, 1784, 1622, 1528, 1401, 1219, 1128, 1031 cm^{-1}. $[\alpha]_D^{25}$ = + 50.3 (c = 0.15, MeOH).

Sodium (*2S*,*4S*,*5R*)-3,3-dimethyl-7-oxo-4-((phenethylcarbamoyl)imino)-4λ^6-thia-1-azabicyclo[3.2.0]heptane-2-carboxylate 4-oxide (37b).

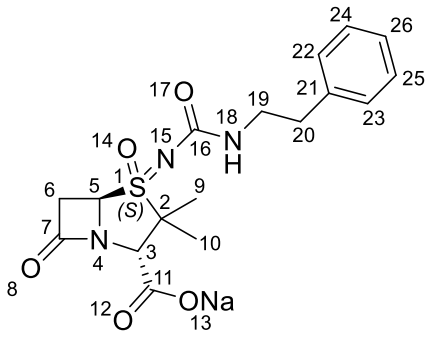

Following General Procedure D, acid **37b** (30 mg, 74 µmol, 49%) was obtained from ester **36b** (77 mg, 1.0 equiv., 0.15 mmol) with 10% (w/w) Pd/C (0.2 equiv.) in anhydrous THF stirring for 3 h under hydrogen atmosphere. The reaction mixture was filtered using Celite®; the Celite® pad was rinsed with DCM, which was then removed *in vacuo*. The residue was redissolved in ethyl acetate before the addition of sodium 2-ethylhexanoate (1.0 equiv.). The resultant mixture was stirred for 15 min before being evaporated *in vacuo*. The product was precipitated by the addition of diethyl ether to the crude residue. Filtration afforded the carboxylate sodium salt.

White solid. **MP**: decomposition > 100 °C. **^{1}H NMR** (500 MHz, 300 K, MeOD-*d*$_4$): δ = 7.31 – 7.24 (m, 2H, *H24*, *H25*), 7.24 – 7.16 (m, 3H, *H22*, *H23*, *H26*), 5.08 (dd, *J* = 4.5, 1.7 Hz, 1H, *H5*), 4.30 (s, 1H, *H3*), 3.67 (dd, *J* = 16.5, 4.5 Hz, 1H, *H6*), 3.41 (dd, *J* = 16.5, 1.7 Hz, 1H, *H6*), 3.35 – 3.32 (m, 2H, *H19*), 2.84 – 2.72 (m, 2H, *H20*), 1.69 (s, 3H, *H10*), 1.43 ppm (s, 3H, *H9*). **^{13}C NMR** (126 MHz, 300 K, MeOD-*d*$_4$): δ = 173.7, 170.7, 162.7, 140.6, 129.9, 129.4, 127.3, 68.2, 68.1, 65.4, 43.3, 39.7, 37.1, 21.4, 19.1

ppm. **HRMS** (ESI): *m/z* calculated for $C_{17}H_{20}N_3O_5S$ $(M–H)^-$ = 378.1123, found 378.1126. **IR** (film): $\tilde{\nu}$ = 3782, 3379, 2839, 2358, 1785, 1621, 1531, 1401, 1219, 1128, 1033 cm^{-1}. $[\alpha]_D^{25}$ = + 88.5 (c = 0.13, MeOH).

Sodium (*2S*,*4S*,*5R*)-4-(((4-methoxybenzyl)carbamoyl)imino)-3,3-dimethyl-7-oxo-4λ⁶-thia-1-azabicyclo[3.2.0]heptane-2-carboxylate 4-oxide (37c).

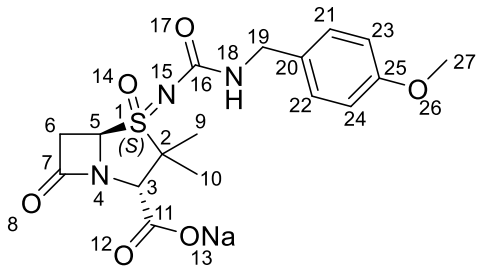

Following General Procedure D, acid **37c** (12 mg, 30 µmol, 45%) was obtained from ester **36c** (35 mg, 1.0 equiv., 68 µmol) with 10% (w/w) Pd/C (0.2 equiv.) in anhydrous THF stirring for 3 h under hydrogen atmosphere. The reaction mixture was filtered using Celite®; the Celite® pad was rinsed with DCM, which was then removed *in vacuo*. The residue was redissolved in ethyl acetate before the addition of sodium 2-ethylhexanoate (1.0 equiv.). The resultant mixture was stirred for 15 min before being evaporated *in vacuo*. The product was precipitated by the addition of diethyl ether to the crude residue. Filtration afforded the carboxylate sodium salt.

White solid. **MP**: decomposition > 100 °C. **^{1}H NMR** (500 MHz, 300 K, MeOD-*d*$_4$): δ = 7.23 – 7.17 (m, 2H, *H21*, *H22*), 6.89 – 6.83 (m, 2H, *H23*, *H24*), 5.17 (dd, *J* = 4.5, 1.7 Hz, 1H, *H5*), 4.33 (s, 1H, *H3*), 4.30 – 4.17 (m, 2H, *H19*), 3.77 (s, 3H, *H27*), 3.68 (dd, *J* = 16.5, 4.5 Hz, 1H, *H6*), 3.44 (dd, *J* = 16.5, 1.8 Hz, 1H, *H6*), 1.70 (s, 3H, *H10*), 1.48 ppm (s, 3H, *H9*). **^{13}C NMR** (126 MHz, 300 K, MeOD-*d*$_4$): δ = 173.9, 170.7 (assigned via HMBC), 162.7, 160.3, 132.5, 129.6, 114.9, 68.2, 68.1, 65.2, 55.7, 44.7, 39.8, 21.4, 19.1 ppm. **HRMS** (ESI): *m/z* calculated for $C_{17}H_{20}N_3O_6S$ $(M–H)^-$ = 394.1078, found 394.1082. **IR** (film): $\tilde{\nu}$ = 3367, 2360, 1795, 1614, 1514, 1246, 1033 cm^{-1}. $[\alpha]_D^{25}$ = + 66.6 (c = 0.42, MeOH).

Sodium (*2S*,*4S*,*5R*)-4-(((4-chlorophenethyl)carbamoyl)imino)-3,3-dimethyl-7-oxo-4λ^6-thia-1-azabicyclo[3.2.0]heptane-2-carboxylate 4-oxide (37d).

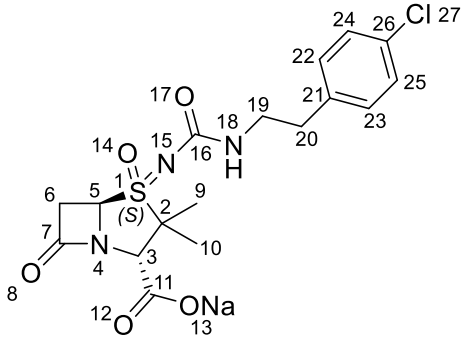

Following General Procedure D, acid **37d** (20 mg, 46 µmol, 61%) was obtained from ester **36d** (40 mg, 1.0 equiv., 75 µmol) with 10% (w/w) Pd/C (0.2 equiv.) in anhydrous THF stirring for 3 h under hydrogen atmosphere. The reaction mixture was filtered using Celite®; the Celite® pad was rinsed with DCM, which was then removed *in vacuo*. The residue was redissolved in ethyl acetate before the addition of sodium 2-ethylhexanoate (1.0 equiv.). The resultant mixture was stirred for 15 min before being evaporated *in vacuo*. The product was precipitated by the addition of diethyl ether to the crude residue. Filtration afforded the carboxylate sodium salt.

White solid. **MP**: decomposition > 100 °C. **^{1}H NMR** (500 MHz, 300 K, MeOD-*d*$_4$): δ = 7.31 – 7.25 (m, 2H, *H24*, *H25*), 7.23 – 7.17 (m, 2H, *H22*, *H23*), 5.10 (dd, *J* = 4.6, 1.7 Hz, 1H, *H5*), 4.33 (s, 1H, *H3*), 3.68 (dd, *J* = 16.5, 4.7 Hz, 1H, *H6*), 3.42 (dd, *J* = 16.5, 1.6 Hz, 1H, *H6*), 3.33 – 3.28 (m, 2H, *H19*), 2.83 – 2.74 (m, 2H, *H20*), 1.69 (s, 3H, *H10*), 1.45 ppm (s, 3H ,*H9*). **^{13}C NMR** (126 MHz, 300 K, MeOD-*d*$_4$): δ = 173.6, 169.7 (assigned via HMBC), 162.7, 139.5, 133.1, 131.5, 129.5, 68.2, 68.1, 65.1 (assigned via HMBC), 43.0, 39.7, 36.3, 21.4, 19.1 ppm. **HRMS** (ESI): *m/z* calculated for $C_{17}H_{19}ClN_3O_5S$ $(M–H)^-$ = 412.0739, found 412.0741. **IR** (film): ṽ = 3658, 3440, 2981, 2889, 2664, 2360, 2342, 1783, 1621, 1473, 1462, 1383, 1251, 1153, 1072, 1033 cm^{-1}. $[\alpha]_D^{25}$ = + 41.5 (c = 0.086, MeOH).

Sodium (*2S*,*4S*,*5R*)-4-(((4-fluorophenethyl)carbamoyl)imino)-3,3-dimethyl-7-oxo-4λ^6-thia-1-azabicyclo[3.2.0]heptane-2-carboxylate 4-oxide (37e).

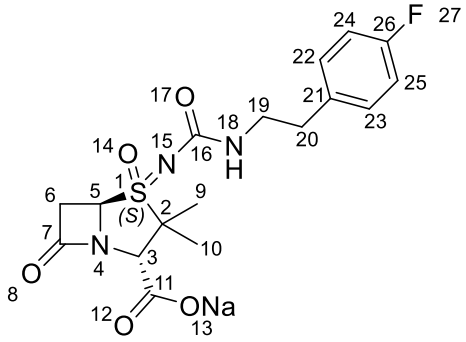

Following General Procedure D, acid **37e** (25 mg, 60 µmol, 51%) was obtained from ester **36e** (60 mg, 1.0 equiv., 0.12 mmol) with 10% (w/w) Pd/C (0.2 equiv.) in anhydrous THF stirring for 3 h under hydrogen atmosphere. The reaction mixture was filtered using Celite®; the Celite® pad was rinsed with DCM, which was then removed *in vacuo*. The residue was redissolved in ethyl acetate before the addition of sodium 2-ethylhexanoate (1.0 equiv.). The resultant mixture was stirred for 15 min before being evaporated *in vacuo*. The product was precipitated by the addition of diethyl ether to the crude residue. Filtration afforded the carboxylate sodium salt.

White solid. **MP**: decomposition > 100 °C. **^{1}H NMR** (500 MHz, 300 K, MeOD-*d*$_4$): δ = 7.26 – 7.18 (m, 2H, *H22*, *H23*), 7.05 – 6.95 (m, 2H, *H24*, *H25*), 5.12 (dd, *J* = 4.5, 1.7 Hz, 1H, *H5*), 4.33 (s, 1H, *H3*), 3.68 (dd, *J* = 16.5, 4.5 Hz, 1H, *H6*), 3.42 (dd, *J* = 16.5, 1.8 Hz, 1H, *H6*), 3.35 – 3.24 (m, 2H, *H19*), 2.83 – 2.72 (m, 2H, *H20*), 1.69 (s, 3H, *H10*), 1.46 ppm (s, 3H, *H9*). **^{19}F NMR** (470 MHz, 300 K, MeOD-*d*$_4$): δ = -119.26 – -119.39 ppm (m). **^{13}C NMR** (126 MHz, 300 K, MeOD-*d*$_4$): δ = 173.6, 170.2, 163.0 (d, *J* = 242.5 Hz), 162.7, 136.5 (d, *J* = 3.2 Hz), 131.5 (d, *J* = 7.8 Hz), 116.0 (d, *J* = 21.3 Hz), 68.2, 68.1, 65.1, 43.2, 39.8, 36.2, 21.4, 19.1 ppm. **HRMS** (ESI): *m/z* calculated for $C_{17}H_{19}FN_3O_5S$ $(M–H)^-$ = 396.1035, found 396.1042. **IR** (film): $\tilde{\nu}$ = 3659, 3423, 2981, 2888, 2664, 2361, 2341, 1784, 1621, 1511, 1473, 1462, 1383, 1251, 1153, 1072 cm^{-1}. $[\alpha]_D^{25}$ = + 107.8 (c = 0.18, MeOH).

Sodium (*2S*,*4S*,*5R*)-3,3-dimethyl-7-oxo-4-(((3-phenylpropyl)carbamoyl)imino)-4λ^6-thia-1-azabicyclo[3.2.0]heptane-2-carboxylate 4-oxide (37f).

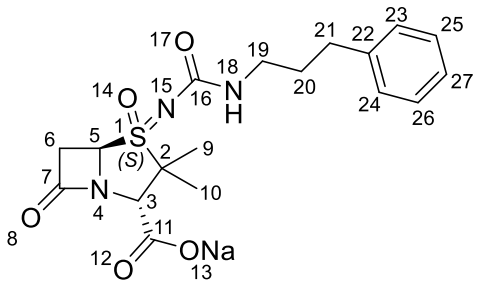

Following General Procedure D, acid **37f** (30 mg, 72 µmol, 62%) was obtained from ester **36f** (60 mg, 1.0 equiv., 0.12 mmol) with 10% (w/w) Pd/C (0.2 equiv.) in anhydrous THF stirring for 3 h under hydrogen atmosphere. The reaction mixture was filtered using Celite®; the Celite® pad was rinsed with DCM, which was then removed *in vacuo*. The residue was redissolved in ethyl acetate before the addition of sodium 2-ethylhexanoate (1.0 equiv.). The resultant mixture was stirred for 15 min before being evaporated *in vacuo*. The product was precipitated by the addition of diethyl ether to the crude residue. Filtration afforded the carboxylate sodium salt.

White solid. **MP**: decomposition > 100 °C. **^{1}H NMR** (500 MHz, 300 K, MeOD-*d*$_4$): δ = 7.31 – 7.08 (m, 5H, *H23*, *H24*, *H25*, *H26*, *H27*), 5.15 (dd, *J* = 4.5, 1.7 Hz, 1H, *H5*), 4.33 (s, 1H, *H3*), 3.68 (dd, *J* = 16.5, 4.6 Hz, 1H, *H6*), 3.43 (dd, *J* = 16.5, 1.7 Hz, 1H, *H6*), 3.18 – 3.07 (m, 2H, *H19*), 2.63 (t, *J* = 7.7 Hz, 2H, *H21*), 1.80 (p, *J* = 7.4 Hz, 2H, *H20*), 1.70 (s, 3H, *H10*), 1.48 ppm (s, 3H, *H9*). **^{13}C NMR** (126 MHz, 300 K, MeOD-*d*$_4$): δ = 173.7, 170.3, 162.8, 143.1, 129.4, 129.3(8), 126.9, 68.1 (2C), 65.1, 41.3, 39.8, 34.2, 32.7, 21.4, 19.0 ppm. **HRMS** (ESI): *m/z* calculated for $C_{18}H_{22}N_3O_5S$ $(M–H)^-$ = 392.1286, found 392.1279. **IR** (film): ṽ = 3658, 3422, 2981, 2889, 2665, 2360, 2341, 1783, 1621, 1473, 1462, 1383, 1251, 1152, 1073 cm^{-1}. $[\alpha]_D^{25}$ = + 101.8 (c = 0.19, MeOH).

Sodium (*2S*,*4S*,*5R*)-4-(((3-chloropropyl)carbamoyl)imino)-3,3-dimethyl-7-oxo-4λ^6-thia-1-azabicyclo[3.2.0]heptane-2-carboxylate 4-oxide (37g).

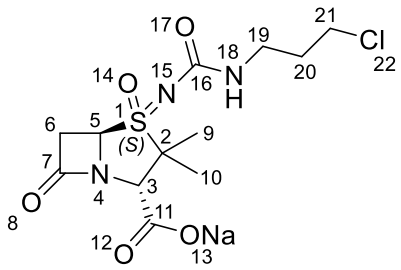

Following General Procedure D, compound **37g** (20 mg, 57 µmol, 55%) was obtained from compound **36g** (49 mg, 1.0 equiv., 0.10 mmol) with 10% (w/w) Pd/C (0.2 equiv.) in anhydrous THF stirring for 3 h under hydrogen atmosphere. The reaction mixture was filtered using Celite®; the Celite® pad was rinsed with DCM, which was then removed *in vacuo*. The residue was redissolved in ethyl acetate before the addition of sodium 2-ethylhexanoate (1.0 equiv.). The resultant mixture was stirred for 15 min before being evaporated *in vacuo*. The product was precipitated by the addition of diethyl ether to the crude residue. Filtration afforded the carboxylate sodium salt.

White solid. **MP**: decomposition > 100 °C. **^{1}H NMR** (500 MHz, 300 K, MeOD-*d*$_4$): δ = 5.16 (dd, *J* = 4.5, 1.7 Hz, 1H, *H5*), 4.32 (s, 1H, *H3*), 3.68 (dd, *J* = 16.5, 4.5 Hz, 1H, *H6*), 3.59 (t, *J* = 6.5 Hz, 2H, *H21*), 3.42 (dd, *J* = 16.5, 1.7 Hz, 1H, *H6*), 3.28 – 3.19 (m, 2H, *H19*), 1.94 (p, *J* = 6.6 Hz, 2H, *H20*), 1.70 (s, 3H, *H10*), 1.47 ppm (s, 3H, *H9*). **^{13}C NMR** (126 MHz, 300 K, MeOD-*d*$_4$): δ = 173.7, 170.5, 162.9, 68.2, 68.1, 65.2, 43.1, 39.7, 39.0, 33.8, 21.4, 19.1 ppm. **HRMS** (ESI): *m/z* calculated for $C_{12}H_{17}ClN_3O_5S$ $(M-H)^-$ = 350.0583, found 350.0600. **IR** (film): $\tilde{\nu}$ = 3824, 3710, 3590, 3394, 3243, 3042, 3004, 2820, 2363, 1793, 1624, 1527, 1407, 1219, 1128, 1086, 1032 cm^{-1}. $[\alpha]_D^{25}$ = + 80.7 (c = 0.25, MeOH).

Sodium (*2S*,*4S*,*5R*)-4-(((4-methoxyphenethyl)carbamoyl)imino)-3,3-dimethyl-7-oxo-4λ^6-thia-1-azabicyclo[3.2.0]heptane-2-carboxylate 4-oxide (36h).

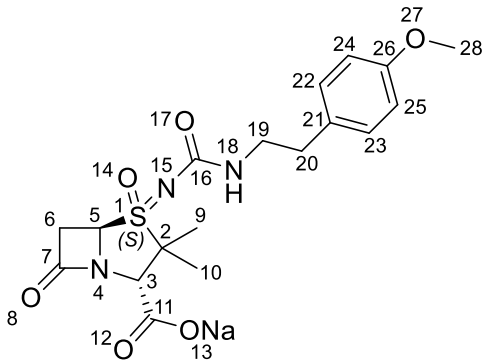

Following General Procedure D, acid **36h** (20 mg, 30 μmol, 41%) was obtained from ester **36h** (60 mg, 1.0 equiv., 0.11 mmol) with 10% (w/w) Pd/C (0.2 equiv.) in anhydrous THF stirring for 3 h under hydrogen atmosphere. The reaction mixture was filtered using Celite®; the Celite® pad was rinsed with DCM, which was then removed *in vacuo*. The residue was redissolved in ethyl acetate before the addition of sodium 2-ethylhexanoate (1.0 equiv.). The resultant mixture was stirred for 15 min before being evaporated *in vacuo*. The product was precipitated by the addition of diethyl ether to the crude residue. Filtration afforded the carboxylate sodium salt.

White solid. **MP**: decomposition > 100 °C. **^{1}H NMR** (500 MHz, 300 K, MeOD-*d*$_4$): δ = 7.16 – 7.09 (m, 2H, *H22*, *H23*), 6.88 – 6.80 (m, 2H, *H24*, *H25*), 5.09 (dd, *J* = 4.5, 1.7 Hz, 1H, *H5*), 4.32 (s, 1H, *H3*), 3.76 (s, 3H, *H28*), 3.67 (dd, *J* = 16.5, 4.5 Hz, 1H, *H6*), 3.42 (dd, *J* = 16.5, 1.7 Hz, 1H, *H6*), 3.30 – 3.25 (m, 2H, *H19*), 2.77 – 2.66 (m, 2H, *H20*), 1.70 (s, 3H, *H10*), 1.45 ppm (s, 3H, *H9*). **^{13}C NMR** (126 MHz, 300 K, MeOD-*d*$_4$): δ = 173.7, 170.4, 162.7, 159.7, 132.5, 130.8, 114.9, 68.2, 68.1, 65.2, 55.7, 43.5, 39.7, 36.2, 21.4, 19.1 ppm. **HRMS** (ESI): *m/z* calculated for $C_{18}H_{22}N_3O_6S$ $(M-H)^-$ = 408.1235, found 408.1253. **IR** (film): $\tilde{\nu}$ = 3351, 2981, 2890, 2838, 2363, 1786, 1614, 1514, 1398, 1247, 1034 cm^{-1}. $[\alpha]_D^{25}$ = + 80.0 (c = 0.16, MeOH).

Sodium (*2S*,*4S*,*5R*)-3,3-dimethyl-7-oxo-4-((((*S*)-1-phenylethyl)carbamoyl)imino)-4λ⁶-thia-1-azabicyclo[3.2.0]heptane-2-carboxylate 4-oxide (37i).

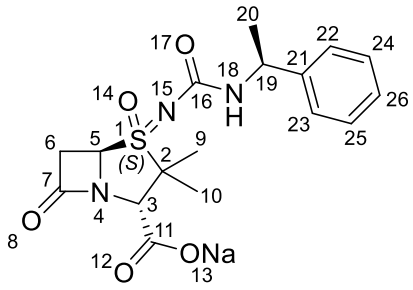

Following General Procedure D, acid **37i** (7 mg, 18 µmol, 37%) was obtained from ester **36i** (25 mg, 1.0 equiv., 50 µmol) with 10% (w/w) Pd/C (0.2 equiv.) in anhydrous THF stirring for 3 h under hydrogen atmosphere. The reaction mixture was filtered using Celite®; the Celite® pad was rinsed with DCM, which was then removed *in vacuo*. The residue was redissolved in ethyl acetate before the addition of sodium 2-ethylhexanoate (1.0 equiv.). The resultant mixture was stirred for 15 min before being evaporated *in vacuo*. The product was precipitated by the addition of diethyl ether to the crude residue. Filtration afforded the carboxylate sodium salt.

White solid. **MP**: decomposition > 100 °C. **^{1}H NMR** (500 MHz, 300 K, MeOD-*d*$_4$): δ = 7.34 – 7.26 (m, 4H, *H22*, *H23*, *H24*, *H25*), 7.24 – 7.16 (m, 1H, *H26*), 5.06 (dd, *J* = 4.5, 1.7 Hz, 1H, *H5*), 4.79 (q, *J* = 7.0 Hz, 1H, *H19*), 4.28 (s, 1H, *H3*), 3.62 (dd, *J* = 16.5, 4.5 Hz, 1H, *H6*), 3.39 (dd, *J* = 16.5, 1.7 Hz, 1H, *H6*), 1.70 (s, 3H, *H10*), 1.47 (s, 3H, *H9*), 1.42 ppm (d, *J* = 7.0 Hz, 3H, H20). **^{13}C NMR** (126 MHz, 300 K, MeOD-*d*$_4$): δ = 173.8, 170.6 (assigned via HMBC), 161.9, 145.9, 129.5, 127.9, 127.0, 68.2, 68.1, 65.5, 51.6, 39.7, 23.1, 21.4, 19.1 ppm. **HRMS** (ESI): *m/z* calculated for $C_{17}H_{20}N_3O_5S$ $(M–H)^-$ = 378.1129, found 378.1120. **IR** (film): ṽ = 3408, 1792, 1623, 1521, 1400, 1237, 1082 cm^{-1}. $[\alpha]_D^{25}$ = + 20.1 (c = 0.25, MeOH).

Sodium (*2S*,*4S*,*5R*)-4-((cyclopropylcarbamoyl)imino)-3,3-dimethyl-7-oxo-4λ^6-thia-1-azabicyclo[3.2.0]heptane-2-carboxylate 4-oxide (37j).

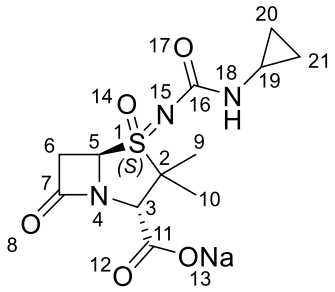

Following General Procedure D, acid **37j** (15 mg, 48 µmol, 59%) was obtained from ester **36j** (35 mg, 1.0 equiv., 80 µmol) with 10% (w/w) Pd/C (0.2 equiv.) in anhydrous THF stirring for 3 h under hydrogen atmosphere. The reaction mixture was filtered using Celite®; the Celite® pad was rinsed with DCM, which was then removed *in vacuo*. The residue was redissolved in ethyl acetate before the addition of sodium 2-ethylhexanoate (1.0 equiv.). The resultant mixture was stirred for 15 min before being evaporated *in vacuo*. The product was precipitated by the addition of diethyl ether to the crude residue. Filtration afforded the carboxylate sodium salt.

White solid. **MP**: decomposition > 100 °C. **^{1}H NMR** (500 MHz, 300 K, MeOD-*d*$_4$): δ = 5.17 (dd, *J* = 4.6, 1.7 Hz, 1H, *H5*), 4.32 (s, 1H, *H3*), 3.70 (dd, *J* = 16.5, 4.5 Hz, 1H, *H6*), 3.43 (dd, *J* = 16.5, 1.7 Hz, 1H, *H6*), 2.52 (tt, *J* = 7.2, 3.8 Hz, 1H, *H19*), 1.68 (s, 3H, *H10*), 1.46 (s, 3H, *H9*), 0.70 – 0.61 (m, 2H, *H20*, *H21*), 0.54 – 0.43 ppm (m, 2H, *H20*, *H21*). **^{13}C NMR** (126 MHz, 300 K, MeOD-*d*$_4$): δ = 173.7, 170.4, 164.1, 68.1(4), 68.1, 65.2, 39.8, 23.8, 21.4, 19.0, 6.7, 6.6 ppm. **HRMS** (ESI): *m/z* calculated for $C_{12}H_{16}N_3O_5S$ $(M–H)^-$ = 314.0816, found 314.0821. **IR** (film): $\tilde{\nu}$ = 3373, 2946, 2359, 1795, 1624, 1524, 1398, 1289, 1235, 1112, 1028 cm^{-1}. $[\alpha]_D^{25}$ = + 106.0 (c = 0.32, MeOH).

4-Methoxybenzyl 2-((*R*)-2-((*S*)-aminosulfinyl)-4-oxoazetidin-1-yl)-3-methylbut-2-enoate (38a).

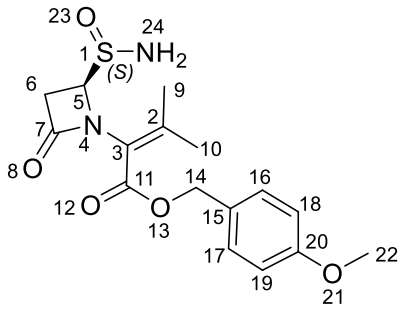

To a solution of *NH*-sulfoximine **32** (75 mg, 1.0 equiv., 0.21 mmol) and dimethyl sulfate (54 mg, 2.0 equiv., 0.43 mmol) in THF (1.1 mL) was added 1 M potassium *tert*-butoxide (29 mg, 0.26 mL, 1 M, 1.2 equiv., 0.26 mmol) dropwise at 0 °C under ambient atmosphere. The reaction mixture was allowed to warm up to ambient temperature before being concentrated. The crude residue was purified using silica column chromatography (5 g Sfär cartridge; 20 mL/min; initially 100% (v/v) cyclohexane (3 CV), followed by a linear gradient (15 CV): 0–55% (v/v) ethyl acetate in cyclohexane) to give sulfyl amide **38a** (35 mg, 65 μmol, 31%). The stereochemistry at the sulfur was tentatively assigned based on that of **32**.

Brown amorphous solid. **^{1}H NMR** (600 MHz, 300 K, $CDCl_3$): δ = 7.34 – 7.29 (m, 2H, *H16*, *H17*), 6.92 – 6.87 (m, 2H, *H18*, *H19*), 5.22 (d, *J* = 11.9 Hz, 1H, *H14*), 5.11 (d, *J* = 11.9 Hz, 1H, *H14*), 4.71 (dd, *J* = 5.2, 2.4 Hz, 1H, *H5*), 4.05 (s, 2H, *H24*), 3.82 (s, 3H, *H22*), 3.31 (dd, *J* = 15.1, 2.4 Hz, 1H, *H6*), 3.16 (dd, *J* = 15.1, 5.2 Hz, 1H, *H6*), 2.21 (s, 3H, *H10*), 1.98 ppm (s, 3H, *H9*). **^{13}C NMR** (151 MHz, 300 K, $CDCl_3$): δ = 164.4, 163.7, 160.0, 154.1, 130.6, 127.6, 120.4, 114.3, 71.3, 67.1, 55.5, 37.3, 24.1, 22.3 ppm. **HRMS** (ESI): *m/z* calculated for $C_{16}H_{19}N_2O_5S$ $(M–H)^-$ = 351.1020, found 351.1020. **IR** (film): $\tilde{\nu}$ = 3649, 2980, 2359, 1772, 1615, 1517, 1459, 1384, 1262, 1176, 1086 cm^{-1}. $[\alpha]_D^{25}$ = – 15.0 (c = 0.10, $CHCl_3$).

4-Methoxybenzyl 3-methyl-2-((*R*)-2-((*S*)-(methylamino)sulfinyl)-4-oxoazetidin-1-yl)but-2-enoate (38b).

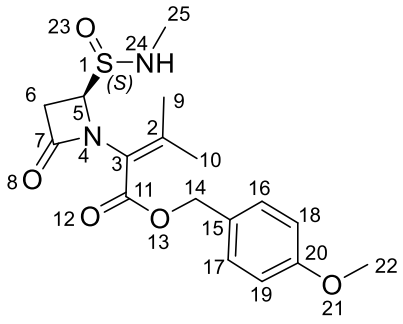

To a solution of *NH*-sulfoximine **32** (50 mg, 1.0 equiv., 0.14 mmol) in THF (1.0 mL) was added trimethylsilyldiazomethane (32 mg, 0.14 mL, 2 M, 2.0 equiv., 0.28 mmol) at ambient temperature and atmosphere. The reaction mixture was stirred at ambient temperature for 1 week before being concentrated. The crude residue was purified using silica column chromatography (5 g Sfär cartridge; 20 mL/min; initially 100% (v/v) cyclohexane (3 CV), followed by a linear gradient (15 CV): 0–40% (v/v) ethyl acetate in cyclohexane) to give sulfyl amide **38b** (27 mg, 74 μmol, 52%). The stereochemistry at the sulfur was tentatively assigned based on that of **32**.

^{1}H NMR (400 MHz, 300 K, $CDCl_3$): δ = 7.33 – 7.27 (m, 2H, *H16*, *H17*), 6.93 – 6.84 (m, 2H, *H18*, *H19*), 5.23, 5.05 (2H, ABq, *J* = 12.0 Hz, *H14*), 5.07 (dd, *J* = 4.1, 1.6 Hz, 1H, *H5*), 3.81 (s, 3H, *H22*), 3.27 (s, 3H, *H25*), 3.02 (dd, *J* = 15.1, 4.1 Hz, 1H, *H6*), 2.81 (dd, *J* = 15.1, 1.6 Hz, 1H, *H6*), 2.22 (s, 3H, *H10*), 2.02 ppm (s, 3H, *H9*). **^{13}C NMR** (101 MHz, 300 K, $CDCl_3$): δ = 165.6, 163.7, 159.9, 153.7, 130.3, 127.9, 120.6, 114.1, 84.6, 66.7, 56.3, 55.4, 43.5, 23.8, 21.9 ppm. **HRMS**: Compound did not ionise using different mass spectrometry techniques (ESI, APCI, and EI). **IR** (film): $\tilde{\nu}$ = 3791, 3661, 3639, 2981, 2838, 1768, 1721, 1614, 1548, 1516, 1462, 1445, 1389, 1298, 1250, 1218, 1177, 1081, 1035 cm^{-1}. $[\alpha]_D^{25}$ = + 1.9 (c = 0.73, $CHCl_3$).

4-Nitrobenzyl (*2S,6S*)-6-bromo-3,3-dimethyl-7-oxo-4-thia-1-azabicyclo[3.2.0]heptane-2-carboxylate (39).

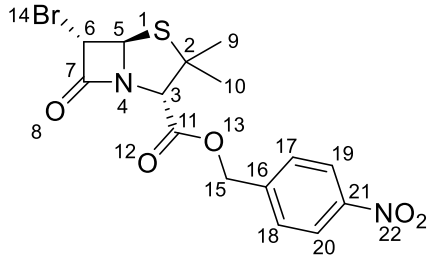

Following General Procedure A, ester **39** (30.0 g, 72 mmol, 73%) was obtained from acid **16** (27.6 g, 1.0 equiv., 99 mmol) and 1-(bromomethyl)-4-nitrobenzene (23.4 g, 1.1 equiv., 108 mmol), following column chromatography (330 g Sfär cartridge; 200 mL/min; initially 100% (v/v) cyclohexane (3 CV), followed by a linear gradient (15 CV): 0–50% (v/v) ethyl acetate in cyclohexane). The analytical data for **39** are consistent with those reported.[182]

White solid. **MP**: 63 – 65 °C (lit. 63 – 65 °C). **^{1}H NMR** (600 MHz, 300 K, $CDCl_3$): δ = 8.28 – 8.22 (m, 2H, *H19*, *H20*), 7.58 – 7.53 (m, 2H, *H17*, *H18*), 5.40 (d, *J* = 1.5 Hz, 1H, *H6*), 5.33, 5.25 (2H, ABq, *J* = 13.0 Hz, *H15*), 4.82 (d, *J* = 1.4 Hz, 1H, *H5*), 4.61 (s, 1H, *H3*), 1.62 (s, 3H, *H10*), 1.41 ppm (s, 3H, *H9*). **^{13}C NMR** (151 MHz, 300 K, $CDCl_3$): δ = 167.5, 166.7, 148.2, 141.8, 129.1, 124.2, 70.7, 70.0, 66.1, 65.1, 49.6, 34.1, 25.9 ppm. **HRMS** (ESI): *m/z* calculated for $C_{15}H_{14}BrN_2O_5S$ $(M–H)^-$ = 412.9812, found 412.9824. **IR** (film): $\tilde{\nu}$ = 3660, 2981, 2360, 2340, 1793, 1752, 1609, 1525, 1460, 1376, 1349, 1298, 1261, 1205, 1183, 1158, 1090, 1015 cm^{-1}. $[\alpha]_D^{25}$ = + 94.8 (c = 0.73, $CHCl_3$).

4-Nitrobenzyl (*2S*,5R*)*-3,3-dimethyl-7-oxo-4-thia-1-azabicyclo[3.2.0]heptane-2-carboxylate (40).

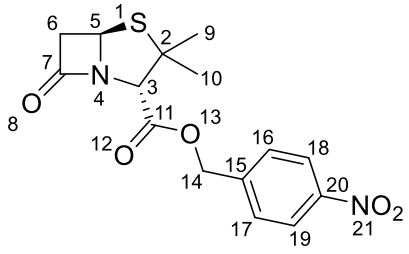

To a solution of **39** (31.8 g, 1.0 equiv., 77 mmol) in anhydrous methanol (153 mL) was added tributylphosphine (15.5 g, 19.0 mL, 1.0 equiv., 77 mmol) dropwise. The reaction mixture was stirred for 1 h at ambient temperature, before being cooled in an ice bath, filtered, and washed

with cold methanol affording ester **40** (22.5 g, 67 mmol, 88%). The analytical data for **40** are consistent with those reported.[183]

White solid. **MP**: 133 – 134 °C. **^{1}H NMR** (600 MHz, 300 K, $CDCl_3$): δ = 8.28 – 8.20 (m, 2H, *H18*, *H19*), 7.58 – 7.52 (m, 2H, *H16*, *H17*), 5.35 – 5.20 (m, 3H, *H5*, *H14*), 4.52 (s, 1H, *H3*), 3.57 (dd, *J* = 16.0, 4.2 Hz, 1H, *H6*), 3.09 (dd, *J* = 15.9, 1.8 Hz, 1H, *H6*), 1.66 (s, 3H, *H10*), 1.41 ppm (s, 3H, *H9*). **^{13}C NMR** (151 MHz, 300 K, $CDCl_3$): δ = 172.5, 167.9, 148.1, 142.1, 129.1, 124.1, 70.4, 65.9, 65.7, 60.9, 46.8, 31.9, 26.8 ppm. **HRMS** (ESI): *m/z* calculated for $C_{15}H_{15}N_2O_5S$ $(M–H)^-$ = 335.0707, found 335.0704. **IR** (film): ṽ = 3661, 2980, 1784, 1754,1609, 1525, 1461, 1350, 1298, 1262, 1207, 1181, 1158, 1132, 1098, 1013 cm^{-1}. $[\alpha]_D^{25}$ = + 211.4 (c = 0.67, $CHCl_3$).

4-Nitrobenzyl (*2S*)-3,3-dimethyl-7-oxo-4-thia-1-azabicyclo[3.2.0]heptane-2-carboxylate 4-oxide (41).

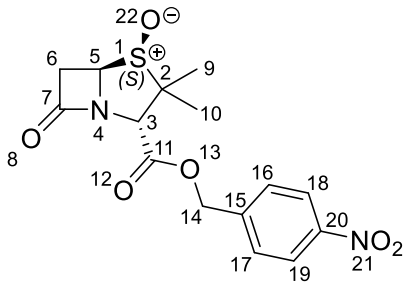

Following General Procedure B, sulfoxide **41** (2.73 g, 7.8 mmol, 59%) was obtained from sulfide **40** (4.4 g, 13.1 mmol), following column chromatography (50 g Sfär cartridge; 120 mL/min; initially 100% (v/v) dichloromethane (3 CV), followed by a linear gradient (15 CV): 0–15% (v/v) acetone in dichloromethane). The analytical data for **41** are consistent with those reported.[95]

White solid. **MP**: 161 – 163 °C. **^{1}H NMR** (600 MHz, 300 K, $CDCl_3$): δ = 8.29 – 8.23 (m, 2H, *H18*, *H19*), 7.58 – 7.53 (m, 2H, *H16*, *H17*), 5.34, 5.29 (2H, ABq, *J* = 13.0 Hz, *H14*), 4.95 (t, *J* = 3.3 Hz, 1H, *H5*), 4.59 (s, 1H, *H3*), 3.36 (d, *J* = 3.3 Hz, 2H, *H6*), 1.69 (s, 3H, *H10*), 1.17 ppm (s, 3H, *H9*). **^{13}C NMR** (151 MHz, 300 K, $CDCl_3$): δ = 170.8, 168.3, 148.3, 141.8, 129.2, 124.2, 74.0, 71.1, 66.4, 65.7, 36.2, 20.3, 18.8 ppm. **HRMS** (ESI): *m/z* calculated for $C_{15}H_{15}N_2O_6S$ $(M–H)^-$ = 351.0656, found 351.0656. **IR** (film):

ṽ = 2981, 1789, 1757, 1609, 1525, 1463, 1349, 1287, 1262 ,1209, 1185, 1161, 1134, 1090, 1057, 1023 cm^{-1}. $[\alpha]_D^{25}$ = + 205.6 (c = 0.67, $CHCl_3$).

4-Nitrobenzyl (*2S,4S,5R*)-4-((methoxycarbonyl)imino)-3,3-dimethyl-7-oxo-4λ⁶-thia-1-azabicyclo[3.2.0]heptane-2-carboxylate 4-oxide (42a).

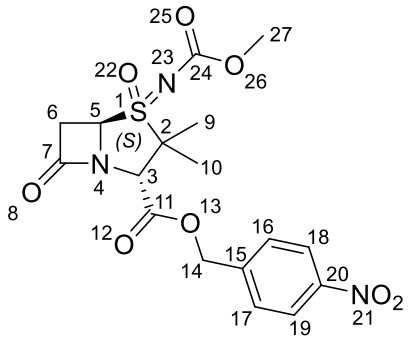

Following General Procedure C, sulfoximine **42a** (161 mg, 0.38 mmol, 95%) was obtained from sulfoxide **41** (141 mg, 1.0 equiv., 0.40 mmol) and methyl carbamate (45 mg, 1.5 equiv., 0.60 mmol), following column chromatography (10 g Sfär cartridge; 40 mL/min; initially 100% (v/v) cyclohexane (3 CV), followed by a linear gradient (15 CV): 0–60% (v/v) ethyl acetate in cyclohexane).

Amorphous solid. **^{1}H NMR** (600 MHz, 300 K, $CDCl_3$): δ = 8.30 – 8.24 (m, 2H, *H18*, *H19*), 7.58 – 7.53 (m, 2H, *H16*, *H17*), 5.33 (m, 2H, *H14*), 4.95 (dd, *J* = 4.3, 2.1 Hz, 1H, *H5*), 4.50 (s, 1H, *H3*), 3.74 (s, 3H, *H27*), 3.72 – 3.61 (m, 2H, *H6*), 1.74 (s, 3H, *H10*), 1.39 ppm (s, 3H, *H9*). **^{13}C NMR** (151 MHz, 300 K, $CDCl_3$): δ = 170.7, 166.6, 160.3, 148.4, 141.2, 129.2, 124.3, 67.7, 66.9(2C), 63.9, 54.2, 39.7, 21.3, 18.9 ppm. **HRMS** (ESI): *m/z* calculated for $C_{17}H_{18}N_3O_8S$ $(M–H)^-$ = 424.0820, found 424.0835. **IR** (film): ṽ = 3660, 2981, 1803, 1761, 1667, 1609, 1525, 1439, 1350, 1281, 1216, 1188, 1088, 1003 cm^{-1}. $[\alpha]_D^{25}$ = + 120.0 (c = 0.67, $CHCl_3$).

4-Nitrobenzyl (*2S,4S,5R*)-4-((*tert*-butoxycarbonyl)imino)-3,3-dimethyl-7-oxo-4λ⁶-thia-1-azabicyclo[3.2.0]heptane-2-carboxylate 4-oxide (42b).

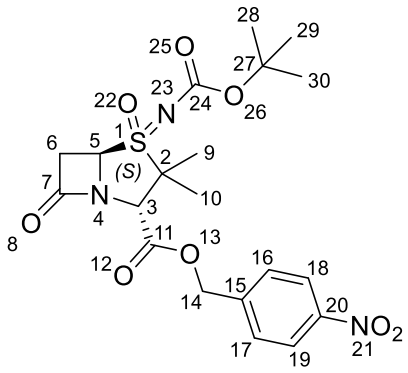

Following General Procedure C, sulfoximine **42b** (384 mg, 0.82 mmol, 96%) was obtained from sulfoxide **41** (300 mg, 1.0 equiv., 0.85 mmol) and *tert*-butyl carbamate (150 mg, 1.5 equiv., 1.27 mmol), following column chromatography (10 g Sfär cartridge; 40 mL/min; initially 100% (v/v) cyclohexane (3 CV), followed by a linear gradient (15 CV): 0-45% (v/v) ethyl acetate in cyclohexane).

Amorphous solid. **^{1}H NMR** (600 MHz, 300 K, $CDCl_3$): δ = 8.27 (m, 2H, *H18*, *H19*), 7.55 (m, 2H, *H16*, *H17*), 5.33 (s, 2H, *H14*), 4.93 (dd, *J* = 4.2, 2.2 Hz, 1H, *H5*), 4.49 (s, 1H, *H3*), 3.69 – 3.59 (m, 2H, *H6*), 1.74 (s, 3H, *H10*), 1.48 (s, 9H, *H28*, *H29*, *H30*), 1.39 ppm (s, 3H, *H9*). **^{13}C NMR** (151 MHz, 300 K, $CDCl_3$): δ = 170.9, 166.7, 158.3, 148.4, 141.3, 129.2, 124.3, 82.3, 67.7, 66.8, 66.7, 63.9, 39.8, 28.2, 21.3, 19.1 ppm. **HRMS** (ESI): *m/z* calculated for $C_{20}H_{24}N_3O_8S$ $(M-H)^-$ = 466.1290, found 466.1289. **IR** (film): ṽ = 3023, 2956, 1800, 1760, 1717, 1669, 1608, 1559, 1523, 1457, 1437, 1396, 1348, 1267, 1214, 1188, 1114, 1084 cm^{-1}. $\boldsymbol{[\alpha]_D^{25}}$ = + 95.4 (c = 0.67, $CHCl_3$).

4-Nitrobenzyl (*2S,4S,5R*)-4-(((benzyloxy)carbonyl)imino)-3,3-dimethyl-7-oxo-4λ^{6}6-thia-1-azabicyclo[3.2.0]heptane-2-carboxylate 4-oxide (42c).

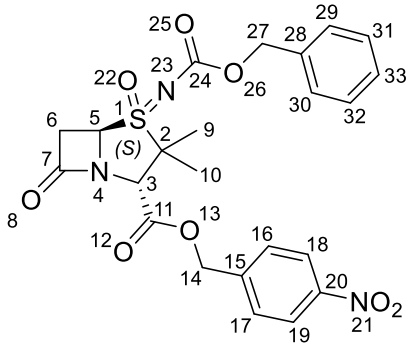

Following General Procedure C, sulfoximine **42c** (224 mg, 0.45 mmol, 57%) was obtained from sulfoxide **41** (300 mg, 1.0 equiv., 0.85 mmol) and benzyl carbamate (191 mg, 1.5 equiv., 1.27 mmol), following column chromatography (10 g Sfär cartridge; 40 mL/min; initially 100% (v/v) cyclohexane (3 CV), followed by a linear gradient (15 CV): 0-50% (v/v) ethyl acetate in cyclohexane).

Amorphous solid. **^{1}H NMR** (600 MHz, 300 K, $CDCl_3$): δ = 8.28 – 8.23 (m, 2H, *H18*, *H19*), 7.57 – 7.51 (m, 2H, *H16*, *H17*), 7.38 – 7.30 (m, 5H, *H29*, *H30*, *H31*, *H32*, *H33*), 5.32 (s, 2H, *H14*), 5.16 (d, *J* = 12.0 Hz, 1H, *H27*), 5.09 (d, *J* = 11.9 Hz, 1H, *H27*), 4.91 (dd, *J* = 3.8, 2.5 Hz, 1H, *H5*), 4.48 (s, 1H, *H3*), 3.50 (dd, *J* = 3.2, 2.3 Hz, 2H, *H6*), 1.72 (s, 3H, *H10*), 1.37 ppm (s, 3H, *H9*). **^{13}C NMR** (151 MHz, 300 K, $CDCl_3$): δ = 170.7, 166.5, 158.9, 148.3, 141.2, 135.5, 129.2, 128.8, 128.7, 128.7, 124.3, 69.1, 67.7, 66.9, 66.8, 63.8, 39.6, 21.2, 18.8 ppm. **HRMS** (ESI): *m/z* calculated for $C_{23}H_{22}N_3O_8S$ $(M\text{-}H)^-$ = 502.1279, found 502.1279. **IR** (film): $\tilde{\nu}$ = 3492, 2964, 1804, 1762, 1727, 1665, 1609, 1526, 1498, 1459, 1379, 1349, 1263, 1217, 1087, 1028 cm^{-1}. $[\alpha]_D^{25}$ = + 70.2 (c = 0.67, $CHCl_3$).

4-Nitrobenzyl (*2S*)-4-((ethoxycarbonyl)imino)-3,3-dimethyl-7-oxo-4λ^6-thia-1-azabicyclo[3.2.0]heptane-2-carboxylate 4-oxide (42d).

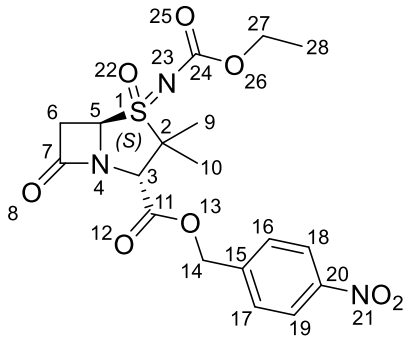

Following General Procedure C, sulfoximine **42d** (325 mg, 0.74 mmol, 87%) was obtained from sulfoxide **41** (300 mg, 1.0 equiv., 0.85 mmol) and ethyl carbamate (113 mg, 1.5 equiv., 1.27 mmol), following column chromatography (10 g Sfär cartridge; 40 mL/min; initially 100% (v/v) cyclohexane (3 CV), followed by a linear gradient (15 CV): 0-45% (v/v) ethyl acetate in cyclohexane).

Amorphous solid. **^{1}H NMR** (600 MHz, 300 K, $CDCl_3$): δ = 8.29 – 8.24 (m, 2H, *H18*, *H19*), 7.57 – 7.53 (m, 2H, *H16*, *H17*), 5.33 (s, 2H, *H14*), 4.95 (dd, *J* = 4.4, 2.1 Hz, 1H, *H5*), 4.50 (s, 1H, *H3*), 4.23 – 4.09 (m, 2H, *H27*), 3.68 (dd, *J* = 16.7, 4.3 Hz, 1H, *H6*), 3.63 (dd, *J* = 16.6, 2.0 Hz, 1H, *H6*), 1.74 (s, 3H, *H10*), 1.39 (s, 3H, *H9*), 1.30 ppm (t, *J* = 7.2, 3H, *H28*). **^{13}C NMR** (151 MHz, 300 K, $CDCl_3$): δ = 170.8, 166.6, 159.9, 148.4, 141.2, 129.2, 124.3, 67.6, 66.8(8), 66.8(5), 63.9, 63.3, 39.7, 21.3, 18.9, 14.5 ppm.

HRMS (ESI): *m/z* calculated for $C_{18}H_{20}N_3O_8S$ $(M-H)^-$ = 438.0977, found 438.0977. **IR** (film): ṽ = 3661, 2981, 1804, 1763, 1664, 1609, 1526, 1464, 1370, 1350, 1263, 1217, 1187, 1091, 1019 cm^{-1}. $[\alpha]_D^{25}$ = + 93.3 (c = 0.67, $CHCl_3$).

4-Nitrobenzyl (*2S,4S,5R*)-3,3-dimethyl-4-((methylsulfonyl)imino)-7-oxo-4λ⁶-thia-1-azabicyclo[3.2.0]heptane-2-carboxylate 4-oxide (42e).

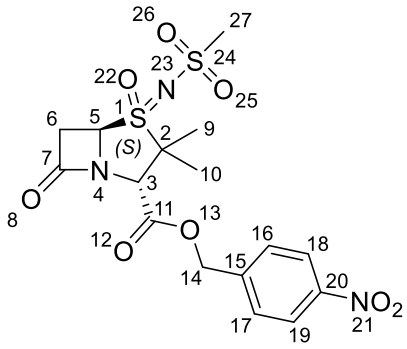

Following General Procedure C, sulfoximine **42e** (219 mg, 0.49 mmol, 58%) was obtained from sulfoxide **41** (300 mg, 1.0 equiv., 0.85 mmol) and methyl sulfonamide (121 mg, 1.5 equiv., 1.27 mmol), following column chromatography (10 g Sfär cartridge; 40 mL/min; initially 100% (v/v) cyclohexane (3 CV), followed by a linear gradient (15 CV): 0-50% (v/v) ethyl acetate in cyclohexane).

Amorphous solid. **^{1}H NMR** (600 MHz, 300 K, $CDCl_3$): δ = 8.30 – 8.23 (m, 2H, *H18*, *H19*), 7.59 – 7.52 (m, 2H, *H16*, *H17*), 5.34 (s, 2H, *H14*), 5.09 (dd, *J* = 4.5, 1.8 Hz, 1H, *H5*), 4.46 (s, 1H, *H3*), 3.69 (dd, *J* = 16.9, 4.5 Hz, 1H, *H6*), 3.54 (dd, *J* = 16.9, 1.8 Hz, 1H, *H6*), 3.16 (s, 3H, *H27*), 1.72 (s, 3H, *H10*), 1.44 ppm (s, 3H, *H9*). **^{13}C NMR** (151 MHz, 300 K, $CDCl_3$): δ = 170.3, 166.2, 148.4, 141.1, 129.3, 124.3, 68.9, 68.2, 67.0, 63.0, 45.3, 39.6, 21.3, 18.6 ppm. **HRMS** (ESI): *m/z* calculated for $C_{16}H_{18}N_3O_8S_2$ $(M-H)^-$ = 444.0541, found 444.0560. **IR** (film): ṽ = 3369, 2981, 1804, 1747, 1658, 1609, 1525, 1462, 1350, 1317, 1261, 1218, 1189, 1165, 1142, 1093, 1063 cm^{-1}. $[\alpha]_D^{25}$ = + 17.7 (c = 0.67, $CHCl_3$).

[1,1'-Biphenyl]-4-ylmethyl (*2S*,*5R*,*6S*)-6-bromo-3,3-dimethyl-7-oxo-4-thia-1-azabicyclo[3.2.0]heptane-2-carboxylate (43).

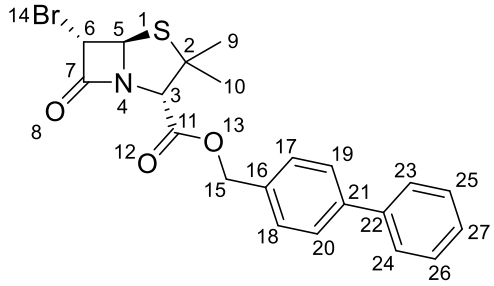

Following General Procedure A, ester **43** (11.81 g, 26.5 mmol, 99%) was obtained from acid **16** (7.5 g, 1.0 equiv., 26.8 mmol) and 4-(bromomethyl)-1,1'-biphenyl (7.28 g, 1.1 equiv., 29.4 mmol), following column chromatography (330 g Sfär cartridge; 200 mL/min; initially 100% (v/v) cyclohexane (3 CV), followed by a linear gradient (15 CV): 0–10% (v/v) ethyl acetate in cyclohexane).

Amorphous solid. **^{1}H NMR** (600 MHz, 300 K, $CDCl_3$): δ = 7.64 – 7.57 (m, 4H, *H19*, *H20*, *H23*, *H24*), 7.48 – 7.42 (m, 4H, *H17*, *H18*, *H25*, *H26*), 7.40 – 7.34 (m, 1H, *H27*), 5.44 (d, *J* = 1.5 Hz, 1H, *H6*), 5.26, 5.22 (2H, ABq, *J* = 12.1 Hz, *H15*), 4.81 (d, *J* = 1.5 Hz, 1H, *H5*), 4.59 (s, 1H, *H3*), 1.61 (s, 3H, *H10*), 1.42 ppm (s, 3H, *H9*). **^{13}C NMR** (151 MHz, 300 K, $CDCl_3$): δ = 167.4, 167.0, 141.9, 140.6, 133.7, 129.3, 129.0, 127.8, 127.6, 127.3, 70.7, 70.1, 67.4, 65.2, 49.6, 34.2, 25.9 ppm. **HRMS** (ESI): *m/z* calculated for $C_{21}H_{19}BrNO_3S$ $(M–H)^-$ = 444.0275, found 444.0267. **IR** (film): ṽ = 2980, 1789, 1746, 1600, 1548, 1486, 1451, 1296, 1203, 1181 cm^{-1}. $[\alpha]_D^{25}$ = + 92.3 (c = 1.83, $CHCl_3$).

[1,1'-Biphenyl]-4-ylmethyl (*2S*,*5R*)-3,3-dimethyl-7-oxo-4-thia-1-azabicyclo[3.2.0]heptane-2-carboxylate (44).

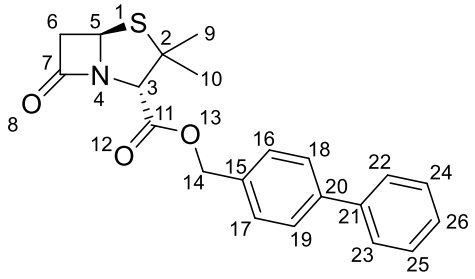

To a solution of **43** (11.8 g, 1.0 equiv., 26.4 mmol) in anhydrous methanol (53 mL) was added tributylphosphine (5.4 g, 6.6 mL, 1.0 equiv., 26.4 mmol) dropwise. The reaction mixture was stirred for 1 h at ambient temperature, before being evaporated. The crude material was purified using silica column chromatography (100 g Sfär cartridge; 120 mL/min; initially 100% (v/v) cyclohexane (3 CV), followed by a linear gradient (15

CV): 0–90% (v/v) dichloromethane in cyclohexane) affording ester **44** (5.78 g. 15.7 mmol, 60%).

Amorphous solid. **^{1}H NMR** (600 MHz, 300 K, $CDCl_3$): δ = 7.63 – 7.57 (m, 4H, *H18*, *H19*, *H22*, *H23*), 7.48 – 7.42 (m, 4H, *H16*, *H17*, *H24*, *H25*), 7.40 – 7.34 (m, 1H, *H26*), 5.30 (dd, *J* = 4.2, 1.8 Hz, 1H, *H5*), 5.24, 5.22 (2H, ABq, *J* = 12.2 Hz, *H14*), 4.51 (s, 1H, *H3*), 3.56 (dd, *J* = 15.9, 4.2 Hz, 1H, *H6*), 3.07 (dd, *J* = 15.9, 1.8 Hz, 1H, *H6*), 1.65 (s, 3H, *H10*), 1.43 ppm (s, 3H, *H9*). **^{13}C NMR** (151 MHz, 300 K, $CDCl_3$) δ 172.5, 168.1, 141.8, 140.6, 134.0, 129.3, 129.0, 127.7, 127.6, 127.3, 70.4, 67.3, 65.9, 60.8, 46.7, 32.0, 26.9 ppm. **HRMS** (ESI): *m/z* calculated for $C_{21}H_{21}NO_3SNa$ $(M+Na)^+$ = 390.1134, found 390.1135. **IR** (film): ṽ = 3847, 3775, 3697, 3663, 3638, 1784, 1691, 1659, 1584, 1549, 1530, 1486, 1463, 1298, 1206 cm^{-1}. $\boldsymbol{[\alpha]_D^{25}}$ = + 129.5 (c = 0.53, $CHCl_3$).

[1,1'-Biphenyl]-4-ylmethyl (*2S*,*5R*)-3,3-dimethyl-7-oxo-4-thia-1-azabicyclo[3.2.0]heptane-2-carboxylate 4-oxide (45).

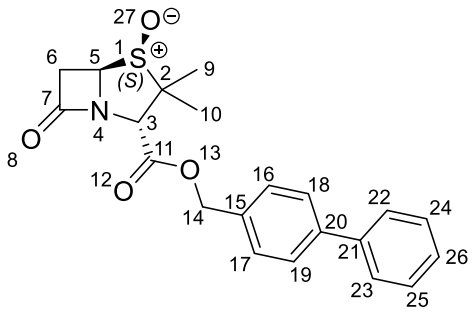

Following General Procedure B, sulfoxide **45** (5.07 g, 13.2 mmol, 84%) was obtained from sulfide **44** (5.78 g, 15.7 mmol), following column chromatography (50 g Sfär cartridge; 120 mL/min; initially 100% (v/v) cyclohexane (3 CV), followed by a linear gradient (15 CV): 0–75% (v/v) ethyl acetate in cyclohexane).

Amorphous solid. **^{1}H NMR** (600 MHz, 300 K, $CDCl_3$): δ = 7.64 – 7.57 (m, 4H, *H18*, *H19*, *H22*, *H23*), 7.48 – 7.42 (m, 4H, *H16*, *H17*, *H24*, *H25*), 7.40 – 7.34 (m, 1H, *H26*), 5.33, 5.21 (2H, ABq, *J* = 12.1 Hz, *H14*), 4.94 (t, *J* = 3.3 Hz, 1H, *H5*), 4.57 (s, 1H, *H3*), 3.38 – 3.32 (m, 2H, *H6*), 1.68 (s, 3H, *H10*), 1.14 ppm (s, 3H, *H9*). **^{13}C NMR** (151

MHz, 300 K, $CDCl_3$): δ = 170.8, 168.4, 141.9, 140.5, 133.8, 129.4, 129.0, 127.8, 127.6, 127.3, 74.1, 71.1, 67.8, 65.8, 36.2, 20.4, 18.7 ppm. **HRMS** (ESI): *m/z* calculated for $C_{21}H_{22}NO_4S$ $(M+H)^+$ = 384.1264, found 384.1264. **IR** (film): ṽ = 3789, 3696, 3662, 1788, 1659, 1584, 1548, 1485, 1206, 1058 cm^{-1}. $[\alpha]_D^{25}$ = + 120.8 (c = 0.69, $CHCl_3$).

[1,1'-Biphenyl]-4-ylmethyl (*2S*,*4S*,*5R*)-4-((methoxycarbonyl)imino)-3,3-dimethyl-7-oxo-4λ⁶-thia-1-azabicyclo[3.2.0]heptane-2-carboxylate 4-oxide (46a).

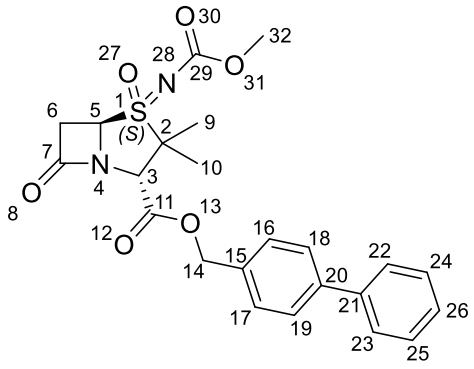

Following General Procedure C, sulfoximine **46a** (250 mg, 0.76 mmol, 65%) was obtained from sulfoxide **45** (450 mg, 1.0 equiv., 1.2 mmol) and methyl carbamate (132 mg, 1.5 equiv., 1.8 mmol), following column chromatography (25 g Sfär cartridge; 80 mL/min; initially 100% (v/v) cyclohexane (3 CV), followed by a linear gradient (15 CV): 0–40% (v/v) ethyl acetate in cyclohexane).

Amorphous solid. **^{1}H NMR** (600 MHz, 300 K, $CDCl_3$): δ = 7.64 – 7.56 (m, 4H, *H18*, *H19*, *H22*, *H23*), 7.48 – 7.42 (m, 4H, *H16*, *H17*, *H24*, *H25*), 7.40 – 7.34 (m, 1H, *H26*), 5.32, 5.25 (2H, ABq, *J* = 12.0 Hz, *H14*), 4.94 (dd, *J* = 4.3, 2.0 Hz, 1H, *H5*), 4.49 (s, 1H, *H3*), 3.73 (s, 3H, *H32*), 3.67 (dd, *J* = 16.8, 4.2 Hz, 1H, *H6*), 3.62 (dd, *J* = 16.6, 2.1 Hz, 1H, *H6*), 1.72 (s, 3H, *H10*), 1.35 ppm (s, 3H, *H9*). **^{13}C NMR** (151 MHz, 300 K, $CDCl_3$): δ = 170.7, 166.7, 160.3, 142.2, 140.4, 133.3, 129.5, 129.0, 127.9, 127.7, 127.3, 68.3, 67.8, 66.9, 63.9, 54.1, 39.6, 21.2, 18.9 ppm. **HRMS** (ESI): *m/z* calculated for $C_{23}H_{25}N_2O_6S$ $(M+H)^+$ = 457.1428, found 457.1430. **IR** (film): ṽ = 3846, 3789, 3696, 3662, 3640, 1804, 1758, 1665, 1583, 1548, 1529, 1485, 1462, 1441, 1282, 1143, 1062 cm^{-1}. $[\alpha]_D^{25}$ = + 93.3 (c = 0.45, $CHCl_3$).

[1,1'-Biphenyl]-4-ylmethyl (*2S*,*4S*,*5R*)-3,3-dimethyl-4-((methylsulfonyl)imino)-7-oxo-4λ^6-thia-1-azabicyclo[3.2.0]heptane-2-carboxylate 4-oxide (46b).

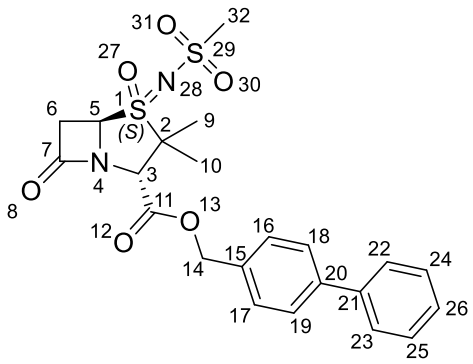

Following General Procedure C, sulfoximine **46b** (362 mg, 0.76 mmol, 65%) was obtained from sulfoxide **45** (450 mg, 1.0 equiv., 1.2 mmol) and methyl sulfonamide (167 mg, 1.5 equiv., 1.8 mmol), following column chromatography (25 g Sfär cartridge; 80 mL/min; initially 100% (v/v) cyclohexane (3 CV), followed by a linear gradient (15 CV): 0-40% (v/v) ethyl acetate in cyclohexane). Amorphous solid. **^{1}H NMR** (600 MHz, 300 K, $CDCl_3$): δ = 7.65 – 7.56 (m, 4H, *H18*, *H19*, *H22*, *H23*), 7.49 – 7.42 (m, 4H, *H16*, *H17*, *H24*, *H25*), 7.41 – 7.35 (m, 1H, *H26*), 5.33, 5.25 (2H, ABq, *J* = 11.9 Hz, *H14*), 5.07 (dd, *J* = 4.4, 1.8 Hz, 1H, *H5*), 4.44 (s, 1H, *H3*), 3.68 (dd, *J* = 16.8, 4.4 Hz, 1H, *H6*), 3.52 (dd, *J* = 16.8, 1.8 Hz, 1H, *H6*), 3.14 (s, 3H, *H32*), 1.70 (s, 3H, *H10*), 1.39 ppm (s, 3H, *H9*). **^{13}C NMR** (151 MHz, 300 K, $CDCl_3$): δ = 170.3, 166.3, 142.3, 140.4, 133.2, 129.6, 129.1, 127.9, 127.8, 127.3, 68.9, 68.5, 68.2, 63.0, 45.3, 39.5, 21.2, 18.6 ppm. **HRMS** (ESI): *m/z* calculated for $C_{22}H_{24}N_2O_6S_2Na$ $(M+Na)^+$ = 499.0968, found 499.0964. **IR** (film): ṽ = 3847, 3811, 3789, 3740, 3696, 3682, 3661, 3638, 1805, 1758, 1710, 1691, 1659, 1641, 1584, 1548, 1529, 1512, 1484, 1467, 1318, 1223, 1189, 1144, 1064 cm^{-1}. $[\alpha]_D^{25}$ = + 91.7 (c = 0.53, $CHCl_3$).

4-Methoxybenzyl (*2S*,*4R*,*5R*)-4-((methoxycarbonyl)imino)-3,3-dimethyl-7-oxo-4λ^6-thia-1-azabicyclo[3.2.0]heptane-2-carboxylate 4-oxide (47).

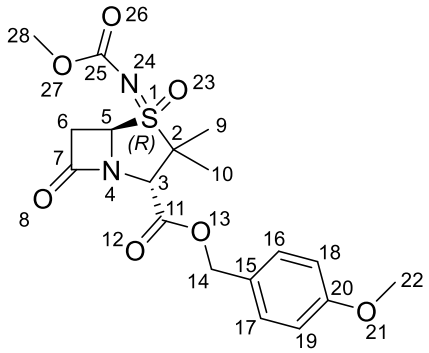

Following General Procedure C, sulfoximine **47** (69 mg, 0.17 mmol, 63%) was obtained by reaction of sulfoxide **25** (90 mg, 1.0 equiv., 0.27 mmol) and methyl carbamate (30 mg, 1.5 equiv., 0.40 mmol), following column chromatography (10 g Sfär cartridge; 40 mL/min; initially 100% (v/v) cyclohexane (3 CV), followed by a linear gradient (15 CV): 0–50% (v/v) ethyl acetate in cyclohexane).

Amorphous solid. **^{1}H NMR** (700 MHz, 300 K, $CDCl_3$): δ = 7.33 – 7.28 (m, 2H, *H16*, *H17*), 6.92 – 6.87 (m, 2H, *H18*, *H19*), 5.24, 5.10 (2H, ABq, *J* = 11.7 Hz, *H14*), 4.91 (dd, *J* = 3.2, 1.1 Hz, 1H, *H5*), 4.49 (s, 1H, *H3*), 3.82 (s, 3H, *H22*), 3.72 (s, 3H, *H28*), 3.60 (dd, *J* = 3.2, 1.2 Hz, 2H, *H6*), 1.62 (s, 3H, *H10*), 1.33 ppm (s, 3H, *H9*). **^{13}C NMR** (176 MHz, 300 K, $CDCl_3$): δ = 169.8, 166.5, 160.3, 159.3, 130.9, 126.6, 114.3, 68.3(2), 68.3, 67.2, 64.0, 55.5, 54.0, 41.3, 20.8, 19.2 ppm. **HRMS** (ESI): *m/z* calculated for $C_{18}H_{20}N_2O_7S$ $(M–H)^-$ = 409.1075, found 409.1087. **IR** (film): ṽ = 2958, 1802, 1754, 1680, 1614, 1517, 1441, 1257 cm^{-1}. $[\alpha]_D^{25}$ = – 17.4 (c = 0.34, $CHCl_3$).

4-Methoxybenzyl (*2S*,*4R*,*5R*)-4-imino-3,3-dimethyl-7-oxo-4λ^6-thia-1-azabicyclo[3.2.0]heptane-2-carboxylate 4-oxide (48).

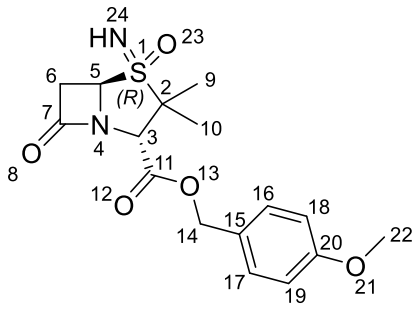

To a solution of sulfoximine **26** (620 mg, 1.0 equiv., 1.27 mmol) in anhydrous ethyl acetate (12.7 mL) was added 10% wt Pd/C (271 mg, 2.0 equiv., 2.55 mmol). Using a Schlenk line, the reaction mixture was evacuated and backfilled with hydrogen gas 3 times. The reaction mixture was stirred at ambient temperature for 6 h under a hydrogen atmosphere before being filtered over Celite®, washed with ethyl acetate, and evaporated. The crude material was purified using silica column chromatography

(25 g Sfär cartridge; 80 mL/min; initially 100% (v/v) cyclohexane (3 CV), followed by a linear gradient (15 CV): 0–100% (v/v) ethyl acetate in cyclohexane) to give compound **48** (200 mg, 0.57 mmol, 45%).

White solid. **MP**: decomposition. **^{1}H NMR** (600 MHz, 300 K, $CDCl_3$): δ = 7.35 – 7.27 (m, 2H, *H16*, *H17*), 6.93 – 6.86 (m, 2H, *H18*, *H19*), 5.24, 5.09 (2H, ABq, *J* = 11.7 Hz, *H14*), 4.60 (dd, *J* = 4.3, 1.7 Hz, 1H, *H5*), 4.30 (s, 1H, *H3*), 3.82 (s, 3H, *H22*), 3.44 (dd, *J* = 16.0, 4.4 Hz, 1H, *H6*), 3.34 (dd, *J* = 16.0, 1.7 Hz, 1H, *H6*), 2.70 (s, 1H, *H24*), 1.56 (s, 3H, *H10*), 1.27 ppm (s, 3H, *H9*). **^{13}C NMR** (151 MHz, 300 K, $CDCl_3$): δ 171.4, 167.5, 160.2, 130.9, 126.8, 114.2, 68.0, 64.4, 64.0, 63.1, 55.5, 38.3, 20.0, 19.0 ppm. **HRMS** (ESI): *m/z* calculated for $C_{16}H_{21}N_2O_5S$ $(M+H)^+$ = 409.1075, found 409.1087. **IR** (film): $\tilde{\nu}$ = 3653, 2980, 2889, 1796, 1752, 1614, 1517, 1463, 1382, 1258, 1174, 1083 cm^{-1}. $[\alpha]_D^{25}$ = + 40.7 (c = 0.23, $CHCl_3$).

4-Methoxybenzyl (*2S*,*4R*,*5R*)-3,3-dimethyl-7-oxo-4-((phenethylcarbamoyl)imino)-4λ^6-thia-1-azabicyclo[3.2.0]heptane-2-carboxylate 4-oxide (49).

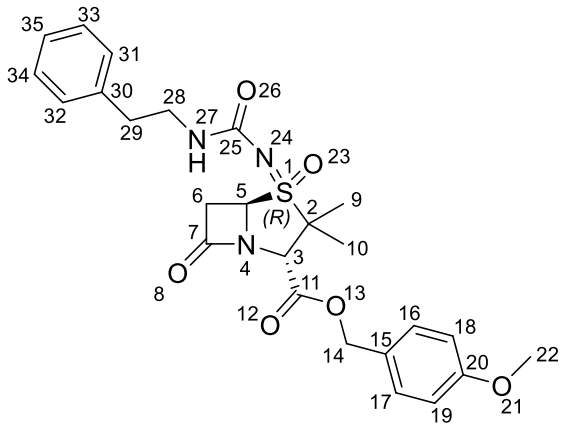

Following General Procedure H, urea **49** (34 mg, 68 μmol, 32%) was obtained from *NH*-sulfoximine **48** (75 mg, 1.0 equiv., 0.21 mmol) and (2-isocyanatoethyl)benzene (50 mg, 1.6 equiv., 0.34 mmol), following column chromatography (5 g Sfär cartridge; 20 mL/min; initially 100% (v/v) cyclohexane (3 CV), followed by a linear gradient (15 CV): 0–55% (v/v) ethyl acetate in cyclohexane). Amorphous solid. **^{1}H NMR** (600 MHz, 300 K, $CDCl_3$): δ = 7.34 – 7.27 (m, 4H, *H16*, *H17*, *H33*, *H34*), 7.25 – 7.14 (m, 3H, *H31*, *H32*, *H35*), 6.93 – 6.88 (m, 2H, *H18*, *H19*),

5.22 (d, *J* = 11.7 Hz, 1H, *H14*), 5.15 – 5.07 (m, 2H, *H14*, *H27*), 4.93 – 4.88 (dd, *J* = 4.5, 1.7 Hz, 1H, *H5*), 4.39 (s, 1H, *H3*), 3.82 (s, 3H, *H22*), 3.69 (dd, *J* = 17.0, 1.7 Hz, 1H, *H6*), 3.53 (dd, *J* = 17.0, 4.5 Hz, 1H, *H6*), 3.50 – 3.38 (m, 2H, *H28*), 2.85 – 2.75 (m, 2H, *H29*), 1.54 (s, 3H, *H10*), 1.30 ppm (s, 3H, *H9*). **^{13}C NMR** (151 MHz, 300 K, $CDCl_3$): δ = 171.0, 166.8, 160.3, 159.1, 139.1, 130.9, 129.0, 128.78 126.7, 126.6, 114.1, 68.2, 67.6, 67.1, 64.1, 55.5, 42.1, 41.2, 36.2, 20.6, 19.2 ppm. **HRMS** (ESI): *m/z* calculated for $C_{25}H_{28}N_3O_6S$ $(M–H)^-$ = 498.1704, found 498.1697. **IR** (film): $\tilde{\nu}$ = 3649, 2980, 2360, 1798, 1750, 1616, 1517, 1459, 1383, 1261, 1086 cm^{-1}. $[\alpha]_D^{25}$ = – 13.1 (c = 0.11, $CHCl_3$).

(*6R*,*7S*)-7-Bromo-3-methyl-8-oxo-5-thia-1-azabicyclo[4.2.0]oct-2-ene-2-carboxylic acid (51).

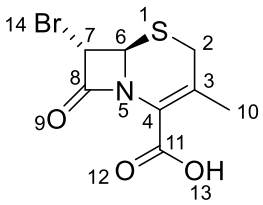

To a solution of HBr (13.8 g, 9.24 mL, 48% wt, 3.5 equiv., 812 mmol) in methanol (30 mL) and 9mL deionized water at -10 °C was added 7-aminodesacetoxycephalosporanic acid (5.00 g, 1.0 equiv., 23 mmol) followed by sodium nitrite (2.4 g, 1.5 equiv., 35 mmol) in 4 mL water dropwise over 30 min. The reaction mixture was stirred for an additional 30 min at ambient temperature before the addition of NaCl (2 g). The reaction mixture was extracted with dichloromethane 3 times. The combined organic extracts were washed with brine, dried over anhydrous Na_2SO_4, and evaporated *in vacuo*. The crude material was purified using silica column chromatography (50 g Sfär cartridge; 120 mL/min; initially 100% (v/v) cyclohexane (3 CV), followed by a linear gradient (15 CV): 0-40% (v/v) ethyl acetate in cyclohexane) to give acid **51** (3.1 g, 11 mmol, 48%). The ^{1}H NMR data for **51** was not consistent with those reported.[149] Previous ^{1}H NMR data were reported at 200 MHz.

Yellow Solid. **MP**: 130 – 132 °C. **^{1}H NMR** (600 MHz, 300 K, $CDCl_3$): δ = 4.85 (d, *J* = 1.6 Hz, 1H, *H7*), 4.70 (d, *J* = 1.6 Hz, 1H, *H6*), 3.48 (dq, *J* = 17.9, 0.9 Hz, 1H, *H2*), 3.30 (d, *J* = 17.8 Hz, 1H, *H2*), 2.25 ppm (s, 3H, *H10*). **^{13}C NMR** (151 MHz, 300 K, $CDCl_3$): δ = 164.2, 160.4, 136.8, 123.4, 59.3, 46.9, 32.2, 20.4 ppm. **HRMS** (ESI): *m/z* calculated for $C_8H_8BrNO_3SNa$ $(M+Na)^+$ = 301.9279, found 301.9280. **IR** (film): ṽ = 3788, 3662, 2981, 1784, 1724, 1631, 1549, 1513, 1381, 1241, 1162, 1070 cm^{-1}. $[\alpha]_D^{25}$ = + 137.1 (c = 0.58, $CHCl_3$).

4-Methoxybenzyl (*6R*,*7S*)-7-bromo-3-methyl-8-oxo-5-thia-1-azabicyclo[4.2.0]oct-2-ene-2-carboxylate (52).

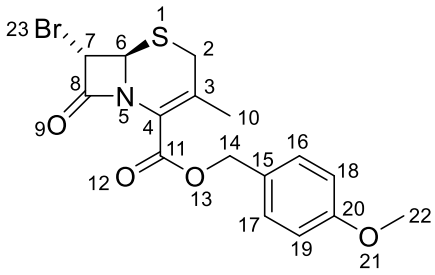

Following General Procedure A, ester **52** (2.86 g, 7.2 mmol, 64%) was obtained from acid **51** (3.1 g, 1.0 equiv., 11.1 mmol) and 1-(bromomethyl)-4-methoxybenzene (2.24 g, 1.0 equiv., 11.1 mmol), following column chromatography (25 g Sfär cartridge; 80 mL/min; initially 100% (v/v) cyclohexane (3 CV), followed by a linear gradient (15 CV): 0-20% (v/v) ethyl acetate in cyclohexane).

Amorphous Solid. **^{1}H NMR** (600 MHz, 300 K, $CDCl_3$): δ = 7.39 – 7.34 (m, 2H, *H16*, *H17*), 6.92 – 6.87 (m, 2H, *H18*, *H19*), 5.29, 5.19 (2H, ABq, *J* = 11.9 Hz, *H14*), 4.79 (d, *J* = 1.6 Hz, 1H, *H7*), 4.66 (d, *J* = 1.6 Hz, 1H, *H6*), 3.81 (s, 3H, *H22*), 3.42 (dd, *J* = 17.7, 1.0 Hz, 1H, *H2*), 3.22 (d, *J* = 17.8 Hz, 1H, *H2*), 2.10 ppm (s, 3H, *H10*). **^{13}C NMR** (151 MHz, 300 K, $CDCl_3$): δ = 161.8, 159.9, 159.2, 131.4, 130.5, 127.4, 124.0, 114.1, 67.6, 58.7, 55.4, 47.3, 31.7, 19.8 ppm. **HRMS** (APCI): *m/z* calculated for $C_{16}H_{16}BrNO_4SNa$ $(M+Na)^+$ = 419.9876, found 419.9878. **IR** (film): ṽ = 3661, 2981, 2890, 1787, 1725, 1613, 1516, 1384, 1361, 1304, 1249, 1177, 1117, 1038 cm^{-1}. $[\alpha]_D^{25}$ = + 217.1 (c = 0.59, $CHCl_3$).

4-Methoxybenzyl (*6R*,*7S*)-7-bromo-3-methyl-8-oxo-5-thia-1-azabicyclo[4.2.0]oct-2-ene-2-carboxylate 5-oxide (53).

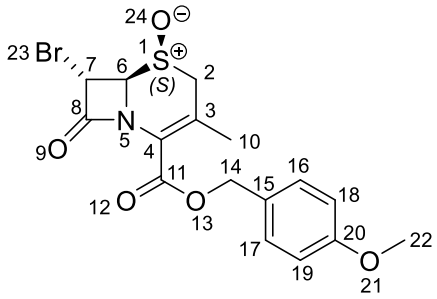

Following General Procedure B, sulfoxide **53** (1.51 g, 3.64 mmol, 51%) was obtained from ester **52** (2.86 g, 1.0 equiv., 7.18 mmol), following column chromatography (25 g Sfär cartridge; 80 mL/min; initially 100% (v/v) cyclohexane (3 CV), followed by a linear gradient (15 CV): 0-45% (v/v) ethyl acetate in cyclohexane).

Amorphous Solid. **^{1}H NMR** (600 MHz, 300 K, $CDCl_3$): δ = 7.41 – 7.35 (m, 2H, *H16*, *H17*), 6.93 – 6.87 (m, 2H, *H18*, *H19*), 5.32, 5.22 (2H, ABq, *J* = 11.8 Hz, *H14*), 5.09 (d, *J* = 1.6 Hz, 1H, *H6*), 4.47 (d, *J* = 1.7 Hz, 1H, *H7*), 3.81 (s, 3H, *H22*), 3.63 (d, *J* = 18.7 Hz, 1H, *H2*), 3.27 (d, *J* = 1.6 Hz, 1H, *H2*), 2.07 ppm (s, 3H, *H10*). **^{13}C NMR** (151 MHz, $CDCl_3$): δ = 160.7, 160.0, 157.9, 130.8, 127.2, 123.8, 120.7, 114.1, 69.2, 68.0, 55.4, 49.9, 42.4, 20.1 ppm. **HRMS** (ESI): *m/z* calculated for $C_{16}H_{15}BrNO_5S$ $(M-H)^-$ = 411.9860, found 411.9862. **IR** (film): ṽ = 3847, 3789, 3717, 3697, 3682, 3662, 3642, 2980, 2900, 1782, 1724, 1691, 1659, 1641, 1612, 1549, 1516, 1463, 1385, 1304, 1263, 1055 cm^{-1}. $[\alpha]_D^{25}$ = + 155.0 (c = 0.41, $CHCl_3$).

4-Methoxybenzyl (*6R*)-3-methyl-8-oxo-5-thia-1-azabicyclo[4.2.0]oct-2-ene-2-carboxylate 5-oxide (54).

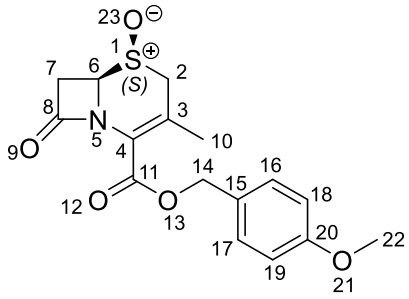

To a solution of sulfoxide **53** (1.51 g, 1.0 equiv., 3.64 mmol) in anhydrous methanol (18 mL) was added tributylphosphine (890 mg, 1.1 mL, 1.2 equiv., 4.4 mmol) dropwise under N_2 atmosphere. The reaction mixture was stirred for 1 h at ambient temperature before being concentrated *in vacuo*. The crude material was purified using column chromatography (25 g Sfär cartridge;

80 mL/min; initially 100% (v/v) cyclohexane (3 CV), followed by a linear gradient (15 CV): 0-100% (v/v) ethyl acetate in cyclohexane) to afford sulfoxide **54** (1.0 g, 3.0 mmol, 82%).

Amorphous Solid. **^{1}H NMR** (600 MHz, 300 K, $CDCl_3$): δ = 7.40 – 7.34 (m, 2H, *H16*, *H17*), 6.93 – 6.86 (m, 2H, *H18*, *H19*), 5.28 – 5.18 (m, 2H, *H14*), 4.35 (dt, *J* = 4.5, 2.0 Hz, 1H, *H6*), 3.81 (s, 3H, *H22*), 3.60 (d, *J* = 18.5 Hz, 1H, *H2*), 3.43 (dd, *J* = 15.5, 4.8 Hz, 1H, *H7*), 3.38 (dd, *J* = 15.5, 2.3 Hz, 1H, *H7*), 3.25 (d, *J* = 18.4, 1.5 Hz, 1H, *H2*), 2.07 ppm (s, 3H, *H10*). **^{13}C NMR** (151 MHz, 300 K, $CDCl_3$): δ = 161.4, 161.4, 160.0, 130.9, 127.3, 124.0, 119.4, 114.1, 67.9, 60.6, 55.4, 49.9, 39.8, 20.1 ppm. **HRMS** (ESI): *m/z* calculated for $C_{16}H_{17}NO_5SNa$ $(M+Na)^+$ = 358.0720, found 358.0720. **IR** (film): ṽ = 3662, 2981, 2889, 2363, 1782, 1725, 1613, 1517, 1462, 1383, 1305, 1252, 1152, 1073 cm^{-1}. $[\alpha]_D^{25}$ = + 123.3 (c = 0.19, $CHCl_3$).

4-Methoxybenzyl (*6R*)-5-(((benzyloxy)carbonyl)imino)-3-methyl-8-oxo-5λ^6-thia-1-azabicyclo[4.2.0]oct-2-ene-2-carboxylate 5-oxide (55a).

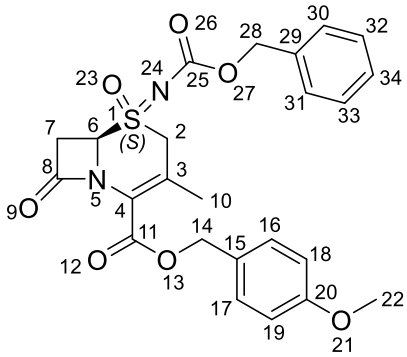

Following General Procedure C, sulfoximine **55a** (125 mg, 0.26 mmol, 72%) was obtained from sulfoxide **54** (120 mg, 1.0 equiv., 0.36 mmol) and benzyl carbamate (81 mg, 1.5 equiv., 0.54 mmol), following column chromatography (10 g Sfär cartridge; 40 mL/min; initially 100% (v/v) cyclohexane (3 CV), followed by a linear gradient (15 CV): 0-35% (v/v) ethyl acetate in cyclohexane).

Amorphous Solid. **^{1}H NMR** (600 MHz, $CDCl_3$): δ = 7.39 – 7.31 (m, 7H, *H16*, *H17*, *H30*, *H31*, *H32*, *H33*, *H34*), 6.93 – 6.86 (m, 2H, *H18*, *H19*), 5.24 (d, *J* = 12.0 Hz, 1H, *H14*), 5.20, 5.14 (2H, ABq, *J* = 11.9 Hz, *H14*), 5.11 (d, *J* = 12.1 Hz, 1H, *H28*), 4.90 (dt, *J* = 4.9, 1.6 Hz, 1H, *H6*), 4.10 (d, *J* = 18.5 Hz, 1H, *H2*), 4.04 (d, *J* = 18.5 Hz, 1H,

H2), 3.81 (s, 3H, *H22*), 3.72 (dd, *J* = 16.3, 2.0 Hz, 1H, *H7*), 3.52 (dd, *J* = 16.4, 4.9 Hz, 1H, *H7*), 2.06 ppm (s, 3H, *H10*). **^{13}C NMR** (151 MHz, $CDCl_3$): δ = 160.9 (2C assigned via HMBC), 160.2, 158.7, 135.7, 130.9, 128.8, 128.6, 128.5, 126.9, 125.4, 123.6, 114.2, 68.8, 68.3, 65.1, 55.4, 54.3, 40.8, 19.5 ppm. **HRMS** (ESI): *m/z* calculated for $C_{24}H_{23}N_2O_7S$ $(M-H)^-$ = 483.1231, found 483.1236. **IR** (film): ṽ = 3788, 3682, 3662, 3020, 2956, 1798, 1727, 1666, 1613, 1548, 1517, 1452, 1381, 1353, 1303, 1271, 1179, 1128, 1047 cm^{-1}. $[\alpha]_D^{25}$ = – 46.3 (c = 0.19, $CHCl_3$).

4-Methoxybenzyl (*6R*)-5-((methoxycarbonyl)imino)-3-methyl-8-oxo-5λ^6-thia-1-azabicyclo[4.2.0]oct-2-ene-2-carboxylate 5-oxide (55b).

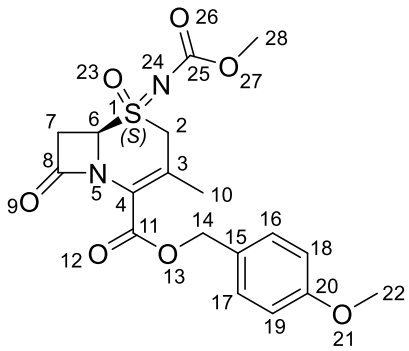

Following General Procedure C, sulfoximine **55b** (84 mg, 0.21 mmol, 57%) was obtained from sulfoxide **54** (120 mg, 1.0 equiv., 0.36 mmol) and methyl carbamate (40 mg, 1.5 equiv., 0.54 mmol), following column chromatography (10 g Sfär cartridge; 40 mL/min; initially 100% (v/v) cyclohexane (3 CV), followed by a linear gradient (15 CV): 0-60% (v/v) ethyl acetate in cyclohexane).

Amorphous Solid. **^{1}H NMR** (600 MHz, 300 K, $CDCl_3$): δ = 7.37 – 7.31 (m, 2H, *H16*, *H17*), 6.93 – 6.86 (m, 2H, *H18*, *H19*), 5.24, 5.21 (2H, ABq, *J* = 11.9 Hz, *H14*), 4.92 (dt, *J* = 4.7, 1.6 Hz, 1H, *H6*), 4.11 (d, *J* = 18.5 Hz, 1H, *H2*), 4.05 (d, *J* = 1.3 Hz, 1H, *H2*), 3.81 (s, 3H, *H22*), 3.76 (dd, *J* = 16.4, 2.0 Hz, 1H, *H7*), 3.73 (s, 3H, *H28*), 3.59 (dd, *J* = 16.4, 4.9 Hz, 1H, *H7*), 2.07 ppm (s, 3H, *H10*). **^{13}C NMR** (151 MHz, 300 K, $CDCl_3$): δ = 161.0, 160.2, 160.2, 159.5, 130.9, 126.9, 125.3, 123.6, 114.2, 68.3, 65.0, 55.4, 54.2, 53.9, 40.8, 19.5 ppm. **HRMS** (ESI): *m/z* calculated for $C_{18}H_{19}N_2O_7S$ $(M-H)^-$ = 407.0918, found 407.0930. **IR** (film): ṽ = 3786, 3697, 3661, 2958, 1792, 1729,

1668, 1612, 1516, 1435, 1381, 1358, 1283, 1177, 1129, 1051 cm^{-1}. $[\alpha]_D^{25}$ = – 61.1 (c = 0.35, $CHCl_3$).

4-Methoxybenzyl (*6R*,*7S*)-7-bromo-3-methyl-8-oxo-5-thia-1-azabicyclo[4.2.0]oct-2-ene-2-carboxylate 5-oxide (57).

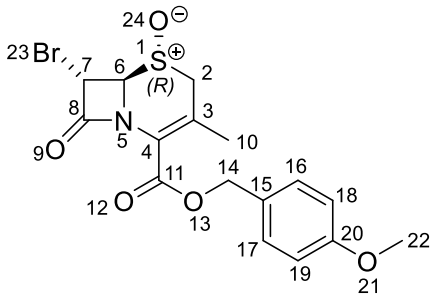

Following General Procedure B, **57** (280 mg, 0.68 mmol, 9%) was obtained from ester **52** (2.86 g, 1.0 equiv., 7.18 mmol), following column chromatography (25 g Sfär cartridge; 80 mL/min; initially 100% (v/v) cyclohexane (3 CV), followed by a linear gradient (15 CV): 0-45% (v/v) ethyl acetate in cyclohexane).

Amorphous Solid. **^{1}H NMR** (600 MHz, 300 K, $CDCl_3$): δ = 7.38 – 7.32 (m, 2H, *H16*, *H17*), 6.93 – 6.87 (m, 2H, *H18*, *H19*), 5.29, 5.19 (2H, ABq, *J* = 11.9 Hz, *H14*), 5.06 (d, *J* = 1.6 Hz, 1H, *H6*), 4.54 (d, *J* = 1.6 Hz, 1H, *H7*), 3.81 (m, 4H, *H2*, *H22*), 3.53 (dd, *J* = 16.9, 1.3 Hz, 1H, *H2*), 2.11 ppm (s, 3H, *H10*). **^{13}C NMR** (151 MHz, 300 K, $CDCl_3$): δ = 160.5, 160.1, 157.4, 130.7, 129.0, 126.9, 124.0, 114.2, 74.8, 68.1, 55.4, 55.0, 44.3, 19.9 ppm. **HRMS** (ESI): *m/z* calculated for $C_{16}H_{15}BrNO_5S$ $(M-H)^-$ = 411.9860, found 411.9852. **IR** (film): $\tilde{\nu}$ = 3789, 3661, 3638, 2981, 2889, 1798, 1726, 1659, 1613, 1549, 1516, 1462, 1384, 1305, 1251, 1177, 1063 cm^{-1}. $[\alpha]_D^{25}$ = – 32.0 (c = 0.24, $CHCl_3$).

4-Methoxybenzyl (*6R*)-3-methyl-8-oxo-5-thia-1-azabicyclo[4.2.0]oct-2-ene-2-carboxylate 5-oxide (58).

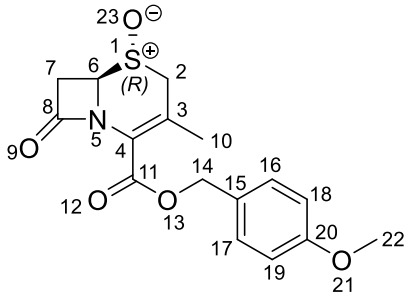

To a solution of sulfoxide **57** (280 mg, 1.0 equiv., 0.68 mmol) in methanol (3 mL) was added tributylphosphine (160 mg, 0.2 mL, 1.2 equiv., 0.81 mmol) dropwise. The reaction mixture was stirred for 1 h at ambient temperature before being

evaporated *in vacuo*. The crude material was purified by column chromatography (10 g Sfär cartridge; 40 mL/min; initially 100% (v/v) cyclohexane (3 CV), followed by a linear gradient (15 CV): 0-100% (v/v) ethyl acetate in cyclohexane) to afford sulfoxide **58** (180 mg, 0.54 mmol, 80%).

Amorphous Solid. **^{1}H NMR** (600 MHz, 300 K, $CDCl_3$): δ = 7.37 – 7.31 (m, 2H, *H16*, *H17*), 6.92 – 6.86 (m, 2H, *H18*, *H19*), 5.24, 5.18 (2H, ABq, *J* = 11.9 Hz, *H14*), 4.37 (dd, *J* = 4.9, 2.1 Hz, 1H, *H6*), 3.84 – 3.78 (m, 4H, *H2*, *H22*), 3.69 (dd, *J* = 16.2, 4.9 Hz, 1H, *H7*), 3.47 (dd, *J* = 17.1, 1.3 Hz, 1H, *H2*), 3.36 (dd, *J* = 16.2, 2.1 Hz, 1H, *H7*), 2.09 ppm (s, 3H, *H10*). **^{13}C NMR** (151 MHz, 300 K, $CDCl_3$): δ = 161.2, 160.8, 160.1, 130.9, 127.3, 127.0, 124.0, 114.2, 68.0, 66.1, 55.4, 54.7, 43.4, 19.8 ppm. **HRMS** (ESI): *m/z* calculated for $C_{16}H_{17}NO_5SNa$ $(M+Na)^+$ = 358.0720, found 358.0720. **IR** (film): ṽ = 3775, 3661, 2981, 2889, 1785, 1726, 1613, 1549, 1517, 1462, 1382, 1305, 1251, 1151, 1072 cm^{-1}. $[\alpha]_D^{25}$ = – 40.6 (c = 0.2, $CHCl_3$).

4-Methoxybenzyl (*6R*)-5-(((benzyloxy)carbonyl)imino)-3-methyl-8-oxo-5λ^6-thia-1-azabicyclo[4.2.0]oct-2-ene-2-carboxylate 5-oxide (59a).

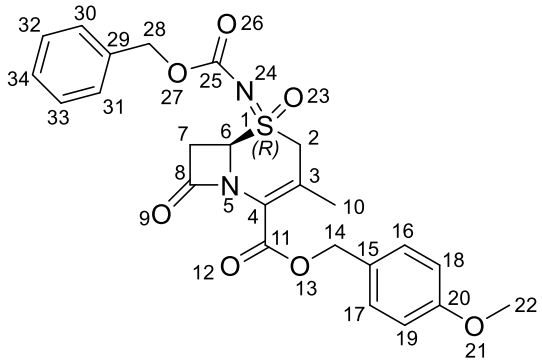

Following General Procedure C, sulfoximine **59a** (62 mg, 0.13 mmol, 36%) was obtained from sulfoxide **58** (120 mg, 1.0 equiv., 0.36 mmol) and benzyl carbamate (81 mg, 1.5 equiv., 0.54 mmol), following column chromatography (10 g Sfär cartridge; 40 mL/min; initially 100% (v/v) cyclohexane (3 CV), followed by a linear gradient (15 CV): 0-35% (v/v) ethyl acetate in cyclohexane).

Amorphous Solid. **^{1}H NMR** (600 MHz, 300 K, $CDCl_3$): δ = 7.41 – 7.29 (m, 7H, *H16*, *H17*, *H30*, *H31*, *H32*, *H33*, *H34*), 6.93 – 6.87 (m, 2H, *H18*, *H19*), 5.26 – 5.14 (m, 3H,

H14, *H28*), 5.09 (d, *J* = 12.3 Hz, 1H, *H28*), 4.85 (d, *J* = 18.0 Hz, 1H, *H2*), 4.74 – 4.70 (m, 1H, *H6*), 3.90 (d, *J* = 18.1 Hz, 1H, *H2*), 3.83 – 3.80 (m, 4H, *H7*, *H22*), 3.48 (dd, *J* = 15.8, 4.9 Hz, 1H, *H7*), 2.06 ppm (s, 3H, *H10*). **^{13}C NMR** (151 MHz, 300 K, $CDCl_3$): δ = 161.0, 160.6, 160.2, 159.2, 135.9, 130.9, 128.7, 128.4, 128.3, 127.8, 126.9, 123.8, 114.2, 68.7, 68.2, 65.2, 55.5, 52.2, 40.6, 19.7 ppm. **HRMS** (ESI): *m/z* calculated for $C_{24}H_{23}N_2O_7S$ $(M\text{-}H)^-$ = 483.1231, found 483.1235. **IR** (film): ṽ = 3661, 2981, 1797, 1727, 1667, 1517, 1462, 1382, 1264, 1126 cm^{-1}. $[\boldsymbol{\alpha}]_{\boldsymbol{D}}^{\mathbf{25}}$ = + 43.0 (c = 0.26, $CHCl_3$).

4-Methoxybenzyl (*6R*)-5-((methoxycarbonyl)imino)-3-methyl-8-oxo-5λ^6-thia-1-azabicyclo[4.2.0]oct-2-ene-2-carboxylate 5-oxide (59b).

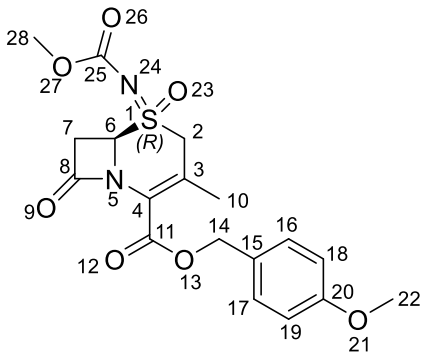

Following General Procedure C, sulfoximine **59b** (95 mg, 0.23 mmol, 65%) was obtained from sulfoxide **58** (120 mg, 1.0 equiv., 0.36 mmol) and methyl carbamate (40 mg, 1.5 equiv., 0.54 mmol), following column chromatography (10 g Sfär cartridge; 40 mL/min; initially 100% (v/v) cyclohexane (3 CV), followed by a linear gradient (15 CV): 0-45% (v/v) ethyl acetate in cyclohexane).

Amorphous Solid. **^{1}H NMR** (600 MHz, 300 K, $CDCl_3$): δ = 7.36 – 7.32 (m, 2H, *H16*, *H17*), 6.93 – 6.86 (m, 2H, *H18*, *H19*), 5.23, 5.19 (2H, ABq, *J* = 11.8 Hz, *H14*), 4.93 (d, *J* = 18.2 Hz, 1H, *H2*), 4.72 (dt, *J* = 4.6, 1.5 Hz, 1H, *H6*), 3.91 (d, *J* = 18.2 Hz, 1H, *H2*), 3.84 (dd, *J* = 15.9, 2.0 Hz, 1H, *H7*), 3.81 (s, 3H, *H22*), 3.73 (s, 3H, *H28*), 3.51 (dd, *J* = 15.8, 4.9 Hz, 1H, *H7*), 2.08 ppm (s, 3H, *H10*). **^{13}C NMR** (151 MHz, 300 K, $CDCl_3$): δ = 161.0, 160.6, 160.2, 159.9, 130.9, 130.5, 126.9, 123.6, 114.2, 68.2, 64.9, 55.5, 54.0, 51.8, 40.4, 19.6 ppm. **HRMS** (ESI): *m/z* calculated for $C_{18}H_{19}N_2O_7S$ $(M\text{-}H)^-$ = 407.0918, found 407.0927. **IR** (film): ṽ = 3662, 2981, 1798, 1727, 1676, 1613, 1517, 1442, 1382, 1265, 1127, 1071 cm^{-1}. $[\boldsymbol{\alpha}]_{\boldsymbol{D}}^{\mathbf{25}}$ = + 49.4 (c = 0.22, $CHCl_3$).

(*6R,7R*)-3-Methyl-8-oxo-7-(2-phenylacetamido)-5-thia-1-azabicyclo[4.2.0]oct-2-ene-2-carboxylic acid (61).

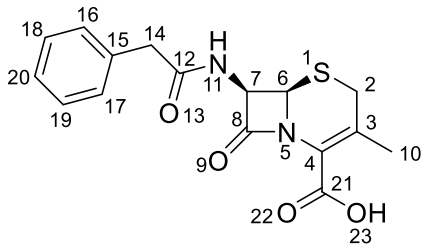

To a solution of 7-aminodesacetoxycephalosporanic acid (5.0 g, 1.0 equiv., 23 mmol) and $NaHCO_3$ (10.7 g, 5.5 equiv., 128 mmol) in deionized water (100 mL) and acetone (18 mL) was added dropwise phenylacetyl chloride (6.1 g, 1.7 equiv., 40 mmol). The reaction mixture was stirred at ambient temperature for 16 h before being acidified to pH 2 with 4 M HCl and extracted with dichloromethane. The combined organic phases were dried over anhydrous Na_2SO_4 and evaporated *in vacuo*. The crude material was purified using silica column chromatography (50 g Sfär cartridge; 120 mL/min; initially 100% (v/v) cyclohexane (3 CV), followed by a linear gradient (15 CV): 0-100% (v/v) ethyl acetate in cyclohexane) affording acid **61** (7.0 g, 22 mmol, 90%). The analytical data for **61** are consistent with those reported.[184]

White solid. **MP**: 198 – 200 °C. **^{1}H NMR** (600 MHz, 300 K, MeOD-*d*$_4$): δ = 7.34 – 7.21 (m, 5H, *H16*, *H17*, *H18*, *H19*, *H20*), 5.63 (d, J = 4.6 Hz, 1H, *H7*), 5.03 (d, J = 4.6 Hz, 1H, *H6*), 3.65 – 3.53 (m, 2H, *H14*), 3.57-3.54 (m, 1H, *H2*), 3.36 – 3.31 (s, 1H, *H2*), 2.14 ppm (s, 3H, *H10*). **^{13}C NMR** (151 MHz, 300 K, MeOD-*d*$_4$): δ = 174.6, 166.2, 165.6, 136.5, 134.3, 130.2, 129.5, 128.0, 124.2, 60.5, 58.8, 43.2, 30.8, 19.9 ppm. **HRMS** (ESI): *m/z* calculated for $C_{16}H_{15}N_2O_4S$ $(M-H)^-$ = 331.0758, found 331.0769. **IR** (film): ṽ = 3530, 3270, 1777, 1727, 1697, 1658, 1629, 1542, 1497, 1413, 1375, 1355, 1293, 1229, 1190, 1162, 1067, 1040 cm^{-1}. $[\alpha]_D^{25}$ = + 102.6 (c = 0.67, CH_3CN).

4-Nitrobenzyl (*6R,7R*)-3-methyl-8-oxo-7-(2-phenylacetamido)-5-thia-1-azabicyclo[4.2.0]oct-2-ene-2-carboxylate (62).

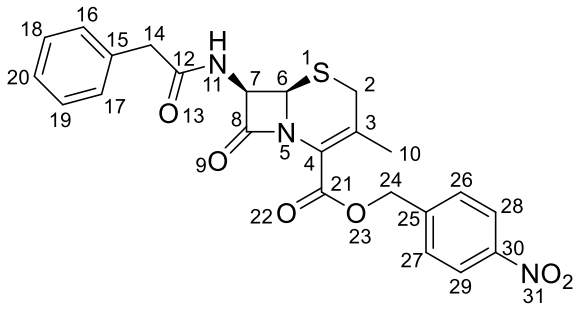

Following General Procedure A, ester **62** (70 mg, 9.7 mmol, 69%) was obtained from acid **61** (5.0 g, 1.0 equiv., 14 mmol) and 1-(bromomethyl)-4-nitrobenzene (3.03, 1.0 equiv., 14 mmol), following column chromatography (50 g Sfär cartridge; 120 mL/min; initially 100% (v/v) cyclohexane (3 CV), followed by a linear gradient (15 CV): 0-50% (v/v) ethyl acetate in cyclohexane). The analytical data for **62** are consistent with those reported.[185]

Yellow solid. **MP**: 142 – 144 °C. **^{1}H NMR** (600 MHz, 300 K, $CDCl_3$) δ 8.26 – 8.19 (m, 2H, *H28*, *H29*), 7.59 – 7.54 (m, 2H, *H26*, *H27*), 7.39 – 7.26 (m, 5H, *H16*, *H17*, *H18*, *H19*, *H20*), 6.02 (d, *J* = 9.0 Hz, 1H, *H11*), 5.79 (dd, *J* = 9.0, 4.7 Hz, 1H, *H7*), 5.35, 5.27 (2H, ABq, *J* = 13.1 Hz, *H24*),v 4.95 (d, *J* = 4.7 Hz, 1H, *H6*), 3.65 (q, *J* = 16.2 Hz, 2H, *H14*), 3.53 – 3.46 (m, 1H, *H2*), 3.22 – 3.11 (m, 1H, *H2*), 2.13 ppm (s, 3H, *H10*). **^{13}C NMR** (151 MHz, 300 K, $CDCl_3$) δ 171.1, 164.7, 161.6, 147.9, 142.3, 133.6, 132.9, 129.5, 129.2, 128.9, 127.8, 123.8, 122.0, 66.0, 59.0, 57.1, 43.4, 30.2, 20.2 ppm. **HRMS** (ESI): *m/z* calculated for $C_{23}H_{21}N_3O_6S$ $(M+Na)^+$ = 490.1043, found 490.1043. **IR** (film): ṽ = 3277, 3029, 2971, 2946, 1766, 1737, 1720, 1654, 1608, 1527, 1497, 1454, 1367, 1349, 1232, 1218, 1200, 1160, 1112, 1070 cm^{-1}. $[\alpha]_D^{25}$ = + 63.5 (c = 0.67, $CHCl_3$).

4-Nitrobenzyl (*5S,6R,7R*)-3-methyl-8-oxo-7-(2-phenylacetamido)-5-thia-1-azabicyclo[4.2.0]oct-2-ene-2-carboxylate 5-oxide (63).

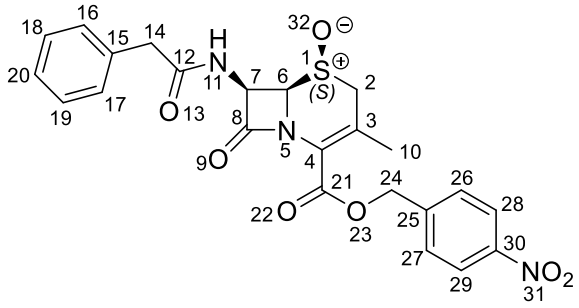

Following General Procedure B, sulfoxide **63** (3.2 g, 6.6 mmol, 57%) was obtained from ester **62** (5.4 g, 11.6 mmol), following column chromatography (50 g Sfär cartridge; 120 mL/min; initially 100% (v/v) dichloromethane (3 CV), followed by a linear gradient (15 CV): 0-20% (v/v) acetone in dichloromethane). The melting point for **63** is consistent with those reported.[186]

White solid. **MP**: 217 – 220 °C. **^{1}H NMR** (600 MHz, 300 K, DMSO-d_6) δ 8.36 (d, *J* = 8.4 Hz, 1H, *H11*), 8.27 – 8.21 (m, 2H, *H28*, *H29*), 7.74 – 7.69 (m, 2H, *H26*, *H27*), 7.32 – 7.29 (m, 4H, *H16*, *H17*, *H18*, *H19*), 7.25 – 7.22 (m, 1H, *H20*), 5.80 (dd, *J* = 8.3, 4.6 Hz, 1H, *H7*), 5.43 (d, *J* = 1.9 Hz, 2H, *H24*), 4.88 (dd, *J* = 4.7, 1.5 Hz, 1H, *H6*), 3.81 (d, *J* = 18.7 Hz, 1H, *H2*), 3.69 (d, *J* = 14.1 Hz, 1H, *H14*), 3.65 (d, *J* = 18.7 Hz, 1H, *H2*), 3.55 (d, *J* = 14.1 Hz, 1H, *H14*), 2.05 ppm (s, 3H, *H10*). **^{13}C NMR** (151 MHz, 300 K, DMSO-d_6): δ = 171.0, 164.2, 160.9, 147.2, 143.2, 135.8, 129.1, 128.8, 128.3, 126.5, 126.3, 123.5, 121.0, 66.3, 65.6, 57.9, 48.6, 41.5, 19.8 ppm. **HRMS** (ESI): *m/z* calculated for $C_{23}H_{22}N_3O_7S$ $(M+H)^+$ = 484.1173, found 484.1172. **IR** (film): ṽ = 3659, 3166, 2981, 2889, 2411, 1738, 1445, 1377, 1259, 1152, 1073, 1040 cm^{-1}. $[\alpha]_D^{25}$ = + 134.3 (c = 0.027, CH_3CN).

Methyl (*6R,7R*)-3-methyl-8-oxo-7-(2-phenylacetamido)-5-thia-1-azabicyclo[4.2.0]oct-2-ene-2-carboxylate (65).

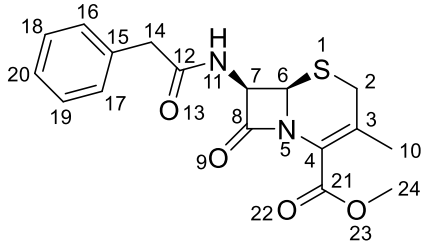

To a solution of acid **61** (3.0 g, 1.0 equiv., 9.0 mmol) in anhydrous dichloromethane (9.0 mL) and anhydrous *N*,*N*-dimethylformamide (9.0 mL) was added K_2CO_3 (1.25 g, 1.0 equiv., 9.0 mmol)

followed by iodomethane (1.92 g, 1.5 equiv., 13.5 mmol). The reaction mixture was stirred in a sealed flask at 35 °C for 3 h before being partitioned between water and ethyl acetate. The organic phase was washed with brine, dried over anhydrous Na_2SO_4, and evaporated *in vacuo*. The crude material was purified using silica column chromatography. (50 g Sfär cartridge; 120 mL/min; initially 100% (v/v) cyclohexane (3 CV), followed by a linear gradient (15 CV): 0-50% (v/v) ethyl acetate in cyclohexane) affording ester **65** (2.61 g, 7.5 mmol, 84%). Reported structure did not have reported characterization data.[187]

White solid. **MP**: 189 – 192 °C. **^{1}H NMR** (600 MHz, 300 K, $CDCl_3$): δ = 7.38 – 7.26 (m, 5H, *H16*, *H17*, *H18*, *H19*, *H20*), 6.10 (d, *J* = 8.9 Hz, 1H, *H11*), 5.76 (dd, *J* = 9.0, 4.7 Hz, 1H, *H7*), 4.94 (d, *J* = 4.6 Hz, 1H, *H6*), 3.82 (s, 3H, *H24*), 3.70 – 3.57 (m, 2H, *H14*), 3.52 – 3.40 (m, 1H, *H2*), 3.20 – 3.08 (m, 1H, *H2*), 2.10 ppm (s, 3H, *H10*). **^{13}C NMR** (151 MHz, 300 K, $CDCl_3$): δ = 171.1, 164.4, 162.5, 133.7, 131.4, 129.5, 129.2, 127.7, 122.5, 59.1, 57.2, 52.4, 43.4, 30.1, 20.0 ppm. **HRMS** (ESI): *m/z* calculated for $C_{17}H_{17}N_2O_4S$ $(M\text{-}H)^-$ = 345.0915, found 345.0916. **IR** (film): $\tilde{\nu}$ = 3273, 3032, 2981, 1770, 1728, 1662, 1537, 1498, 1454, 1437, 1378, 1356, 1308, 1246, 1199, 1161, 1112, 1071, 1056, 1056 cm^{-1}. $\boldsymbol{[\alpha]_D^{25}}$ = + 71.0 (c = 0.67, $CHCl_3$).

Methyl (*5S,6R,7R*)-3-methyl-8-oxo-7-(2-phenylacetamido)-5-thia-1-azabicyclo[4.2.0]oct-2-ene-2-carboxylate 5-oxide (66).

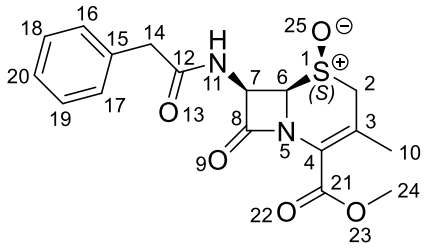

Following General Procedure B, sulfoxide **66** (520 mg, 1.4 mmol, 82%) was obtained from ester **65** (610 mg, 1.8 mmol), following column chromatography (25 g Sfär cartridge; 80 mL/min; initially 100% (v/v) cyclohexane (3 CV), followed by a linear gradient (15 CV): 0-

60% (v/v) ethyl acetate in cyclohexane). The analytical data for **66** are consistent with those reported.[188]

White solid. **MP**: 211 – 213 °C. **^{1}H NMR** (600 MHz, 300 K, DMSO-d_6): δ = 8.35 (d, *J* = 8.3 Hz, 1H, *H11*), 7.30 (m, 4H, *H16*, *H17*, *H18*, *H19*), 7.23 (m, 1H, *H20*), 5.75 (dd, *J* = 8.3, 4.6 Hz, 1H, *H7*), 4.84 (dd, *J* = 4.7, 1.5 Hz, 1H, *H6*), 3.78 (s, 3H, *H24*), 3.76 (m, 1H, *H2*), 3.69 (d, *J* = 14.1 Hz, 1H, *H14*), 3.64 – 3.59 (m, 1H, *H2*), 3.53 (d, *J* = 14.1 Hz, 1H, *H14*), 2.01 ppm (s, 3H, *H10*). **^{13}C NMR** (151 MHz, 300 K, DMSO-d_6): δ = 171.0, 164.0, 161.7, 135.8, 129.1, 128.2, 126.5, 124.7, 121.3, 66.2, 58.0, 52.2, 48.5, 41.5, 19.7 ppm. **HRMS** (ESI): *m/z* calculated for $C_{17}H_{17}N_2O_5S$ $(M-H)^-$ = 361.0864, found 361.0866. **IR** (film): ṽ = 3680, 3659, 3637, 3623, 3602, 3572, 3541, 3284, 3166, 3007, 2964, 2408, 1776, 1727, 1646, 1536, 1443, 1377, 1309, 1262, 1097, 1038 cm^{-1}. $[\alpha]_D^{25}$ = + 77.4 (c = 0.067, CH_3CN).

Methyl (*5S,6R,7R*)-5-((*tert*-butoxycarbonyl)imino)-3-methyl-8-oxo-7-(2-phenylacetamido)-5λ^6-thia-1-azabicyclo[4.2.0]oct-2-ene-2-carboxylate 5-oxide (67).

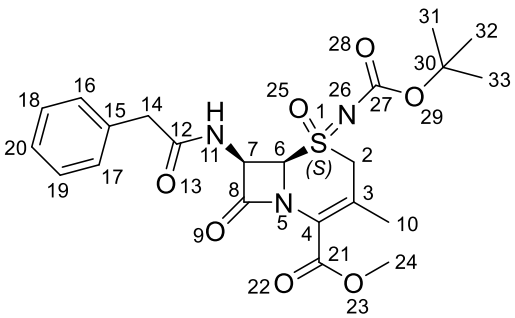

Following General Procedure C, sulfoximine **67** (150 mg, 0.31 mmol, 46%) was obtained from sulfoxide **66** (250 mg, 1.0 equiv., 0.69 mmol) and *tert*-butyl carbamate (121 mg, 1.5 equiv., 1.0 mmol) in dichloromethane, following column chromatography (10 g Sfär cartridge; 40 mL/min; initially 100% (v/v) dichloromethane (3 CV), followed by a linear gradient (15 CV): 0-10% (v/v) acetone in dichloromethane).

White solid. **MP**: 174 – 175 °C. **^{1}H NMR** (600 MHz, 300 K, DMSO-d_6): δ = 8.63 (d, *J* = 9.3 Hz, 1H, *H11*), 7.31 – 7.20 (m, 5H, *H16*, *H17*, *H18*, *H19*, *H20*), 6.06 (dd, *J* =

9.3, 4.6 Hz, 1H, *H7*), 5.35 (d, *J* = 4.6 Hz, 1H, *H6*), 4.62 (d, *J* = 18.1 Hz, 1H, *H2*), 4.49 (d, *J* = 17.9 Hz, 1H, *H2*), 3.79 (s, 3H, *H24*), 3.65 (d, *J* = 14.7 Hz, 1H, *H14*), 3.55 (d, *J* = 14.7 Hz, 1H, *H14*), 2.06 (s, 3H, *H10*), 1.43 ppm (s, 9H, *H31*, *H32*, *H33*). **^{13}C NMR** (151 MHz, 300 K, DMSO-d_6): δ = 170.9, 163.9, 161.5, 157.1, 135.6, 130.6, 129.2, 128.2, 126.4, 120.5, 80.0, 67.4, 58.9, 54.5, 52.6, 41.3, 27.8, 18.9 ppm. **HRMS** (ESI): *m/z* calculated for $C_{22}H_{26}N_3O_7S$ $(M-H)^-$ = 476.1497, found 476.1494. **IR** (film): ṽ = 2980, 1779, 1736, 1699, 1676, 1514, 1370, 1316, 1274, 1252, 1154, 1111, 1051 cm^{-1}. $[\alpha]_D^{25}$ = – 113.0 (c = 0.087, CH_3CN).

2-(Trimethylsilyl)ethyl (*7R*)-3-methyl-8-oxo-7-(2-phenylacetamido)-5-thia-1-azabicyclo[4.2.0]oct-2-ene-2-carboxylate (68).

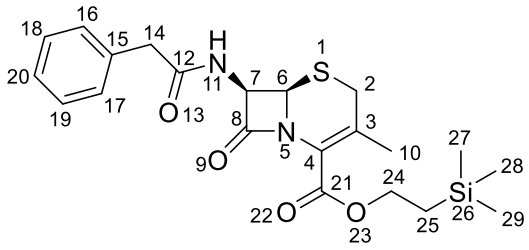

To a solution of acid **61** (1.5 g, 1.0 equiv., 4.5 mmol) in anhydrous dichloromethane (9.0 mL) was added 4-*N*,*N*-dimethylaminopyridine (1.1 g, 2.0 equiv., 9.0 mmol) and DCC (1.02 g, 1.1 equiv., 5.0 mmol) at 0 °C. The reaction was stirred for 5 minutes and 2-(trimethylsilyl)ethan-1-ol (620 mg, 1.2 equiv., 5.4 mmol) was added. The reaction mixture was slowly allowed to warm up to ambient temperature over 30 min before being evaporated and partitioned between ethyl acetate and water. The organic phase was sequentially washed with water and brine, dried over anhydrous Na_2SO_4, and evaporated *in vacuo*. The crude material was purified using silica column chromatography (25 g Sfär cartridge; 80 mL/min; initially 100% (v/v) cyclohexane (3 CV), followed by a linear gradient (15 CV): 0-60% (v/v) ethyl acetate in cyclohexane) affording ester **68** (1.64 g, 3.8 mmol, 84%).

Amorphous solid. **^{1}H NMR** (600 MHz, 300 K, CD_3CN): δ = 7.36 – 7.24 (m, 5H, *H16*, *H17*, *H18*, *H19*, *H20*), 7.18 (d, *J* = 8.8 Hz, 1H, *H11*), 5.64 (dd, *J* = 8.7, 4.7 Hz, 1H,

H7), 4.98 (d, *J* = 4.7 Hz, 1H, *H6*), 4.35 – 4.24 (m, 2H, *H24*), 3.60 – 3.50 (m, 3H, *H2*, *H14*), 3.29 – 3.22 (m, 1H, *H14*), 2.03 (s, 3H, *H10*), 1.07 – 1.00 (m, 2H, *H25*), 0.04 ppm (s, 9H, *H27*, *H28*, *H29*). **^{13}C NMR** (151 MHz, 300 K, CD_3CN): δ = 172.2, 165.6, 163.5, 136.5, 131.3, 130.2, 129.5, 127.8, 123.7, 64.5, 60.2, 58.1, 43.1, 30.3, 19.8, 17.8, -1.6 ppm. **HRMS** (ESI): *m/z* calculated for $C_{21}H_{27}N_2O_4SSi$ $(M-H)^-$ = 431.1466, found 431.1445. **IR** (film): ṽ = 3659, 3602, 3280, 2955, 1770, 1722, 1658, 1542, 1498, 1454, 1388, 1365, 1310, 1250, 1185, 1160, 1065 cm^{-1}. $[\alpha]_D^{25}$ = + 66.7 (c = 0.2, $CHCl_3$).

2-(Trimethylsilyl)ethyl (*5S,6R,7R*)-3-methyl-8-oxo-7-(2-phenylacetamido)-5-thia-1-azabicyclo[4.2.0]oct-2-ene-2-carboxylate 5-oxide (69).

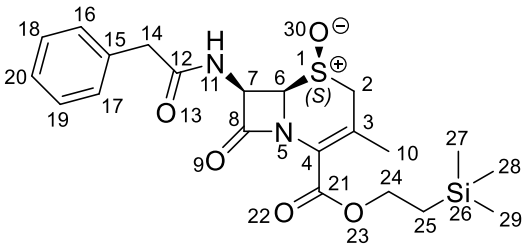

Following General Procedure B, sulfoxide **69** (1.4 g, 3.2 mmol, 83%) was obtained from ester **68** (1.6 g, 3.8 mmol), following column chromatography (25 g Sfär cartridge; 80 mL/min; initially 100% (v/v) cyclohexane (3 CV), followed by a linear gradient (15 CV): 0-100% (v/v) ethyl acetate in cyclohexane).

White solid. **MP**: 180 – 183 °C. **^{1}H NMR** (600 MHz, 300 K, $CDCl_3$): δ = 7.37 – 7.31 (m, 2H, *H18*, *H19*), 7.31 – 7.26 (m, 3H, *H16*, *H17*, *H20*), 6.75 (d, *J* = 9.9 Hz, 1H, *H11*), 6.01 (dd, *J* = 9.9, 4.6 Hz, 1H, *H7*), 4.44 (dd, *J* = 4.7, 1.6 Hz, 1H, *H6*), 4.42 – 4.28 (m, 2H, *H24*), 3.66 – 3.58 (m, 2H, *H14*), 3.55 (d, *J* = 18.7 Hz, 1H, *H2*), 3.20 (d, J = 18.7 Hz, 1H, *H2*), 2.13 (s, 3H, *H10*), 1.14 – 1.03 (m, 2H, *H25*), 0.07 ppm (s, 9H, *H27*, *H28*, *H29*). **^{13}C NMR** (151 MHz, 300 K, $CDCl_3$): δ = 171.4, 163.9, 161.3, 133.9, 129.5, 129.1, 127.7, 123.3, 123.1, 66.9, 64.6, 59.1, 49.4, 43.6, 20.3, 17.5, -1.4 ppm. HRMS (ESI): *m/z* calculated for $C_{21}H_{27}N_2O_5SSi$ $(M-H)^-$ = 447.1415, found 447.1420. **IR** (film): ṽ = 3283, 3032, 2955, 1772, 1721, 1654, 1532, 1499, 1455, 1392, 1364, 1305, 1251, 1239, 1188, 1162, 1050, 1037 cm^{-1}. $[\alpha]_D^{25}$ = + 118.6 (c = 0.67, $CHCl_3$).

2-(Trimethylsilyl)ethyl (*5S,6R,7R*)-5-((*tert*-butoxycarbonyl)imino)-3-methyl-8-oxo-7-(2-phenylacetamido)-5λ^6-thia-1-azabicyclo[4.2.0]oct-2-ene-2-carboxylate 5-oxide (70).

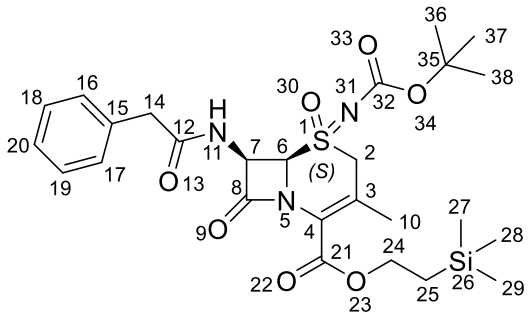

Following General Procedure C, sulfoximine **70** (102 mg, 0.18 mmol, 33%) was obtained from sulfoxide **69** (250 mg, 1.0 equiv., 0.56 mmol) and *tert*-butyl carbamate (98 mg, 1.5 equiv., 0.84 mmol) in dichloromethane (2.8 mL), following column chromatography (10 g Sfär cartridge; 40 mL/min; initially 100% (v/v) cyclohexane (3 CV), followed by a linear gradient (15 CV): 0-40% (v/v) ethyl acetate in cyclohexane).

White solid. **MP**: 163 – 164 °C. **^{1}H NMR** (600 MHz, 300 K, $CDCl_3$): δ = 7.36 – 7.26 (m, 5H, *H16*, *H17*, *H18*, *H19*, *H20*), 6.63 (d, *J* = 10.5 Hz, 1H, *H11*), 6.18 (dd, *J* = 10.4, 4.6 Hz, 1H, *H7*), 4.95 (d, *J* = 1.1 Hz, 1H, *H6*), 4.40 – 4.27 (m, 2H, *H24*), 4.25 (d, *J* = 18.7 Hz, 1H, *H2*), 4.03 (d, *J* = 18.7 Hz, 1H, *H2*), 3.73 – 3.59 (m, 2H, *H14*), 2.13 (s, 3H, *H10*), 1.52 (s, 9H, *H36*, *H37*, *H38*), 1.09 – 1.03 (m, 2H, *H25*), 0.04 ppm (s, 9H, *H27*, *H28*, *H29*). **^{13}C NMR** (151 MHz, 300 K, $CDCl_3$): δ = 171.0, 163.4, 160.9, 157.5, 133.5, 129.9, 129.1, 128.1, 127.7, 122.6, 82.1, 68.5, 65.0, 59.9, 55.9, 43.4, 28.3, 19.6, 17.5, -1.4 ppm. **HRMS** (ESI): *m/z* calculated for $C_{26}H_{36}N_3O_7SSi$ $(M-H)^-$ = 562.2049, found 562.2058. **IR** (film): ṽ = 3406, 3000, 2956, 1768, 1729, 1703, 1675, 1519, 1440, 1394, 1370, 1345, 1320, 1278, 1252, 1227, 1184, 1156, 1112, 1068 cm^{-1}. $[\alpha]_D^{25}$ = – 106.0 (c = 0.67, $CHCl_3$).

Allyl (*7R*)-3-methyl-8-oxo-7-(2-phenylacetamido)-5-thia-1-azabicyclo[4.2.0]oct-2-ene-2-carboxylate (71).

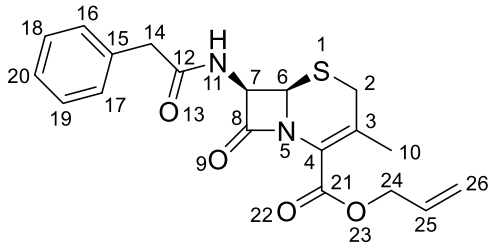

Following General Procedure A, ester **71** (1.1 g, 1.5 mmol, 49%) was obtained from acid **61** (1.0 g, 1.0 equiv., 3.0 mmol) and 3-bromoprop-1-ene (550 mg, 1.5 equiv., 4.5 mmol), following column chromatography (25 g Sfär cartridge; 80 mL/min; initially 100% (v/v) cyclohexane (3 CV), followed by a linear gradient (15 CV): 0-40% (v/v) ethyl acetate in cyclohexane). Reported structure did not have reported characterization data.[189]

Amorphous solid. **^{1}H NMR** (600 MHz, 300 K, $CDCl_3$): δ = 7.39 – 7.26 (m, 5H, *H16*, *H17*, *H18*, *H19*, *H20*), 6.07 (d, *J* = 9.0 Hz, 1H, *H11*), 5.94 (ddt, *J* = 17.1, 10.4, 5.9 Hz, 1H, *H25*), 5.77 (dd, *J* = 9.0, 4.7 Hz, 1H, *H7*), 5.36 (dd, *J* = 17.2, 1.5 Hz, 1H, *H26*), 5.26 (dd, *J* = 10.4, 1.2 Hz, 1H, *H26*), 4.94 (d, *J* = 4.7 Hz, 1H, *H6*), 4.72 (qdt, *J* = 13.1, 6.0, 1.3 Hz, 2H, *H24*), 3.70 – 3.59 (m, 2H, *H14*), 3.50 – 3.43 (m, 1H, *H2*), 3.18 – 3.11 (m, 1H, *H2*), 2.11 ppm (s, 3H, *H10*). **^{13}C NMR** (151 MHz, 300 K, $CDCl_3$): δ = 171.3, 164.5, 161.9, 133.9, 131.7, 131.5, 129.6, 129.3, 127.9, 122.7, 119.2, 66.4, 59.2, 57.3, 43.6, 30.2, 20.2 ppm. **HRMS** (ESI): *m/z* calculated for $C_{19}H_{19}N_2O_4S$ $(M-H)^-$ = 371.1071, found 371.1078. **IR** (film): $\tilde{\nu}$ = 3339, 3029, 2946, 1780, 1729, 1704, 1674, 1519, 1498, 1454, 1383, 1321, 1278, 1251, 1228, 1193, 1157, 1069 cm^{-1}. $[\alpha]_D^{25}$ = + 118.6 (c = 0.17, $CHCl_3$).

Allyl (*5S,6R,7R*)-3-methyl-8-oxo-7-(2-phenylacetamido)-5-thia-1-azabicyclo[4.2.0]oct-2-ene-2-carboxylate 5-oxide (72).

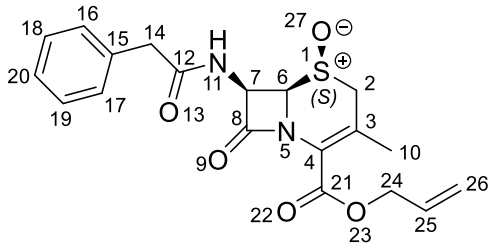

Following General Procedure B, sulfoxide **72** (273 mg, 0.70 mmol, 49%) was obtained from ester **71** (540 mg, 1.5 mmol), following column chromatography (25 g Sfär cartridge;

80 mL/min; initially 100% (v/v) cyclohexane (3 CV), followed by a linear gradient (15 CV): 0-100% (v/v) ethyl acetate in cyclohexane).

Amorphous solid. **^{1}H NMR** (600 MHz, 300 K, $CDCl_3$): δ = 7.38 – 7.27 (m, 5H, *H16*, *H17*, *H18*, *H19*, *H20*), 6.70 (d, *J* = 10.0 Hz, 1H, *H11*), 6.04 (dd, *J* = 10.0, 4.6 Hz, 1H, *H7*), 5.96 (ddt, *J* = 17.1, 10.3, 5.9 Hz, 1H, *H25*), 5.38 (dq, *J* = 17.2, 1.5 Hz, 1H, *H24*), 5.28 (dq, *J* = 10.4, 1.2 Hz, 1H, *H24*), 4.82 – 4.71 (m, 2H, *H26*), 4.45 (dd, *J* = 4.7, 1.6 Hz, 1H, *H6*), 3.68 – 3.56 (m, 3H, *H2*, *H14*), 3.24 – 3.17 (m, 1H, *H2*), 2.15 ppm (s, 3H, *H10*). **^{13}C NMR** (151 MHz, 300 K, $CDCl_3$): δ = 171.3, 163.9, 160.8, 133.8, 131.5, 129.5, 129.2, 127.7, 123.9, 123.0, 119.5, 66.9, 66.8, 59.2, 49.5, 43.6, 20.4 ppm. **HRMS** (ESI): *m/z* calculated for $C_{19}H_{19}N_2O_5S$ $(M-H)^-$ = 387.1020, found 387.1016. **IR** (film): $\tilde{\nu}$ = 3694, 3284, 3020, 2928, 2856, 1770, 1729, 1704, 1676, 1656, 1519, 1499, 1466, 1380, 1320, 1280, 1251, 1190, 1158, 1068 cm^{-1}. $[\alpha]_D^{25}$ = + 31.8 (c = 0.47, $CHCl_3$).

(9H-Fluoren-9-yl)methyl (*6R,7R*)-3-methyl-8-oxo-7-(2-phenylacetamido)-5-thia-1-azabicyclo[4.2.0]oct-2-ene-2-carboxylate (74).

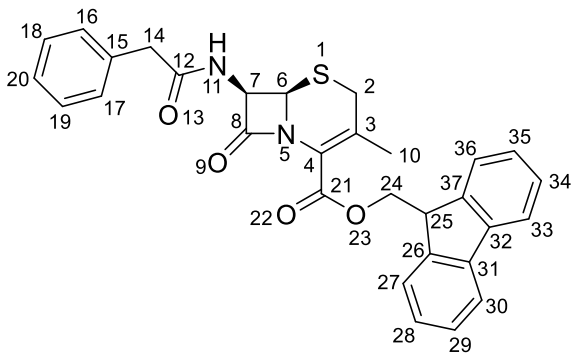

To a solution of acid **61** (1.5 g, 1.0 equiv., 4.5 mmol) in anhydrous dichloromethane (22 mL) was added 4-dimethylaminopyridine (55 mg, 0.1 equiv., 0.45 mmol) and EDC (1.3 g, 1.5 equiv., 6.8 mmol) at 0 °C. The reaction was stirred for 5 min and (9H-fluoren-9-yl)methanol (1.1 g, 1.2 equiv., 5.4 mmol) was added. The reaction mixture was allowed to slowly warm up to ambient temperature before being evaporated *in vacuo* and partitioned between ethyl acetate and water. The organic phase was sequentially washed with water and brine, dried over anhydrous Na2SO4, and evaporated *in vacuo*. The crude material was purified using silica column chromatography (25 g Sfär

cartridge; 80 mL/min; initially 100% (v/v) cyclohexane (3 CV), followed by a linear gradient (15 CV): 0-60% (v/v) ethyl acetate in cyclohexane) ester **74** (1.88 g, 3.7 mmol, 82%).

White solid. **MP**: 200 – 204 °C. **^{1}H NMR** (600 MHz, 300 K, $CDCl_3$): δ = 7.75 (d, *J* = 7.6 Hz, 2H, *H30*, *H33*), 7.59 – 7.54 (m, 2H, *H27*, *H36*), 7.39 (m, 2H, *H29*, *H34*), 7.37 – 7.32 (m, 2H, *H28*, *H35*), 7.32 – 7.25 (m, 5H, *H16*, *H17*, *H18*, *H19*, *H20*), 6.14 (d, *J* = 8.9 Hz, 1H, *H11*), 5.77 (dd, *J* = 8.9, 4.6 Hz, 1H, *H7*), 4.95 (d, *J* = 4.6 Hz, 1H, *H6*), 4.68 (dd, *J* = 10.9, 6.0 Hz, 1H, *H24*), 4.53 (dd, *J* = 10.9, 6.9 Hz, 1H, *H24*), 4.26 (t, *J* = 6.5 Hz, 1H, *H25*), 3.67 (d, *J* = 16.1 Hz, 1H, *H14*), 3.61 (d, *J* = 16.0 Hz, 1H, *H14*), 3.43 – 3.37 (m, 1H, *H2*), 3.15 – 3.02 (m, 1H, *H2*), 1.90 ppm (s, 3H, *H10*). **^{13}C NMR** (151 MHz, 300 K, $CDCl_3$): δ = 171.3, 164.7, 162.2, 144.0, 143.5, 141.5, 141.4, 133.9, 132.6, 129.6, 129.3, 128.0, 127.9, 127.8, 127.3, 127.2, 125.2, 125.1, 122.7, 120.1, 120.1, 67.4, 59.2, 57.5, 46.9, 43.5, 30.3, 20.0 ppm. **HRMS** (ESI): *m/z* calculated for $C_{30}H_{25}N_2O_4S$ $(M\text{-}H)^-$ = 509.1540, found 509.1521. **IR** (film): $\tilde{\nu}$ = 3694, 3339, 3029, 2929, 1778, 1676, 1536, 1497, 1478, 1452, 1390, 1320, 1225, 1195, 1159 cm^{-1}. $[\alpha]_D^{25}$ = + 211.8 (c = 0.67, $CHCl_3$).

(9H-Fluoren-9-yl)methyl (*5S,6R,7R*)-3-methyl-8-oxo-7-(2-phenylacetamido)-5-thia-1-azabicyclo[4.2.0]oct-2-ene-2-carboxylate 5-oxide (75).

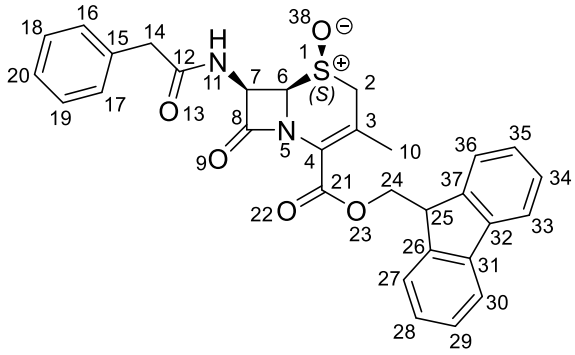

Following General Procedure B, sulfoxide **75** (600 mg, 1.1 mmol, 31%) was obtained from ester **74** (1.88 g, 3.7 mmol), following column chromatography (25 g Sfär cartridge; 80 mL/min; initially 100% (v/v) dichloromethane (3 CV), followed by a linear gradient (15 CV): 0-4% (v/v) acetone in dichloromethane).

Amorphous solid. **^{1}H NMR** (600 MHz, 300 K, DMSO-d_6): δ = 8.33 (d, *J* = 8.4 Hz, 1H, *H11*), 7.89 (d, *J* = 7.6 Hz, 2H, *H30*, *H33*), 7.75 – 7.63 (m, 2H, *H27*, *H36*), 7.41 (tdt, *J* = 7.5, 2.0, 0.9 Hz, 2H, *H29*, *H34*), 7.33 (tt, *J* = 7.4, 1.4 Hz, 2H, *H28*, *H35*), 7.31 – 7.20 (m, 5H, *H16*, *H17*, *H18*, *H19*, *H20*), 5.76 (dd, J = 8.4, 4.6 Hz, 1H, *H7*), 4.84 (dd, J = 4.6, 1.5 Hz, 1H, *H6*), 4.73 (dd, J = 10.9, 5.9 Hz, 1H, *H24*), 4.65 (dd, J = 10.9, 5.9 Hz, 1H, *H24*), 4.33 (t, J = 5.9 Hz, 1H, *H25*), 3.74 – 3.65 (m, 2H, *H2*, *H14*), 3.59 – 3.50 (m, 2H, *H2*, *H14*), 1.66 ppm (s, 3H, *H10*). **^{13}C NMR** (151 MHz, 300 K, DMSO-*d*6): δ = 171.5, 164.5, 161.7, 144.1, 143.9, 141.3, 141.2, 136.3, 129.6, 128.7, 128.2, 128.1, 127.7, 127.6, 127.0, 125.6, 125.5, 125.4, 121.8, 120.6, 120.5, 67.0, 66.7, 58.4, 49.0, 46.8, 42.0, 19.8 ppm. **HRMS** (ESI): *m/z* calculated for $C_{30}H_{25}N_2O_5S$ $(M-H)^-$ = 525.1494, found 525.1490. **IR** (film): ṽ = 3322, 3028, 2931, 1777, 1745, 1678, 1535, 1497, 1479, 1452, 1391, 1331, 1277, 1221, 1198 cm^{-1}. $[\alpha]_D^{25}$ = + 224.4 (c = 0.57, $CHCl_3$).

4-Methoxybenzyl (*2S*,*3S*,*5R*)-3-((1H-1,2,3-triazol-1-yl)methyl)-3-methyl-7-oxo-4-thia-1-azabicyclo[3.2.0]heptane-2-carboxylate (78).

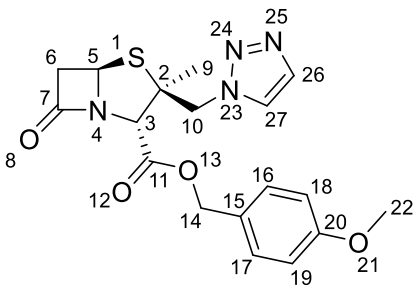

To a solution of **19** (500 mg, 1.48 mmol) in anhydrous acetonitrile (7.4 mL) was added 2-(trimethylsilyl)-2H-1,2,3-triazole (522 mg, 3.7 mmol). The reaction mixture was stirred at 115 °C for 5 h in a sealed tube. The crude material was used in the subsequent step without further purification due to product instability.

4-Methoxybenzyl (*2S*,*3S*,*5R*)-3-((1H-1,2,3-triazol-1-yl)methyl)-3-methyl-7-oxo-4-thia-1-azabicyclo[3.2.0]heptane-2-carboxylate 4-oxide (79).

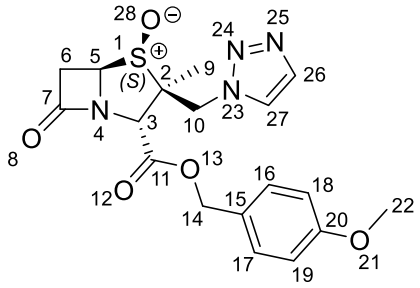

Following General Procedure B, sulfoxide **79** (120 mg, 0.30 mmol, 75%) was obtained from sulfide **78** (150 mg, 0.40 mmol), following column chromatography (25 g Sfär cartridge; 80 mL/min; initially 100% (v/v) cyclohexane with 0.1% (v/v) triethylamine (3 CV), followed by a linear gradient (15 CV): 0–100% (v/v) ethyl acetate with 0.1% (v/v) triethylamine in cyclohexane with 0.1% (v/v) triethylamine).

^{1}H NMR (500 MHz, 300 K, $CDCl_3$): δ = 7.75 (s, 1H, *H26*), 7.70 (s, 1H, *H27*), 7.40 – 7.35 (m, 2H, *H16*, *H17*), 6.97 – 6.91 (m, 2H, *H18*, *H19*), 5.27 (d, *J* = 11.7 Hz, 1H, *H14*), 5.19 (d, *J* = 11.6 Hz, 1H, *H14*), 5.06 (d, *J* = 14.8 Hz, 1H, *H10*), 4.97 (d, *J* = 14.7 Hz, 1H, *H10*), 4.94 – 4.90 (m, 1H, *H5*), 4.62 (s, 1H, *H3*), 3.82 (s, 3H, *H22*), 3.44 (dd, *J* = 16.0, 4.2 Hz, 1H, *H6*), 3.38 (dd, *J* = 15.8, 1.8 Hz, 1H, *H6*), 0.96 ppm (s, 3H, *H9*).

^{13}C NMR (126 MHz, 300K, $CDCl_3$): δ = 170.1, 167.3, 160.4, 134.5, 131.1, 126.5, 125.1, 114.5, 78.5, 71.5, 68.6, 63.6, 55.5, 49.9, 36.7, 13.9 ppm. **HRMS** (ESI): *m/z* calculated for $C_{18}H_{19}N_4O_5S$ $(M-H)^-$ = 403.1082, found 403.1098.

Appendix

Appendix 7.1 Selected crystallographic data for penam (*S*)- and (*R*)-sulfoximines 32 and 48

Compound	**32**	**48**
Empirical Formula	C16 H20 N2 O5 S	C16 H20 N2 O5 S
Formula weight	352.41	352.41
Crystal system	Orthorhombic	Monoclinic
Space group	P 2_1 2_1 2_1	P 1 2_1 1
Unit cell dimensions	a = 7.15180(10) Å α = 90° b = 7.86090(10) Å β = 90° c = 29.7867(3) Å γ = 90°	a = 11.63590(10) Å α = 90° b = 6.08650(10) Å β = 108.6110(10)° c = 12.50120(10) Å γ = 90°
Volume	1674.60(4) $Å^3$	839.061(18) Å3
Z	4	2
Density (calculated)	1.398 Mg/m^3	1.395 Mg/m^3
F(000)	744	372
Reflections collected	35223	32026
Independent reflections	3489 [R(int) = 0.042]	3339 [R(int) = 0.034]
Data / restraints / parameters	3489 / 0 / 218	3339 / 4 / 222
Goodness-of-fit on F^2	0.9946	1.0034
Final R indices [I>2σ(I)]	R1 = 0.0230, wR2 = 0.0596	R1 = 0.0275, wR2 = 0.0763
R indices (all data)	R1 = 0.0242, wR2 = 0.0603	R1 = 0.0277, wR2 = 0.0767
Absolute structure parameter (Flack parameter)[126]	–0.003(5)	–0.006(5)

Appendix 7.2 Selected crystallographic data for (*S*)-cephem sulfoxide 54

Compound	**54**
Empirical Formula	C 16 H17 N O5 S
Formula weight	335.38
Crystal system	Monoclinic
Space group	P 2_1
Unit cell dimensions	a = 11.1894(2) Å α = 90° b = 5.83630(10) Å β = 105.1994(17)°. c = 12.3264(2) Å γ = 90°
Volume	776.81(2) $Å^3$
Z	2
Density (calculated)	1.434 Mg/m^3
F(000)	352
Reflections collected	12191
Independent reflections	3150 [R(int) = 0.025]
Data / restraints / parameters	3150 / 1 / 210
Goodness-of-fit on F^2	1.0027
Final R indices [I>2σ(I)]	R1 = 0.0311, wR2 = 0.0869
R indices (all data)	R1 = 0.0320, wR2 = 0.0875
Absolute structure parameter (Flack parameter)[126]	0.000(6)

Appendix 7.3 Mass spectrometric investigations on the covalent reaction of sulbactam sulfoximine derivatives with AmpC. Sulbactam or a sulbactam sulfoximine derivative (10 µM) was added to isolated recombinant AmpC (1 µM) in buffer (50 mM Tris, pH 7.5). After the indicated time, 50 µL of the solution was injected onto a C4 Solid-Phase Extraction cartridge, washed, and eluted into an iFunnel Agilent 6550 accurate mass quadrupole time-of-flight (Q-TOF) mass spectrometer operated in the positive ionization mode, as reported.[39] Data were analyzed using MassHunter Qualitative Analysis software (Agilent Technologies) using the maximum entropy deconvolution algorithm. See the Methods Section for assay details.

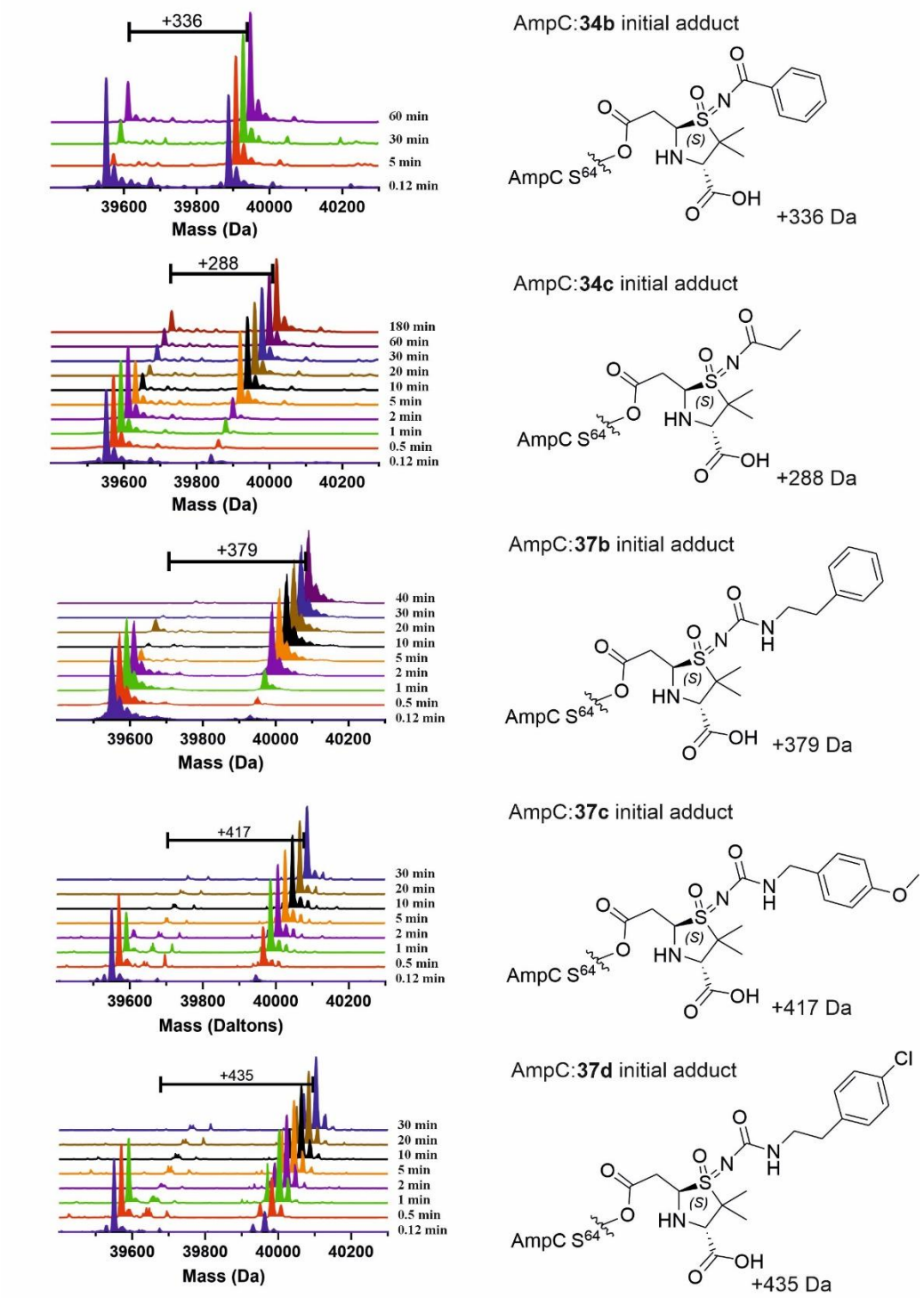

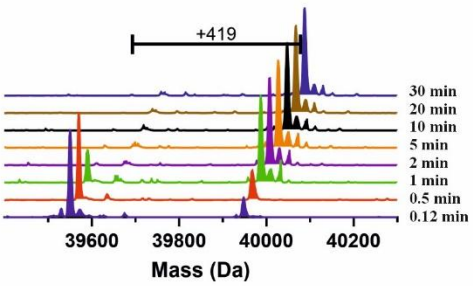

AmpC:**37e** initial adduct

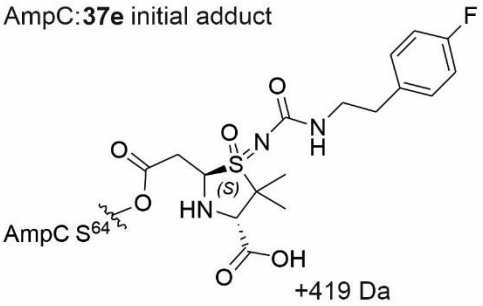

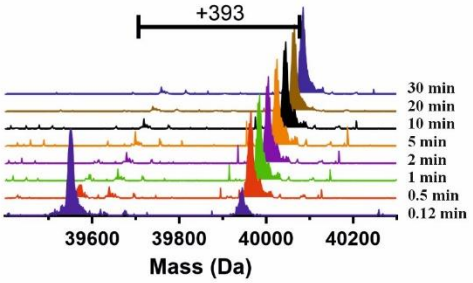

AmpC:**37f** initial adduct

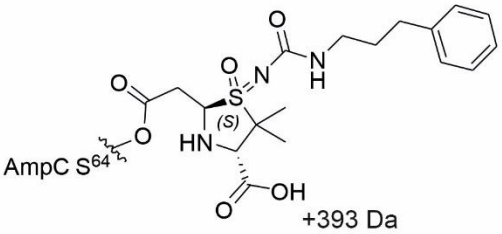

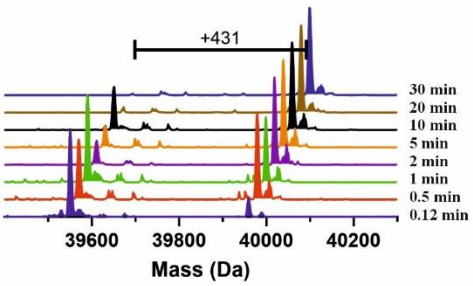

AmpC:**37h** initial adduct

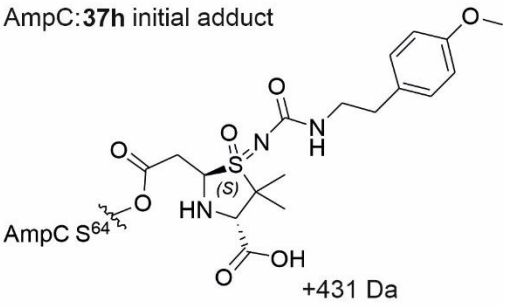

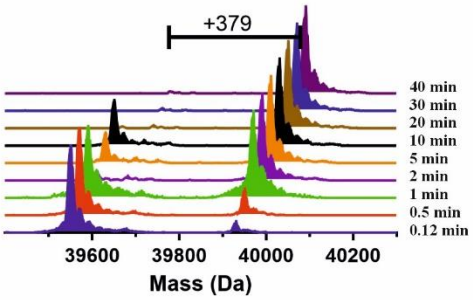

AmpC:**37i** initial adduct

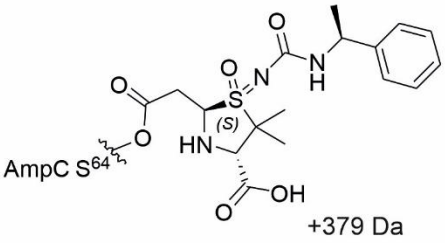

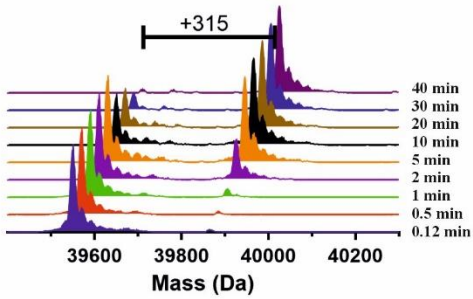

AmpC:**37j** initial adduct

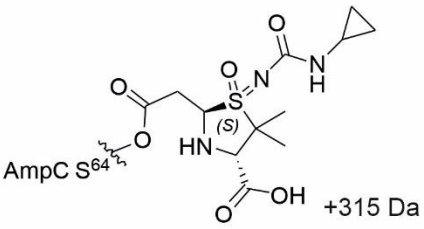

Appendix 7.4 Mass spectrometric investigations on the covalent reaction of sulbactam sulfoximine derivatives with OXA-10. Sulbactam or a sulbactam sulfoximine derivative (10 µM) was added to isolated recombinant OXA-10 (1 µM) in buffer (50 mM Tris, pH 7.5). After the indicated time, 50 µL of the solution was injected onto a C4 Solid-Phase Extraction cartridge, washed, and eluted into an iFunnel Agilent 6550 accurate mass quadrupole time-of-flight (Q-TOF) mass spectrometer operated in the positive ionization mode, as reported.[39] Data were analyzed using MassHunter Qualitative Analysis software (Agilent Technologies) using the maximum entropy deconvolution algorithm.

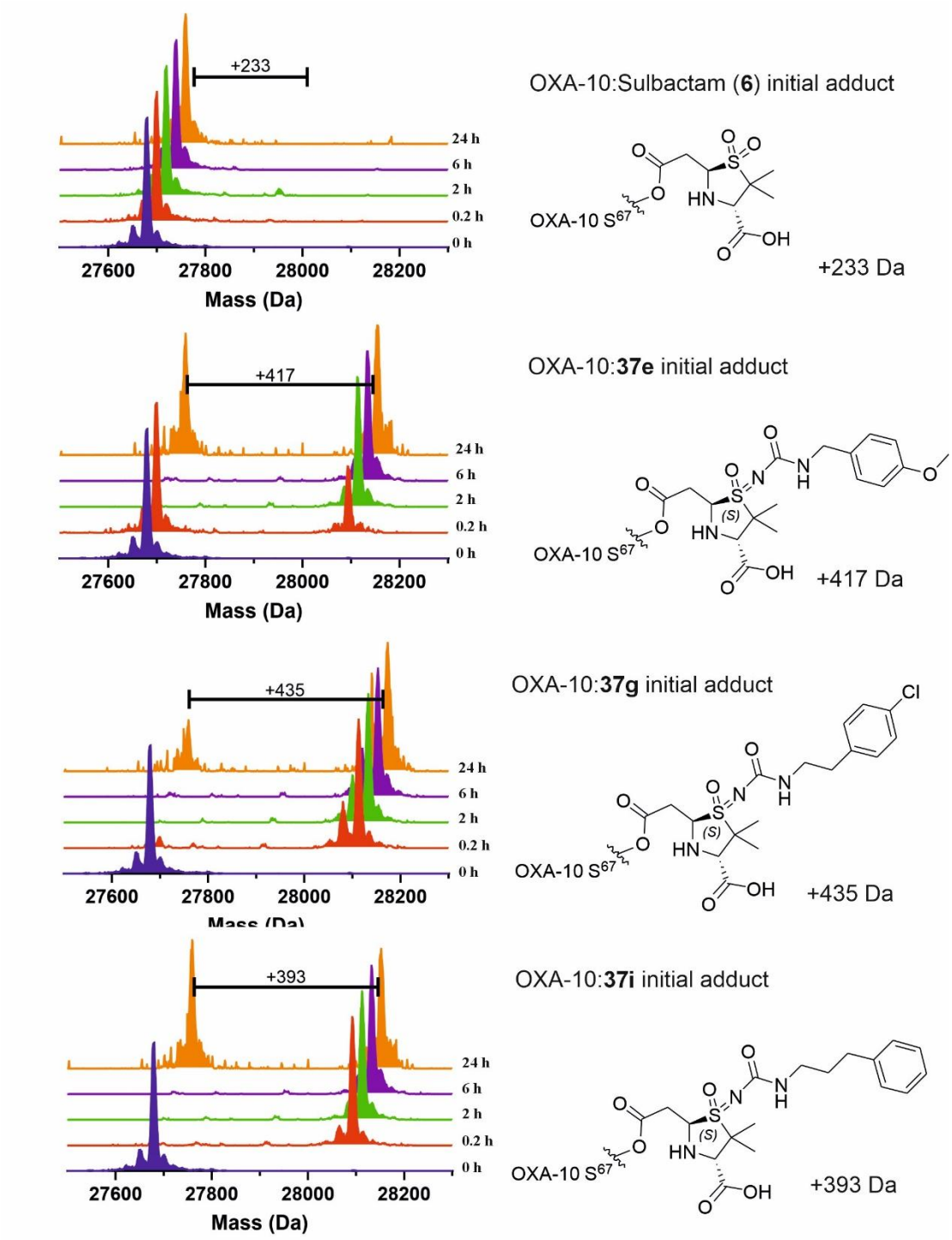

Appendix 7.5 Crystallization conditions, data collection, and refinement statistics for the AmpC$_{EC}$: 37a complex crystal structure.

	AmpC$_{EC}$: 37a
PDB ID	9I5D
Crystallization	
Precipitation conditions[a]	AmpC$_{EC}$ (25 mg/mL in: 50 nM Tris, pH 7.5), 1.6 M K_3PO_4, pH 8.8, 10 mM **37a**, 20%$_{w/v}$ glycerol
Data collection	
Space group	C 1 2 1
Cell dimensions:	
a, *b*, *c* (Å)	118.11, 77.31, 97.67
α, β, γ (°)	90.00, 116.79, 90.00
X-Ray source[b]	Breamline i03
Resolution (Å)[c]	45.32 – 1.43 (1.45 – 1.43)
R_{merge}	0.08594 (1.373)
R_{meas}	0.09267 (1.497)
R_{pim}	0.0344 (0.5838)
I / σI	10.69 (0.92)
CC (1/2)	0.999 (0.437)
CC*	1 (0.78)
Total number of reflections	1036854 (28893)
Total number unique reflections	144090 (4636)
Completeness (%)	99.69 (96.22)
Multiplicity	7.2 (6.2)
Wilson B-factor	17.58
Refinement	
R_{work} / R_{free}	0.1595 / 0.1746
No. atoms:	6411
B-factors:	23.85
R.m.s. deviations:	
Bond lengths (Å)	0.018
Bond angles (°)	1.12

[**a**] Experimental details are described in the Experimental Section. [**b**] DLS: Diamond Light Source. [**c**] Values in parentheses are for the highest-resolution shell.

References

(1) Fleming, A. On the Antibacterial Action of Cultures of a Penicillium, with Special Reference to their Use in the Isolation of B. influenzæ. *The British Journal of Experimental Pathology* **1929**, *10* (3), 226–236.
(2) Chain, E.; Florey, H. W.; Gardner, A. D.; Heatley, N. G.; Jennings, M. A.; Orr-Ewing, J.; Sanders, A. G. PENICILLIN AS A CHEMOTHERAPEUTIC AGENT. *The Lancet* **1940**, *236* (6104), 226–228. DOI: 10.1016/S0140-6736(01)08728-1.
(3) Abraham, E. P.; Chain, E.; Fletcher, C. M.; Gardner, A. D.; Heatley, N. G.; Jennings, M. A.; Florey, H. W. FURTHER OBSERVATIONS ON PENICILLIN. *The Lancet* **1941**, *238* (6155), 177–189. DOI: 10.1016/S0140-6736(00)72122-2.
(4) Bush, K.; Bradford, P. A. β-Lactams and β-Lactamase Inhibitors: An Overview. *Cold Spring Harb. Perspect. Med.* **2016**, *6* (8). DOI: 10.1101/cshperspect.a025247.
(5) Tipper, D. J.; Strominger, J. L. Mechanism of action of penicillins: a proposal based on their structural similarity to acyl-D-alanyl-D-alanine. *Proc. Natl. Acad. Sci. U. S. A.* **1965**, *54* (4), 1133–1141. DOI: 10.1073/pnas.54.4.1133.
(6) Goffin, C.; Ghuysen, J. M. Multimodular penicillin-binding proteins: an enigmatic family of orthologs and paralogs. *Microbiol Mol Biol Rev* **1998**, *62* (4), 1079–1093. DOI: 10.1128/mmbr.62.4.1079-1093.1998.
(7) Zapun, A.; Contreras-Martel, C.; Vernet, T. Penicillin-binding proteins and beta-lactam resistance. *FEMS Microbiol Rev* **2008**, *32* (2), 361–385. DOI: 10.1111/j.1574-6976.2007.00095.x.
(8) Abraham, E. P.; Chain, E. An Enzyme from Bacteria able to Destroy Penicillin. *Nature* **1940**, *146* (3713), 837–837. DOI: 10.1038/146837a0.
(9) Bush, K. Past and Present Perspectives on β-Lactamases. *Antimicrob Agents Chemother* **2018**, *62* (10). DOI: 10.1128/aac.01076-18.
(10) Drawz, S. M.; Bonomo, R. A. Three decades of beta-lactamase inhibitors. *Clin. Microbiol. Rev.* **2010**, *23* (1), 160–201. DOI: 10.1128/cmr.00037-09.
(11) Ambler, R. P. The structure of beta-lactamases. *Philos. Trans. R. Soc. Lond. B Biol. Sci.* **1980**, *289* (1036), 321–331. DOI: 10.1098/rstb.1980.0049.
(12) Hall, B. G.; Barlow, M. Revised Ambler classification of {beta}-lactamases. *J. Antimicrob. Chemother.* **2005**, *55* (6), 1050–1051. DOI: 10.1093/jac/dki130.
(13) Mora-Ochomogo, M.; Lohans, C. T. β-Lactam antibiotic targets and resistance mechanisms: from covalent inhibitors to substrates. *RSC Med Chem* **2021**, *12* (10), 1623–1639. DOI: 10.1039/d1md00200g.
(14) Farley, A.; Ermolovich, Y.; Calvopina, K.; Rabe, P.; Panduwawala, T.; Brem, J.; Björkling, F.; Schofield, C. Structural Basis of Metallo-β-lactamase Inhibition by N -Sulfamoylpyrrole-2-carboxylates. *ACS Infectious Diseases* **2021**, *XXXX*. DOI: 10.1021/acsinfecdis.1c00104.
(15) Paterson, D. L.; Bonomo, R. A. Extended-spectrum beta-lactamases: a clinical update. *Clin. Microbiol. Rev.* **2005**, *18* (4), 657–686. DOI: 10.1128/cmr.18.4.657-686.2005.
(16) Nordmann, P.; Cuzon, G.; Naas, T. The real threat of Klebsiella pneumoniae carbapenemase-producing bacteria. *Lancet Infect. Dis.* **2009**, *9* (4), 228–236. DOI: 10.1016/s1473-3099(09)70054-4.
(17) Walsh, T. R.; Toleman, M. A.; Poirel, L.; Nordmann, P. Metallo-beta-lactamases: the quiet before the storm? *Clin. Microbiol. Rev.* **2005**, *18* (2), 306–325. DOI: 10.1128/cmr.18.2.306-325.2005.
(18) Palzkill, T. Metallo-β-lactamase structure and function. *Ann. N. Y. Acad. Sci.* **2013**, *1277*, 91–104. DOI: 10.1111/j.1749-6632.2012.06796.x.
(19) Jacoby George, A. AmpC β-Lactamases. *Clin. Microbiol. Rev.* **2009**, *22* (1), 161–182. DOI: 10.1128/cmr.00036-08.
(20) Lobkovsky, E.; Moews, P. C.; Liu, H.; Zhao, H.; Frere, J. M.; Knox, J. R. Evolution of an enzyme activity: crystallographic structure at 2-A resolution of cephalosporinase from the

ampC gene of Enterobacter cloacae P99 and comparison with a class A penicillinase. *Proc. Natl. Acad. Sci. U. S. A.* **1993**, *90* (23), 11257–11261. DOI: 10.1073/pnas.90.23.11257.
(21) Rodríguez-Martínez, J. M.; Poirel, L.; Nordmann, P. Extended-spectrum cephalosporinases in Pseudomonas aeruginosa. *Antimicrob Agents Chemother* **2009**, *53* (5), 1766–1771. DOI: 10.1128/aac.01410-08.
(22) Philippon, A.; Arlet, G.; Jacoby, G. A. Plasmid-determined AmpC-type beta-lactamases. *Antimicrob Agents Chemother* **2002**, *46* (1), 1–11. DOI: 10.1128/aac.46.1.1-11.2002.
(23) Pérez-Pérez, F. J.; Hanson, N. D. Detection of plasmid-mediated AmpC beta-lactamase genes in clinical isolates by using multiplex PCR. *J. Clin. Microbiol.* **2002**, *40* (6), 2153–2162. DOI: 10.1128/jcm.40.6.2153-2162.2002.
(24) Livermore, D. M.; Mushtaq, S.; Warner, M.; Zhang, J.; Maharjan, S.; Doumith, M.; Woodford, N. Activities of NXL104 combinations with ceftazidime and aztreonam against carbapenemase-Producing Enterobacteriaceae. *Antimicrob Agents Chemother* **2011**, *55* (1), 390–394. DOI: 10.1128/aac.00756-10.
(25) Yoon, E. J.; Jeong, S. H. Class D β-lactamases. *J. Antimicrob. Chemother.* **2021**, *76* (4), 836–864. DOI: 10.1093/jac/dkaa513.
(26) Evans, B. A.; Amyes, S. G. OXA β-lactamases. *Clin. Microbiol. Rev.* **2014**, *27* (2), 241–263. DOI: 10.1128/cmr.00117-13.
(27) Walther-Rasmussen, J.; Høiby, N. OXA-type carbapenemases. *J. Antimicrob. Chemother.* **2006**, *57* (3), 373–383. DOI: 10.1093/jac/dki482.
(28) Poirel, L.; Héritier, C.; Tolün, V.; Nordmann, P. Emergence of oxacillinase-mediated resistance to imipenem in Klebsiella pneumoniae. *Antimicrob Agents Chemother* **2004**, *48* (1), 15–22. DOI: 10.1128/aac.48.1.15-22.2004.
(29) Poirel, L.; Potron, A.; Nordmann, P. OXA-48-like carbapenemases: the phantom menace. *J. Antimicrob. Chemother.* **2012**, *67* (7), 1597–1606. DOI: 10.1093/jac/dks121.
(30) Jean, S. S.; Lee, W. S.; Lam, C.; Hsu, C. W.; Chen, R. J.; Hsueh, P. R. Carbapenemase-producing Gram-negative bacteria: current epidemics, antimicrobial susceptibility and treatment options. *Future Microbiol.* **2015**, *10* (3), 407–425. DOI: 10.2217/fmb.14.135.
(31) Brown, A. G.; Butterworth, D.; Cole, M.; Hanscomb, G.; Hood, J. D.; Reading, C.; Rolinson, G. N. Naturally-occurring beta-lactamase inhibitors with antibacterial activity. *J. Antibiot. (Tokyo)* **1976**, *29* (6), 668–669. DOI: 10.7164/antibiotics.29.668.
(32) Fisher, J. W.; Belasco, J. G.; Charnas, R. L.; Khosla, S.; Knowles, J. R. β-Lactamase inactivation by mechanism-based reagents. *Philosophical Transactions of the Royal Society of London. B, Biological Sciences* **1980**, *289* (1036), 309–319. DOI: 10.1098/rstb.1980.0048.
(33) Lang, P. A.; de Munnik, M.; Oluwole, A. O.; Claridge, T. D. W.; Robinson, C. V.; Brem, J.; Schofield, C. J. How Clavulanic Acid Inhibits Serine β-Lactamases. *ChemBioChem* **2024**, *25* (22), e202400280. DOI: 10.1002/cbic.202400280.
(34) Reading, C.; Cole, M. Clavulanic acid: a beta-lactamase-inhiting beta-lactam from Streptomyces clavuligerus. *Antimicrob Agents Chemother* **1977**, *11* (5), 852–857. DOI: 10.1128/aac.11.5.852.
(35) White, A. R.; Kaye, C.; Poupard, J.; Pypstra, R.; Woodnutt, G.; Wynne, B. Augmentin (amoxicillin/clavulanate) in the treatment of community-acquired respiratory tract infection: a review of the continuing development of an innovative antimicrobial agent. *J. Antimicrob. Chemother.* **2004**, *53 Suppl 1*, i3–20. DOI: 10.1093/jac/dkh050.
(36) Brogden, R. N.; Heel, R. C.; Speight, T. M.; Avery, G. S. Ticarcillin: a review of its pharmacological properties and therapeutic efficacy. *Drugs* **1980**, *20* (5), 325–352. DOI: 10.2165/00003495-198020050-00001.
(37) Richmond, M. H.; Sykes, R. B. The beta-lactamases of gram-negative bacteria and their possible physiological role. *Adv. Microb. Physiol.* **1973**, *9*, 31–88. DOI: 10.1016/s0065-2911(08)60376-8.

(38) English, A. R.; Retsema, J. A.; Girard, A. E.; Lynch, J. E.; Barth, W. E. CP-45,899, a Beta-Lactamase Inhibitor That Extends the Antibacterial Spectrum of Beta-Lactams: Initial Bacteriological Characterization. *Antimicrobial Agents and Chemotherapy* **1978**, *14* (3), 414–419. DOI: doi:10.1128/aac.14.3.414.
(39) Lang, P. A.; Raj, R.; Tumber, A.; Lohans, C. T.; Rabe, P.; Robinson, C. V.; Brem, J.; Schofield, C. J. Studies on enmetazobactam clarify mechanisms of widely used β-lactamase inhibitors. *Proc. Natl. Acad. Sci. USA* **2022**, *119* (18), e2117310119. DOI: 10.1073/pnas.2117310119.
(40) Wexler, H. M.; Harris, B.; Carter, W. T.; Finegold, S. M. In vitro efficacy of sulbactam combined with ampicillin against anaerobic bacteria. *Antimicrob Agents Chemother* **1985**, *27* (5), 876–878. DOI: 10.1128/aac.27.5.876.
(41) Stefani, S.; Russo, G.; Pellegrino, M. B.; Mezzatesta, M. L.; Cocuzza, C.; Nicoletti, G. In-vitro activity of ampicillin/sulbactam and other antibiotics against clinical isolates of Haemophilus sp. and Branhamella catarrhalis. *J. Chemother.* **1990**, *2* (1), 26–30. DOI: 10.1080/1120009x.1990.11738976.
(42) Jones, R. N.; Wilson, H. W.; Thornsberry, C.; Barry, A. L. In vitro antimicrobial activity of cefoperazone-sulbactam combinations against 554 clinical isolates including a review and beta-lactamase studies. *Diagn Microbiol Infect Dis* **1985**, *3* (6), 489–499. DOI: 10.1016/s0732-8893(85)80005-5.
(43) Aronoff, S. C.; Jacobs, M. R.; Johenning, S.; Yamabe, S. Comparative activities of the beta-lactamase inhibitors YTR 830, sodium clavulanate, and sulbactam combined with amoxicillin or ampicillin. *Antimicrobial Agents and Chemotherapy* **1984**, *26* (4), 580–582. DOI: 10.1128/aac.26.4.580.
(44) Desai, N. R.; Shah, S. M.; Cohen, J.; McLaughlin, M.; Dalal, H. R. Zosyn (piperacillin/tazobactam) reformulation: Expanded compatibility and coadministration with lactated Ringer's solutions and selected aminoglycosides. *Ther. Clin. Risk Manag.* **2008**, *4* (2), 303–314. DOI: 10.2147/tcrm.s2564.
(45) Sader, H. S.; Jones, R. N.; Andrade-Baiocchi, S.; Biedenbach, D. J. Four-year evaluation of frequency of occurrence and antimicrobial susceptibility patterns of bacteria from bloodstream infections in Latin American medical centers. *Diagn Microbiol Infect Dis* **2002**, *44* (3), 273–280. DOI: 10.1016/s0732-8893(02)00469-8.
(46) Livermore, D. M.; Mushtaq, S.; Warner, M.; Turner, S. J.; Woodford, N. Potential of high-dose cefepime/tazobactam against multiresistant Gram-negative pathogens. *J. Antimicrob. Chemother.* **2017**, *73* (1), 126–133. DOI: 10.1093/jac/dkx360.
(47) Morrissey, I.; Magnet, S.; Hawser, S.; Shapiro, S.; Knechtle, P. In Vitro Activity of Cefepime-Enmetazobactam against Gram-Negative Isolates Collected from U.S. and European Hospitals during 2014-2015. *Antimicrob Agents Chemother* **2019**, *63* (7). DOI: 10.1128/aac.00514-19.
(48) Bhowmick, T.; Canton, R.; Pea, F.; Quevedo, J.; Santerre Henriksen, A.; Timsit, J. F.; Kaye, K. S. Cefepime-enmetazobactam: first approved cefepime-β- lactamase inhibitor combination for multi-drug resistant Enterobacterales. *Future Microbiol.* **2025**, *20* (4), 277–286. DOI: 10.1080/17460913.2025.2468112.
(49) Kaye, K. S.; Belley, A.; Barth, P.; Lahlou, O.; Knechtle, P.; Motta, P.; Velicitat, P. Effect of Cefepime/Enmetazobactam vs Piperacillin/Tazobactam on Clinical Cure and Microbiological Eradication in Patients With Complicated Urinary Tract Infection or Acute Pyelonephritis: A Randomized Clinical Trial. *JAMA* **2022**, *328* (13), 1304–1314. DOI: 10.1001/jama.2022.17034.
(50) Falagas, M. E.; Romanos, L. T.; Kontogiannis, D. S.; Tsiara, K.; Kakoullis, S. A. Resistance of Gram-Negative Bacteria to Cefepime-Enmetazobactam: A Systematic Review. *Pathogens* **2025**, *14* (8). DOI: 10.3390/pathogens14080777.

(51) Ehmann, D. E.; Jahić, H.; Ross, P. L.; Gu, R.-F.; Hu, J.; Kern, G.; Walkup, G. K.; Fisher, S. L. Avibactam is a covalent, reversible, non–β-lactam β-lactamase inhibitor. *Proceedings of the National Academy of Sciences* **2012**, *109* (29), 11663–11668. DOI: doi:10.1073/pnas.1205073109.
(52) Drawz, S. M.; Papp-Wallace, K. M.; Bonomo, R. A. New β-lactamase inhibitors: a therapeutic renaissance in an MDR world. *Antimicrob Agents Chemother* **2014**, *58* (4), 1835–1846. DOI: 10.1128/aac.00826-13.
(53) Zasowski, E. J.; Rybak, J. M.; Rybak, M. J. The β-Lactams Strike Back: Ceftazidime-Avibactam. *Pharmacotherapy* **2015**, *35* (8), 755–770. DOI: 10.1002/phar.1622.
(54) Castanheira, M.; Sader, H. S.; Farrell, D. J.; Mendes, R. E.; Jones, R. N. Activity of ceftaroline-avibactam tested against Gram-negative organism populations, including strains expressing one or more β-lactamases and methicillin-resistant Staphylococcus aureus carrying various staphylococcal cassette chromosome mec types. *Antimicrob Agents Chemother* **2012**, *56* (9), 4779–4785. DOI: 10.1128/aac.00817-12.
(55) Zhanel, G. G.; Lawson, C. D.; Adam, H.; Schweizer, F.; Zelenitsky, S.; Lagacé-Wiens, P. R.; Denisuik, A.; Rubinstein, E.; Gin, A. S.; Hoban, D. J.; et al. Ceftazidime-avibactam: a novel cephalosporin/β-lactamase inhibitor combination. *Drugs* **2013**, *73* (2), 159–177. DOI: 10.1007/s40265-013-0013-7.
(56) Shirley, M. Ceftazidime-Avibactam: A Review in the Treatment of Serious Gram-Negative Bacterial Infections. *Drugs* **2018**, *78* (6), 675–692. DOI: 10.1007/s40265-018-0902-x.
(57) van Duin, D.; Lok, J. J.; Earley, M.; Cober, E.; Richter, S. S.; Perez, F.; Salata, R. A.; Kalayjian, R. C.; Watkins, R. R.; Doi, Y.; et al. Colistin Versus Ceftazidime-Avibactam in the Treatment of Infections Due to Carbapenem-Resistant Enterobacteriaceae. *Clin. Infect. Dis.* **2018**, *66* (2), 163–171. DOI: 10.1093/cid/cix783.
(58) Mansour, H.; Ouweini, A. E. L.; Chahine, E. B.; Karaoui, L. R. Imipenem/cilastatin/relebactam: A new carbapenem β-lactamase inhibitor combination. *Am. J. Health Syst. Pharm.* **2021**, *78* (8), 674–683. DOI: 10.1093/ajhp/zxab012.
(59) Papp-Wallace, K. M.; Barnes, M. D.; Alsop, J.; Taracila, M. A.; Bethel, C. R.; Becka, S. A.; van Duin, D.; Kreiswirth, B. N.; Kaye, K. S.; Bonomo, R. A. Relebactam Is a Potent Inhibitor of the KPC-2 β-Lactamase and Restores Imipenem Susceptibility in KPC-Producing Enterobacteriaceae. *Antimicrob Agents Chemother* **2018**, *62* (6). DOI: 10.1128/aac.00174-18.
(60) Karlowsky, J. A.; Lob, S. H.; Young, K.; Motyl, M. R.; Sahm, D. F. In Vitro Activity of Imipenem/Relebactam Against Gram-Negative Bacilli from Pediatric Patients-Study for Monitoring Antimicrobial Resistance Trends (SMART) global surveillance program 2015-2017. *J Pediatric Infect Dis Soc* **2021**, *10* (3), 274–281. DOI: 10.1093/jpids/piaa056.
(61) Durand-Réville, T. F.; Guler, S.; Comita-Prevoir, J.; Chen, B.; Bifulco, N.; Huynh, H.; Lahiri, S.; Shapiro, A. B.; McLeod, S. M.; Carter, N. M.; et al. ETX2514 is a broad-spectrum β-lactamase inhibitor for the treatment of drug-resistant Gram-negative bacteria including Acinetobacter baumannii. *Nature Microbiology* **2017**, *2* (9), 17104. DOI: 10.1038/nmicrobiol.2017.104.
(62) McLeod, S. M.; Moussa, S. H.; Hackel, M. A.; Miller, A. A. In Vitro Activity of Sulbactam-Durlobactam against Acinetobacter baumannii-calcoaceticus Complex Isolates Collected Globally in 2016 and 2017. *Antimicrob Agents Chemother* **2020**, *64* (4). DOI: 10.1128/aac.02534-19.
(63) Keam, S. J. Sulbactam/Durlobactam: First Approval. *Drugs* **2023**, *83* (13), 1245–1252. DOI: 10.1007/s40265-023-01920-6.
(64) Hecker, S. J.; Reddy, K. R.; Totrov, M.; Hirst, G. C.; Lomovskaya, O.; Griffith, D. C.; King, P.; Tsivkovski, R.; Sun, D.; Sabet, M.; et al. Discovery of a Cyclic Boronic Acid β-Lactamase

Inhibitor (RPX7009) with Utility vs Class A Serine Carbapenemases. *J. Med. Chem.* **2015**, *58* (9), 3682–3692. DOI: 10.1021/acs.jmedchem.5b00127.
(65) McCarthy, M. W.; Walsh, T. J. Meropenem/vaborbactam fixed combination for the treatment of patients with complicated urinary tract infections. *Drugs Today (Barc)* **2017**, *53* (10), 521–530. DOI: 10.1358/dot.2017.53.10.2721815.
(66) Lomovskaya, O.; Sun, D.; Rubio-Aparicio, D.; Nelson, K.; Tsivkovski, R.; Griffith, D. C.; Dudley, M. N. Vaborbactam: Spectrum of Beta-Lactamase Inhibition and Impact of Resistance Mechanisms on Activity in Enterobacteriaceae. *Antimicrob Agents Chemother* **2017**, *61* (11). DOI: 10.1128/aac.01443-17.
(67) Ackley, R.; Roshdy, D.; Meredith, J.; Minor, S.; Anderson, W. E.; Capraro, G. A.; Polk, C. Meropenem-Vaborbactam versus Ceftazidime-Avibactam for Treatment of Carbapenem-Resistant Enterobacteriaceae Infections. *Antimicrob Agents Chemother* **2020**, *64* (5). DOI: 10.1128/aac.02313-19.
(68) Kaye, K. S.; Bhowmick, T.; Metallidis, S.; Bleasdale, S. C.; Sagan, O. S.; Stus, V.; Vazquez, J.; Zaitsev, V.; Bidair, M.; Chorvat, E.; et al. Effect of Meropenem-Vaborbactam vs Piperacillin-Tazobactam on Clinical Cure or Improvement and Microbial Eradication in Complicated Urinary Tract Infection: The TANGO I Randomized Clinical Trial. *JAMA* **2018**, *319* (8), 788–799. DOI: 10.1001/jama.2018.0438.
(69) Wunderink, R. G.; Giamarellos-Bourboulis, E. J.; Rahav, G.; Mathers, A. J.; Bassetti, M.; Vazquez, J.; Cornely, O. A.; Solomkin, J.; Bhowmick, T.; Bishara, J.; et al. Effect and Safety of Meropenem–Vaborbactam versus Best-Available Therapy in Patients with Carbapenem-Resistant Enterobacteriaceae Infections: The TANGO II Randomized Clinical Trial. *Infectious Diseases and Therapy* **2018**, *7* (4), 439–455. DOI: 10.1007/s40121-018-0214-1.
(70) Penwell, W. F.; Shapiro, A. B.; Giacobbe, R. A.; Gu, R.-F.; Gao, N.; Thresher, J.; McLaughlin, R. E.; Huband, M. D.; DeJonge, B. L. M.; Ehmann, D. E.; et al. Molecular Mechanisms of Sulbactam Antibacterial Activity and Resistance Determinants in Acinetobacter baumannii. *Antimicrobial Agents and Chemotherapy* **2015**, *59* (3), 1680–1689. DOI: doi:10.1128/aac.04808-14.
(71) Poulikakos, P.; Tansarli, G. S.; Falagas, M. E. Combination antibiotic treatment versus monotherapy for multidrug-resistant, extensively drug-resistant, and pandrug-resistant Acinetobacter infections: a systematic review. *Eur. J. Clin. Microbiol. Infect. Dis.* **2014**, *33* (10), 1675–1685. DOI: 10.1007/s10096-014-2124-9.
(72) Manning, J. M.; Moore, S.; Rowe, W. B.; Meister, A. Identification of L-methionine S-sulfoximine as the diastereoisomer of L-methionine SR-sulfoximine that inhibits glutamine synthetase. *Biochemistry* **1969**, *8* (6), 2681–2685. DOI: 10.1021/bi00834a066.
(73) Rowe, W. B.; Ronzio, R. A.; Meister, A. Inhibition of glutamine synthetase by methionine sulfoximine. Studies On Methionine sulfoximine phosphate. *Biochemistry* **1969**, *8* (6), 2674–2680. DOI: 10.1021/bi00834a065.
(74) Lücking, U. Sulfoximines: A Neglected Opportunity in Medicinal Chemistry. *Angew. Chem. Int. Ed.* **2013**, *52* (36), 9399–9408. DOI: 10.1002/anie.201302209.
(75) Sirvent, J. A.; Lücking, U. Novel Pieces for the Emerging Picture of Sulfoximines in Drug Discovery: Synthesis and Evaluation of Sulfoximine Analogues of Marketed Drugs and Advanced Clinical Candidates. *ChemMedChem* **2017**, *12* (7), 487–501. DOI: 10.1002/cmdc.201700044.
(76) Reggelin, M.; Zur, C. Sulfoximines: Structures, Properties and Synthetic Applications. *Synthesis* **2000**, *2000* (01), 1–64. DOI: 10.1055/s-2000-6217.
(77) Mäder, P.; Kattner, L. Sulfoximines as Rising Stars in Modern Drug Discovery? Current Status and Perspective on an Emerging Functional Group in Medicinal Chemistry. *J. Med. Chem.* **2020**, *63* (23), 14243–14275. DOI: 10.1021/acs.jmedchem.0c00960.

(78) Andresini, M.; Tota, A.; Degennaro, L.; Bull, J. A.; Luisi, R. Synthesis and Transformations of NH-Sulfoximines. *Chemistry – A European Journal* **2021**, *27* (69), 17293–17321. DOI: 10.1002/chem.202102619.
(79) Bhalani, D. V.; Nutan, B.; Kumar, A.; Singh Chandel, A. K. Bioavailability Enhancement Techniques for Poorly Aqueous Soluble Drugs and Therapeutics. *Biomedicines* **2022**, *10* (9). DOI: 10.3390/biomedicines10092055.
(80) Altenburg, B.; Frings, M.; Schöbel, J.-H.; Goßen, J.; Pannen, K.; Vanderliek, K.; Rossetti, G.; Koschmieder, S.; Chatain, N.; Bolm, C. Chiral Analogues of PFI-1 as BET Inhibitors and Their Functional Role in Myeloid Malignancies. *ACS Med. Chem. Lett.* **2020**, *11* (10), 1928–1934. DOI: 10.1021/acsmedchemlett.9b00625.
(81) Meanwell, N. A. Synopsis of Some Recent Tactical Application of Bioisosteres in Drug Design. *J. Med. Chem.* **2011**, *54* (8), 2529–2591. DOI: 10.1021/jm1013693.
(82) Lücking, U.; Jautelat, R.; Krüger, M.; Brumby, T.; Lienau, P.; Schäfer, M.; Briem, H.; Schulze, J.; Hillisch, A.; Reichel, A.; et al. The Lab Oddity Prevails: Discovery of Pan-CDK Inhibitor (R)-S-Cyclopropyl-S-(4-{[4-{[(1R,2R)-2-hydroxy-1-methylpropyl]oxy}-5-(trifluoromethyl)pyrimidin-2-yl]amino}phenyl)sulfoximide (BAY 1000394) for the Treatment of Cancer. *ChemMedChem* **2013**, *8* (7), 1067–1085. DOI: 10.1002/cmdc.201300096.
(83) Lücking, U.; Scholz, A.; Lienau, P.; Siemeister, G.; Kosemund, D.; Bohlmann, R.; Briem, H.; Terebesi, I.; Meyer, K.; Prelle, K.; et al. Identification of Atuveciclib (BAY 1143572), the First Highly Selective, Clinical PTEFb/CDK9 Inhibitor for the Treatment of Cancer. *ChemMedChem* **2017**, *12* (21), 1776–1793. DOI: 10.1002/cmdc.201700447.
(84) Lücking, U.; Kosemund, D.; Böhnke, N.; Lienau, P.; Siemeister, G.; Denner, K.; Bohlmann, R.; Briem, H.; Terebesi, I.; Bömer, U.; et al. Changing for the Better: Discovery of the Highly Potent and Selective CDK9 Inhibitor VIP152 Suitable for Once Weekly Intravenous Dosing for the Treatment of Cancer. *J. Med. Chem.* **2021**, *64* (15), 11651–11674. DOI: 10.1021/acs.jmedchem.1c01000.
(85) Foote, K. M.; Nissink, J. W. M.; McGuire, T.; Turner, P.; Guichard, S.; Yates, J. W. T.; Lau, A.; Blades, K.; Heathcote, D.; Odedra, R.; et al. Discovery and Characterization of AZD6738, a Potent Inhibitor of Ataxia Telangiectasia Mutated and Rad3 Related (ATR) Kinase with Application as an Anticancer Agent. *J. Med. Chem.* **2018**, *61* (22), 9889–9907. DOI: 10.1021/acs.jmedchem.8b01187.
(86) Wilson, Z.; Odedra, R.; Wallez, Y.; Wijnhoven, P. W. G.; Hughes, A. M.; Gerrard, J.; Jones, G. N.; Bargh-Dawson, H.; Brown, E.; Young, L. A.; et al. ATR Inhibitor AZD6738 (Ceralasertib) Exerts Antitumor Activity as a Monotherapy and in Combination with Chemotherapy and the PARP Inhibitor Olaparib. *Cancer Res.* **2022**, *82* (6), 1140–1152. DOI: 10.1158/0008-5472.Can-21-2997.
(87) Gege, C.; Bravo, F. J.; Uhlig, N.; Hagmaier, T.; Schmachtenberg, R.; Elis, J.; Burger-Kentischer, A.; Finkelmeier, D.; Hamprecht, K.; Grunwald, T.; et al. A helicase-primase drug candidate with sufficient target tissue exposure affects latent neural herpes simplex virus infections. *Sci. Transl. Med.* **2021**, *13* (598), eabf8668. DOI: doi:10.1126/scitranslmed.abf8668.
(88) Sparks, T. C.; Watson, G. B.; Loso, M. R.; Geng, C.; Babcock, J. M.; Thomas, J. D. Sulfoxaflor and the sulfoximine insecticides: chemistry, mode of action and basis for efficacy on resistant insects. *Pestic Biochem Physiol* **2013**, *107* (1), 1–7. DOI: 10.1016/j.pestbp.2013.05.014.
(89) Zhu, Y.; Loso, M. R.; Watson, G. B.; Sparks, T. C.; Rogers, R. B.; Huang, J. X.; Gerwick, B. C.; Babcock, J. M.; Kelley, D.; Hegde, V. B.; et al. Discovery and characterization of sulfoxaflor, a novel insecticide targeting sap-feeding pests. *J Agric Food Chem* **2011**, *59* (7), 2950–2957. DOI: 10.1021/jf102765x.
(90) Yamagishi, F. G.; Rayner, D. R.; Zwicker, E. T.; Cram, D. J. Stereochemistry of sulfur compounds. V. Stereochemical reaction cycles that involve cyclic sulfoxides, sulfimides, and

sulfoximides. *Journal of the American Chemical Society* **1973**, *95* (6), 1916–1925. DOI: 10.1021/ja00787a036.
(91) Swern, D.; Ikeda, I.; Whitfield, G. F. Tetracovalent sulfur intermediates in iminosulfurane synthesis. Genesis of a potentially general ylid preparation. *Tetrahedron Lett.* **1972**, *13* (26), 2635–2638. DOI: 10.1016/S0040-4039(01)84894-2.
(92) Huang, S.-L.; Swern, D. Oxidation of N-acyl-, N-sulfonyl-, and N-arylsulfilimines to sulfoximines by m-chloroperoxybenzoate anion. *The Journal of Organic Chemistry* **1979**, *44* (14), 2510–2513. DOI: 10.1021/jo01328a039.
(93) Wang, J.; Zhang, J.; Miao, K.; Yun, H.; Shen, H. C.; Zhao, W.; Liang, C. Eaton's reagent-mediated metal-free and efficient synthesis of NH-sulfoximines. *Tetrahedron Lett.* **2017**, *58* (4), 333–337. DOI: 10.1016/j.tetlet.2016.12.031.
(94) Tamura, Y.; Sumoto, K.; Minamikawa, J.; Ikeda, M. A novel method for sulfilimines and sulfoximines. *Tetrahedron Lett.* **1972**, *13* (40), 4137–4140. DOI: 10.1016/S0040-4039(01)94257-1.
(95) Kemp, J. E. G.; Closier, M. D.; Stefaniak, M. H. Penicillin and cephalosporin sulphoximines. *Tetrahedron Lett.* **1979**, *20* (39), 3785–3788. DOI: 10.1016/S0040-4039(01)95524-8.
(96) Siu, T.; Yudin, A. K. Electrochemical Imination of Sulfoxides Using N-Aminophthalimide. *Org. Lett.* **2002**, *4* (11), 1839–1842. DOI: 10.1021/ol0257530.
(97) Miao, J.; Richards, N. G. J.; Ge, H. Rhodium-catalyzed direct synthesis of unprotected NH-sulfoximines from sulfoxides. *Chem. Commun.* **2014**, *50* (68), 9687–9689, 10.1039/C4CC04349A. DOI: 10.1039/C4CC04349A.
(98) Zenzola, M.; Doran, R.; Degennaro, L.; Luisi, R.; Bull, J. A. Transfer of Electrophilic NH Using Convenient Sources of Ammonia: Direct Synthesis of NH Sulfoximines from Sulfoxides. *Angew. Chem. Int. Ed.* **2016**, *55* (25), 7203–7207. DOI: 10.1002/anie.201602320.
(99) Johnson, C. R.; Schroeck, C. W. Chemistry of sulfoxides and related compounds. XLV. Asymmetric syntheses using optically active oxosulfonium alkylides. *Journal of the American Chemical Society* **1973**, *95* (22), 7418–7423. DOI: 10.1021/ja00803a034.
(100) Johnson, C. R.; Kirchhoff, R. A.; Corkins, H. G. Chemistry of sulfoxides and related compounds. XLIX. Synthesis of optically active sulfoximines from optically active sulfoxides. *The Journal of Organic Chemistry* **1974**, *39* (16), 2458–2459. DOI: 10.1021/jo00930a044.
(101) Tamura, Y.; Minamikawa, J.; Sumoto, K.; Fujii, S.; Ikeda, M. Synthesis and some properties of O-acyl-and O-nitrophenylhydroxylamines. *The Journal of Organic Chemistry* **1973**, *38* (6), 1239–1241. DOI: 10.1021/jo00946a045.
(102) Tota, A.; Zenzola, M.; Chawner, S. J.; John-Campbell, S. S.; Carlucci, C.; Romanazzi, G.; Degennaro, L.; Bull, J. A.; Luisi, R. Synthesis of NH-sulfoximines from sulfides by chemoselective one-pot N- and O-transfers. *Chem. Commun.* **2017**, *53* (2), 348–351, 10.1039/C6CC08891K. DOI: 10.1039/C6CC08891K.
(103) Lohier, J.-F.; Glachet, T.; Marzag, H.; Gaumont, A.-C.; Reboul, V. Mechanistic investigation of the NH-sulfoximination of sulfide. Evidence for λ6-sulfanenitrile intermediates. *Chem. Commun.* **2017**, *53* (12), 2064–2067, 10.1039/C6CC09940H. DOI: 10.1039/C6CC09940H.
(104) Zenzola, M.; Doran, R.; Luisi, R.; Bull, J. A. Synthesis of Sulfoximine Carbamates by Rhodium-Catalyzed Nitrene Transfer of Carbamates to Sulfoxides. *J. Org. Chem.* **2015**, *80* (12), 6391–6399. DOI: 10.1021/acs.joc.5b00844.
(105) Yoshimura, A.; Nemykin, V. N.; Zhdankin, V. V. o-Alkoxyphenyliminoiodanes: Highly Efficient Reagents for the Catalytic Aziridination of Alkenes and the Metal-Free Amination of Organic Substrates. *Chem. Eur. J.* **2011**, *17* (38), 10538–10541. DOI: 10.1002/chem.201102265.

(106) Lacôte, E.; Amatore, M.; Fensterbank, L.; Malacria, M. Catalytic Synthesis of Sulfoximines using Copper(II) Salts. *Synlett* **2002**, *2002* (1), 116–118. DOI: 10.1055/s-2002-19338.
(107) Leca, D.; Song, K.; Amatore, M.; Fensterbank, L.; Lacôte, E.; Malacria, M. Iodine(III)-Mediated Preparations of Nitrogen-Containing Sulfur Derivatives: Dramatic Influence of the Sulfur Oxidation State. *Chem. Eur. J.* **2004**, *10* (4), 906–916. DOI: 10.1002/chem.200305525.
(108) Okamura, H.; Bolm, C. Rhodium-Catalyzed Imination of Sulfoxides and Sulfides: Efficient Preparation of N-Unsubstituted Sulfoximines and Sulfilimines. *Org. Lett.* **2004**, *6* (8), 1305–1307. DOI: 10.1021/ol049715n.
(109) Mancheño, O. G.; Bolm, C. Iron-Catalyzed Imination of Sulfoxides and Sulfides. *Org. Lett.* **2006**, *8* (11), 2349–2352. DOI: 10.1021/ol060640s.
(110) Kemp, J. E. G.; Ellis, D.; Closier, M. D. Penicillin N-cyanosulphilmines; cyanamide/iodobenzene diacetate, a convenient cyanonitrene reagent for N-cyano sulphilmines, sulphoximines, phosphinimines and aziridines. *Tetrahedron Lett.* **1979**, *20* (39), 3781–3784. DOI: 10.1016/S0040-4039(01)95523-6.
(111) Zheng, W.; Chen, X.; Chen, F.; He, Z.; Zeng, Q. Syntheses and Transformations of Sulfoximines. *Chem. Rec.* **2021**, *21* (2), 396–416. DOI: 10.1002/tcr.202000134.
(112) Hosseinian, A.; Zare Fekri, L.; Monfared, A.; Vessally, E.; Nikpassand, M. Transition-metal-catalyzed C–N cross-coupling reactions of N-unsubstituted sulfoximines: a review. *J. Sulfur Chem.* **2018**, *39* (6), 674–698. DOI: 10.1080/17415993.2018.1471142.
(113) Kemp, J. E. G.; Closier, M. D.; Stefaniak, M. H. Penicillin and cephalosporin sulphoximines. *Tetrahedron Lett.* **1979**, *20* (39), 3785–3788. DOI: 10.1016/S0040-4039(01)95524-8.
(114) Micetich, R. G.; Maiti, S. N.; Spevak, P.; Tanaka, M.; Yamazaki, T.; Ogawa, K. Synthesis of 2β-Azidomethylpenicillin-1,1-Dioxides and 3β-Azido-3α-methylcepham-1,1-Dioxides. *Synthesis* **1986**, (4), 292–296. DOI: 10.1055/s-1986-31587.
(115) Osborne, N. F.; Atkins, R. J.; Broom, N. J. P.; Coulton, S.; Harbridge, J. B.; Harris, M. A.; Stirling-François, I.; Walker, G. Synthesis of (5R)-(Z)-6-(1-methyl-1,2,3-triazol-4-ylmethylene)penem-3-carboxylic acid, a potent broad spectrum β-lactamase inhibitor, from 6-aminopenicillanic acid. *J. Chem. Soc., Perkin Trans. 1* **1994**, (2), 179–188. DOI: 10.1039/P19940000179.
(116) Richter, H. G. F.; Angehrn, P.; Hubschwerlen, C.; Kania, M.; Page, M. G. P.; Specklin, J.-L.; Winkler, F. K. Design, Synthesis, and Evaluation of 2β-Alkenyl Penam Sulfone Acids as Inhibitors of β-Lactamases. *J. Med. Chem.* **1996**, *39* (19), 3712–3722. DOI: 10.1021/jm9601967.
(117) Ishiwata, A.; Kotra, L. P.; Miyashita, K.; Nagase, T.; Mobashery, S. Stereoselective Reduction of α-Bromopenicillanates by Tributylphosphine. *Org. Lett.* **2000**, *2* (18), 2889–2892. DOI: 10.1021/ol000185e.
(118) Micetich, R. G.; Maiti, S. N.; Tanaka, M.; Yamazaki, T.; Ogawa, K. Studies on 6-halo- and 6,6-dihalopenicillins: the rearrangement of methyl 6,6-dibromopenicillanate to 1,4-thiazepine. *J. Org. Chem.* **1986**, *51* (6), 853–858. DOI: 10.1021/jo00356a020.
(119) Buynak, J. D.; Ghadachanda, V. R.; Vogeti, L.; Zhang, H.; Chen, H. Synthesis and Evaluation of 3-(Carboxymethylidene)- and 3-(Carboxymethyl)penicillinates as Inhibitors of β-Lactamase. *J. Org. Chem.* **2005**, *70* (11), 4510–4513. DOI: 10.1021/jo050004s.
(120) Yang, Y.; Tang, S.; Liu, Z.; Wang, Y.; Pang, J.; You, X.; Song, D.; Li, Y.; Lu, X. Synthesis and antibacterial evaluation of sulbactam derivatives against Acinetobacter baumannii. *Pharmazie* **2018**, *73* (8), 433–437. DOI: 10.1691/ph.2018.8487.
(121) Sacripante, G.; Just, G. Stereoselective synthesis of α-alkylazetidinones by a free radical chain reaction. *J. Org. Chem.* **1987**, *52* (16), 3659–3661. DOI: 10.1021/jo00392a030.

(122) Bandini, E.; Favi, G.; Martelli, G.; Panunzio, M.; Piersanti, G. A Trans-Stereoselective Synthesis of 3-Halo-4-alkyl(aryl)-NH-azetidin-2-ones. *Org. Lett.* **2000**, *2* (8), 1077–1079. DOI: 10.1021/ol005633x.
(123) Volkmann, R. A.; Carroll, R. D.; Drolet, R. B.; Elliott, M. L.; Moore, B. S. Efficient preparation of 6,6-dihalopenicillanic acids. Synthesis of penicillanic acid S,S-dioxide (sulbactam). *J. Org. Chem.* **1982**, *47* (17), 3344–3345. DOI: 10.1021/jo00138a035.
(124) Zenzola, M.; Doran, R.; Luisi, R.; Bull, J. A. Synthesis of Sulfoximine Carbamates by Rhodium-Catalyzed Nitrene Transfer of Carbamates to Sulfoxides. *The Journal of Organic Chemistry* **2015**, *80* (12), 6391–6399. DOI: 10.1021/acs.joc.5b00844.
(125) Miao, J.; Richards, N. G. J.; Ge, H. Rhodium-catalyzed direct synthesis of unprotected NH-sulfoximines from sulfoxides. *Chem. Commun.* **2014**, *50* (68), 9687–9689, 10.1039/C4CC04349A. DOI: 10.1039/C4CC04349A.
(126) Flack, H. On enantiomorph-polarity estimation. *Acta Crystallographica Section A* **1983**, *39* (6), 876–881. DOI: doi:10.1107/S0108767383001762.
(127) Hackenberger, C. P. R.; Raabe, G.; Bolm, C. Synthetic and Spectroscopic Investigation of N-Acylated Sulfoximines. *Chem. Eur. J.* **2004**, *10* (12), 2942–2952. DOI: 10.1002/chem.200306016.
(128) Chan, D. M. T.; Monaco, K. L.; Wang, R.-P.; Winters, M. P. New N- and O-arylations with phenylboronic acids and cupric acetate. *Tetrahedron Lett.* **1998**, *39* (19), 2933–2936. DOI: 10.1016/S0040-4039(98)00503-6.
(129) Evans, D. A.; Katz, J. L.; West, T. R. Synthesis of diaryl ethers through the copper-promoted arylation of phenols with arylboronic acids. An expedient synthesis of thyroxine. *Tetrahedron Lett.* **1998**, *39* (19), 2937–2940. DOI: 10.1016/S0040-4039(98)00502-4.
(130) Lam, P. Y. S.; Clark, C. G.; Saubern, S.; Adams, J.; Winters, M. P.; Chan, D. M. T.; Combs, A. New aryl/heteroaryl C-N bond cross-coupling reactions via arylboronic acid/cupric acetate arylation. *Tetrahedron Lett.* **1998**, *39* (19), 2941–2944. DOI: 10.1016/S0040-4039(98)00504-8.
(131) Borst, M. L. G.; Ouairy, C. M. J.; Fokkema, S. C.; Cecchi, A.; Kerckhoffs, J. M. C. A.; de Boer, V. L.; van den Boogaard, P. J.; Bus, R. F.; Ebens, R.; van der Hulst, R.; et al. Polycyclic Sulfoximines as New Scaffolds for Drug Discovery. *ACS Comb. Sci.* **2018**, *20* (6), 335–343. DOI: 10.1021/acscombsci.7b00150.
(132) Schuemacher, A. C.; Hoffmann, R. W. Condensation Between Isocyanates and Carboxylic Acids in the Presence of 4-Dimethylaminopyridine (DMAP), a Mild and Efficient Synthesis of Amides. *Synthesis* **2001**, *2001* (02), 0243–0246. DOI: 10.1055/s-2001-10813.
(133) Sheehan, J.; Cruickshank, P.; Boshart, G. Notes- A Convenient Synthesis of Water-Soluble Carbodiimides. *The Journal of Organic Chemistry* **1961**, *26* (7), 2525–2528. DOI: 10.1021/jo01351a600.
(134) Neises, B.; Steglich, W. Einfaches Verfahren zur Veresterung von Carbonsäuren. *Angew. Chem.* **1978**, *90* (7), 556–557. DOI: 10.1002/ange.19780900718.
(135) Moessner, C.; Bolm, C. $Cu(OAc)_2$-Catalyzed N-Arylations of Sulfoximines with Aryl Boronic Acids. *Org. Lett.* **2005**, *7* (13), 2667–2669. DOI: 10.1021/ol050816a.
(136) Barton, D. H. R.; Elliott, J. D.; Géro, S. D. The synthesis and properties of a series of strong but hindered organic bases. *J. Chem. Soc., Chem. Commun.* **1981**, (21), 1136–1137, 10.1039/C39810001136. DOI: 10.1039/C39810001136.
(137) Bolm, C.; Hackenberger, C. P. R.; Simić, O.; Verrucci, M.; Müller, D.; Bienewald, F. A Mild Synthetic Procedure for the Preparation of N-Alkylated Sulfoximines. *Synthesis* **2002**, *2002* (07), 0879–0887. DOI: 10.1055/s-2002-28514.
(138) Abdel-Magid, A. F.; Carson, K. G.; Harris, B. D.; Maryanoff, C. A.; Shah, R. D. Reductive Amination of Aldehydes and Ketones with Sodium Triacetoxyborohydride. Studies on Direct and Indirect Reductive Amination Procedures1. *The Journal of Organic Chemistry* **1996**, *61* (11), 3849–3862. DOI: 10.1021/jo960057x.

(139) Rulev, A. Y. Weak Nucleophiles in the Aza-Michael Reaction. *Adv. Synth. Catal.* **2023**, *365* (12), 1908–1925. DOI: 10.1002/adsc.202300316.
(140) Xu, L.-W.; Li, L.; Xia, C.-G.; Zhou, S.-L.; Li, J.-W.; Hu, X.-X. Highly Efficient Aza-Michael Reactions of Enones with Carbamates Using a Combination of Quaternary Ammonium Salts and BF3·OEt2 as a Catalyst. *Synlett* **2003**, *2003* (15), 2337–2340. DOI: 10.1055/s-2003-43333.
(141) Mitsunobu, O. The Use of Diethyl Azodicarboxylate and Triphenylphosphine in Synthesis and Transformation of Natural Products. *Synthesis* **1981**, *1981* (01), 1–28. DOI: 10.1055/s-1981-29317.
(142) De Bernardo, S.; Tengi, J. P.; Sasso, G. J.; Weigele, M. Clavalanine (Ro 22-5417), a new clavam antibiotic from Streptomyces clavuligerus. 4. A stereorational synthesis. *The Journal of Organic Chemistry* **1985**, *50* (19), 3457–3462. DOI: 10.1021/jo00219a008.
(143) Stelakatos, G. C.; Paganou, A.; Zervas, L. New methods in peptide synthesis. Part III. Protection of carboxyl group. *Journal of the Chemical Society C: Organic* **1966**, (0), 1191–1199, 10.1039/J39660001191. DOI: 10.1039/J39660001191.
(144) Kametani, T.; Sekine, H.; Honda, T. The Deblocking of Cephalosporin Benzhydryl Esters with Formic Acid. *Chem. Pharm. Bull. (Tokyo)* **1982**, *30* (12), 4545–4547. DOI: 10.1248/cpb.30.4545.
(145) Froussios, C.; Kolovos, M. Preparation of Diphenylmethyl Esters and Ethers of Unprotected Amino Acids and β-Hydroxy-α-amino Acids. *Synthesis* **1987**, *1987* (12), 1106–1108. DOI: 10.1055/s-1987-28185.
(146) Williams, J. M.; Brands, K. M. J.; Skerlj, R. T.; Jobson, R. B.; Marchesini, G.; Conrad, K. M.; Pipik, B.; Savary, K. A.; Tsay, F.-R.; Houghton, P. G.; et al. Practical Synthesis of the New Carbapenem Antibiotic Ertapenem Sodium. *The Journal of Organic Chemistry* **2005**, *70* (19), 7479–7487. DOI: 10.1021/jo0501442.
(147) Comito, M.; Monguzzi, R.; Tagliapietra, S.; Maspero, A.; Palmisano, G.; Cravotto, G. From Batch to the Semi-Continuous Flow Hydrogenation of pNB, pNZ-Protected Meropenem. *Pharmaceutics* **2023**, *15* (5). DOI: 10.3390/pharmaceutics15051322.
(148) Page, M. I. The mechanisms of reactions of .beta.-lactam antibiotics. *Acc. Chem. Res.* **1984**, *17* (4), 144–151. DOI: 10.1021/ar00100a005.
(149) De Angelis, F.; Attorrese, G.; Cavicchio, G.; Ciampa, S.; Di Tullio, A.; Fattori, D.; Nicoletti, R.; Domenici, E. Synthesis and Preliminary Biological Evaluation of 3'-Substituted Cephem Sulfones as Potential β-Lactamase Inhibitors. *European Journal of Organic Chemistry* **2001**, *2001* (16), 3075–3081. DOI: 10.1002/1099-0690(200108)2001:16.
(150) Laganis, E. D.; Chenard, B. L. Metal silanolates: organic soluble equivalents for O−2. *Tetrahedron Lett.* **1984**, *25* (51), 5831–5834. DOI: 10.1016/S0040-4039(01)81697-X.
(151) Fisher, J. W.; Trinkle, K. L. Iodide dealkylation of benzyl, PMB, PNB, and t-Butyl N-acyl amino acid esters via lithium ion coordination. *Tetrahedron Lett.* **1994**, *35* (16), 2505–2508. DOI: 10.1016/S0040-4039(00)77156-5.
(152) Ogilvie, K. K.; Beaucage, S. L. Fluoride ion promoted deprotection and transesterification in nucleotide triesters. *Nucleic Acids Res.* **1979**, *7* (3), 805–823. DOI: 10.1093/nar/7.3.805.
(153) Jeong, S. H.; Bae, I. K.; Lee, J. H.; Sohn, S. G.; Kang, G. H.; Jeon, G. J.; Kim, Y. H.; Jeong, B. C.; Lee, S. H. Molecular Characterization of Extended-Spectrum Beta-Lactamases Produced by Clinical Isolates of Klebsiella pneumoniae and Escherichia coli from a Korean Nationwide Survey. *J. Clin. Microbiol.* **2004**, *42* (7), 2902–2906. DOI: doi:10.1128/jcm.42.7.2902-2906.2004.
(154) Jacoby George, A. AmpC β-lactamases. *Clin. Microbiol. Rev.* **2009**, *22* (1), 161–182. DOI: 10.1128/cmr.00036-08.

(155) Paetzel, M.; Danel, F.; de Castro, L.; Mosimann, S. C.; Page, M. G. P.; Strynadka, N. C. J. Crystal structure of the class D β-lactamase OXA-10. *Nat. Struct. Biol.* **2000**, *7* (10), 918–925. DOI: 10.1038/79688.
(156) Poirel, L.; Potron, A.; Nordmann, P. OXA-48-like carbapenemases: the phantom menace. *J. Antimicrob. Chemother.* **2012**, *67* (7), 1597–1606. DOI: 10.1093/jac/dks121.
(157) van Berkel, S. S.; Brem, J.; Rydzik, A. M.; Salimraj, R.; Cain, R.; Verma, A.; Owens, R. J.; Fishwick, C. W. G.; Spencer, J.; Schofield, C. J. Assay Platform for Clinically Relevant Metallo-β-lactamases. *J. Med. Chem.* **2013**, *56* (17), 6945–6953. DOI: 10.1021/jm400769b.
(158) Goddard, J.-P.; Reymond, J.-L. Enzyme assays for high-throughput screening. *Curr. Opin. Biotechnol.* **2004**, *15* (4), 314–322. DOI: 10.1016/j.copbio.2004.06.008.
(159) van Berkel, S. S.; Brem, J.; Rydzik, A. M.; Salimraj, R.; Cain, R.; Verma, A.; Owens, R. J.; Fishwick, C. W. G.; Spencer, J.; Schofield, C. J. Assay Platform for Clinically Relevant Metallo-β-lactamases. *J. Med. Chem.* **2013**, *56* (17), 6945–6953. DOI: 10.1021/jm400769b.
(160) Usher, K. C.; Blaszczak, L. C.; Weston, G. S.; Shoichet, B. K.; Remington, S. J. Three-Dimensional Structure of AmpC β-Lactamase from Escherichia coli Bound to a Transition-State Analogue: Possible Implications for the Oxyanion Hypothesis and for Inhibitor Design. *Biochemistry* **1998**, *37* (46), 16082–16092. DOI: 10.1021/bi981210f.
(161) McLeod, S. M.; Carter, N. M.; Huband, M. D.; Traczewski, M. M.; Bradford, P. A.; Miller, A. A. Sulbactam-durlobactam susceptibility test method development and quality control ranges for MIC and disk diffusion tests. *J. Clin. Microbiol.* **2024**, *62* (1), e01228–01223. DOI: doi:10.1128/jcm.01228-23.
(162) Cortes-Clerget, M.; Yu, J.; Kincaid, J. R. A.; Walde, P.; Gallou, F.; Lipshutz, B. H. Water as the reaction medium in organic chemistry: from our worst enemy to our best friend. *Chemical Science* **2021**, *12* (12), 4237–4266, 10.1039/D0SC06000C. DOI: 10.1039/D0SC06000C.
(163) Page, M. I. The reactivity of beta-lactams, the mechanism of catalysis and the inhibition of beta-lactamases. *Curr. Pharm. Des.* **1999**, *5* (11), 895–913.
(164) Zapun, A.; Contreras-Martel, C.; Vernet, T. Penicillin-binding proteins and β-lactam resistance. *FEMS Microbiol. Rev.* **2008**, *32* (2), 361–385. DOI: 10.1111/j.1574-6976.2007.00095.x.
(165) Lee, C.-R.; Lee, J. H.; Park, M.; Park, K. S.; Bae, I. K.; Kim, Y. B.; Cha, C.-J.; Jeong, B. C.; Lee, S. H. Biology of Acinetobacter baumannii: Pathogenesis, Antibiotic Resistance Mechanisms, and Prospective Treatment Options. *Frontiers in Cellular and Infection Microbiology* **2017**, *Volume 7 - 2017*, Review. DOI: 10.3389/fcimb.2017.00055.
(166) Di, L.; Kerns, E. H. Profiling drug-like properties in discovery research. *Curr. Opin. Chem. Biol.* **2003**, *7* (3), 402–408. DOI: 10.1016/S1367-5931(03)00055-3.
(167) Zhang, Z.; Tang, W. Drug metabolism in drug discovery and development. *Acta Pharm Sin B* **2018**, *8* (5), 721–732. DOI: 10.1016/j.apsb.2018.04.003.
(168) Rex, J. H.; Eisenstein, B. I.; Alder, J.; Goldberger, M.; Meyer, R.; Dane, A.; Friedland, I.; Knirsch, C.; Sanhai, W. R.; Tomayko, J.; et al. A comprehensive regulatory framework to address the unmet need for new antibacterial treatments. *The Lancet Infectious Diseases* **2013**, *13* (3), 269–275. DOI: 10.1016/S1473-3099(12)70293-1.
(169) Drusano, G. L. Pharmacokinetics and Pharmacodynamics of Antimicrobials. *Clin. Infect. Dis.* **2007**, *45* (Supplement_1), S89–S95. DOI: 10.1086/518137.
(170) Lang, P. A.; Parkova, A.; Leissing, T. M.; Calvopiña, K.; Cain, R.; Krajnc, A.; Panduwawala, T. D.; Philippe, J.; Fishwick, C. W. G.; Trapencieris, P.; et al. Bicyclic Boronates as Potent Inhibitors of AmpC, the Class C β-Lactamase from Escherichia coli. *Biomolecules* **2020**, *10* (6), 899.
(171) Lohans, C. T.; Freeman, E. I.; Groesen, E. v.; Tooke, C. L.; Hinchliffe, P.; Spencer, J.; Brem, J.; Schofield, C. J. Mechanistic Insights into β-Lactamase-Catalysed Carbapenem

Degradation Through Product Characterisation. *Sci. Rep.* **2019**, *9* (1), 13608. DOI: 10.1038/s41598-019-49264-0.
(172) McCoy, A. J.; Grosse-Kunstleve, R. W.; Adams, P. D.; Winn, M. D.; Storoni, L. C.; Read, R. J. Phaser crystallographic software. *J. Appl. Crystallogr.* **2007**, *40* (4), 658–674. DOI: doi:10.1107/S0021889807021206.
(173) Adams, P. D.; Grosse-Kunstleve, R. W.; Hung, L.-W.; Ioerger, T. R.; McCoy, A. J.; Moriarty, N. W.; Read, R. J.; Sacchettini, J. C.; Sauter, N. K.; Terwilliger, T. C. PHENIX: building new software for automated crystallographic structure determination. *Acta Crystallographica Section D* **2002**, *58* (11), 1948–1954. DOI: doi:10.1107/S0907444902016657.
(174) Emsley, P.; Lohkamp, B.; Scott, W. G.; Cowtan, K. Features and development of Coot. *Acta Crystallographica Section D* **2010**, *66* (4), 486–501. DOI: doi:10.1107/S0907444910007493.
(175) Young, J. Y.; Westbrook, J. D.; Feng, Z.; Sala, R.; Peisach, E.; Oldfield, T. J.; Sen, S.; Gutmanas, A.; Armstrong, D. R.; Berrisford, J. M.; et al. OneDep: Unified wwPDB System for Deposition, Biocuration, and Validation of Macromolecular Structures in the PDB Archive. *Structure* **2017**, *25* (3), 536–545. DOI: 10.1016/j.str.2017.01.004.
(176) Lewis, J. S. *CLSI M100 Performance Standards for Antimicrobial Susceptibility Testing*; Clinical and Laboratory Standards Institute (CLSI), 2025.
(177) Harris, D. A.; Powers, M. E.; Romesberg, F. E. Synthesis and biological evaluation of penem inhibitors of bacterial signal peptidase. *Bioorg. Med. Chem. Lett.* **2009**, *19* (14), 3787–3790. DOI: 10.1016/j.bmcl.2009.04.034.
(178) Zenzola, M.; Doran, R.; Luisi, R.; Bull, J. A. Synthesis of Sulfoximine Carbamates by Rhodium-Catalyzed Nitrene Transfer of Carbamates to Sulfoxides. *J. Org. Chem.* **2015**, *80* (12), 6391–6399. DOI: 10.1021/acs.joc.5b00844.
(179) Moessner, C.; Bolm, C. Cu(OAc)2-Catalyzed N-Arylations of Sulfoximines with Aryl Boronic Acids. *Org. Lett.* **2005**, *7* (13), 2667–2669. DOI: 10.1021/ol050816a.
(180) Tanaka, H.; Tanaka, M.; Nakai, A.; Katayama, Y.; Torii, S. A Facile Reductive Removal of Bromine Atom(s) of 6,6-Dibromo- and 6-Bromopenicillanate Derivatives in a Pb/Al Bimetal System. *Bull. Chem. Soc. Jpn.* **1989**, *62* (2), 627–629. DOI: 10.1246/bcsj.62.627.
(181) Franceschi, G.; Alpegiani, M.; Bedeshci, A.; Bissolino, P.; Visentin, G.; Zarini, F.; Perrone, E. Reactivity parameters of the metal assisted 1,2-cleavage of penicillins. *Heterocycles* **1990**, *31*, 617–628. DOI: 10.3987/COM-89-5257.
(182) Brennan, J.; Hussain, F. H. S. The Synthesis of Penicillanate Esters from Ultrasonically Formed Organozinc Intermediates. *Synthesis* **1985**, *1985* (08), 749–751. DOI: 10.1055/s-1985-31331.
(183) Beels, C. M. D.; Abu-Rabie, M. S.; Murray-Rust, P.; Murray-Rust, J. Chiral conversion of 6-aminopenicillanic acid into an antibacterial pen-2-em-3-carboxylic acid derivative: absolute structure from X-ray analysis. *J. Chem. Soc., Chem. Commun.* **1979**, (15), 665–666, 10.1039/C39790000665. DOI: 10.1039/C39790000665.
(184) Chauvette, R. R.; Pennington, P. A.; Ryan, C. W.; Cooper, R. D. G.; Jose, F. L.; Wright, I. G.; Van Heyningen, E. M.; Huffman, G. W. Chemistry of cephalosporin antibiotics. XXI. Conversion of penicillins to cephalexin. *The Journal of Organic Chemistry* **1971**, *36* (9), 1259–1267. DOI: 10.1021/jo00808a021.
(185) Barton, D. H. R.; Comer, F.; Greig, D. G. T.; Sammes, P. G.; Cooper, C. M.; Hewitt, G.; Underwood, W. G. E. Transformations of penicillin. Part I. Preparation and rearrangements of 6β-phenylacetamidopenicillanic sulphoxides. *Journal of the Chemical Society C: Organic* **1971**, (0), 3540–3550, 10.1039/J39710003540. DOI: 10.1039/J39710003540.
(186) Gunda, T. E. Mannich Reactions of Cephalosporin Sulphoxides and Sulphones with Imonium Salts. An Improved Synthesis of 2-Methylene-cephalosporins. *Synth. Commun.* **1992**, *22* (20), 2979–2986. DOI: 10.1080/00397919208021124.

(187) Ninomiya, K.; Shioiri, T.; Yamada, S. Phosphorus in Organic Synthesis. XII. Amino Acids and Peptides. XXII. Reaction of Penicillin Sulfoxides with Diethyl Phosphorocyanidate (DEPC). *Chem. Pharm. Bull. (Tokyo)* **1976**, *24* (11), 2711–2715. DOI: 10.1248/cpb.24.2711.
(188) Claes, P. G.; Decoster, G.; Kerremans, L. A.; Vanderhaeghe, H. PREPARATION OF Δ3-7α-PHENYLACETAMIDODESACETOXY-CEPHALOSPORANIC ACID. *The Journal of Antibiotics* **1979**, *32* (8), 820–827.
(189) Torii, S.; Tanaka, H.; Katoh, T.; Morisaki, K. Pd(O)-catalyzed electroreductive cleavage of allylic acetates. *Tetrahedron Lett.* **1984**, *25* (30), 3207–3208. DOI: 10.1016/S0040-4039(01)91010-X.